NASA CR-72784
TRW 09849-6001-R0-00

FINAL REPORT

INVESTIGATION OF THRUSTERS FOR CRYOGENIC REACTION CONTROL SYSTEMS

VOLUME I

By
R. J. JOHNSON

TRW
SYSTEMS GROUP

PREPARED FOR

NATIONAL AERONAUTICS AND SPACE ADMINISTRATION
NASA Lewis Research Center
Contract NAS 3-11227

P. N. HERR,
Project Manager

NOTICE

This report was prepared as an account of Government-sponsored work. Neither the United States, nor the National Aeronautics and Space Administration (NASA), nor any person acting on behalf of NASA:

A. Makes any warranty or representation, expressed or implied, with respect to the accuracy, completeness, or usefulness of the information contained in this report, or that the use of any information, apparatus, method, or process disclosed in this report may not infringe privately-owned rights; or

B. Assumes any liabilities with respect to the use of, or for damages resulting from the use of, any information, apparatus, method or process disclosed in this report.

As used above, "person acting on behalf of NASA" includes any employee or contractor of NASA, or employee of such contractor, to the extent that such employee or contractor of NASA or employee of such contractor prepares, disseminates, or provides access to any information pursuant to this employment or contract with NASA, or his employment with such contractor.

Requests for copies of this report should be referred to

National Aeronautics and Space Administration
Scientific and Technical Information Facility
P. O. Box 33
College Park, Md. 20740

NASA CR-72784
TRW 09849-6001-R0-00

FINAL REPORT

INVESTIGATION OF THRUSTERS FOR CRYOGENIC REACTION CONTROL SYSTEMS

Volume I

by

R. J. Johnson

TRW SYSTEMS GROUP
One Space Park
Redondo Beach, California 90278

prepared for

NATIONAL AERONAUTICS AND SPACE ADMINISTRATION

November 13, 1970

CONTRACT NAS 3-11227

NASA Lewis Research Center
Cleveland, Ohio
P. N. Herr, Project Manager
Liquid Rocket Technology Branch

FOREWORD

This report was prepared by the Science and Technology Division of the TRW Systems Group at One Space Park, Redondo Beach, California, under Contract NAS 3-11227. The contract was administered by the Lewis Research Center of the National Aeronautics and Space Administration, Cleveland, Ohio. The NASA Project Manager for the contract was Mr. P. N. Herr of the Liquid Rocket Technology Branch. This is the final report on the subject contract and summarizes the technical effort conducted during the period from June 1968 to October 1969.

The following personnel at TRW contributed to the technical accomplishments of this program: R. J. Johnson, Program Manager; Dr. H. L. Burge and S. J. Van Grouw, Technical Advisors; Dr. N. C. Rodewald, Data Evaluation; Dr. J. L. Blumenthal, R. J. Grassi, and M. J. Santy, Laboratory Investigations; K. J. Mock, Design; W. W. Fellows, Test Operations; and G. P. Starr, Data Acquisition.

CONTENTS

CONTENTS (Continued)

CONTENTS (Continued)

ILLUSTRATIONS

ILLUSTRATIONS (Continued)

ILLUSTRATIONS (Continued)

ILLUSTRATIONS (Continued)

ILLUSTRATIONS (Continued)

ILLUSTRATIONS (Continued)

ILLUSTRATIONS (Continued)

TABLES

TABLES (Continued)

ABSTRACT

An experimental and analytical program was conducted to evaluate the ignition characteristics and delivered performance of gaseous hydrogen-oxygen reaction control thrusters. Specific goals were to establish design criteria for a pilot bed catalytic igniter and to define an operating map for reliable thruster ignition at two chamber pressure levels. The relative activities of Shell 405 and Engelhard MFSA catalysts at cryogenic temperatures were determined by both laboratory investigations and test hardware reactor firings. Repeatable ignitions, high performance, and pulse mode operation of each pressure level thruster were demonstrated with propellant temperatures from ambient to -250°F (117°K).

1. SUMMARY

The experimental results of contract NAS 3-11227 have demonstrated the feasibility of catalytic pilot bed ignition of gaseous hydrogen-oxygen thrusters. Pilot bed design criteria and thruster/igniter operational limits were established for a wide range of environmental and propellant inlet conditions.

The specific goals of the "Investigation of Thrusters for Cryogenic Reaction Control Systems" program were:

- Establish design criteria for pilot bed catalytic reactors capable of igniting 20 lbf (89N) gaseous hydrogen-oxygen thrusters at chamber pressures of 10 and 100 psia (69 and 690 kN/m^2).

- Define an operating map for reliable thruster ignition and operation at each chamber pressure level, including the operating variables of propellant temperatures, helium dilution of propellants, vacuum effects, and catalyst bed temperature.

To accomplish these goals, an extensive experimental effort of 857 tests was conducted, including laboratory catalyst activity evaluations, catalytic reactor igniter tests, and combined thruster/igniter firings, both steady state and pulse mode.

Laboratory experimental studies performed with candidate Shell 405-ABSG and Engelhard MFSA catalysts led to the following conclusions:

- The activity of either catalyst at temperatures below -25°C (248°K) is strongly dependent upon the condition of the catalyst surface. Absorbed oxygen was found to be extremely detrimental to low temperature H_2-O_2 reaction, while preabsorbed hydrogen enhanced the activity of the catalysts.

- The Shell 405-ABSG catalyst has a greater capacity for H_2-O_2 reaction than the Engelhard MFSA catalyst at temperatures below -125°C (148°K). However, above this temperature, the Engelhard catalyst appeared to be at least equal to and perhaps superior in activity to the Shell catalyst.

- High vacuum exposure (10^{-6} mm Hg) at temperatures up to 816°C (1089°K) for time periods of several hours had little effect on the surface structure of either catalyst or their capacity to promote low temperature H_2-O_2 reaction.

Catalytic reactor experiments with hardware capable of igniting a 20 lbf (89N) O_2/H_2 thruster were conducted to further evaluate each candidate catalyst formulation and determine effects of catalyst bed lengths, vacuum environment, and propellant inlet conditions. The major results of the reactor experiments were:

- Reaction was achieved at propellant temperatures as low as -250°F (117°K) with the Shell 405-ABSG catalyst, while the Engelhard MFSA catalyst did not sustain reaction below -100°F (200°K).

- Helium dilutions in oxygen as high as 50 percent by weight for the high pressure reactor and 25 percent at low pressure did not preclude ambient temperature reaction. Helium-hydrogen dilutions up to 10 percent by weight were reacted at both pressure levels.

- No significant degradation of reactor ignition response resulted when the catalyst bed was exposed to high vacuum (10^{-5} mm Hg) prior to reaction (consistent with the laboratory activity investigation results).

Combined thruster/igniter test firings were performed at each chamber pressure level to investigate minimum ignition energy level requirements, evaluate effects of catalyst bed variations, establish steady-state baseline performance, and determine pulse mode performance characteristics. In summary, the results of these tests were:

- Satisfactory thruster ignitions were achieved with igniter effluent temperatures as low as 1250°F (950°K) and igniter flow rates as low as 2 percent of thruster propellant flows.

- Thruster ignition was found to be very sensitive to injection geometry. Successful ignitions were attained by secondary injection of pure oxygen into the fuel-rich igniter effluent gases.

- Combustion efficiencies of 95 percent of theoretical equilibrium C^* were measured with the high pressure thruster, and 90 percent of theoretical C^* with the low pressure thruster. No extensive injector optimizations were conducted during this program.

- Pulse mode tests were performed at each chamber pressure level with propellant inlet temperatures of -250°F (117°K). Repeatable pulses were attained with a number of different pulse duty cycles.

Recommendations for further investigations include the performance and durability evaluation of flightweight thruster designs at each chamber pressure level. Preliminary designs of flight-type thrusters, based on the results of this program, are also presented in the report.

2. INTRODUCTION

The "Investigation of Thrusters for Cryogenic Reaction Control Systems" program effort, NASA/LeRC Contract NAS 3-11227, was comprised of an experimental and supporting analytical evaluation of the igniter delay, reactor design, thruster response times, and delivered performance for a gaseous hydrogen-oxygen reaction control thruster. The thruster design concept for this program incorporated a pilot bed igniter, through which only a small portion (less than 10 percent) of the thruster propellants was passed. Previous NASA sponsored investigations of hydrogen-oxygen thrusters utilized by-pass bed designs, wherein all of the hydrogen and part of the oxygen (mixture ratio 1.0) flowed through the catalyst bed, and additional oxygen was injected downstream to increase overall mixture ratio and attain higher performance. The catalyst formulations evaluated during this investigation, Shell 405-ABSG and Engelhard MFSA, were also employed in previous hydrogen-oxygen catalytic ignition programs.

The thruster nominal design/operation conditions evaluated during this program were:

- Vacuum thrust - 20 lbf (89N)
- Chamber pressures - 10, 100 psia (69, 690 kN/m^2)
- Overall mixture ratio - 2.5
- Propellant temperatures - ambient to -250°F (117°K)
- Helium dilution in oxygen - 0, 5, 25, 50 percent by weight
- Helium dilution in hydrogen - 0, 5, 10 percent by weight
- Igniter mixture ratio - 1.0 nominal
- Igniter flow rates - 2, 5, 10 percent of thruster flow
- Duty cycle - steady state/pulse mode

The primary objectives of this investigation were to establish pilot bed reactor design criteria and to define an operating map for reliable thruster ignition and operation. To accomplish these goals, the following tasks were conducted:

- Laboratory investigations to determine the relative activities of the Shell 405-ABSG and Engelhard MFSA catalysts over a range of environmental conditions
- Catalytic reactor experiments to further evaluate each catalyst under actual firing conditions and to determine reactor response times
- Combined thruster/igniter test firings to establish ignition requirements and operational limits for both steady-state and pulse mode duty cycles.

Test hardware, procedures, and experimental results for each task are discussed in the subsequent report sections. A summary of program results and recommendations for further investigations are presented in the concluding remarks.

3. CATALYST ACTIVITY LABORATORY INVESTIGATIONS

This section describes the laboratory experimental studies performed with the candidate Shell 405 and Engelhard MFSA catalysts. The selection of these two catalyst formulations was based upon the results of previous NASA-sponsored experimental investigations. The objectives of this task effort were as follows:

- Determine over a range of operating parameters the relative activities of the Shell 405 and Engelhard MFSA catalysts for hydrogen-oxygen reaction at cryogenic temperatures
- Evaluate the effects of vacuum soaking at elevated temperatures on the catalytic activity at cryogenic temperatures
- Determine the best practical pretreatment conditions for the catalysts in order to maximize their low temperature hydrogen-oxygen ignition properties
- Obtain empirical reaction rate data at low temperatures which can be utilized in an analytical model for predicting the ignition transient and in the engineering design of practical thruster systems

In conducting these investigations, two independant experimental techniques were employed. First, preliminary hydrogen and oxygen chemisorption screening experiments were performed to identify the important variables. Next, pulsed flow, isothermal, differential reactor tests were then conducted to investigate the catalytic H_2-O_2 reaction under simulated igniter/thruster operating conditions.

3.1 PRELIMINARY CHEMISORPTION SCREENING EXPERIMENTS

The large number of environmental conditions to which the catalysts could be exposed prior to engine ignition made it essential that some preliminary experiments be conducted to determine those soak conditions which were most critical, and hence should be included in the differential reactor test matrix. The approach which was used in the preliminary experimentation involved hydrogen and/or oxygen chemisorption measurements following exposure of the catalysts to well-defined pretreatment and soak conditions. TRW established the effectiveness of this general method under a previous NASA contract (NAS 7-520) which was aimed at correlating the low temperature, high vacuum, hydrazine ignition properties of the Shell 405 catalyst with the various concentrations of chemisorbed gas species (O_2, N_2, NH_3, H_2) present on the catalyst surface. It was found that the adsorption of hydrogen and/or oxygen was very sensitive to the amount of active surface metal available to catalyze the reaction. Hence, chemisorption measurements provided a simple and rapid method of distinguishing the effects on

catalyst surface activity of various soak environments. Moreover, measurements of the low temperature rates of adsorption (and/or reaction) of hydrogen on catalyst surfaces which were previously exposed to oxygen (and vice versa) provided qualitative data on the important initial steps in the ignition of the catalyst-thruster system (i.e., does a hydrogen or oxygen lead help or hinder ignition of the thruster at cryogenic temperature?).

Studies of the catalyst surface properties, pretreatment effects and soak effects by hydrogen and oxygen chemisorption measurements (both isotherm and rate data) are described in the following sections.

3.1.1 Description of Chemisorption Apparatus

The chemisorption apparatus is an all-glass, constant volume, adsorption system. It consists of a manifold and gas sample bulb, catalyst sample tube thermally isolated from the manifold, a gas analysis sampling outlet, a high vacuum pumping system, a sample furnace, temperature measurement and control systems, and a very precise pressure measuring system. Figure 1 shows a schematic diagram of the apparatus. The amount of gas adsorbed on a sample of catalyst is determined by measuring the pressure drop in the calibrated constant volume system.

3.1.2 Test Matrix for Preliminary Experiments

Table 1 presents the chemisorption screening test matrix used to establish probable effects of catalyst soak conditions on the activity of the candidate catalysts. The most important soak conditions were then used for the differential reactor investigation described in Section 3.2.

The test matrix covers the effect of time, temperature and environment (air, vacuum, hydrogen, helium) upon the catalysts. Included in the matrix are chemisorption kinetic measurements to determine the relative rates of chemisorption of hydrogen and oxygen upon the catalysts and the effect of preadsorbed oxygen and hydrogen upon the chemisorption rates.

3.1.3 Experimental Procedure

To make an equilibrium adsorption isotherm measurement a known weight of catalyst was pretreated and then was allowed to thermally equilibrate at the predetermined isotherm temperature. A quantity of gas was initially bled into the evacuated manifold from the gas storage bulb. The number of molecules initially in the gas phase was calculated from the known volume of the manifold and the measured manifold pressure. A stopcock connecting the evacuated sample bulb to the gas manifold was then opened and the gas introduced into the sample bulb. As the gas species (e.g., hydrogen) adsorbed on the catalyst sample, the pressure decreased. When there was no appreciable further change in pressure, the system was assumed to be at equilibrium and the final gas phase pressure recorded. The number of molecules of gas remaining in the gas phase was calculated from the known dead space of the manifold and sample tube. The difference between the original and the final number of molecules in the gas phase was

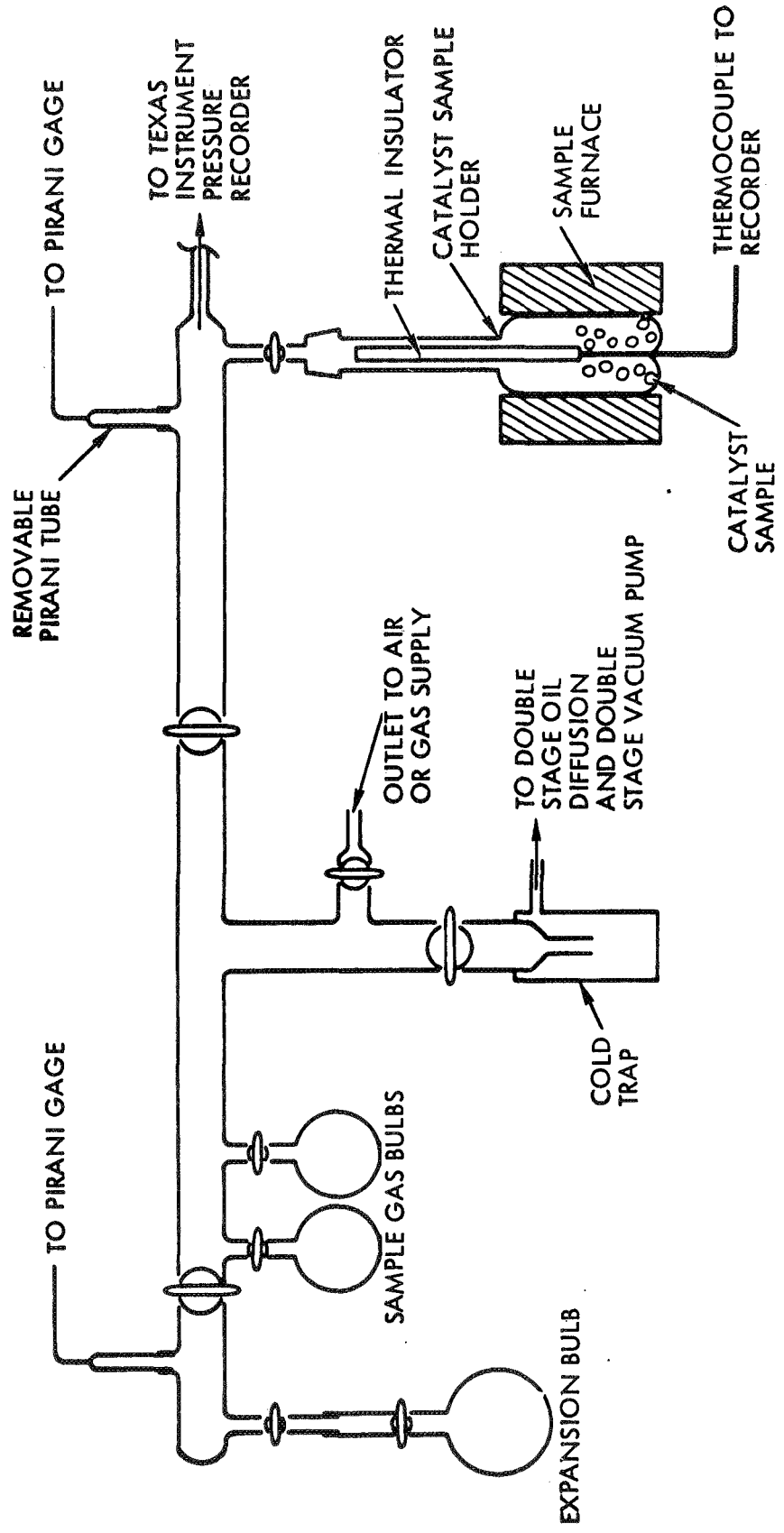

Figure 1. Schematic Diagram of All-Glass Constant Volume Adsorption System

Table 1. Preliminary Chemisorption Screening Tests to Establish Catalyst Soak Conditions for the Differential Reactor Investigation

Experiment No.	Catalyst Type		Catalyst Pretreatment		Soak Temperature		Soak Time (hrs)			Soak Environment				Chemisorption Isotherm Measurement		Chemisorption Kinetic Measurement			
	Shell 405	MFSA	Standard H_2 and Vacuum Pretreatment to Clean Surface	"As Received" Catalyst Outgassed Only	1500°F (1089°K)	-108°F (195°K)	1	5	50	10^{-5} Torr Vacuum	Air 1 atm	H_2 1 atm	He 1 atm	O_2 400°F (478°K)	H_2 400°F (478°K)	H_2 at -108°F (195°K) Clean Surface	H_2 at -108°F (195°K) Surface Presaturated With O_2	O_2 at -108°F (195°K) Clean Surface	O_2 at -108°F (195°K) Surface Presaturated With H_2
1	X			X										X					
2	X			X											X				
3	X		X											X					
4	X		X												X				
5	X		X													X			
6	X		X														X		
7	X		X															X	
8	X		X				X			X					X				
9	X		X		X			X		X					X				
10	X		X		X				X	X					X				
11	X		X		X				X	X					X				
12	X		X		X				X				X		X				
13	X		X		X			X			X			X					
14	X		X		X			X				X			X				
15	X		X			X		X			X			X					
16	X		X			X		X				X			X				
17		X		X										X					
18		X		X											X				
19		X	X											X					
20		X	X												X				
21		X	X													X			
22		X	X															X	
23		X	X																X
24		X	X																
25		X	X		X		X			X					X				
26		X	X		X			X		X					X				
27		X	X		X				X	X					X				
28		X	X		X				X				X		X				
29		X	X		X			X			X			X					
30		X	X		X			X				X			X				
31		X	X			X		X			X			X					
32		X	X			X		X				X			X				

the number of molecules adsorbed on the sample at the isotherm temperature and the final equilibrium pressure. The amount of gas adsorbed at the final equilibrium pressure thus represents one point on the adsorption isotherm. The stopcock connecting the sample tube to the gas manifold was then closed again, fresh gas admitted to the manifold, and the process repeated. A new higher equilibrium pressure was obtained with a corresponding larger quantity of gas adsorbed. This process was repeated up to an equilibrium pressure of 200 torr (mm Hg).

3.1.4 Chemisorption Isotherm Studies with Hydrogen

Hydrogen chemisorption experiments with Shell 405 ABSG catalyst and Engelhard MFSA catalysts are described below. The studies included "as received" catalysts and catalysts which were pretreated in order to remove all initial surface oxides and preadsorbed gases. The pretreated catalysts are called "clean" catalysts.

3.1.4.1 Hydrogen Chemisorption Isotherm Studies with Shell 405 ABSG* Catalyst

The hydrogen chemisorption isotherm results are given in Table 2. The adsorption temperature of 200°C (472°K) and equilibrium pressure of 200 torr were selected from previous studies as the best conditions for determining catalyst changes. Typical adsorption isotherms are shown in Figure 2.

The first column of Table 2 shows the pretreatment conditions to which the Shell catalyst was exposed prior to the hydrogen chemisorption isotherm measurements. The standard pretreatment was to evacuate the catalyst sample for 16 hours at 200°C (473°K) and then expose the sample to 200 torr hydrogen gas for 7 hours followed by an additional 16 hours of evacuation at 600°C (873°K). Based on previous experimental studies, this pretreatment procedure removed the very strongly chemisorbed oxygen (from air exposure of the "as received" catalyst).

The second column in Table 2 shows the various soak conditions to which the "clean" catalyst was exposed prior to equilibrium hydrogen chemisorption measurements. The soak conditions were: exposure of the catalyst to 10^{-6} torr vacuum at 816°C (1089°K) for time periods of 1, 5, and 50 hours; to helium (1 atm) at 816°C (1089°K) for 50 hours; and to hydrogen (1 atm) at 816°C (1089°K) and at -78°C (195°K) for 5 hours.

*The Shell 405 ABSG catalyst used, Lot 5-Lem-402, was equivalent to Lot 4-Jem-402 except that the alumina support was rounded by water attrition. The final pellet size, 14-18 mesh, is identical to Lot 4-Jem-402.

TABLE 2

SUMMARY OF HYDROGEN CHEMISORPTION ISOTHERM EXPERIMENTS AT 473°K ON SHELL 405-ABSG CATALYST

Pretreatment Conditions	Soak Conditions	Equilibrium Hydrogen Adsorption* at 473°K and 200 torr Hydrogen Atoms x 10^{-18}
"As Received" Catalyst Outgassed in 10^{-6} torr for 16 hours	None	765 ± 61**
Standard***	None	336 ± 26**
Standard***	1 hour at 1089°K in 10^{-6} torr vacuum	288 ± 60****
Standard***	5 hours at 1089°K in 10^{-6} torr vacuum	298 ± 20****
Standard***	50 hours at 1089°K in 10^{-6} torr vacuum	198 ± 16**
Standard***	50 hours at 1089°K in 1 atm helium	234 ± 18**
Standard***	5 hours at 1089°K in 1 atm hydrogen	148 ± 12**
Standard***	5 hours at 195°K in 1 atm hydrogen	188 ± 15**

NOTES

*For comparison purposes, it should be noted that 1 gram of Shell 405 contains ~1000 x 10^{18} iridium atoms. If all atoms of iridium in the catalyst were surface atoms (iridium distributed in a monomolecular layer on the support), the catalyst would adsorb at 473°K (after standard pretreatment) ~1000 x 10^{18} atoms of hydrogen.

**Based on previous replicate experiments, the uncertainty was taken as ± 8% of the measured value.

***The standard pretreatment to remove very strongly adsorbed oxygen (from air exposure of the catalyst) consists of 16 hours evacuation at 473°K followed by exposure to 200 torr hydrogen at 773°K for seven hours followed by 16 hours evacuation at 873°K in 10^{-6} torr vacuum.

****Duplicate experiments were run for each of these cases and the listed uncertainty represents the span between the experiments.

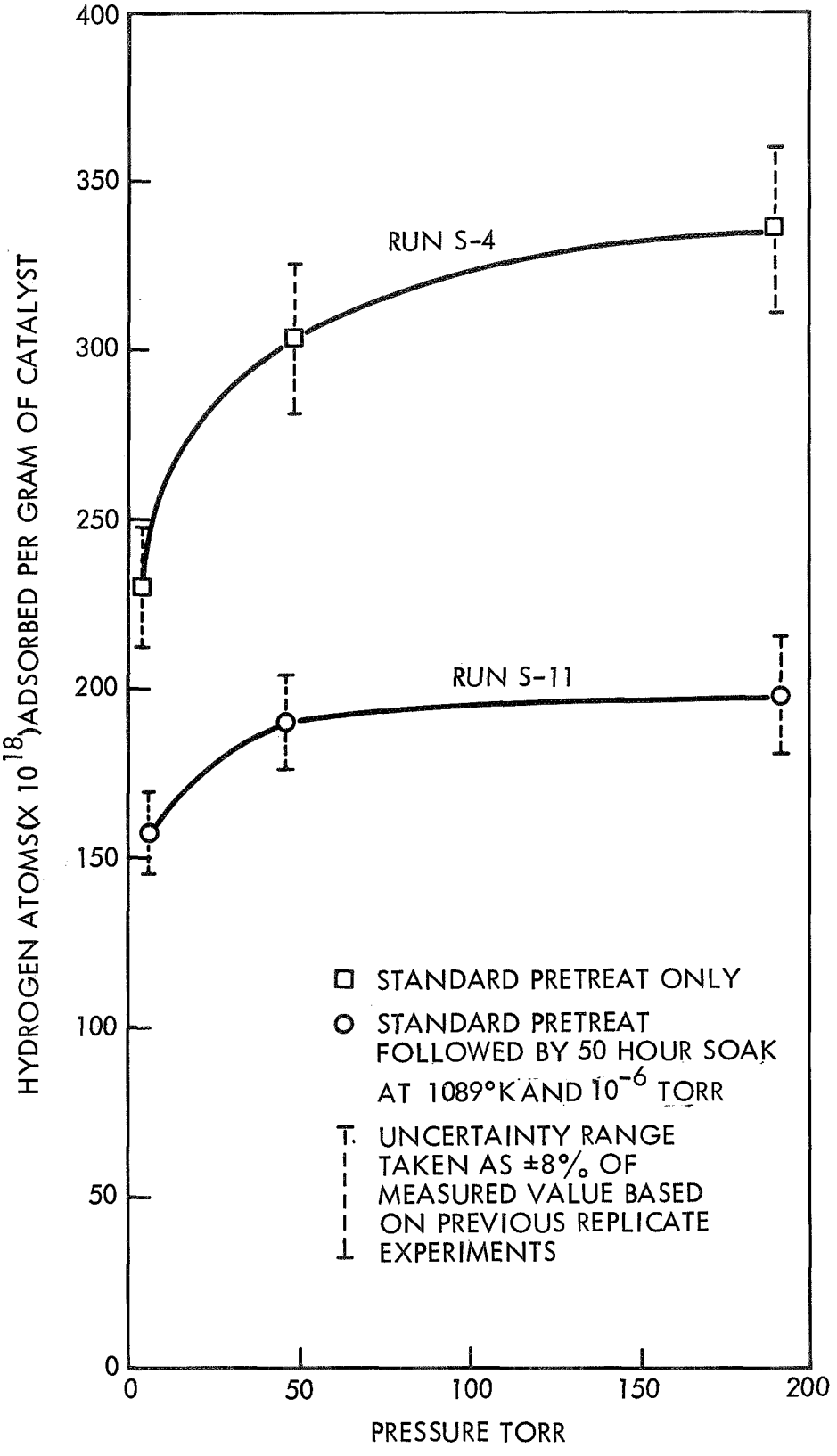

Figure 2. Typical Hydrogen Chemisorption Isotherms on Shell 405 ABSG Catalyst

The third column of Table 2 shows the number of hydrogen atoms chemisorbed at 200°C (473°K) and 200 torr pressure. Previous experiments with the Shell 405 ABSG catalyst showed that adsorption at 200°C (473°K) and 200 torr essentially saturates the surface. This is seen from the typical adsorption isotherms shown in Figure 2.

The results show that soaking at 816°C (1089°K) in hydrogen for 1 to 5 hours decreased the capacity of the catalyst to adsorb hydrogen at 200°C (473°K) by a factor of 2. This is very likely a sintering effect rather than the result of residually adsorbed hydrogen since at 816°C (1089°K) previous temperature scanning experiments showed that very little, if any, hydrogen would remain adsorbed. It is further seen that the effect of soaking in helium for 50 hours at 816°C (1089°K) was less than a soak in 10^{-6} torr vacuum for 50 hours at 816°C (1089°K).

These experiments showed that the two soaking conditions, 1 atm of hydrogen at 816°C (1089°K) for 5 hours and at 10^{-6} torr vacuum at 816°C (1089°K) for 50 hours, had the greatest effect on the catalyst. These two conditions were also kinetically evaluated in the differential pulse flow reactor to determine their actual effect on the catalyst reaction rate at low temperatures.

3.1.4.2 Hydrogen Chemisorption Studies with Engelhard MFSA Catalysts

Experiments to determine the best pretreating conditions for removal of the oxides and residual gases from the Engelhard MFSA catalysts are shown in Table 3. Column 1 shows the pretreating conditions, column 2 the adsorption gas, and column 3 the number of atoms adsorbed at equilibrium. The results showed that the pretreating conditions used with Shell 405 ABSG catalysts were also applicable to the Engelhard catalysts. Therefore, the standard method for preparing these catalysts for the adsorption and soaking experiments was to outgas the catalyst at 200°C (473°K) for 16 hours at 10^{-6} torr, then to expose the catalyst to 200 torr hydrogen at 500°C (773°K) for 7 hours, and to evacuate the catalyst at 600°C (873°K) in 10^{-6} torr vacuum for 16 hours.

The hydrogen chemisorption experiments for Engelhard MFSA 1/8-inch catalyst are summarized in Table 4. Column 1 describes the pretreating conditions, column 2 describes the soaking conditions, and column 3 shows the number of hydrogen atoms adsorbed per gram of catalyst at 200°C (473°K) and 200 torr pressure.

These experiments revealed that the active surface of the Engelhard MFSA catalyst was not affected by high temperature vacuum soaks. However, exposure to helium at 816°C (1089°K) for 50 hours decreased the active surface by about 75 percent. These results can be seen in Table 4.

Comparative measurements were also made with the 1/16-inch Engelhard MFSA catalyst and are given in Table 5, which also includes adsorption of oxygen. Column 1 describes the soak conditions, column 2

Table 3. Effect of Pretreatment on Chemisorption by Engelhard MFSA 1/8" (0.318 cm) Catalyst at 473°K

Pretreatment	Adsorbing Gas	Equilibrium Chemisorption at 473°K and 200 torr Atoms X 10^{-18}
"As received catalyst" outgassed at 473°K for 16 hours at 10^{-6} torr vacuum	oxygen	1.1 ± 1
Standard*	oxygen	15.6 ± 2
Outgassed at 473°K for 16 hours, followed by exposure to 200 torr hydrogen at 573°K for 7 hours, followed by 16 hours at 673°K in 10^{-6} torr vacuum	oxygen	15.9 ± 2
"As received catalyst" outgassed at 473°K for 16 hours at 10^{-6} torr vacuum	hydrogen	29.0 ± 2
Standard*	hydrogen	10.4 ± 1
Outgassed at 473°K for 16 hours, followed by exposure to 200 torr hydrogen at 573°K for 7 hours, followed by 16 hours at 673°K in 10^{-6} torr vacuum	hydrogen	8.2 ± 1

*Outgassed at 473°K for 16 hours at 10^{-6} torr, followed by exposure to 200 torr hydrogen at 773°K for 7 hours, then evacuated 16 hours at 873°K in 10^{-6} torr vacuum.

Table 4. Summary of Hydrogen Chemisorption Isotherm Experiments at 473°K on 1/8" (0.318 cm) Engelhard MFSA Catalyst

Pretreatment Conditions	Soak Conditions	Equilibrium Chemisorption at 473°K and 200 Torr Atoms x 10^{-18}/gm
"As Received" Catalyst outgassed in 10^{-6} torr vacuum for 16 hours	None	29.9 ± 2.0
Standard*	None	10.4 ± 2.0
Standard*	1 Hour @ 1089°K in 10^{-6} Torr Vacuum	9.94 ± 2.0
Standard*	5 Hours @ 1089°K in 10^{-6} Torr Vacuum	13.68 ± 2.7
Standard*	50 Hours @ 1089°K in 10^{-6} Torr Vacuum	13.40 ± 2.6
Standard*	50 Hours @ 1089°K in 1 atm of Helium	3.13 ± 0.6
Standard*	5 Hours @ 1089°K in 1 atm of Hydrogen	7.92 ± 1.6
Standard*	5 Hours @ 195°K in 1 atm Hydrogen	9.67 ± 1.9

*The standard pretreatment to remove strongly absorbed oxygen (from air exposure of the catalyst) consists of 16 hour evacuation at 473°K, followed by exposure to 200 torr hydrogen at 773°K for seven hours, followed by 16 hours evacuation at 873°K in 10^{-6} torr vacuum.

**Based on previous replicate experiments; the uncertainty was taken as ±8% of the measured value.

***Based on triplicate experiments, the uncertainty represents the span between each experiment.

Table 5. Summary of Comparative Chemisorption Isotherm Experiments at 473°K on 1/8" (0.318 cm) and 1/16" (0.159 cm) "Clean" Engelhard MFSA Catalysts*

Soak Conditions	Adsorbing Gas	Equilibrium Chemisorption at 473°K and 200 Torr Atoms x 10^{-18}/gm	
		Engelhard 1/8" (.318 cm) MFSA	Engelhard 1/16" (.159 cm) MFSA
None	Hydrogen	10.4 ± 2.0	38.0 ± 4.0
50 Hours at 1089°K in 1 atm of helium	Hydrogen	3.13 ± 0.6	12.0 ± 2.0
5 Hours at 1089°K in 1 atm of hydrogen	Hydrogen	7.92 ± 1.6	10.1 ± 2.6
None	Oxygen	15.9 ± 3	23.7 ± 4

*All catalyst samples were pretreated by the standard pretreatment to remove very strongly adsorbed oxygen (from air exposure of the catalyst). This consists of 16-hour evacuation at 473°K, followed by exposure to 200 torr hydrogen at 773°K for seven hours, followed by 16 hours evacuation at 873°K in 10^{-6} torr vacuum.

the adsorbing gas, and columns 3 and 4 the chemisorption values [the number of atoms of hydrogen or oxygen adsorbed per gram of catalyst at 200°C (473°K) and 200 torr pressure]. When both catalysts were pretreated, followed by chemisorption of oxygen, the amount of oxygen adsorbed by the 1/16-inch catalyst was greater than that of the 1/8-inch catalyst. This fact, plus the fact that the amount of hydrogen adsorbed by the 1/16-inch catalyst was greater than that of the 1/8-inch catalyst, indicated that the metal content of the 1/16-inch catalyst was higher than the 1/8-inch catalyst even though the two catalysts were supposed to have identical metal contents. These experiments also indicated a reduction of active surface by about 70 percent when the samples were exposed to helium at 816°C (1089°K) for 50 hours.

Table 6 shows the number of atoms of metal per gram of catalyst found by three independent spectrographic analyses of the 1/8- and 1/16-inch catalysts. The average deviation of these analyses is high because the small amount of metal present on these catalysts is close to the minimum amount detected by this type of analysis. The data show that the 1/16-inch catalyst has approximately 1.6 times more metal than the 1/8-inch catalyst.*

*Engelhard has confirmed these findings based on their own laboratory analysis of catalyst samples from the same lots.

Table 6. Summary of Spectographic Analysis of Metal Content of Engelhard Catalysts

Metal	Atoms x 10^{-18} Per Gram	
	Engelhard MFSA 1/8" (.318 cm)	Engelhard MFSA 1/16" (.159 cm)
Platinum	7.72 ± 0.96	12.30 ± 1.84
Rhodium	4.73 ± 0.59	7.68 ± 2.30
Lead	Less than 0.87	Less than 1.45

3.1.5 Chemisorption Isotherm Studies with Oxygen

The following paragraphs describe the oxygen chemisorption studies with Shell 405 ABSG catalysts and Engelhard MFSA catalysts. The adsorption studies were performed with "as received" and "clean" catalysts subjected to soaking in specific environments.

3.1.5.1 Oxygen Chemisorption Studies with Shell 405 ABSG Catalyst

The oxygen chemisorption studies with Shell 405 ABSG catalyst are summarized in Table 7. Columns 1 and 2 give the pretreating and soaking conditions, respectively, and column 3 gives the number of oxygen atoms adsorbed per gram of catalyst at 200°C (473°K) and 200 torr oxygen.

Based on the fact that the total number of iridium atoms per gram of catalyst is 1000 x 10^{18} atoms, and the "as received" catalyst has a surface composition of about $IrO_{0.3}$ at ambient temperature, it is seen that catalyst surface oxygen composition increases to $IrO_{0.6}$ at 200°C (473°K) and 200 torr oxygen pressure. At -78°C (195°K), a "clean" catalyst exposed to air at 1 atm takes on a surface composition of about $IrO_{0.2}$ (600 x 10^{18} atoms of oxygen/per gram less 400 x 10^{18} atoms of oxygen/gram after soaking at -78°C). The oxygen uptake on the catalyst

Table 7. Summary of Oxygen Chemisorption Isotherm Experiments at 473°K on Shell 405 ABSG Catalyst*

Pretreatment Conditions	Soak Conditions	Equilibrium Chemisorption at 200°C and 200 torr atoms x 10^{-18}/gram
Outgassed 16 hours at 10^{-6} torr	None	321 ± 25
Standard*	None	600 ± 48
Standard*	5 hours at 1089°K 1 atm of air	22 ± 2
Standard*	5 hours at 195°K 1 atm of air	400 ± 32 (additional oxygen atoms added to the surface)

*Standard pretreatment consists of 16 hours evacuation at 473°K, followed by exposure to 200 torr hydrogen at 773°K for seven hours, followed by 16 hours evacuation at 873°K in 10^{-6} torr vacuum.

exposed to 1 atm of air for 5 hours at 816°C (1089°K) corresponds to the surface coverage of about $IrO_{1.5}$, a stable oxide form (based on previous research). The oxygen adsorbed after soaking in air for 5 hours at 816°C (1089°K) when the catalyst is subject to 200°C (473°K) and 200 torr oxygen, is probably the amount physically adsorbed on the oxide surface.

3.1.5.2 Oxygen Chemisorption Studies with Engelhard MFSA Catalysts

The oxygen chemisorption experiments with Engelhard MFSA catalysts are summarized in Tables 8 and 9. The equilibrium values of the amount of oxygen atoms adsorbed per gram of 1/8-inch catalyst are given in Table 8 and a comparison of the equilibrium values for the 1/8-inch catalyst and the 1/16-inch catalyst are given in Table 9.

3.1.6 Alternate Chemisorption of Hydrogen and Oxygen on Engelhard MFSA 1/8-inch Catalyst at -78°C

A series of alternate hydrogen and oxygen chemisorptions on samples of Engelhard MFSA 1/8-inch catalyst at -78°C (195°K) was performed to determine if the water molecules formed on the active surface sites of the catalyst remained at the site or moved off the site to permit further reaction between oxygen and hydrogen. Duplicate experiments were performed; the catalysts were pretreated in the standard way, and then hydrogen was chemisorbed on the surface at -78°C (195°K) and 200 torr until equilibrium was established, followed by expansion of the resident gas phase in the system down to a pressure of 1 micron. Oxygen was then adsorbed at 200 torr and -78°C until equilibrium was established, followed by expansion. This process was repeated several times, as shown in Table 10.

Column 1 of Table 10 shows the sequence of adsorption-desorption experiments. Columns 2 and 4 show the amount of hydrogen adsorbed on the catalyst, and columns 3 and 5 show the amount of oxygen adsorbed on the catalyst.

The total number of hydrogen and oxygen atoms adsorbed is also shown. Table 10 shows that the number of oxygen atoms adsorbed on the surface covered with preadsorbed hydrogen was approximately three times the number of hydrogen atoms adsorbed. This could be accounted for by the initial reaction of 2 atoms of hydrogen and 1 atom of oxygen to form 1 molecule of water, which moves off the active catalyst site followed by the formation of multiple metal oxide and some physical adsorption of oxygen.

The experiments indicate that the formation of water is not necessarily accompanied by permanent retention of the H_2O molecule on the active site, but that water may move off the catalyst site to free it for further reaction. The differences shown by the adsorption of oxygen and hydrogen within parallel experiments indicate the complexity of the reaction on the catalyst.

Table 8. Summary of Oxygen Chemisorption Isotherm Experiments at 473°K on Engelhard MFSA 1/8" (0.318 cm) Catalyst

Pretreatment	Soak Conditions	Equilibrium Chemisorption at 473°K and 200 Torr Atoms x 10^{-18}/gram
"As received" catalyst outgassed at 473°K for 16 hours at 10^{-6} torr vacuum	None	1.1 ± 1
Standard*	None	15.6 ± 2
Outgassed at 473°K for 16 hours, followed by exposure to 200 torr hydrogen at 573°K for 7 hours, followed by 16 hours at 673°K in 10^{-6} torr vacuum	None	15.9 ± 2
Standard*	5 hours @ 1089°K in 1 atm of air	0.0
Standard	5 hours @ 195°K in 1 atm of air	5.86 ± 1.2

*This consists of 16-hour evacuation at 473°K, followed by exposure to 200 torr hydrogen at 773°K for seven hours, followed by 16 hours evacuation at 873°K in 10^{-6} torr vacuum.

Table 9. Summary of Comparative Oxygen Chemisorption Isotherm Experiments at 473°K on 1/8" (0.318 cm) and 1/16" (0.159 cm) "Clean" Engelhard MFSA Catalyst*

Soak Conditions	Equilibrium Chemisorption at 473°K and 200 torr oxygen atoms x 10^{-18}/gram	
	Engelhard 1/8" (.318 cm) MFSA	Engelhard 1/16" (.159 cm) MFSA
None	15.9 ± 3	23.7 ± 4
5 hours at 1089°K in 1 atmosphere of air	0.0	0.0
5 hours at 195°K in 1 atmosphere of air	5.86 ± 1.2	22.0 ± 4

*All catalyst samples were pretreated by the standard pretreatment to remove very strongly absorbed oxygen (from air exposure of the catalyst). This consists of 16-hour evacuation at 473°K, followed by exposure to 200 torr hydrogen at 773°K for seven hours, followed by 16 hours evacuation at 873°K in 10^{-6} torr vacuum.

Table 10. Repeated Alternated Chemisorption of Hydrogen and Oxygen on Engelhard MFSA 1/8" (0.318 cm) Catalyst at 200 torr and 195°K

Adsorption Sequence	SAMPLE 1		SAMPLE 2	
	Hydrogen Atoms x 10^{-18}/gm Adsorbed	Oxygen Atoms x 10^{-18}/gm Adsorbed	Hydrogen Atoms x 10^{-18}/gm Adsorbed	Oxygen Atoms x 10^{-18}/gm Adsorbed
1	11.3 ± 2		10.4 ± 2	
2		35.4 ± 7		27.1 ± 5
3	14.7 ± 3		14.0 ± 3	
4		31.4 ± 6		21.2 ± 4
5	16.9 ± 3		14.5 ± 3	
6	5.5 ± 1		7.2 ± 2	
7		30.1 ± 6		21.7 ± 4
8		18.3 ± 4		17.5 ± 4
9		14.8 ± 2		19.3 ± 4
TOTAL	48.4 ± 1.5	130.0 ± 3	46.2 ± 1.5	106.8 ± 3

3.1.7 Chemisorption Rate Measurements

The following paragraphs describe chemisorption rate measurements made with hydrogen and oxygen on both the Shell 405 ABSG and Engelhard 1/8-inch MFSA catalyst.

In conducting a chemisorption rate experiment, the procedure followed was to take a known weight of pretreated catalyst sample and allow it to thermally equilibrate at the selected temperature. The gas was then admitted to the sample and the pressure change recorded as a function of time. When pressure decreased to about 10 percent below the preselected nominal experimental pressure, an additional amount of gas was rapidly admitted to the sample and the pressure was again recorded as a function of time. This sequence was repeated until the rate of pressure change with time was very small.

3.1.7.1 Hydrogen and Oxygen Chemisorption Rate Measurements with Shell 405 ABSG Catalyst

Experiments to study the rate of chemisorption of hydrogen and oxygen on the Shell 405 ABSG catalyst were done at -78°C (195°K). Adsorption versus time measurements were made at a total pressure of 1 torr under the following set of conditions:

- Hydrogen chemisorption on a "clean" (standard pretreatment) sample of Shell 405 ABSG catalyst
- Hydrogen chemisorption on a sample of Shell 405 ABSG catalyst upon which oxygen had been preadsorbed at 200°C (473°K)
- Oxygen chemisorption on a "clean" (standard pretreatment) sample of Shell 405 ABSG catalyst
- Oxygen chemisorption on a sample of Shell 405 ABSG catalyst upon which hydrogen had been preadsorbed at 200°C (473°K)

Figures 3 and 4 present the results of these experiments in terms of the number of atoms of gas adsorbed as a function of time. From these figures it is apparent that at -78°C (195°K) hydrogen adsorbs much more slowly on Shell 405 catalyst when it has preadsorbed oxygen. However, when the Shell 405 catalyst has preadsorbed hydrogen, the rate of oxygen adsorption is much greater than on a "clean" shell catalyst.

3.1.7.2 Hydrogen and Oxygen Chemisorption Rate Measurements with Engelhard MFSA 1/8-inch Catalyst

Experiments to study the rate of chemisorption of hydrogen and oxygen on the Engelhard MFSA catalysts (1/8-inch) were performed at -78°C (195°K). Adsorption versus time measurements were made at a

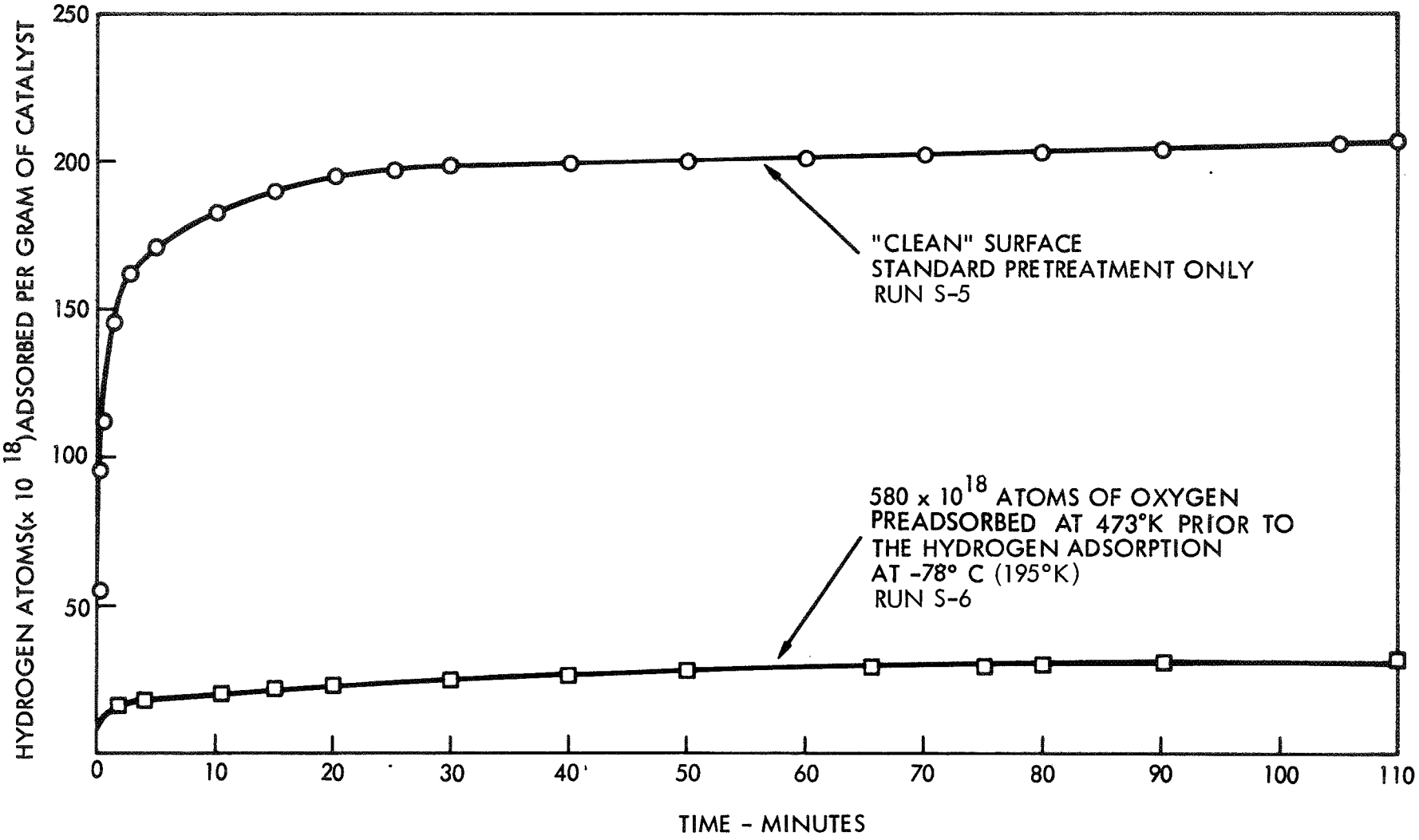

Figure 3. Hydrogen Chemisorption on Shell ABSG Catalyst as a Function of Time
Hydrogen Pressure 1 Torr, Temperature -78°C (195°K)

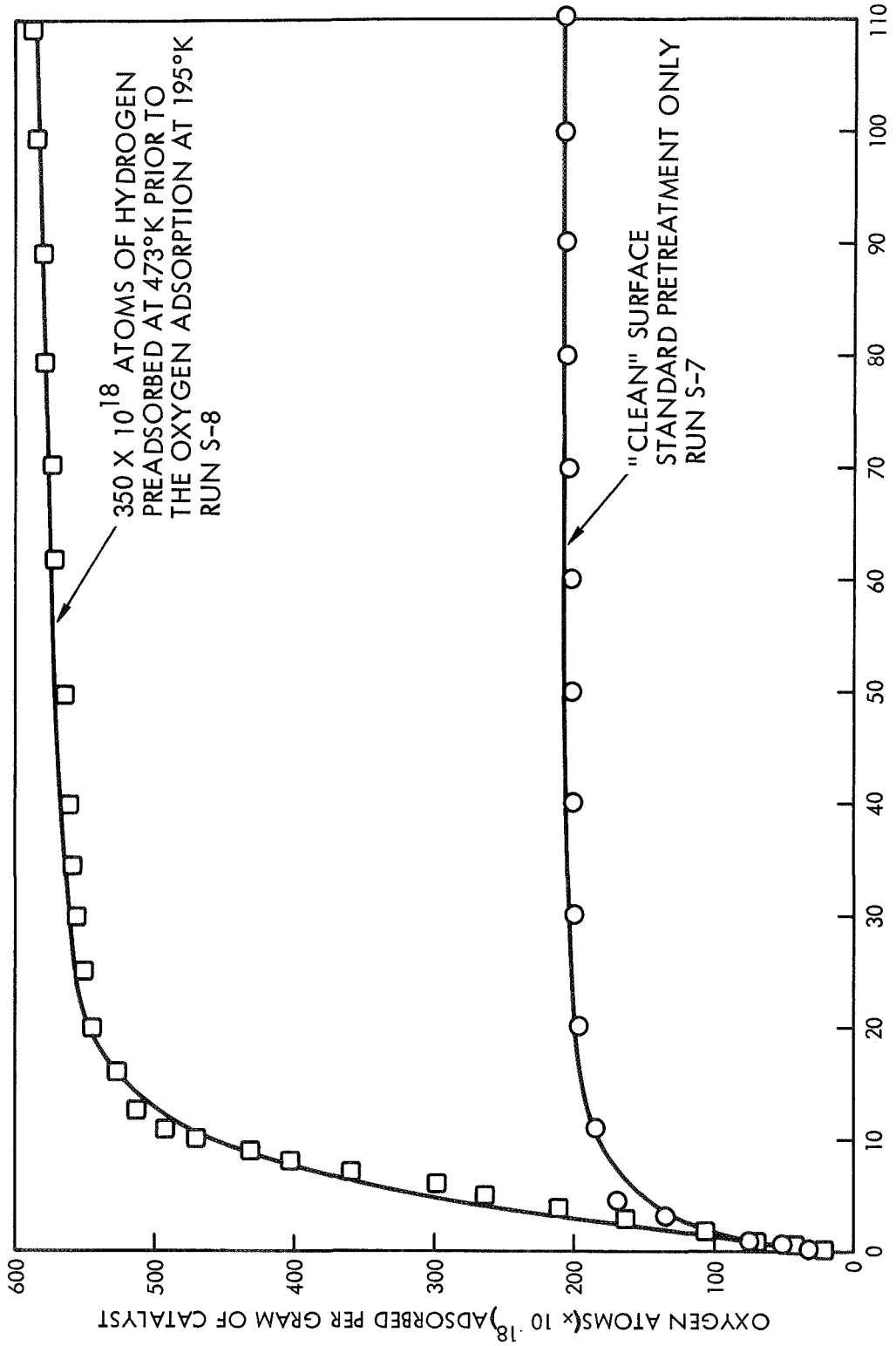

Figure 4. Oxygen Chemisorption on Shell 405 ABSG Catalyst as a Function of Time
Oxygen Pressure 1 Torr, Temperature -78°C (195°K)

total pressure of 1 torr under the following set of conditions:

- Hydrogen chemisorption on a "clean" (standard pretreatment) sample of Engelhard MFSA 1/8-inch catalyst
- Hydrogen chemisorption on a sample of the Engelhard MFSA 1/8-inch catalyst upon which oxygen had been preadsorbed at 200°C (473°K)
- Oxygen chemisorption on a "clean" (standard pretreatment) sample of Engelhard MFSA 1/8-inch catalyst
- Oxygen chemisorption on a sample of the Engelhard MFSA 1/8-inch catalyst upon which hydrogen had been preadsorbed at 200°C (473°K)

Figures 5 and 6 present the results of these experiments in terms of the number of atoms of gas adsorbed per gram of catalyst as a function of time. From these figures, it is apparent that at -78°C (195°K), the rate of adsorption of hydrogen gas takes place more slowly on the Engelhard MFSA catalyst which is saturated with preadsorbed oxygen. Much more oxygen will chemisorb on a sample of the Engelhard MFSA catalyst which is saturated with preadsorbed hydrogen than on an equivalent sample of "clean" Engelhard MFSA catalyst.

From these results, it would appear quite likely that oxygen preadsorbed on the surface of the Engelhard MFSA catalyst would decrease the ability of the catalyst to ignite a hydrogen-oxygen mixture at cryogenic temperatures.

3.2 KINETIC STUDIES WITH THE PULSE FLOW ISOTHERMAL DIFFERENTIAL REACTOR

An isothermal, pulse-flow, differential reactor was utilized to evaluate the relative capacities of Shell 405 catalyst and Engelhard MFSA catalyst to promote cryogenic hydrogen-oxygen reaction. Semiquantitative reaction kinetics studies were also performed under a variety of testing conditions. The following paragraphs present discussions of the design and operation of the pulse flow differential reactor, the method of obtaining experimental data, and the results of the experimentation.

3.2.1 Description of Reactor and Pretreatment Systems

The isothermal differential reactor and the catalyst pretreating and soaking system are schematically shown in Figures 7 and 8, respectively. Photographs of these systems are presented in Figures 9 through 12.

The differential reactor system is a pulsed flow type using a Carle sampling valve to introduce a reproducible plug of reactant ($H_2 + O_2$) gas into a helium stream that continuously passes over the catalyst (or over

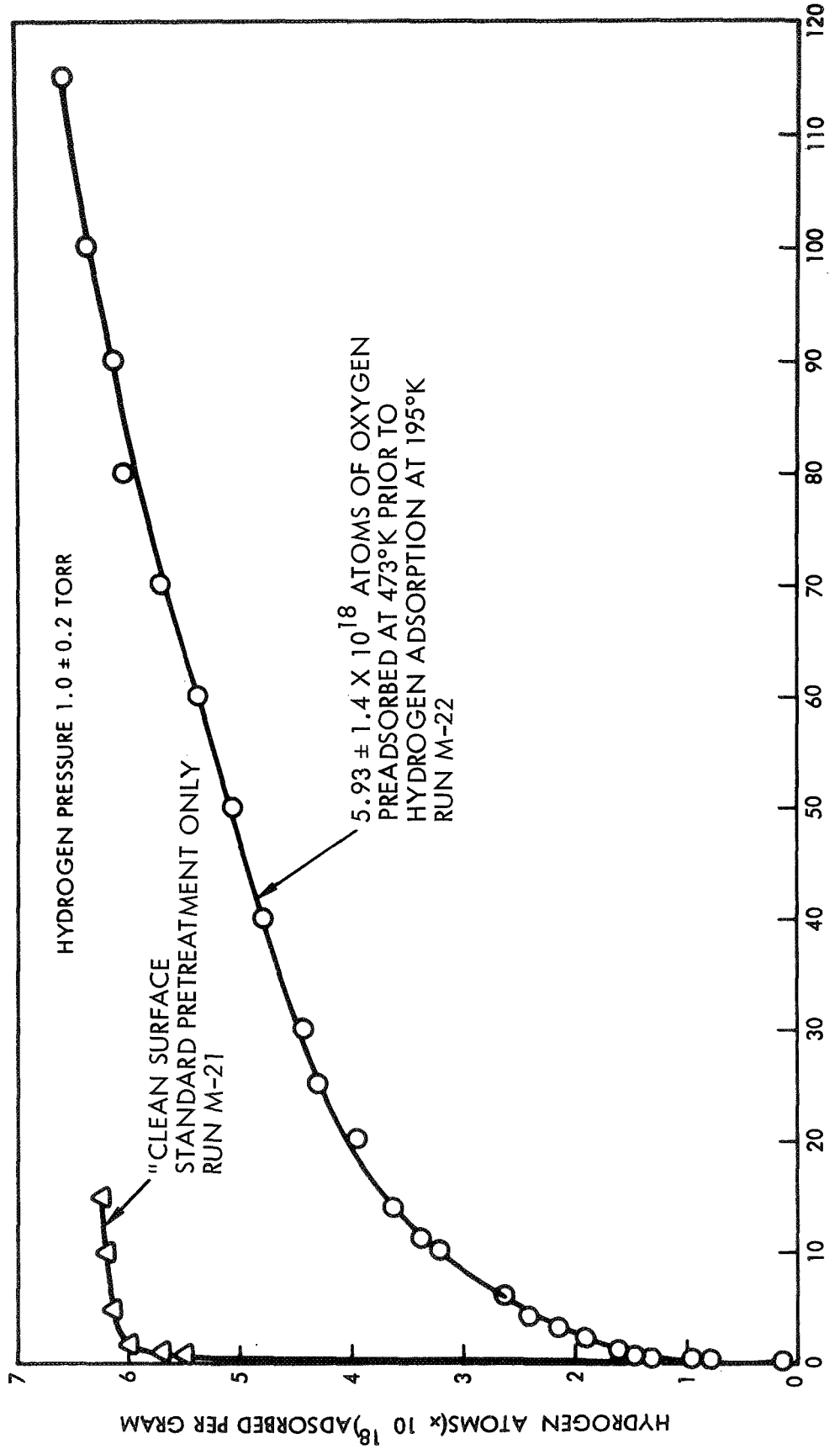

Figure 5. Hydrogen Adsorption at -78°C (195°K) on 1/8" (.318 cm) Engelhard MFSA Catalyst

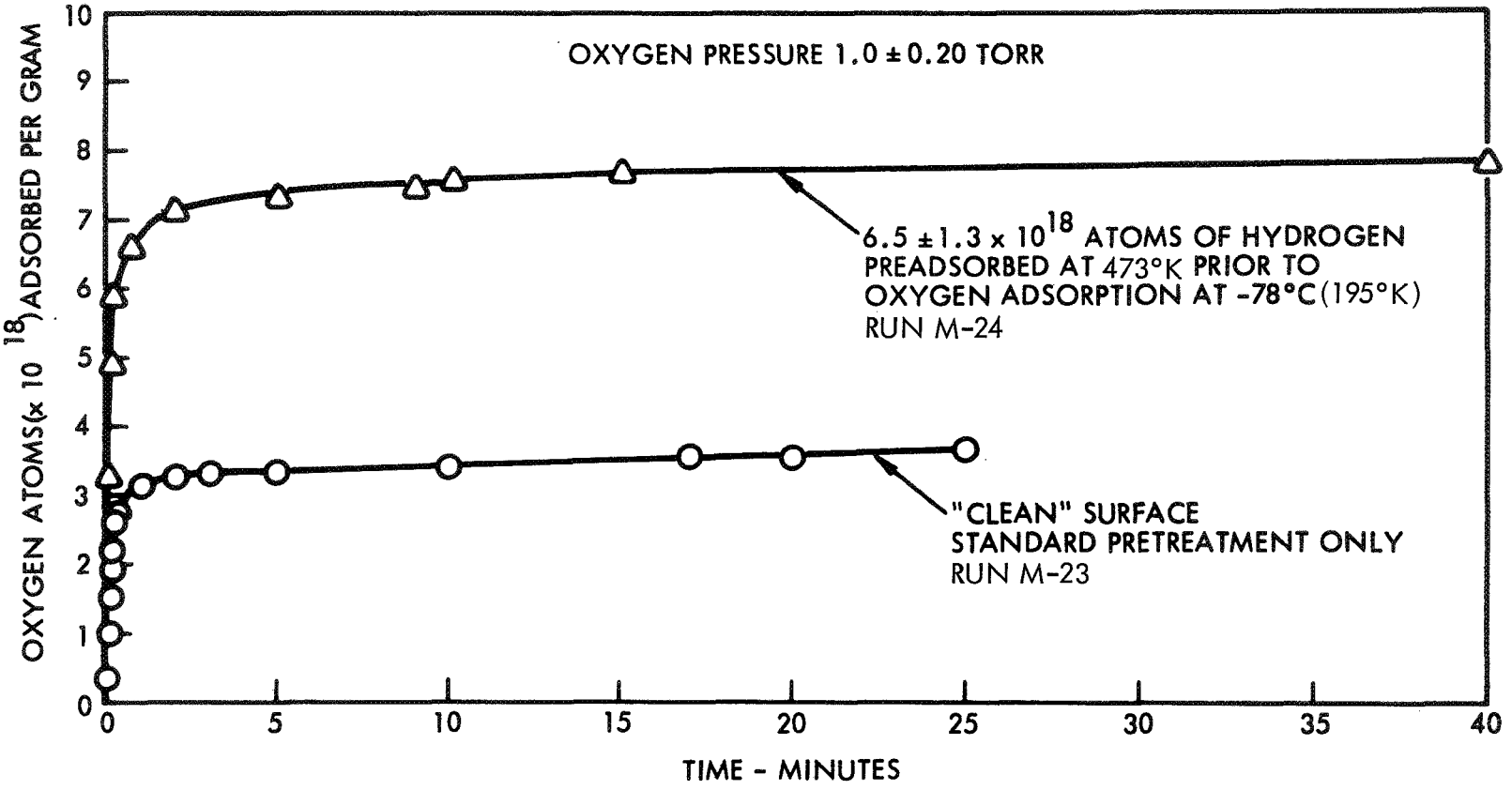

Figure 6. Oxygen Adsorption at -78°C (195°K) on 1/8" (.318 cm) Engelhard MFSA Catalyst

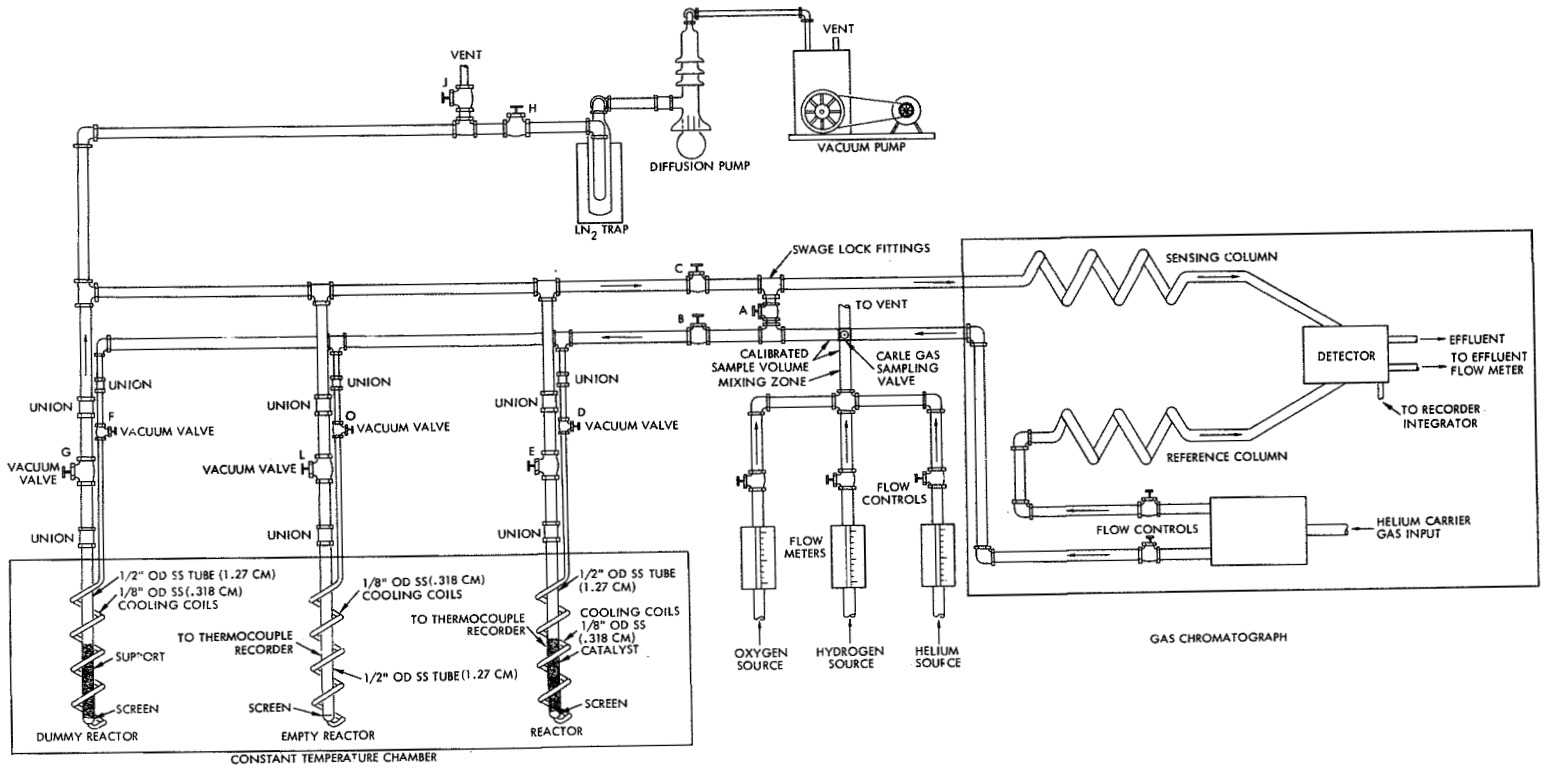

Figure 7. Layout of the Isothermal Differential Reactor

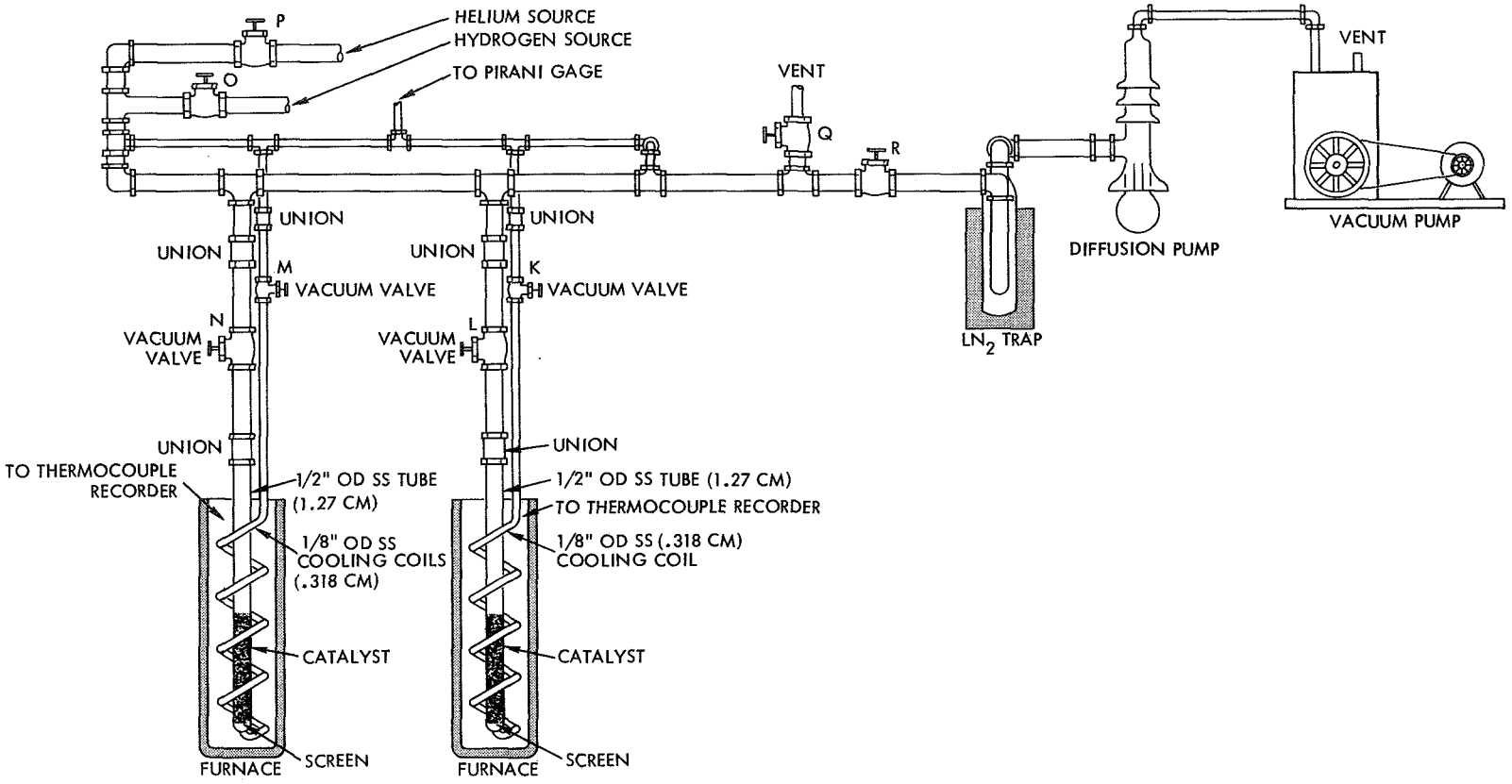

Figure 8. Layout of the Catalyst Pretreating and Soaking System

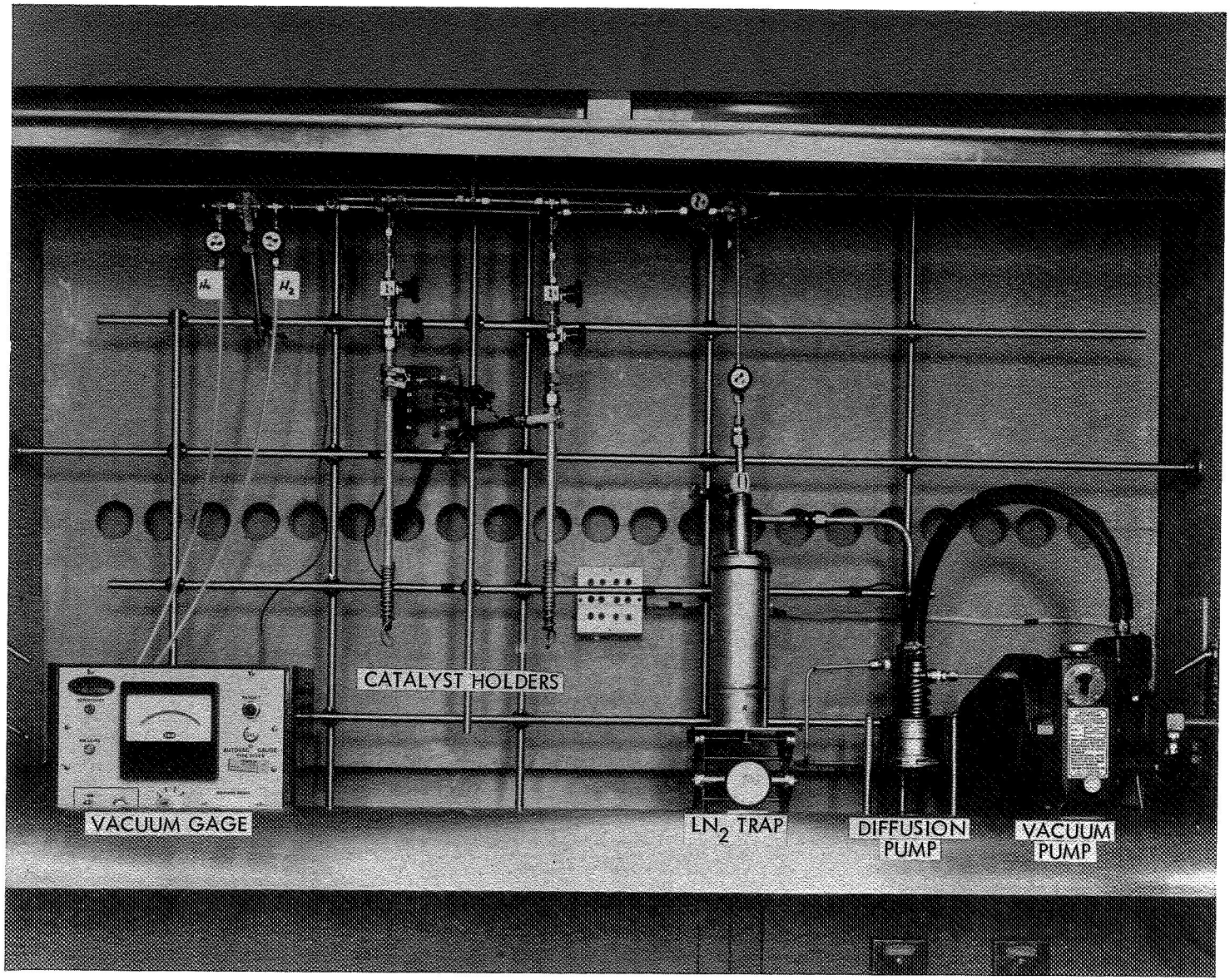

Figure 9. Front View of the Pretreating and Soaking System

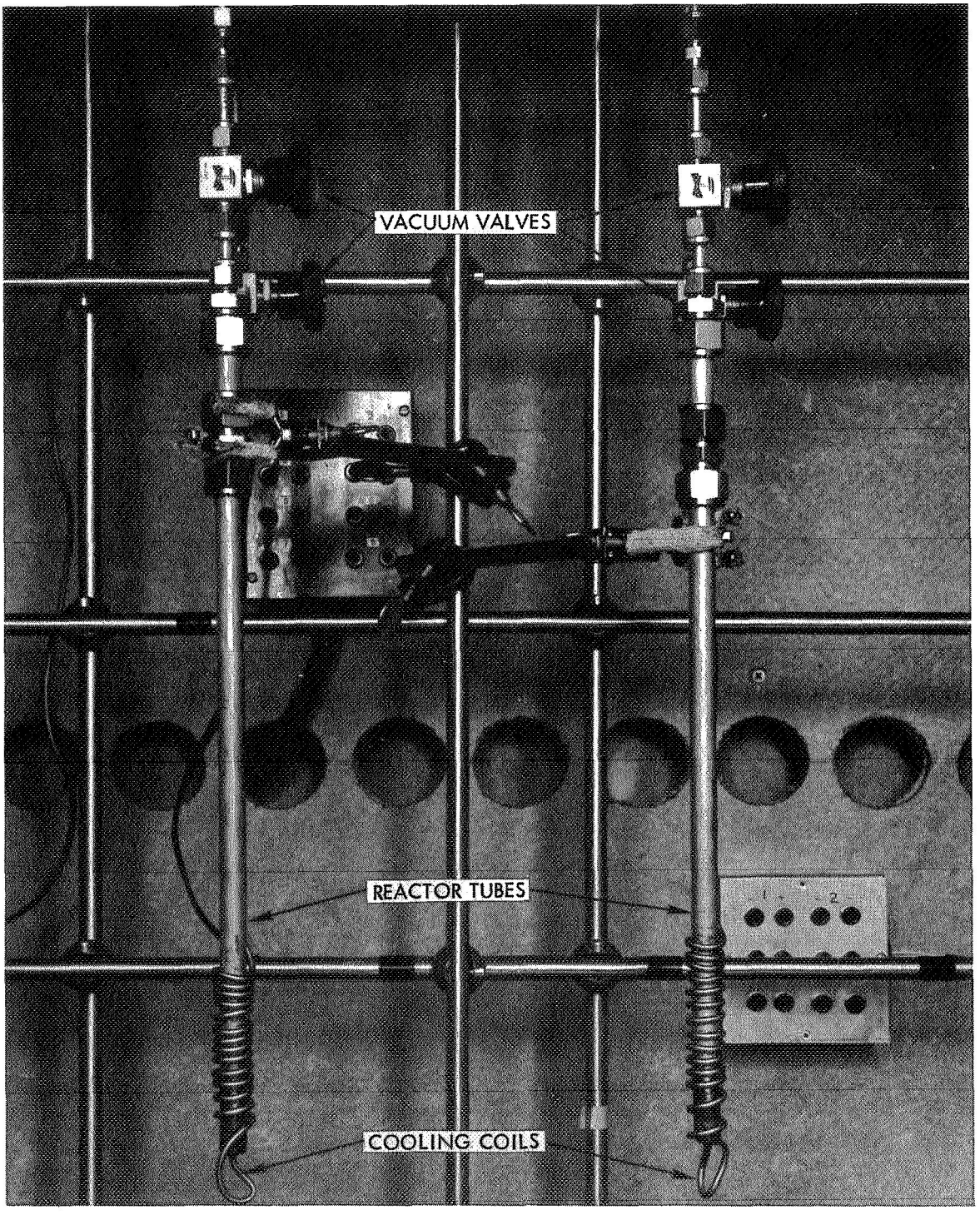

Figure 10. Close-Up View of the Catalyst Reactor Tubes

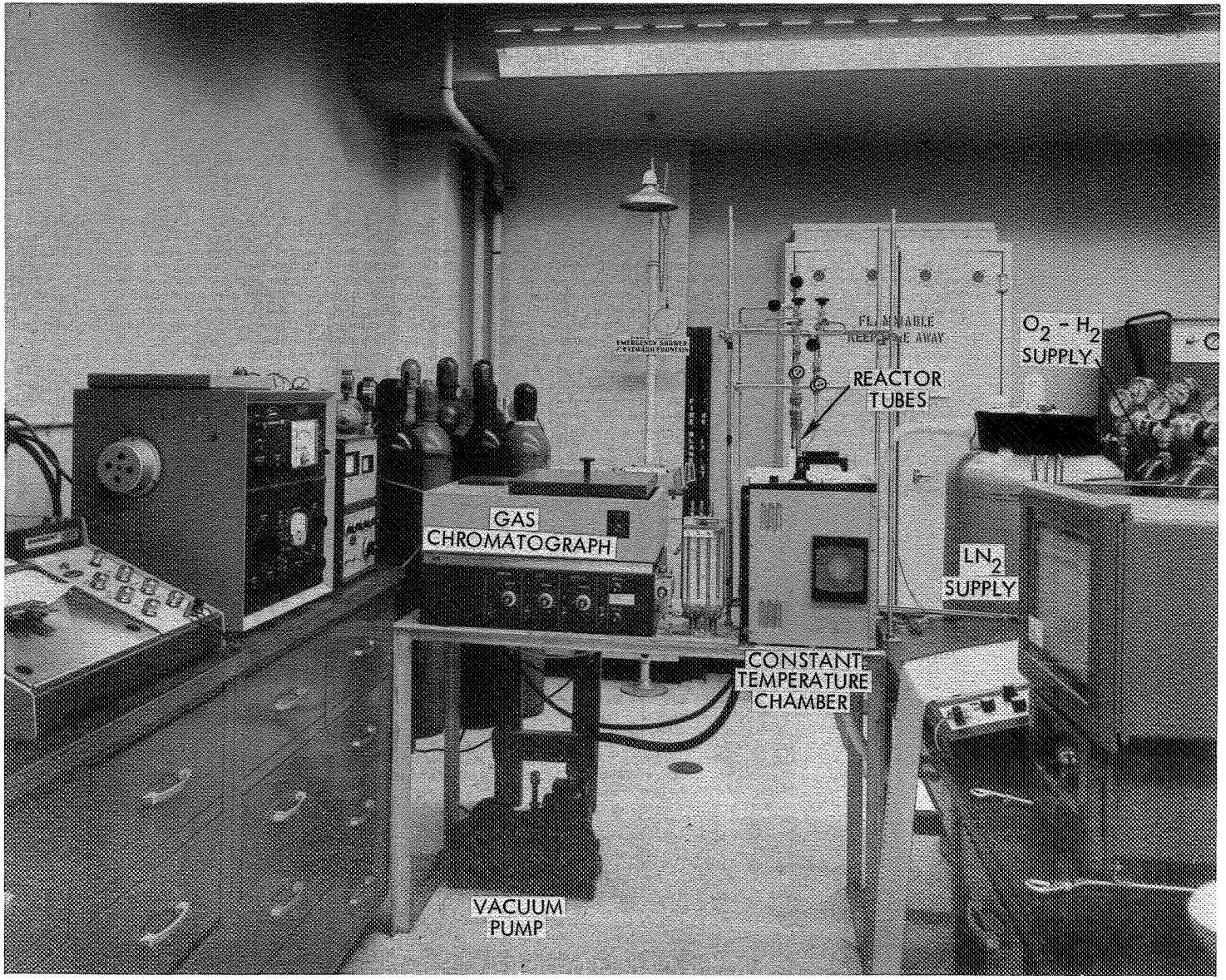

Figure 11. Wide Angle View of the Isothermal Differential Reactor System

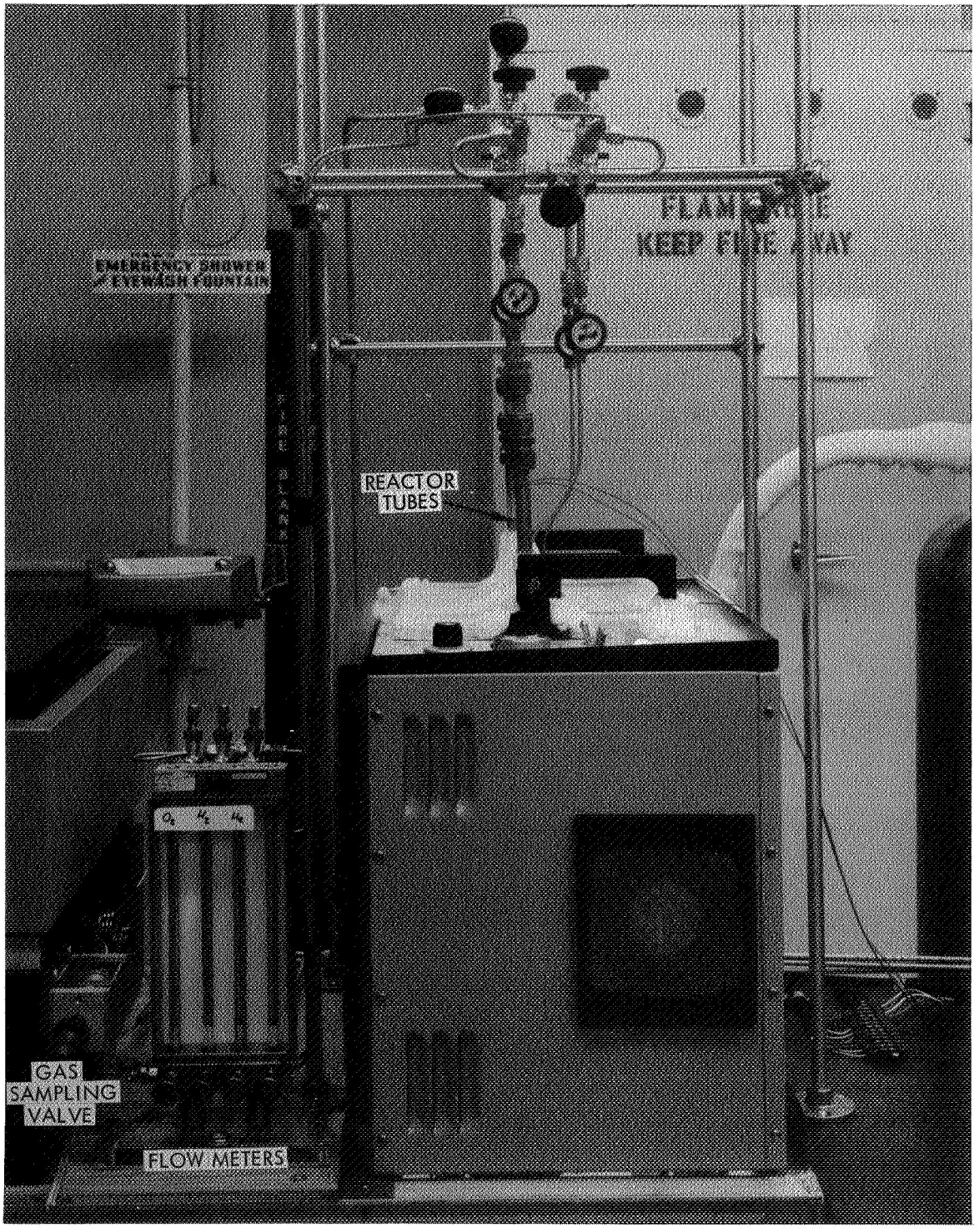

Figure 12. Close-Up View of the Isothermal Differential Reactor Flow System and Constant Temperature Chamber

a dummy reactor which contains only catalyst support or through an empty tube) and then through the gas chromatograph. The plug of gas is carried over the catalyst by the helium stream and then into the gas chromatograph for analysis to determine the amount of gas reacted and/or adsorbed. A constant temperature chamber with a range from -196°C (77°K) to 300°C (573°K) and a reproducibility of ±0.05°C controls the reactor temperature. The total pressure of the system can be varied from 30 to 90 psia (2.068×10^5 to 6.205×10^5 N/m^2) depending on the length of the gas chromatograph column. The pulse flow mode of operation insures isothermal or very nearly isothermal conditions. Kinetic experiments were performed using the differential reactor with one sample of catalyst while other catalyst samples are pretreated and conditioned in the separate pretreating and soaking system (Figures 8, 9 and 10).

3.2.2 Operation of Reactor

A dummy reactor tube containing only the alumina catalyst support material and the kinetic reactor tube which contains the same amount of active catalyst were initially pretreated and exposed to a predetermined soaking environment, evacuated, and then removed from the heating and soaking zones (Figures 8, 9 and 10) by closing the vacuum valves and disconnecting at the unions. These reactors were then carefully connected to the differential reactor system as shown in Figure 9. Valve A was opened and valves C and B were closed during connecting of the reactor lines. Valve H was first opened to remove air (by the vacuum system) and then valves H and A were closed and valves C and B were opened. Valve J was then opened and helium flowed through the lines for about 15 minutes to insure removal of all traces of air. Valve J was then closed and valves D, E, F, G, L, and O were opened and helium passed through the reactor tubes for a few minutes to establish equilibrium, and then valves C and B were closed and valve A was opened. The constant temperature chamber was set at the predetermined temperature and while equilibrium conditions were established, the hydrogen-oxygen-helium mixture ratio was set by adjusting the flow of the gases through the Carle sampling valve. The composition of the gas mixture was determined by turning the handle of the Carle sampling valve which caused a reproducible sample of the mixture of gas to enter the chromatograph for analysis. When a reference chromatogram was obtained of the established mixture ratio and the reactor tubes were at the predetermined temperature, then valve A was closed and valves C, B, L, and O were opened to establish a steady flow of helium through the empty reactor tube.

At cryogenic temperatures, the flow through the reactor changes causing a corresponding change in the gas chromatogram shape and area which was detected by comparison of the empty reactor chromatogram with the original sample mixture chromatogram. Next the Carle valve was activated to introduce a reproducible plug of the reactant gases to flow over the catalyst support and then into the gas chromatograph for analysis as shown in Figure 8. Then valves F and G were closed and valves D and E were opened and the procedure was repeated for the actual

catalyst. The reactant gases were alternately pulsed over the support and catalyst at regular intervals until the gas chromatograph analysis showed that hydrogen and oxygen no longer reacted or chemisorbed on the catalyst.

3.2.3 Experimental Procedure

The procedure generally used in the kinetic experiments is described below.

A catalyst sample and corresponding support were preweighed and placed in separate reactor tubes. These tubes were connected to the pretreating section and outgassed at 500°C (773°K) for 2 hours. Hydrogen at 20 psig (1.379×10^5 N/m^2) was put into the reactors and allowed to react with the oxides present on the catalyst surface for a period of 1 hour. Then the hydrogen was pumped off at 10^{-6} torr. Removal of the hydrogen and reaction products was performed three more times. The catalyst and supports were outgassed at 10^{-6} torr vacuum at 600°C (873°K) for 16 hours. The reactor tubes were cooled to room temperature in vacuum, and helium was placed over the catalyst and support at 20 psig (1.379×10^5 N/m^2). The reactor tubes were removed from the pretreating section and transferred to the kinetic reactor section described in the previous section.

After connection to the kinetic reactor system, helium was then passed over the catalyst support and through the empty reactor tube (called the dummy reactor) until equilibrium was established through the system and the gas chromatograph.

In experiments subsequent to the initial studies, hydrogen at room temperature was pulsed over the catalyst sample to post-treat the sample for reaction, and the reactor was then cooled to the operating temperature for the kinetic experiments. During the time for establishing thermal equilibrium, the gas flows were adjusted to correspond to the reactant mixture selected for the experiments. After equilibrium was established, the reactant mixture was pulsed first through the empty reactor to permit an accurate determination of the gas composition; then, the reactants were pulsed through the catalyst support to determine the change in the gas chromatograph peaks caused by the physical hold-up of the gases in passing through the supports at the low temperature (physical adsorption). Then the reactant mixture was pulsed through the catalyst bed and the amount of hydrogen and oxygen remaining in the mixture was recorded on the gas chromatograph. The reactant mixture was pulsed at definite time intervals through the catalyst until the amount adsorbed or reacted approached zero.

3.2.4 Analysis of Experimental Data

For each experiment, the rate of disappearance (by reaction and/or chemisorption) of oxygen and/or hydrogen was tabulated as a function of the total number of molecules of gas which had previously adsorbed or

reacted. The average adsorption or reaction rate for each pulse was computed from the measured conversion by the relationship:

$$\bar{r}_{ave} = \frac{F}{W} \Delta_X \tag{1}$$

where

$\bar{r}_{ave}$ = average rate of disappearance of a particular reactant (H_2 or O_2) atoms/sec-gram of catalyst

F = flow rate of a particular reactant (H_2 or O_2) entering the catalyst bed atoms/sec

W = weight of catalyst sample

Δ_X = measured conversion of particular reactant (H_2 or O_2)

$$\Delta_X \cong \frac{\left(\begin{array}{c}\text{number of counts through} \\ \text{dummy reactor}\end{array}\right) - \left(\begin{array}{c}\text{number of counts through} \\ \text{catalyst bed}\end{array}\right)}{\text{number of counts through dummy reactor}}$$

The total amount of reactant (O_2 or H_2) which had adsorbed or reacted at the end of each pulse was computed by summing the product of the measured conversions times the number of reactant molecules (H_2 or O_2) per pulse over all of the previous pulses:

$$n_i = \sum_{1}^{i} n_j^o \Delta x_j \tag{2}$$

where

n_i = number of molecules of oxygen or hydrogen adsorbed or reacted at the end of the ith pulse

Δ_{x_j} = conversion of oxygen or hydrogen on the jth pulse

n^o_j = number of reactant molecules (O_2 or H_2) introduced to the catalyst bed on the jth pulse

3.2.5 Post-Treatment Effects

Initial experiments in the differential reactor system indicated that little or no reaction would occur at low temperatures on a catalyst which had been subjected to the standard pretreatment. Experimental results showing the effects of post-treatment, particularly with hydrogen, are given in Table 11. Further results indicated that a hydrogen lead was required over the "clean" catalyst in order to obtain reaction at lower temperatures. Consequently, the standard pretreatment of the catalyst was supplemented by pulsing hydrogen over the catalyst at room temperature prior to cooling to the preselected reaction temperature.

Table 11. Effect of Post-Treatment on Catalyst Activity at -125°C (148°K)

Experiment Number	Catalyst	Pre-Treatment	Post-Treatment	Reactants	Results
R-1	0.5 grams Shell 405 ABSG	Outgassed at 773°K for 2 hrs at 10^{-6} vacuum torr	None	H_2 at 64 psia (4.4126×10^5 N/M^2) O_2 at 16 psia (1.1032×10^5 N/M^2) He at 6 psia (4.1369×10^4 N/M^2) Sample pulse 2cc	No Reaction Occurred
R-2	Same as Above	Standard	None	H_2 at 64 psia (4.4126×10^5 N/M^2) O_2 at 16 psia (1.1032×10^5 N/M^2) He at 5 psia (3.4474×10^4 N/M^2) Sample pulse 2cc	Small amount of reaction on the first pulse, no reaction thereafter
R-3	Same as Above	Standard	None	Same as Above	No Reaction at all
R-4	Same as Above	Standard	None	Same as Above	No Reaction at all
R-5	Same as Above	Standard	Hydrogen pulsed over the catalyst at -148°K	Same as Above	Reaction occurred and continued to occur for several pulses
R-6	Same as Above	Standard	Hydrogen pulsed over the catalyst at room temperature	Same as Above	Same as Above
R-7	Same as Above	Standard	Same as Above	Same as Above	Reaction Occurred
R-8	Same as Above	Standard	Same as Above	Same as Above	Reaction Occurred
R-15	Engelhard MFSA 1/16-inch (.159 cm)	Standard	None	Same as Above	20% conversion on the first pulse and a decrease to about 0% after the third pulse
R-14	Same as Above	Standard	Hydrogen pulsed over the catalyst at room temperature	Same as Above	50% conversion on the first pulse gradually decreasing to 0% after the seventh pulse

*Standard pretreatment consists of outgassing for two hours at 773°K under 10^{-6} torr vacuum followed by an exposure to hydrogen and reaction products at 10^{-6} torr vacuum for 10 minutes. This cycle is repeated three more times and is then followed by outgassing of the catalyst at 873°K for 16 hours at 10^{-6} torr vacuum.

3.2.6 Experimental Test Matrix

Table 12 outlines the final experimental test matrix. Experiments 1 through 9 were aimed at determining the effect of temperature and reactant partial pressure on the rate of hydrogen-oxygen reaction and/or chemisorption on the Shell 405 ABSG catalyst. A total system pressure of 75 psia (5.171×10^5 N/m^2) was maintained in these experiments by utilizing helium as a diluent. In experiments 1 through 9, the hydrogen to oxygen mixture ratio entering the catalyst bed was maintained at 4 moles of hydrogen per mole of oxygen while the partial pressure of reactants (hydrogen plus oxygen) was varied from 7.5 to 75 psia (5.171×10^4 to 5.171×10^5 N/m^2). Experiments 10 and 11 investigated the effect of catalyst bed length on the reaction rates for Shell 405 ABSG catalyst under a single set of experimental conditions.

Experiments 12 and 13 evaluated the effect of soaking "clean" Shell 405 catalyst in hydrogen at low temperature, -160°C (113°K); and at high temperature, 816°C, (1089°K), respectively. Experiments 14 and 15 determined the effect of soaking a clean Shell 405 catalyst at 816°C (1089°K) in high vacuum and in oxygen, respectively. The effect of increased mixture ratio, 16 moles of hydrogen per mole of oxygen, was determined in experiment 16. The effect of total system pressure (reactants plus helium diluent) was evaluated in experiments 9 and 17. Experiments 18 through 30 were essentially the same as experiments 1 through 9 and 12 through 15, but used Engelhard MFSA 1/16-inch catalyst in place of the Shell 405 ABSG catalyst.

3.2.7 Experimental Kinetic Studies with Shell 405 ABSG Catalyst

The following paragraphs describe the kinetic experiments with Shell 405 ABSG catalyst, showing the change in the reaction rate as a function of bed length, temperature, partial pressure, total pressure, and soaking environment.

3.2.7.1 Reaction Rate as a Function of Bed Length

The change in reaction rate with bed length is shown in Figure 13. The bed diameter was constant for each test, therefore the 1-gram catalyst bed was twice the length of the 1/2-gram bed, etc. The experimental data in Figure 13 indicate that the initial phase of the reaction was independent of the sample size, i.e., the reaction rate (O_2 atoms/sec/gram of catalyst), multiplied by the catalyst sample weight in grams, is a constant (19×10^{18} O_2 atoms reacted per second) for all three experiments. However, the results also show that the maximum oxygen atoms taken up per gram of catalyst were directly related to the bed length, i.e., the 2-gram catalyst bed, which was four times the length of the 1/2-gram bed, reacted four times the oxygen atoms per gram as the shorter bed.

Table 12. Test Matrix for H_2-O_2 Reaction Kinetics Study in the Isothermal Differential Reactor

Experiment Number	Catalyst Type	Catalyst Sample Size Grams	Soak Conditions (after standard pretreatment)	Temperature °K	P_{O_2} psia	P_{O_2} N/M^2	P_{H_2} psia	P_{H_2} N/M^2	P_{Helium} psia	P_{Helium} N/M^2	P_{Total} psia	P_{Total} N/M^2	Volume Flow Rate Ml/Min STP	Pulse Size Ml STP
1	Shell 405	0.5	None	113	15.0	1.0342×10^5	60.0	4.1369×10^5	--	--	75	5.1711×10^5	120	2.0
2	↑	↑	↑	113	1.5	1.0342×10^4	6.0	4.1369×10^4	67.5	4.6539×10^5	↑	↑	↑	↑
3	↑	↑	↑	113	4.0	2.7579×10^4	16.0	1.1032×10^5	55.0	3.7921×10^5	↑	↑	↑	↑
4	↑	↑	↑	123	15.0	1.0342×10^5	60.0	4.1369×10^5	--	--	↑	↑	↑	↑
5	↑	↑	↑	123	1.5	1.0342×10^4	6.0	4.1369×10^4	67.5	4.6539×10^5	↑	↑	↑	↑
6	↑	↑	↑	123	4.0	2.7579×10^4	16.0	1.1032×10^5	55.0	3.7921×10^5	↑	↑	↑	↑
7	↑	↑	↑	148	15.0	1.0342×10^5	60.0	4.1369×10^5	--	--	↑	↑	↑	↑
8	↑	↑	↑	148	1.5	1.0342×10^4	6.0	4.1369×10^4	67.5	4.6539×10^5	↑	↑	↑	↑
9	↑	0.5	↑	148	4.0	2.7579×10^4	16.0	1.1032×10^5	55.0	3.7921×10^5	↑	↑	↑	↑
10	↑	1.0	↑	148	15.0	1.0342×10^5	60.0	4.1369×10^5	--	--	↑	↑	↑	↑
11	↑	2.0	None	148	↑	↑	↑	↑	--	--	↑	↑	↑	↑
12	↑	0.5	60 psia (4.1369×10^5 N/M^2) H_2 at 98°K, 1 hour	123	↑	↑	↑	↑	--	--	↑	↑	↑	↑
13	↑	↑	15 psia (1.0342×10^5 N/M^2) H_2 at 1089°K, 5 hours	123	↑	↑	↑	↑	--	--	↑	↑	↑	↑
14	↑	↑	10^{-6} torr vacuum, 1089°K, 5 hours	123	↑	↑	↑	↑	--	--	↑	↑	↑	↑
15	↑	↑	15 psia (1.0342×10^5 N/M^2) O_2 at 1089°K, 5 hours	123	15.0	1.0342×10^5	60.0	4.1369×10^5	--	--	↑	↑	↑	↑
16	↑	↑	None	148	4.0	2.7579×10^4	64.0	4.4126×10^5	5.0	3.4474×10^4	75	5.1711×10^5	↑	↑
17	Shell 405	↑	↑	148	4.0	2.7579×10^4	16.0	1.1032×10^5	1.0	6.8948×10^3	35	2.4132×10^5	↑	2.0
18	MFSA 1/16"	↑	↑	123	15.0	1.0342×10^5	60.0	4.1369×10^5	--	--	75	5.1711×10^5	↑	0.5
19	↑	↑	↑	123	1.5	1.0342×10^4	6.0	4.1369×10^4	67.5	4.6539×10^5	↑	↑	↑	↑
20	↑	↑	↑	123	4.0	2.7579×10^4	16.0	1.1032×10^5	55.0	3.7921×10^5	↑	↑	↑	↑
21	↑	↑	↑	148	15.0	1.0342×10^5	60.0	4.1369×10^5	--	--	↑	↑	↑	↑
22	↑	↑	↑	148	1.5	1.0342×10^4	6.0	4.1369×10^4	67.5	4.6539×10^5	↑	↑	↑	↑
23	↑	↑	↑	148	4.0	2.7579×10^4	16.0	1.1032×10^5	55.0	3.7921×10^5	↑	↑	↑	↑
24	↑	↑	↑	173	15.0	1.0342×10^5	60.0	4.1369×10^5	--	--	↑	↑	↑	↑
25	↑	↑	↑	173	1.5	1.0342×10^4	6.0	4.1369×10^4	67.5	4.6539×10^5	↑	↑	↑	↑
26	↑	↑	None	173	4.0	2.7579×10^4	16.0	1.1032×10^5	55.0	3.7921×10^5	↑	↑	↑	↑
27	↑	↑	60 psia (4.1369×10^5 N/M^2) H_2 at 223°K, 1 hour	148	15.0	1.0342×10^5	60.0	4.1369×10^5	--	--	↑	↑	↑	↑
28	↑	↑	15 psia (1.0342×10^5 N/M^2) He at 1089°K, 5 hours	148	↑	↑	↑	↑	--	--	↑	↑	↑	↑
29	↑	↑	10^{-6} torr vacuum, 1089°K, 5 hours	148	↑	↑	↑	↑	--	--	↑	↑	↑	↑
30	MFSA 1/16"	0.5	15 psia (1.0342×10^5 N/M^2) O_2 at 1089°K, 5 hours	148	15.0	1.0342×10^5	60.0	4.1369×10^5	--	--	75	5.1711×10^5	120	0.5

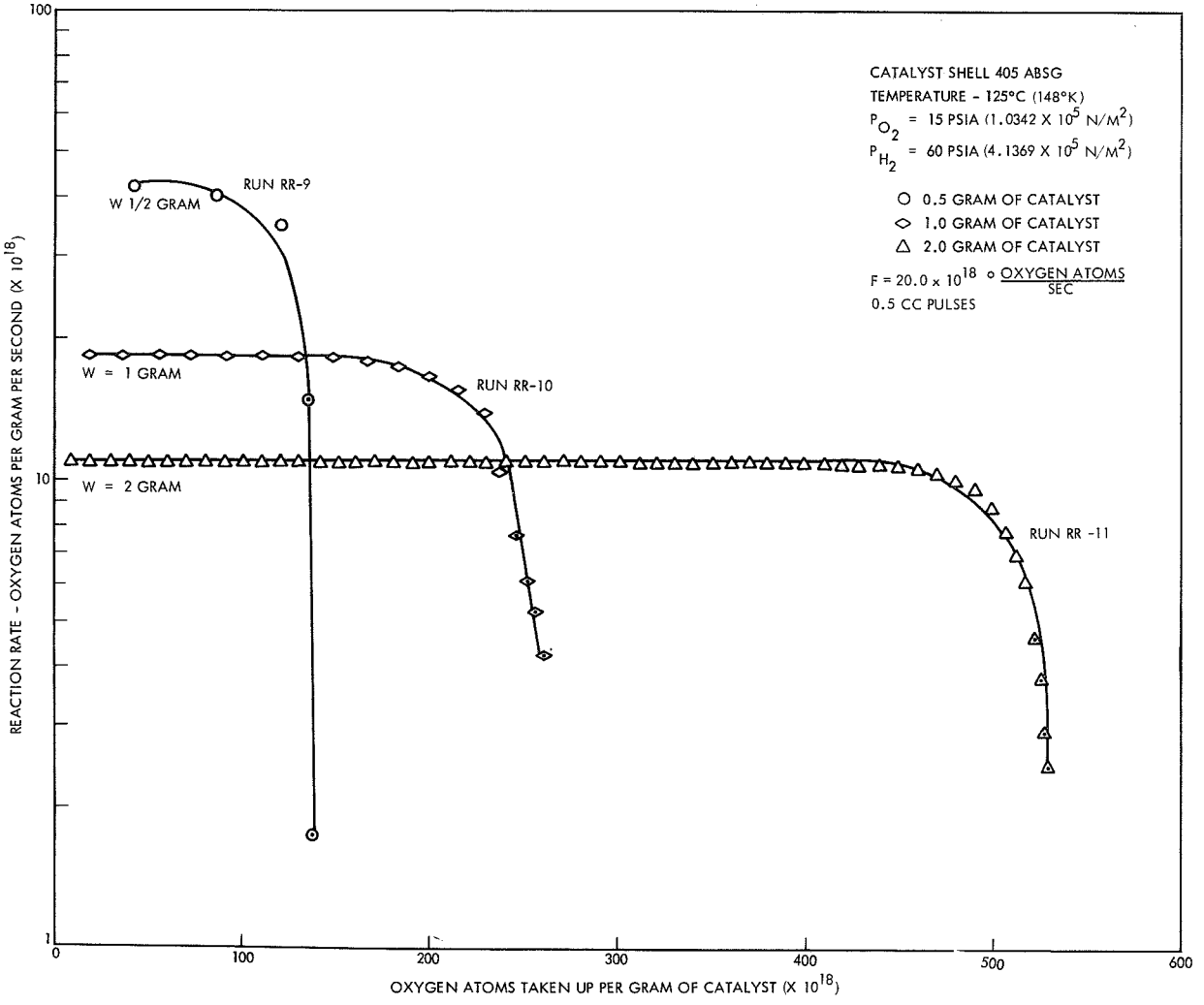

Figure 13. Reaction Rate of the Hydrogen-Oxygen System as a Function of Bed Length

3.2.7.2 Reaction Rate as a Function of Temperature

The effects of temperature variation at different reactant gas pressures (total pressure of hydrogen plus oxygen) can be seen in Figures 14 through 17. In these experiments, the total gas pressure was maintained at 75 psia (5.171×10^5 N/m^2) and the reactant mixture ratio was held at 4 moles of hydrogen per mole of oxygen. Helium was used as the diluent at the lower hydrogen-oxygen partial pressures. Figure 14 shows the reproducibility of a typical set of experiments while Figures 15, 16, and 17 relate the temperature effects at reactant gas (hydrogen plus oxygen) pressures of 75, 20, and 7.5 psia (5.171×10^5, 1.379×10^5, and 5.171×10^4 N/m^2), respectively.

3.2.7.3 Reaction Rate as a Function of Reactant Partial Pressure and Total System Pressure

The change in the reaction rate at various temperatures as a function of the hydrogen-oxygen partial pressure can be seen in Figures 18, 19 and 20, which show the results obtained at -125°, -150° and -160°C, (148°, 123° and 113°K), respectively. In all the experiments, the total system pressure was held at 75 psia (5.171×10^5 N/m^2) while the reactant gas (hydrogen plus oxygen) pressure was varied from 7.5 to 75 psia (5.171×10^4 to 5.171×10^5 N/m^2). Figure 21 shows the effect of varying the total system pressure from 75 to 30 psia at a temperature of -125°C (148°K). The hydrogen-to-oxygen-to-helium molar ratios were maintained at 16 to 40 to 55.5, respectively. It was found that at higher pressures, the reaction continues at a higher rate to a higher surface coverage.

3.2.7.4 Reaction Rate as a Function of Soaking Environment

The effects of various soaking environments on the hydrogen-oxygen reaction rate are shown in Figure 22. It was observed that soaking at 816°C (1089°K) for 4 hours had a strong depressing effect upon the reaction rate. Soaking in hydrogen at 816°C (1089°K) for 5 hours had an intermediate depressing effect while soaking in 10^{-6} torr vacuum at 816°C (1089°K) for 5 hours resulted in no effect upon the catalytic reaction rate.

3.2.8 Experimental Studies with Engelhard MFSA Catalyst

The following paragraphs describe the kinetic experiments with Engelhard MFSA 1/16-inch catalysts. These experiments evaluated the effects of reactant partial pressure, temperature, and soaking environment with respect to reaction rate.

3.2.8.1 Reaction Rate as a Function of Temperature

The effect of temperature variation at different hydrogen-oxygen partial pressures can be seen in Figures 23, 24 and 25. In these experiments, the total gas pressure was maintained at 75 psia (5.171×10^5 N/m^2) and the reactant mixture ratio was held at 4 moles of hydrogen per mole of oxygen. Helium was used as the diluent at the lower hydrogen-oxygen

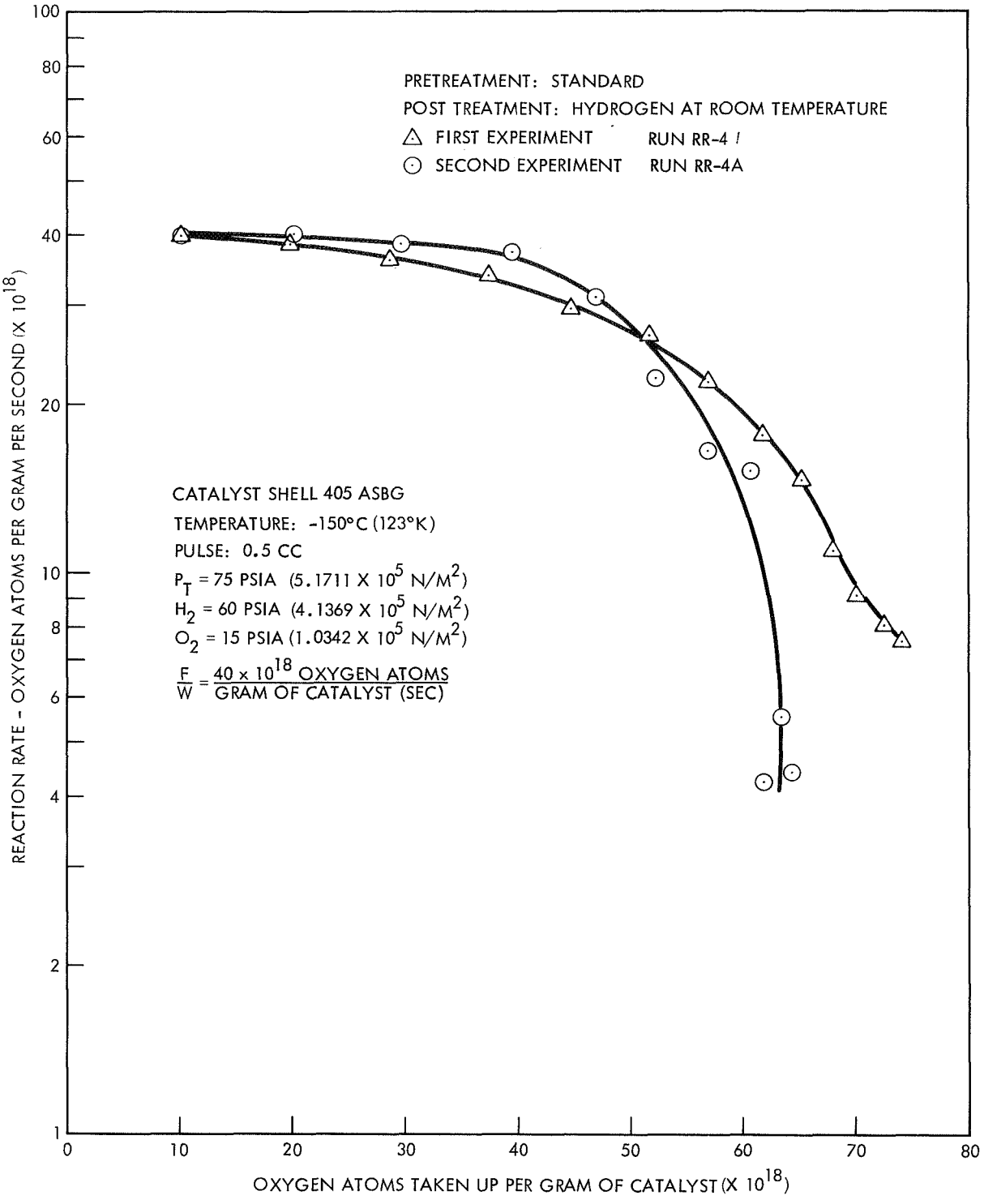

Figure 14. Reproducibility of Reaction Rate Measurements

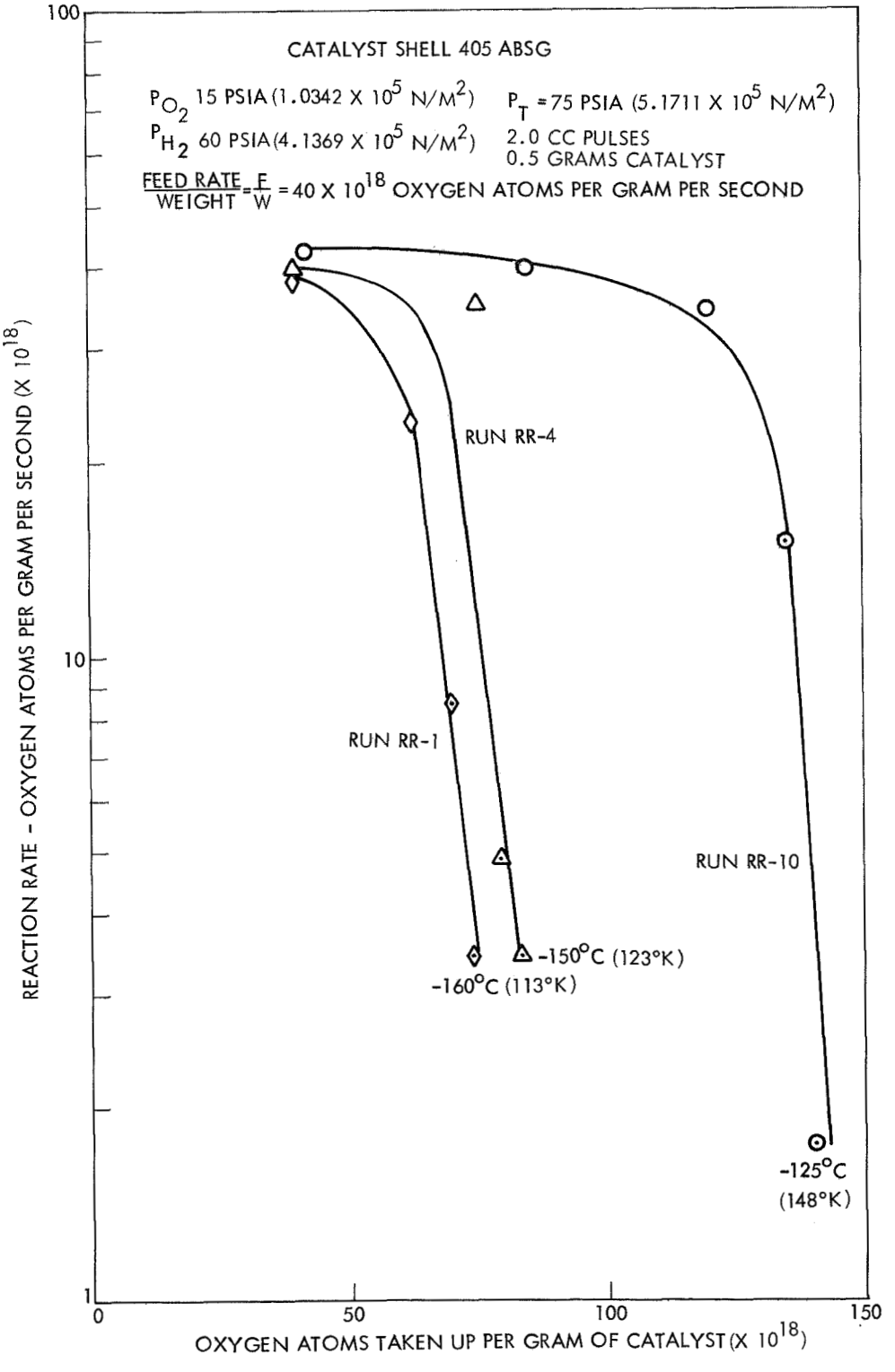

Figure 15. Reaction Rate of the Hydrogen-Oxygen System as a Function of Temperature, Total Reactant Gas Pressure = 75 psia (5.1711 X 10^5 N/M^2)

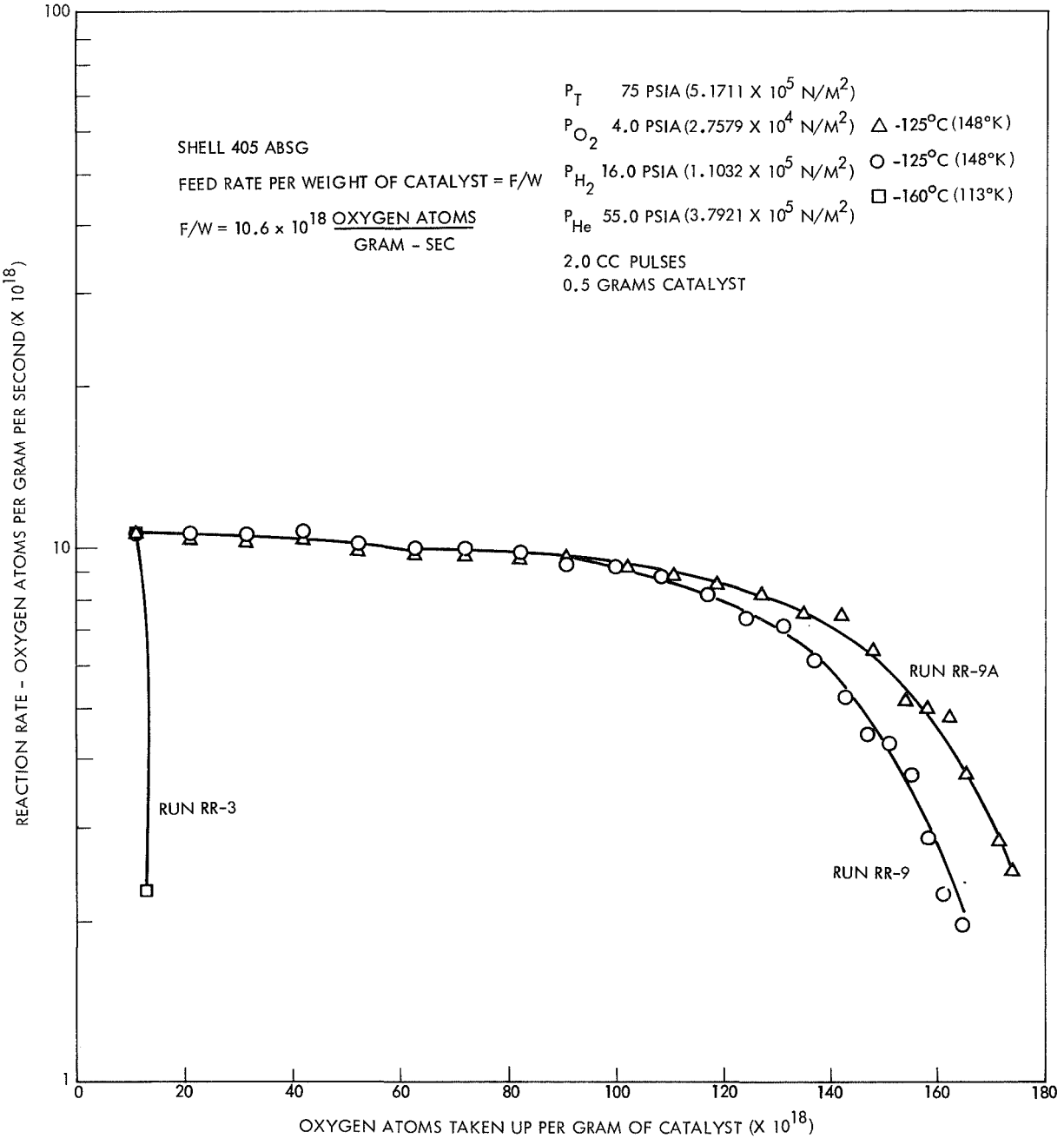

Figure 16. Reaction Rate of the Hydrogen-Oxygen System as a Function of Temperature, Total Reactant Gas Pressure = 20 psia (1.3790×10^5 N/M^2)

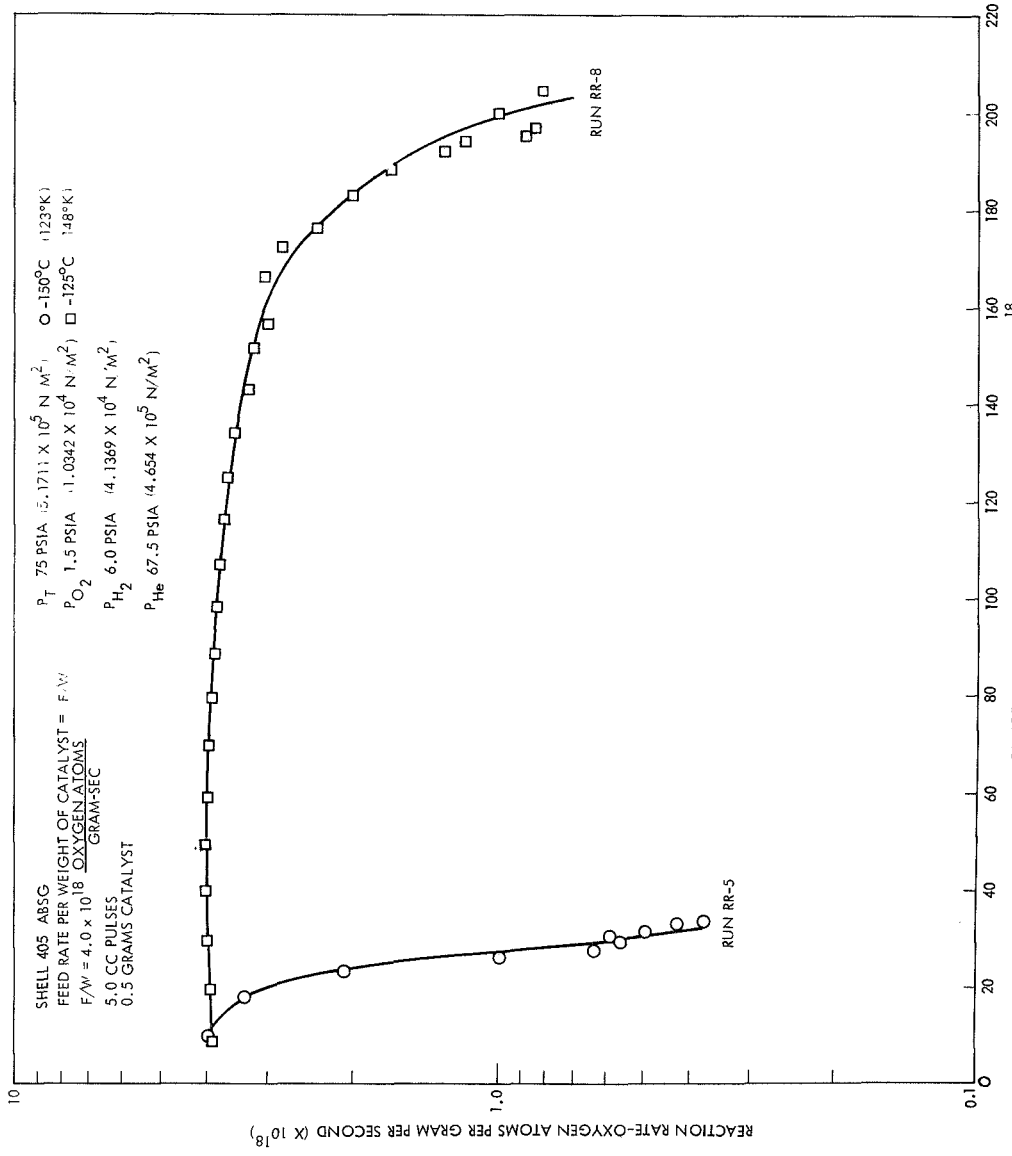

Figure 17. Reaction Rate of the Hydrogen-Oxygen System as a Function of Temperature, Total Reactant Gas Pressure = 7.5 psia (5.1711×10^4 N/M^2)

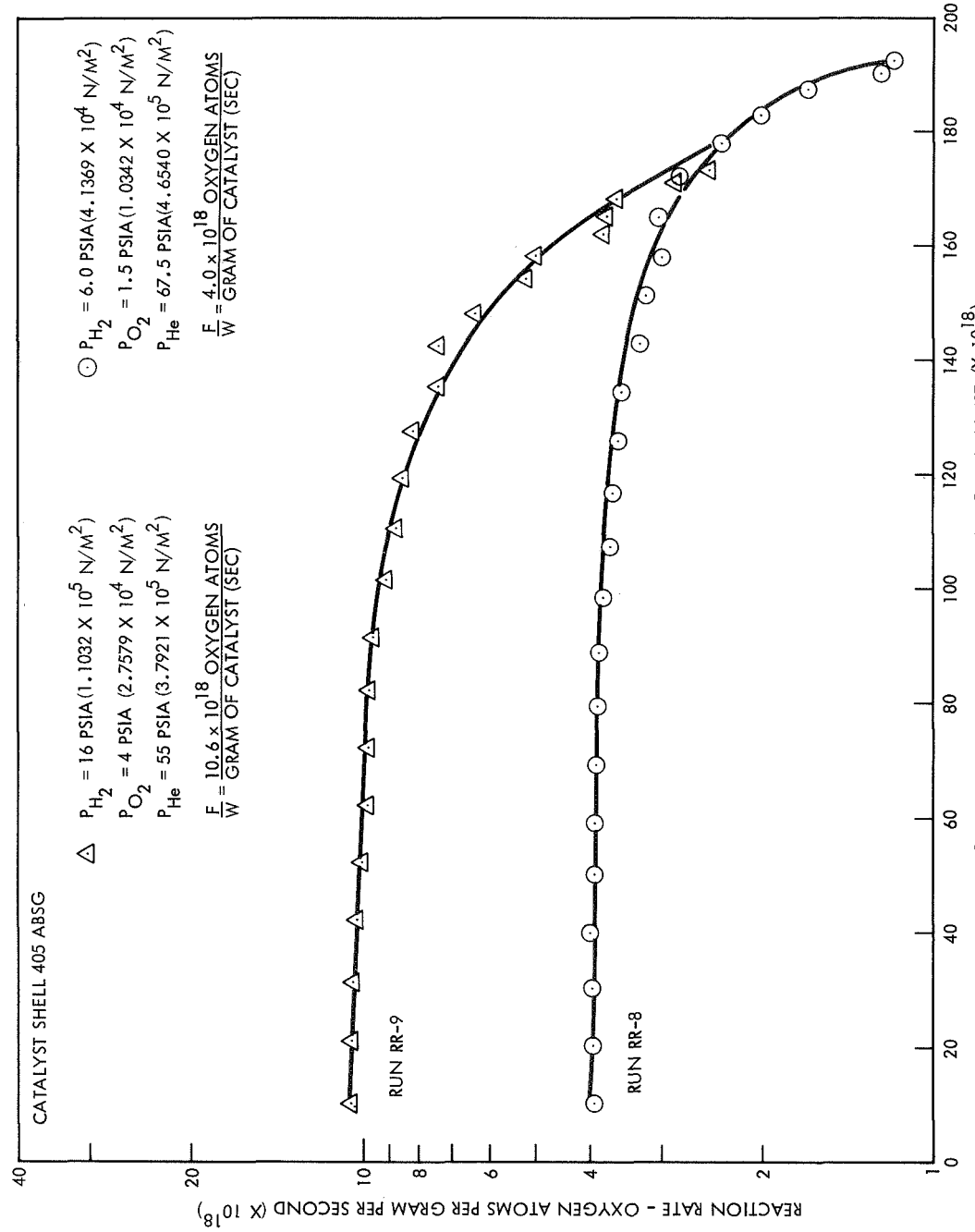

Figure 18. Reaction Rate as a Function of the Hydrogen-Oxygen Partial Pressures at -125°C (148°K)

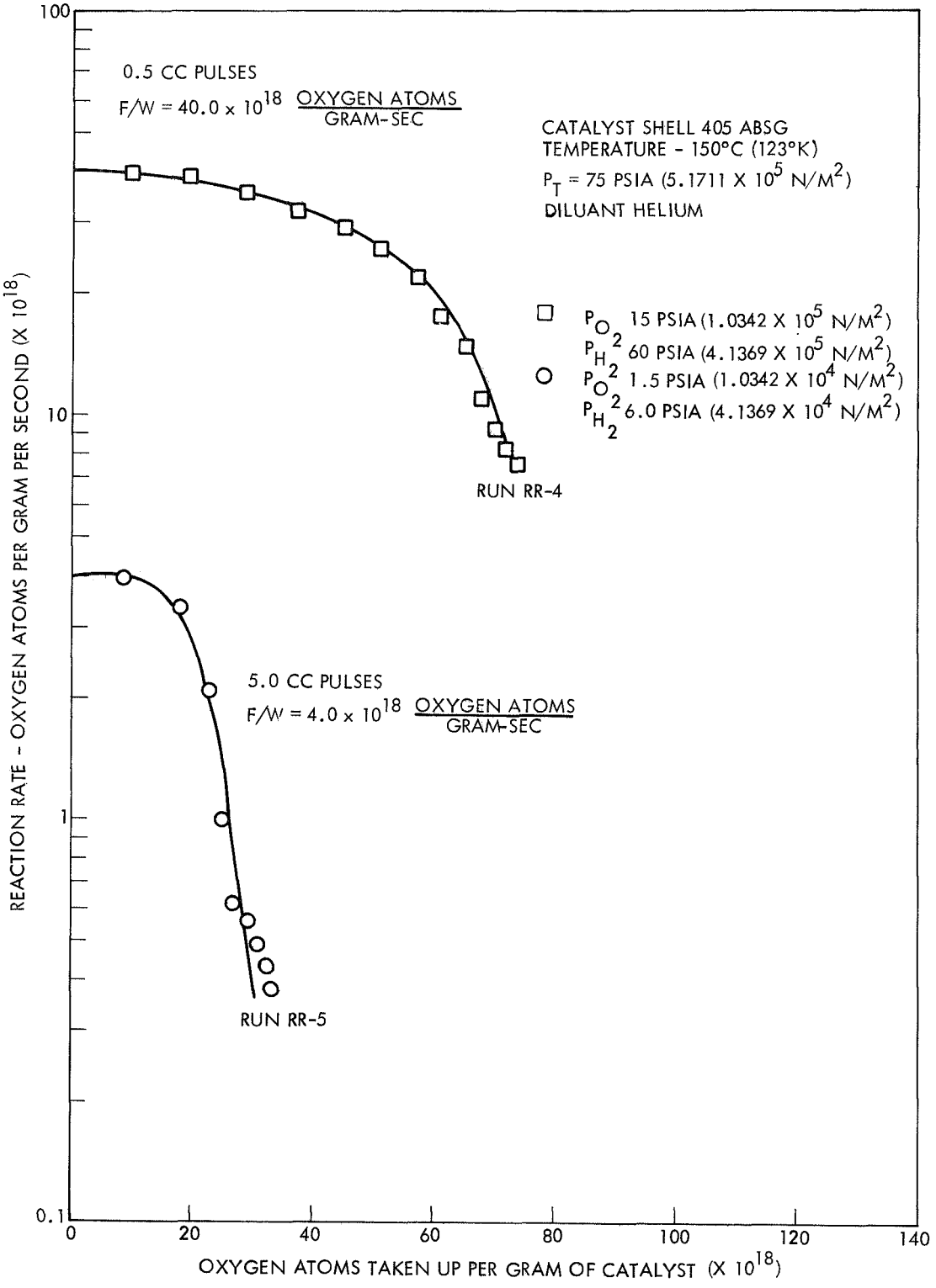

Figure 19. Reaction Rate as a Function of the Hydrogen-Oxygen Partial Pressures at -150°C (123°K)

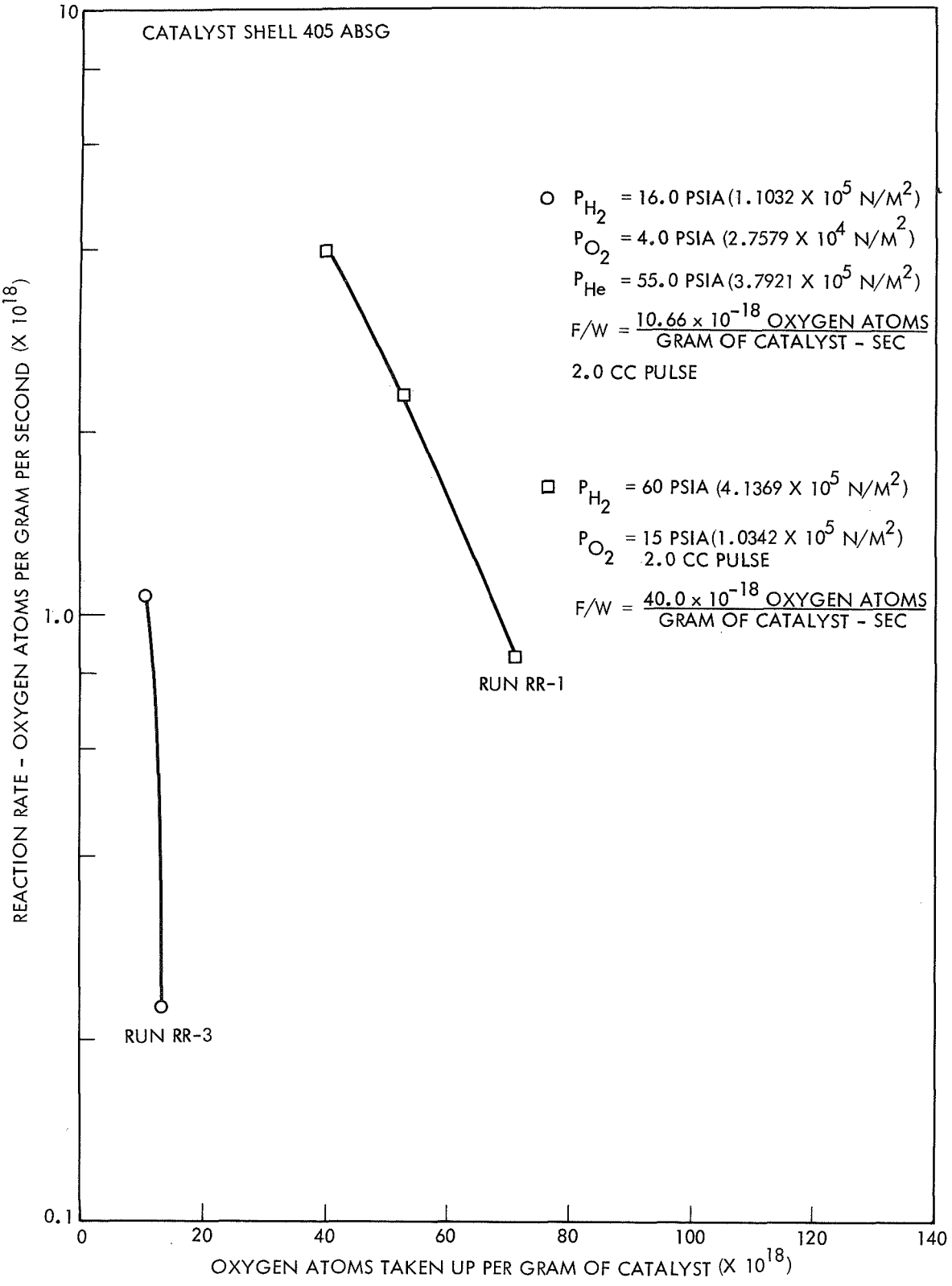

Figure 20. Reaction Rate as a Function of the Hydrogen-Oxygen Partial Pressures at -160°C (113°K)

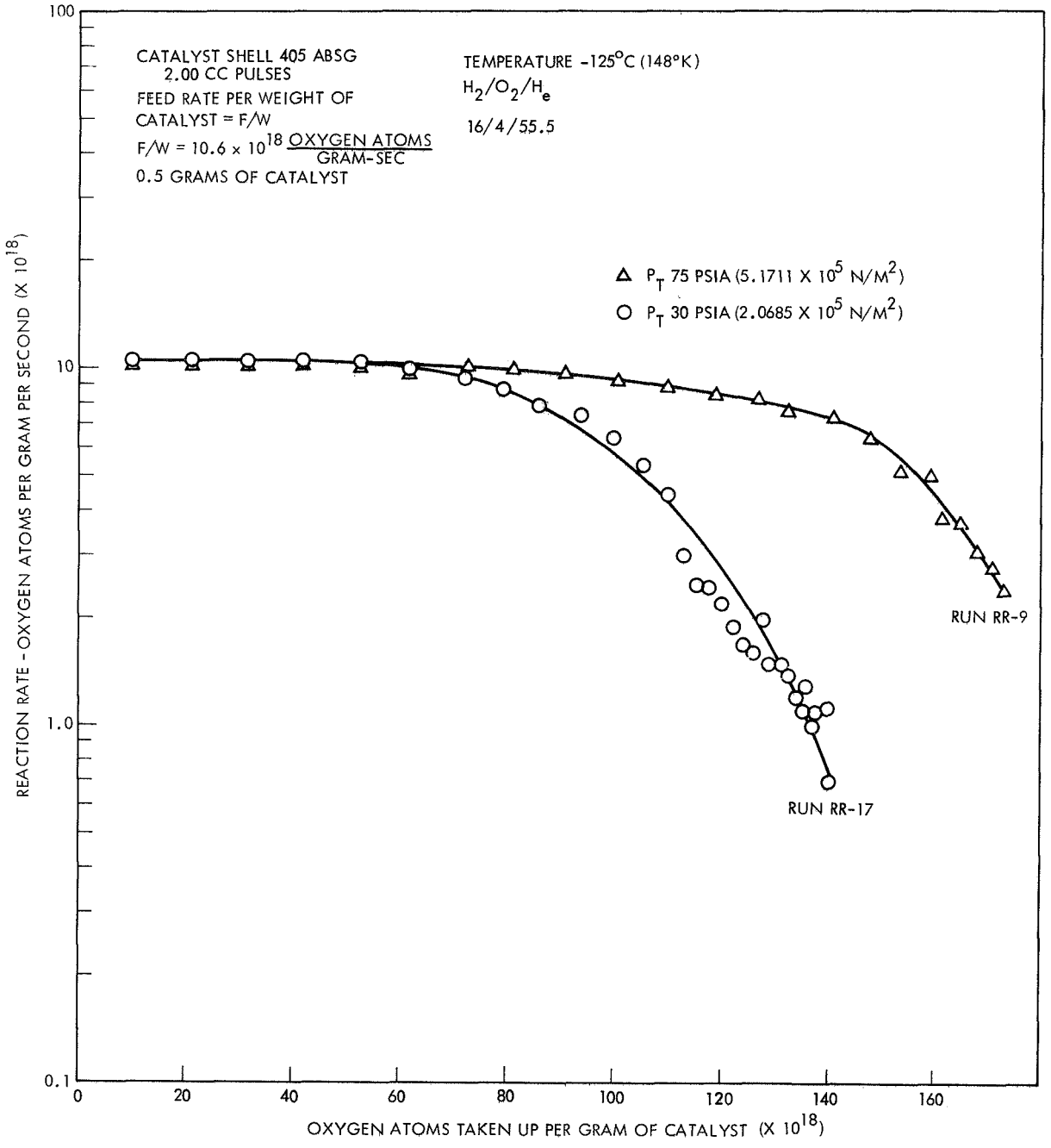

Figure 21. Reaction Rate as a Function of Total System Pressure

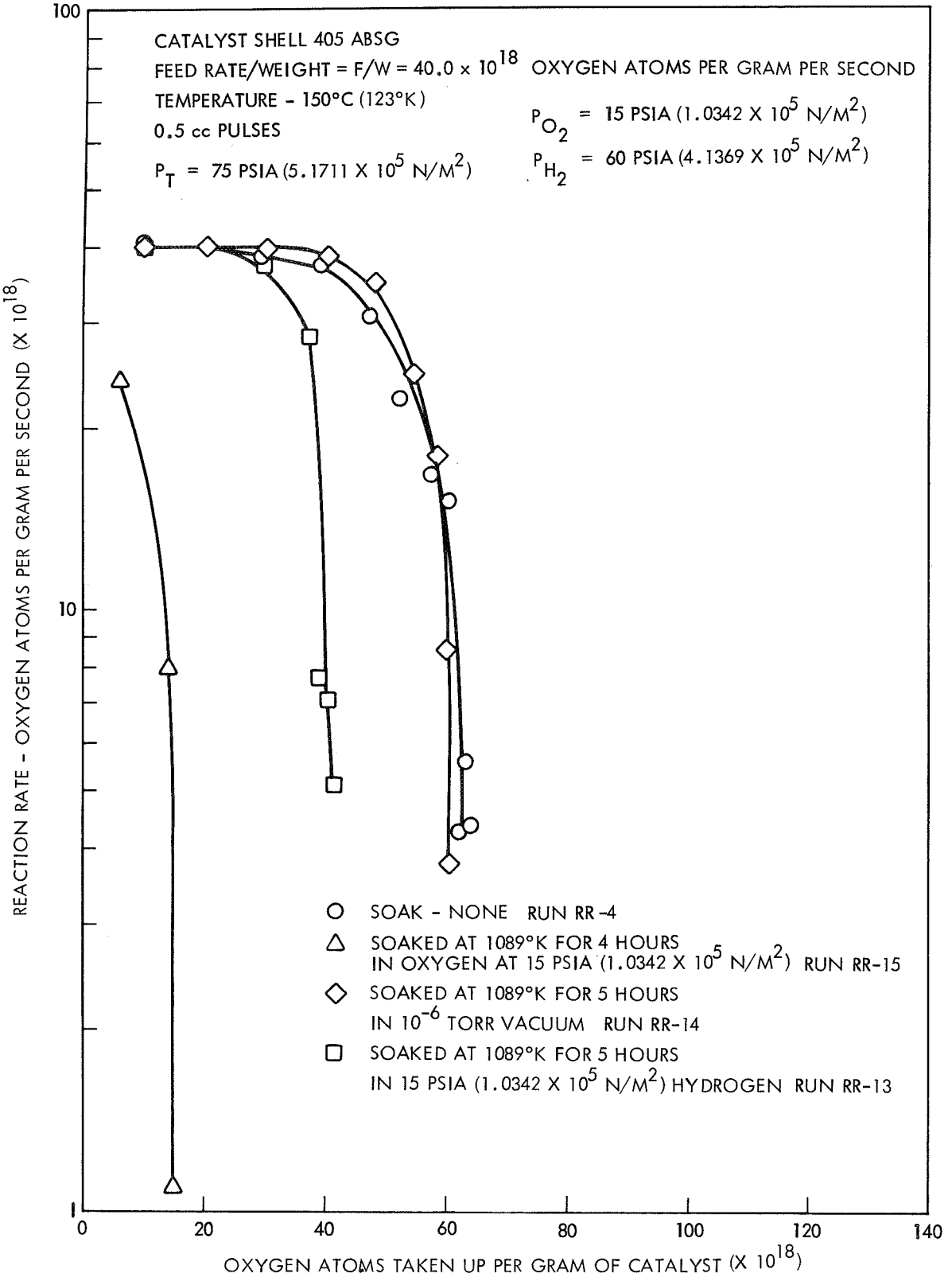

Figure 22. Reaction Rate as a Function of Soaking Environment

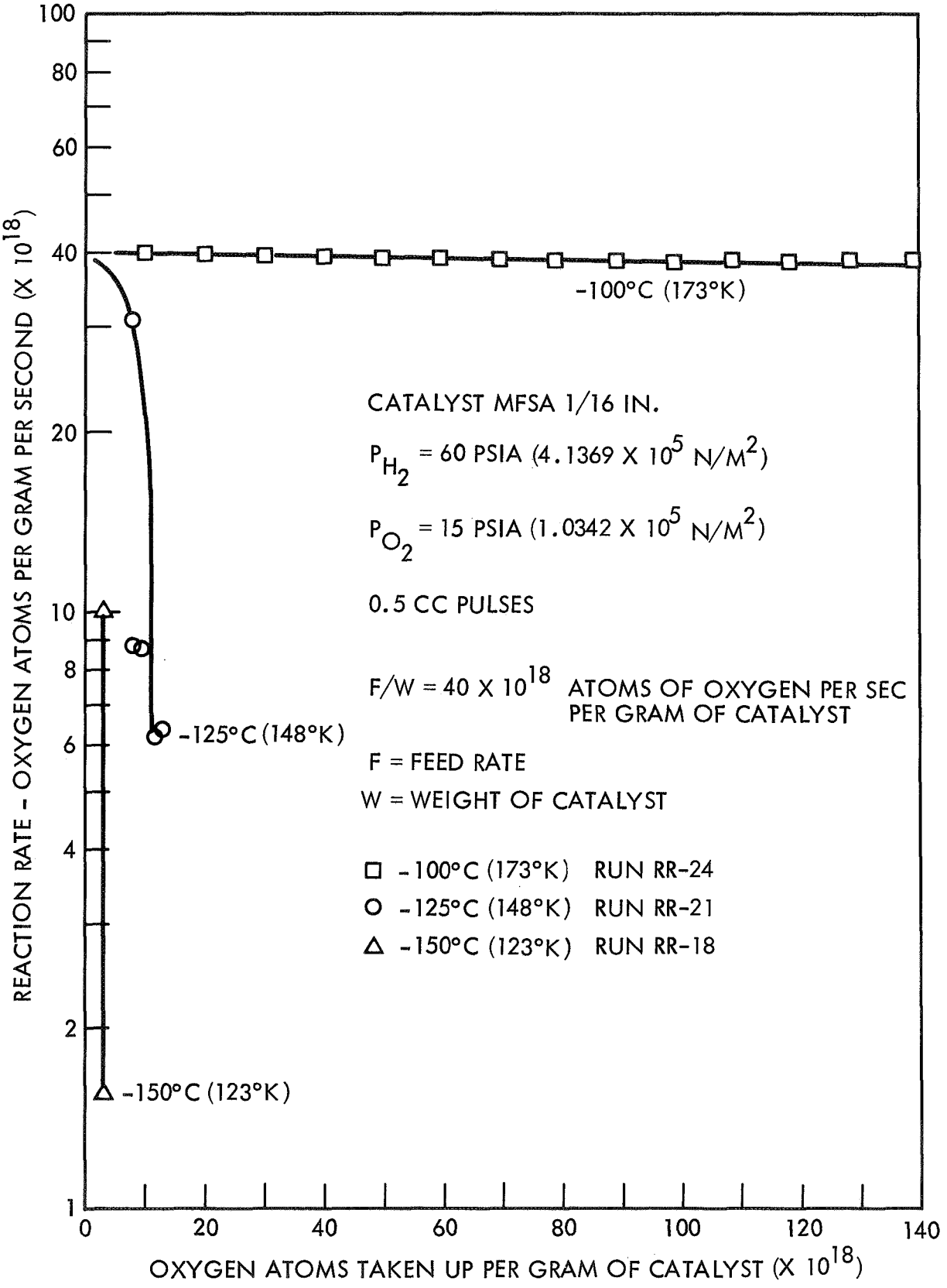

Figure 23. Reaction Rate of the Hydrogen-Oxygen System as a Function of Temperature, Total Reactant Gas Pressure = 75 psia (5.1711×10^5 N/M^2)

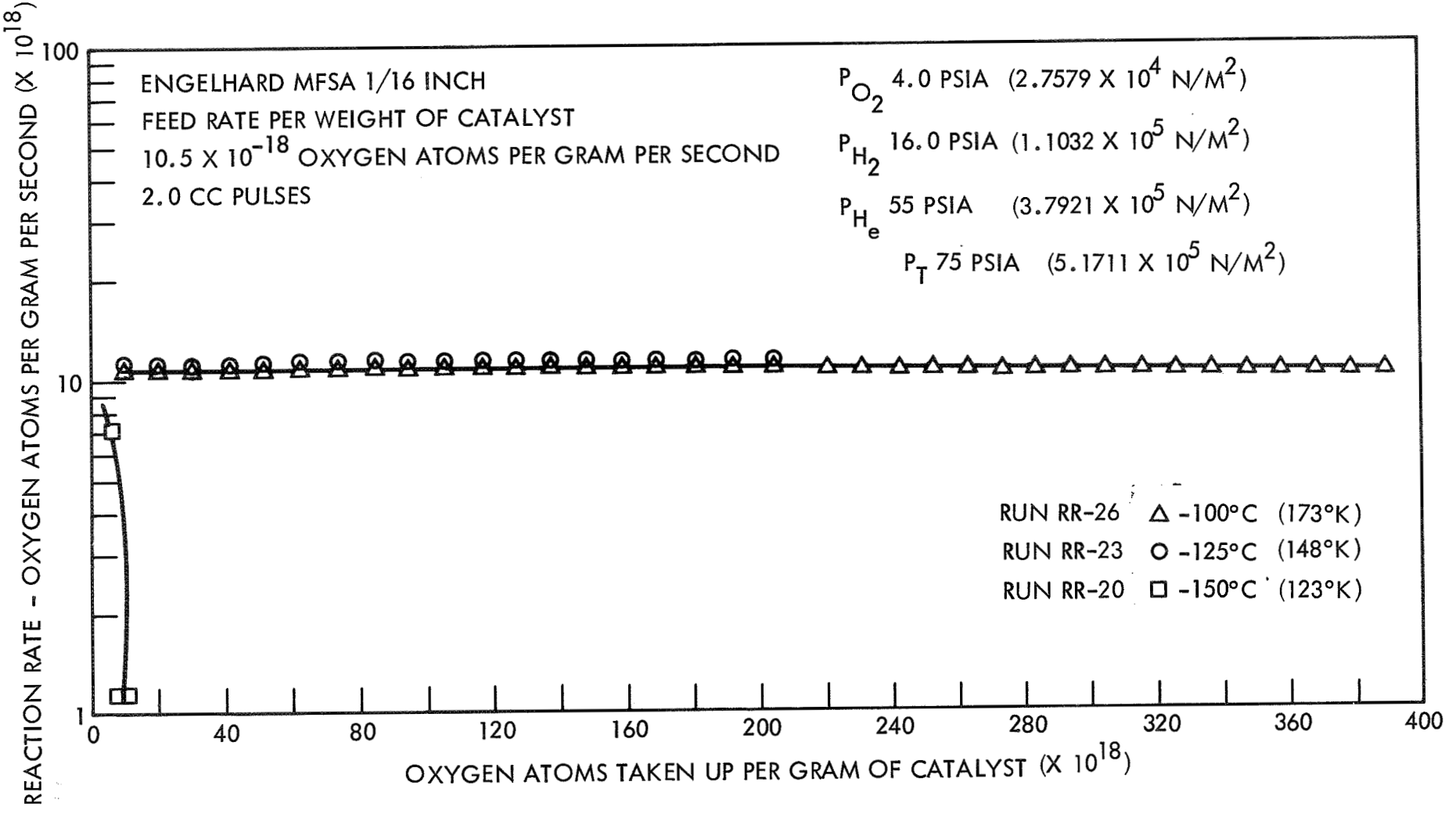

Figure 24. Reaction Rate of the Hydrogen-Oxygen System as a Function of Temperature, Total Reactant Gas Pressure = 20 psia (1.3790×10^5 N/M^2)

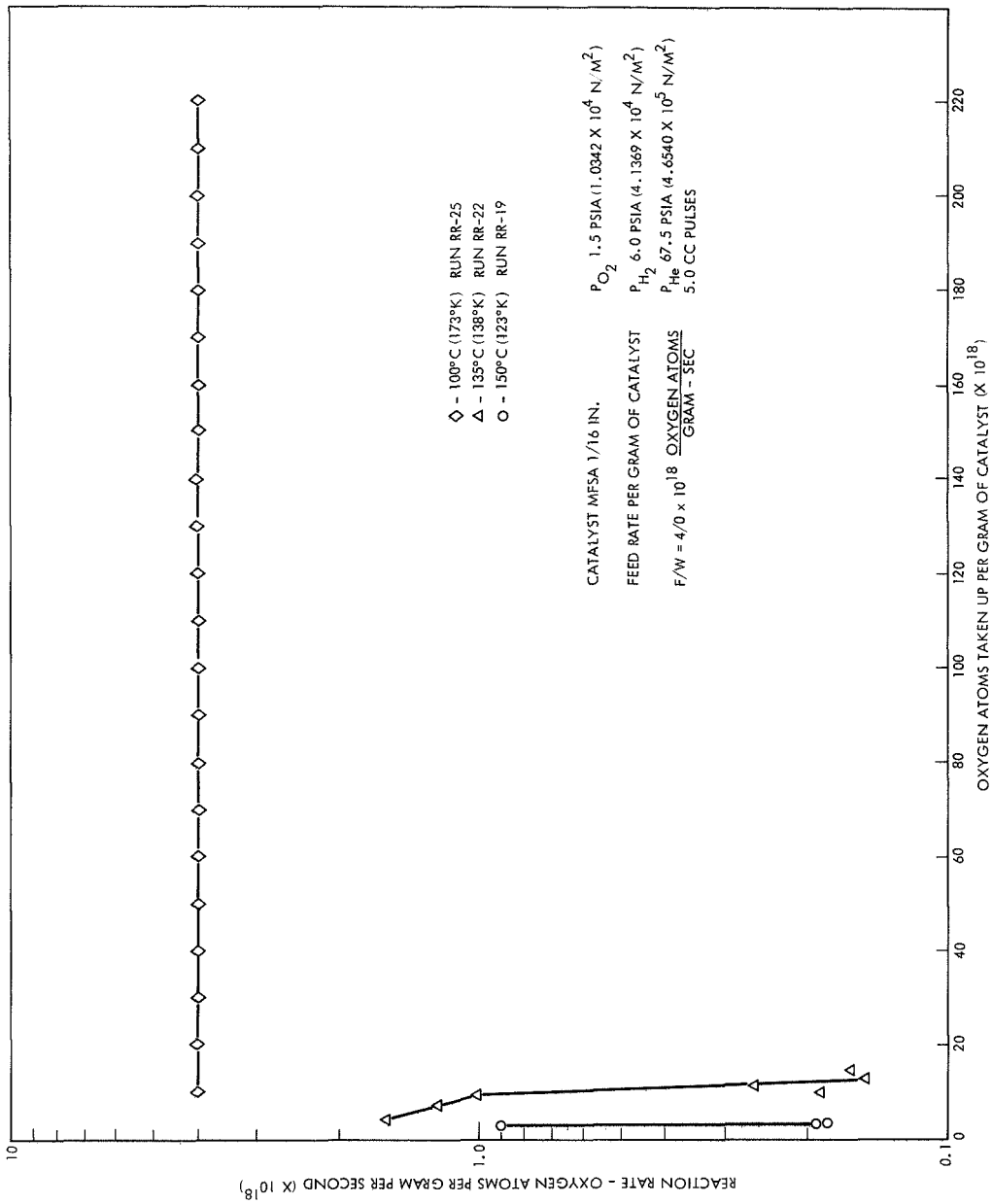

Figure 25. Reaction Rate of the Hydrogen-Oxygen System as a Function of Temperature, Total Reactant Gas Pressure = 7.5 psia (5.1711 X 10^4 N/M^2)

partial pressures. Figures 23, 24 and 25 relate the temperature effects at reactant gas (hydrogen plus oxygen) pressures of 75, 20 and 7.5 psia (5.171×10^5, 1.379×10^5, and 5.171×10^4 N/m^2), respectively.

3.2.8.2 Reaction Rate as a Function of Reactant Partial Pressure

It can be seen from Figures 23, 24 and 25 that no change in the reaction rate with respect to surface coverage occurred at -100°C (173°K) when the partial pressures of the reactant mixture were varied. At -125°C (148°K) and -150°C (123°K), the variations in the reaction rates with respect to surface coverage were well within the experimental limits of the apparatus.

3.2.8.3 Reaction Rate as a Function of Hydrogen-Oxygen Mixture Ratio

The effect of the hydrogen-to-oxygen mixture ratio on the reaction rate with respect to surface uptake of oxygen is shown in Figure 26. It was found that at a temperature of -125°C (148°K) the reaction rates seemed to intersect at a surface coverage of 18×10^{18} atoms of oxygen per gram of catalyst. This occurred when the mole ratio of hydrogen-to-oxygen was varied from 16/1 to 4/1.

3.2.8.4 Reaction Rate as a Function of Soak Environment

The effects of various soaking environments on the MFSA 1/16-inch catalyst are shown in Figure 27. These data curves indicate that the 15 psia helium soak for 5 hours at 815°C (1089°K) resulted in the most pronounced loss of catalyst activity at -125°C (148°K). Soaking in oxygen for 5 hours at 815°C (1089°K) and 15 psia (1.034×10^5 N/m^2) had the least detrimental effect on catalyst activity of any of the soak conditions evaluated, as shown in Figure 27.

3.2.9 Comparison of Shell 405 ABSG and Engelhard MFSA 1/15-inch Catalysts

In Figures 28, 29 and 30, the catalytic activity of Shell 405 ABSG catalyst is compared to that of Engelhard MFSA catalyst. These comparisons were made under the same reactor conditions except that the hydrogen-oxygen partial pressures were varied. In every case, it was found that at temperatures below -100°C (173°K), the Shell 405 ABSG catalyst was superior. However, at -100°C (173°K), the Engelhard MFSA catalyst appeared to be as active as the Shell catalyst.

3.3 CONCLUSIONS FROM EXPERIMENTAL RESULTS

Based on the chemisorption measurements and pulsed flow reactor experiments, the conclusions pertinent to the design of a H_2-O_2 catalytic reactor were:

- The activity of both the Shell 405 and Engelhard MFSA catalysts, with respect to promoting low temperature H_2-O_2 reaction, depends very strongly on the condition of the catalyst surface. A freshly prepared catalyst which is exposed to ambient air rapidly adsorbs oxygen which is extremely detrimental to the activity of the catalyst. Indeed, it was found with both types of catalysts that it is essential to preadsorb a layer of hydrogen gas on a "cleaned" catalyst surface in order to achieve appreciable H_2-O_2 catalyst activity at temperatures below -25°C (248°K). To obtain an active catalyst surface in an H_2-O_2 thruster system the following procedure is recommended:

  (1) Operate the thruster at a high H_2-O_2 mixture ratio (ambient temperature ignition) for a period of seconds to drive adsorbed oxygen off the catalyst. Keep the catalyst surface temperature below 1800°F (~1260°K) during this operation.

  (2) Shut the engine down with a hydrogen lag and continue to purge hydrogen over the catalyst while it is cooling to ambient temperature.

  (3) Exclude oxygen from the above treated catalyst prior to low temperature firing.

  (4) Initiate and terminate reactor operation with a hydrogen purge.

- The pulsed flow reactor experiments indicated that the Shell 405 catalyst has a greater capacity than the MFSA catalyst to promote H_2-O_2 reaction at temperatures below -125°C (148°K). On the other hand, at temperatures above -125°C (148°K) the MFSA catalysts appear to be at least equal to and perhaps better than the Shell 405 catalyst. This latter result is surprising in light of the chemisorption experiments which showed that the Shell 405 catalyst has a much greater number of surface metal sites (per unit weight of catalyst) than the Engelhard MFSA catalyst. A possible explanation is as follows:

  (1) The Shell catalyst particle with its much greater metal content is likely to consist of a continuous or nearly continuous thermally conductive metal film supported by the high surface area alumina. On the other hand, the MFSA catalyst particle probably consists of small crystallites or islands of active metal which are thermally insulated from each other by the supporting alumina.

(2) When H_2 and O_2 react to form water on an active site on the Shell 405 catalyst much of the heat of reaction is rapidly conducted away by the continuous metal film and, hence, localized hot spots within the catalyst particle are minimized. On the other hand, the more thermally isolated active sites on the MFSA catalysts promote hot spots within the catalyst particle.

(3) If reaction sites on the MFSA catalyst are self-heated (because of reaction and/or chemisorption) much more rapidly than the bulk of the catalyst particle itself, then it is possible that the product of reaction (H_2O) can be desorbed from the active sites and readsorbed on the alumina support, thus freeing the active sites to promote further reaction. That is to say, at bulk particle temperatures well below the freezing point of water, it may still be possible for the water molecules to be transported from the active reaction site to some other part of the catalyst pellet. This hypothesis is supported by the observations that at temperaturs of -125°C (148°K) and above, on the Engelhard MFSA catalyst, many times more oxygen atoms were reacted than could be accounted for in terms of the total number of active metal sites present.

- At temperatures up to 815°C (1088°K) for time periods of several hours, exposure of either the Shell or Engelhard catalysts to high vacuum environments has little effect on either the surface structure or the catalysts or their capacity to promote low temperature H_2-O_2 reaction.

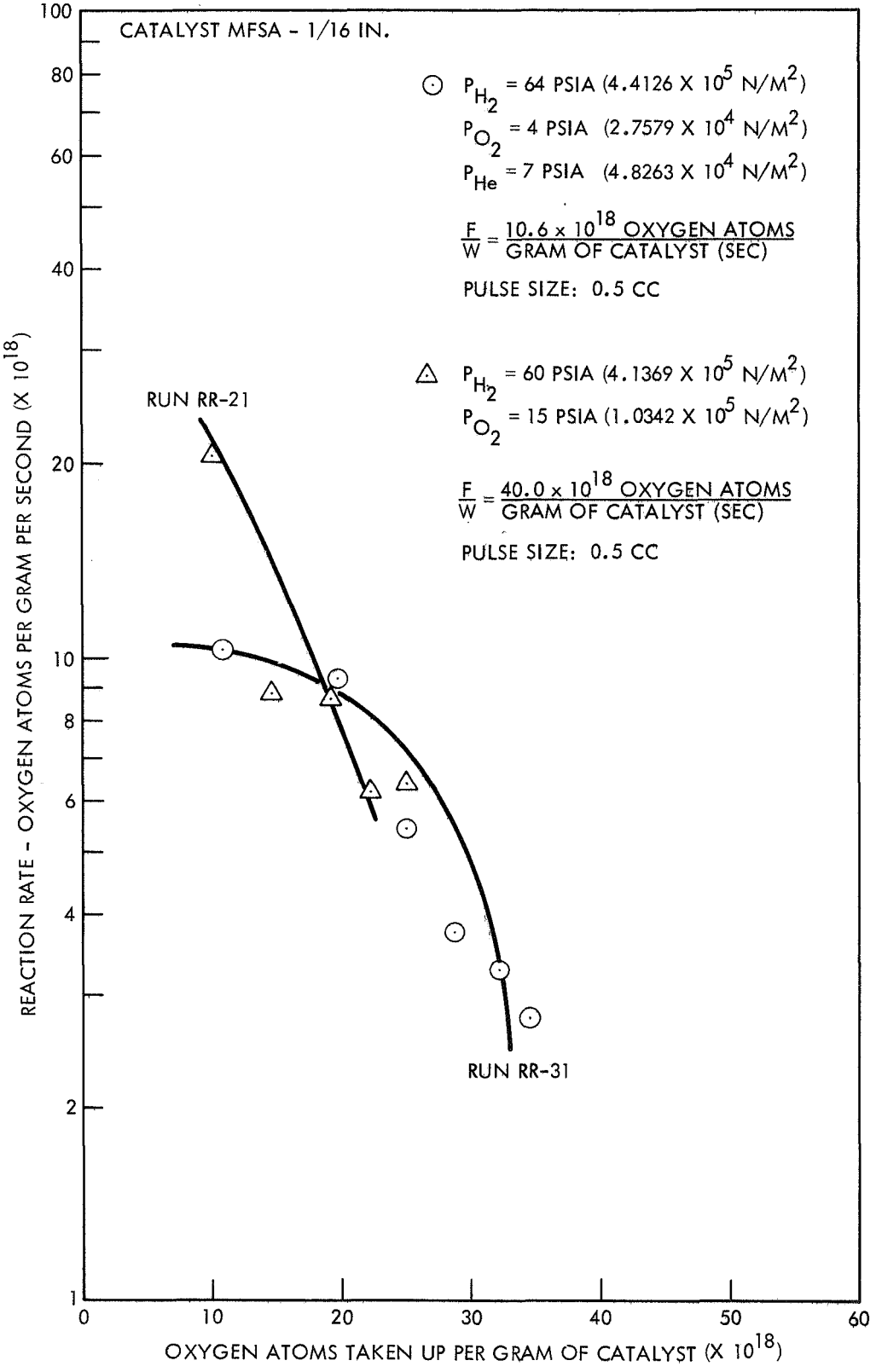

Figure 26. Reaction Rate as a Function of the Hydrogen-to-Oxygen Mixture Ratio at -125°C (148°K)

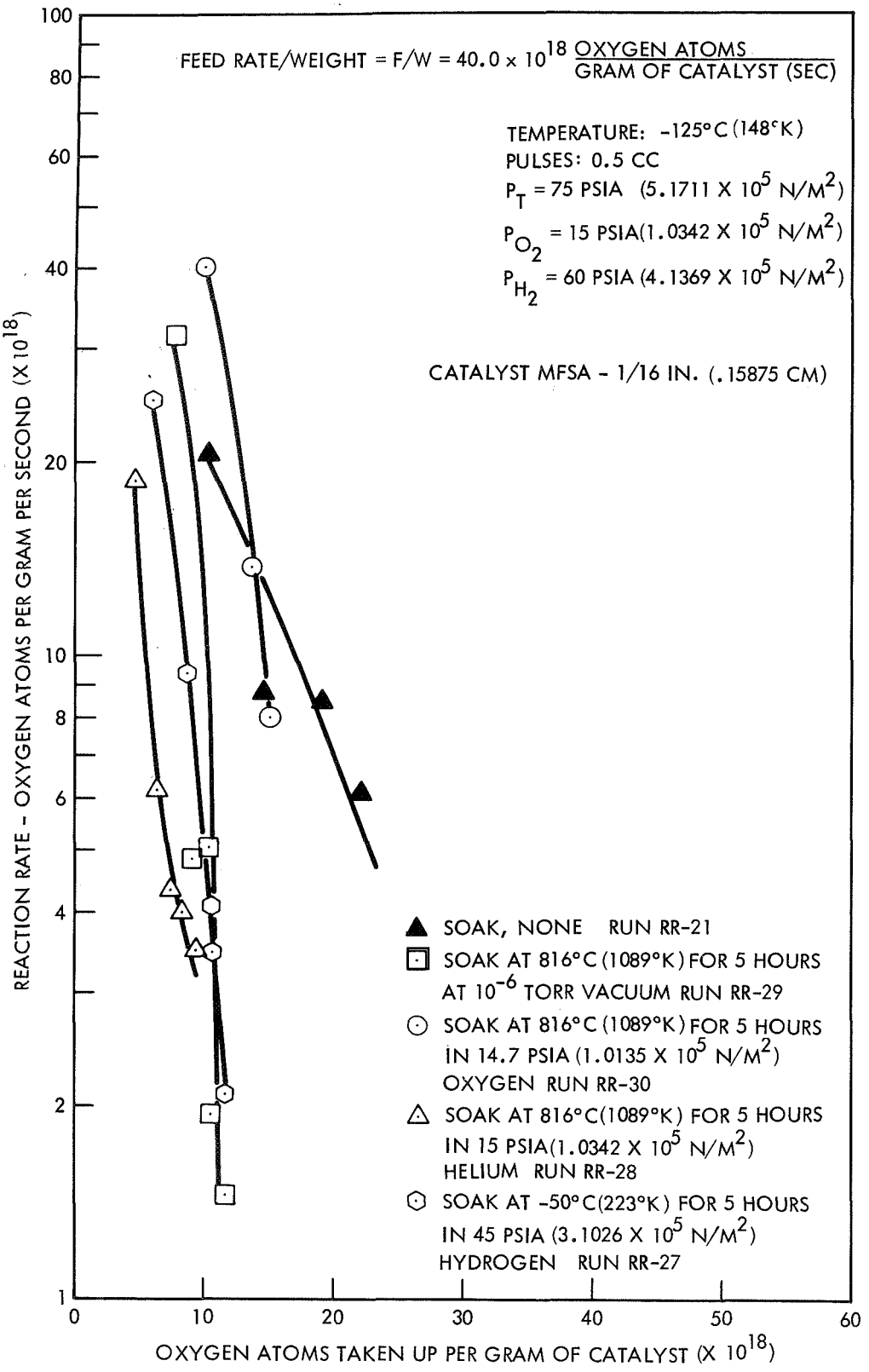

Figure 27. Reaction Rate as a Function of Soak Environment

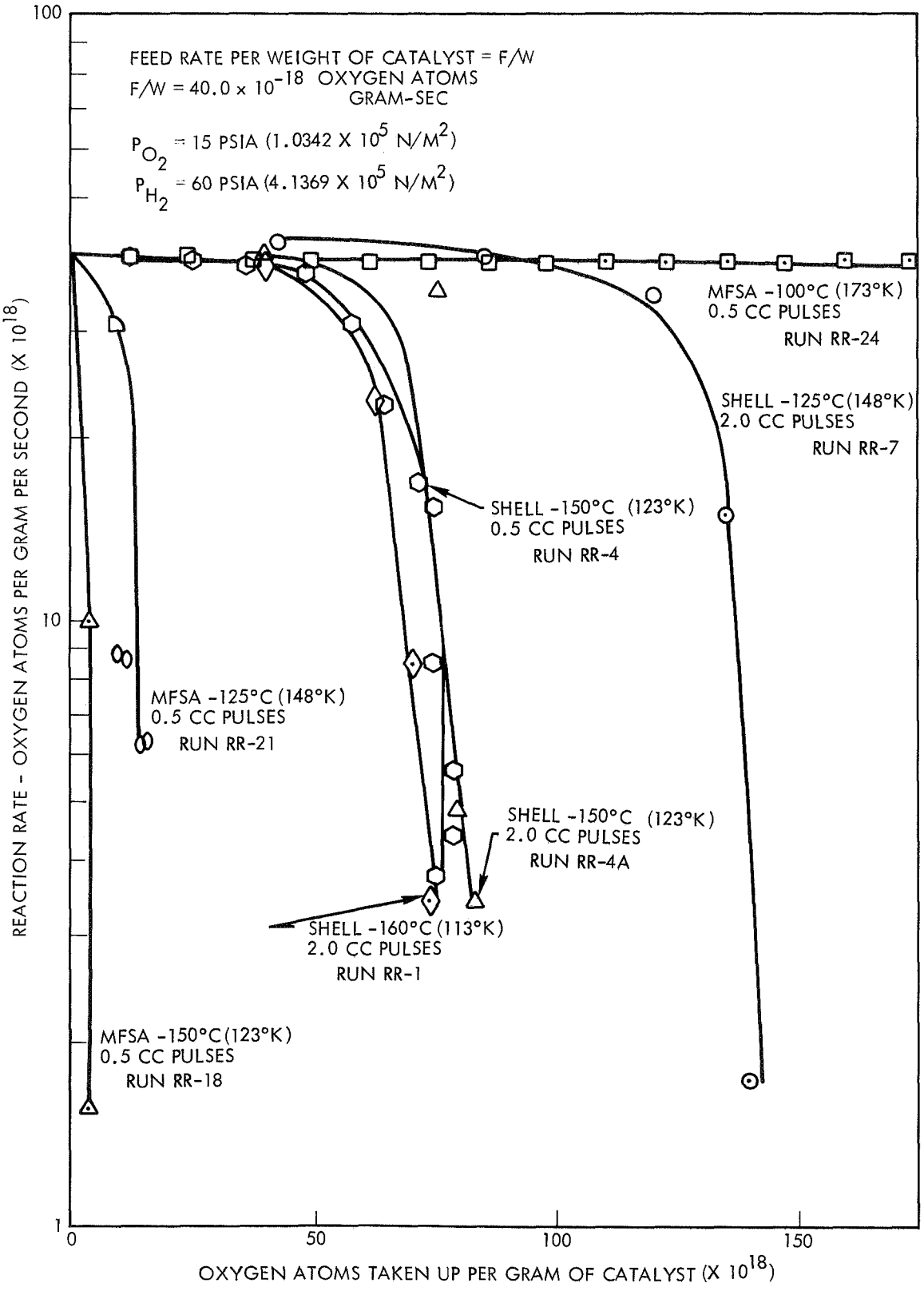

Figure 28. Low Temperature Reaction Rates — Shell 405 ABSG and Engelhard MFSA Catalysts

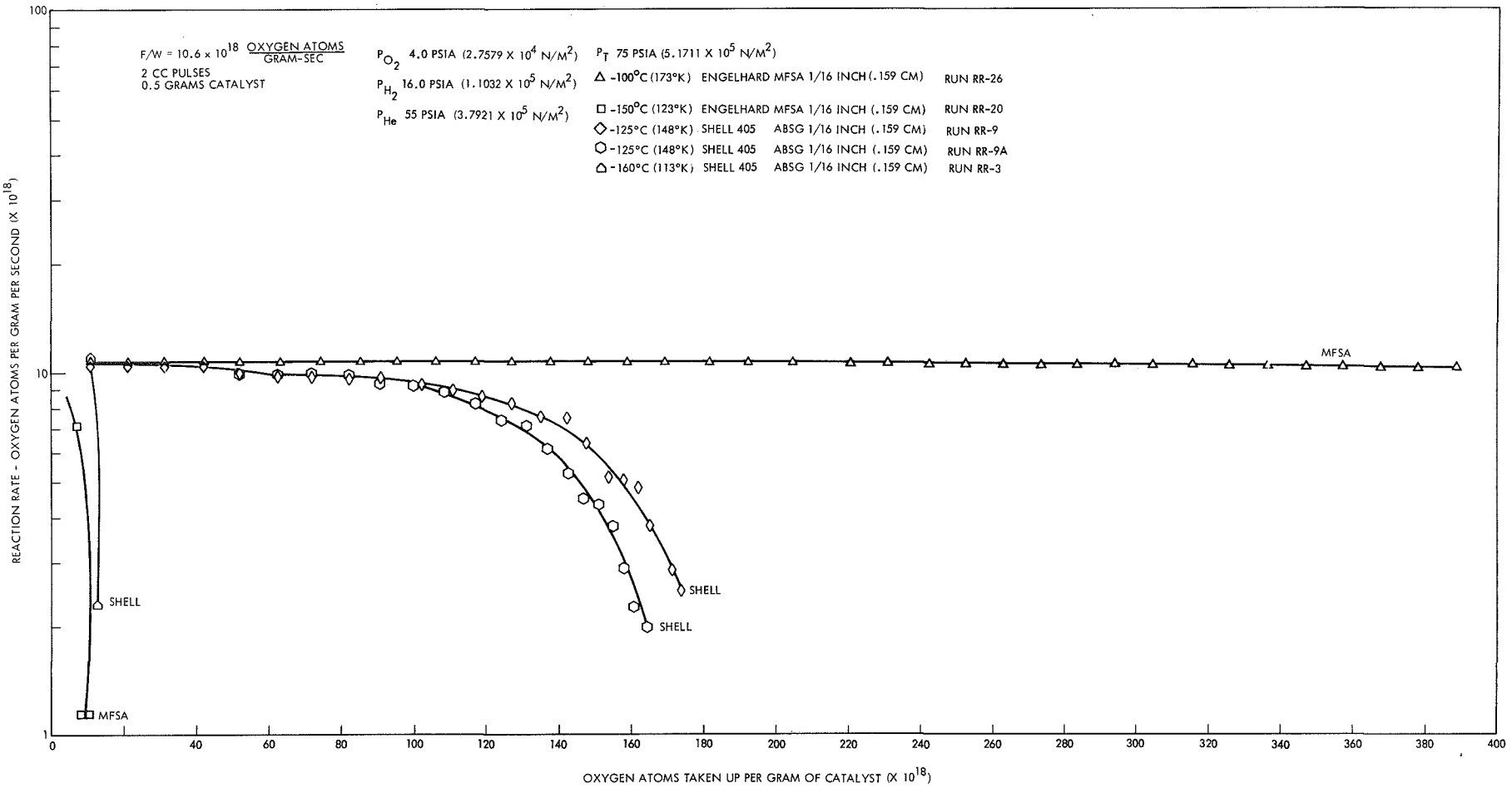

Figure 29. Comparison of Shell 405 ABSG and Engelhard MFSA Catalysts as a Function of Temperature, Total Reactant Gas Pressure = 20 psia (1.3790×10^5 N/M^2)

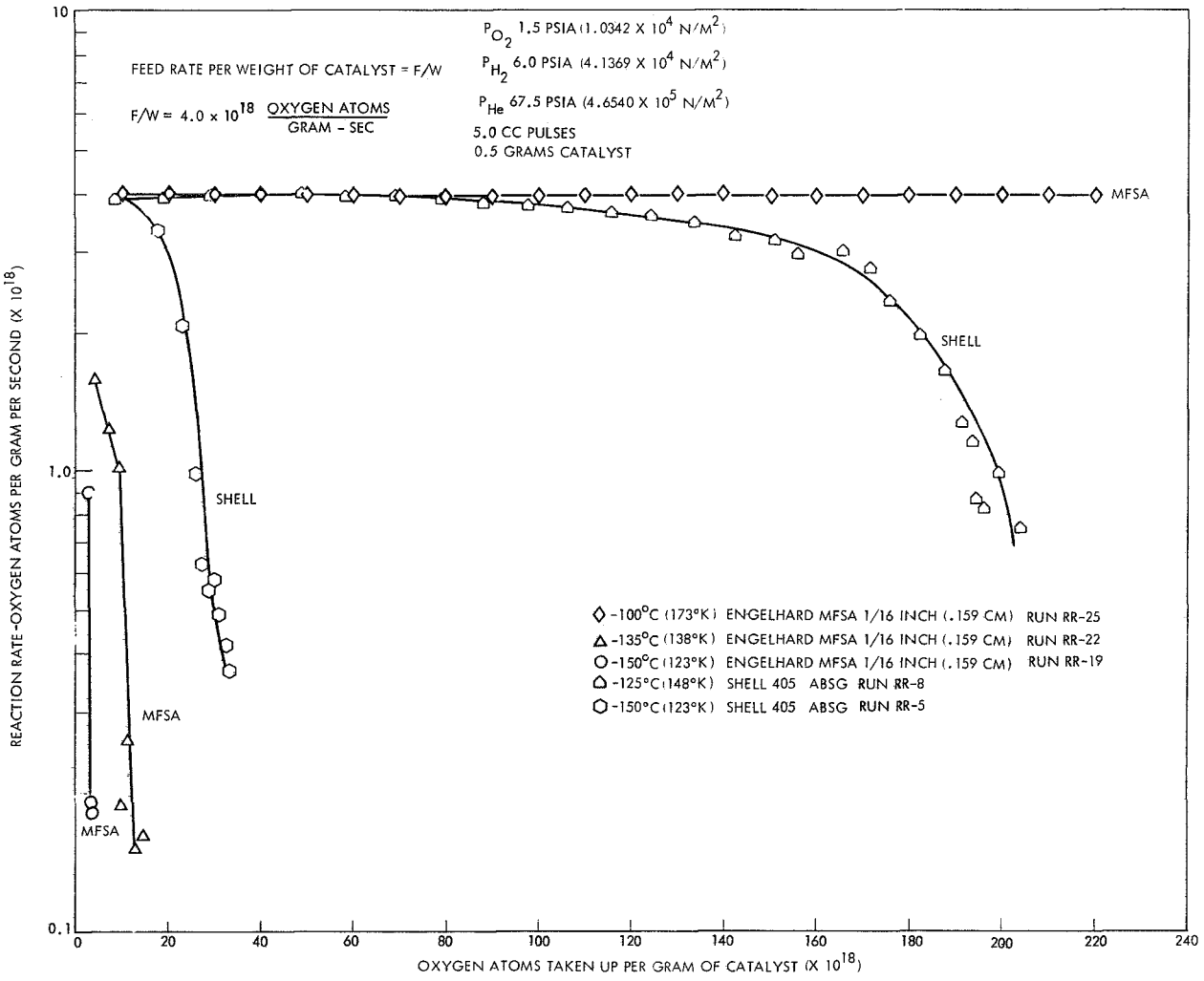

Figure 30. Comparison of Shell 405 ABSG and Engelhard MFSA Catalysts as a Function of Temperature, Total Reactant Gas Pressure = 7.5 psia (5.1711×10^4 N/M^2)

4. CATALYTIC REACTOR EXPERIMENTS

A series of reactor test firings were performed to determine the effects of vacuum on ignition delay time for each of the two candidate catalyst formulations. The catalysts evaluated, Shell 405 and Engelhard MFSA, were the same two types investigated during the laboratory studies described in the previous report section. The objectives of this task were:

- Design and fabricate catalytic reactors for each pressure level thruster.
- Establish ignition delay times for each catalyst type by reactor test firings.
- Determine the combined effect on reactor ignition delay caused by variables such as length of catalyst bed, vacuum environment, propellant and bed temperatures prior to ignition, and helium dilution of propellants.
- Determine the most significant environmental conditions and the superior catalyst formulation for combined thruster/igniter optimization.

The following paragraphs describe in detail the reactor hardware and test procedures utilized, and discuss the experimental results obtained.

4.1 REACTOR HARDWARE DESCRIPTION

A separate catalytic reactor was designed and fabricated for each thruster chamber pressure level, 10 and 100 psia (69 and 690 kN/m^2). Each reactor was to incorporate extensive pressure and temperature instrumentation capability and to accommodate catalyst bed length variations.

4.1.1 Low Pressure Reactor Igniter

The basic design of the igniter for the low chamber pressure thruster is illustrated in Figure 31. The igniter components were fabricated almost entirely from 1-inch (2.54 cm) standard stainless steel fittings and tubing for ease of modification. Pre-mixing of the propellants was accomplished by injecting the oxygen radially through a series of orifices into the hydrogen inlet flow. Further mixing of the gases occurs within the injection volume, mixing section, and diffusion bed.

The igniter assembly required only two seals, and the major components were threaded together as indicated. The mixing section contained replaceable sleeve and orifice plate inserts, which provided the capability of changing the gas velocity through the mixing section to prevent flashback from the catalyst bed over the required range of propellant inlet temperatures. Variations in catalyst bed length were tested by inserting bed cartridge tubes of different lengths and changing the length of the adjustment spacer.

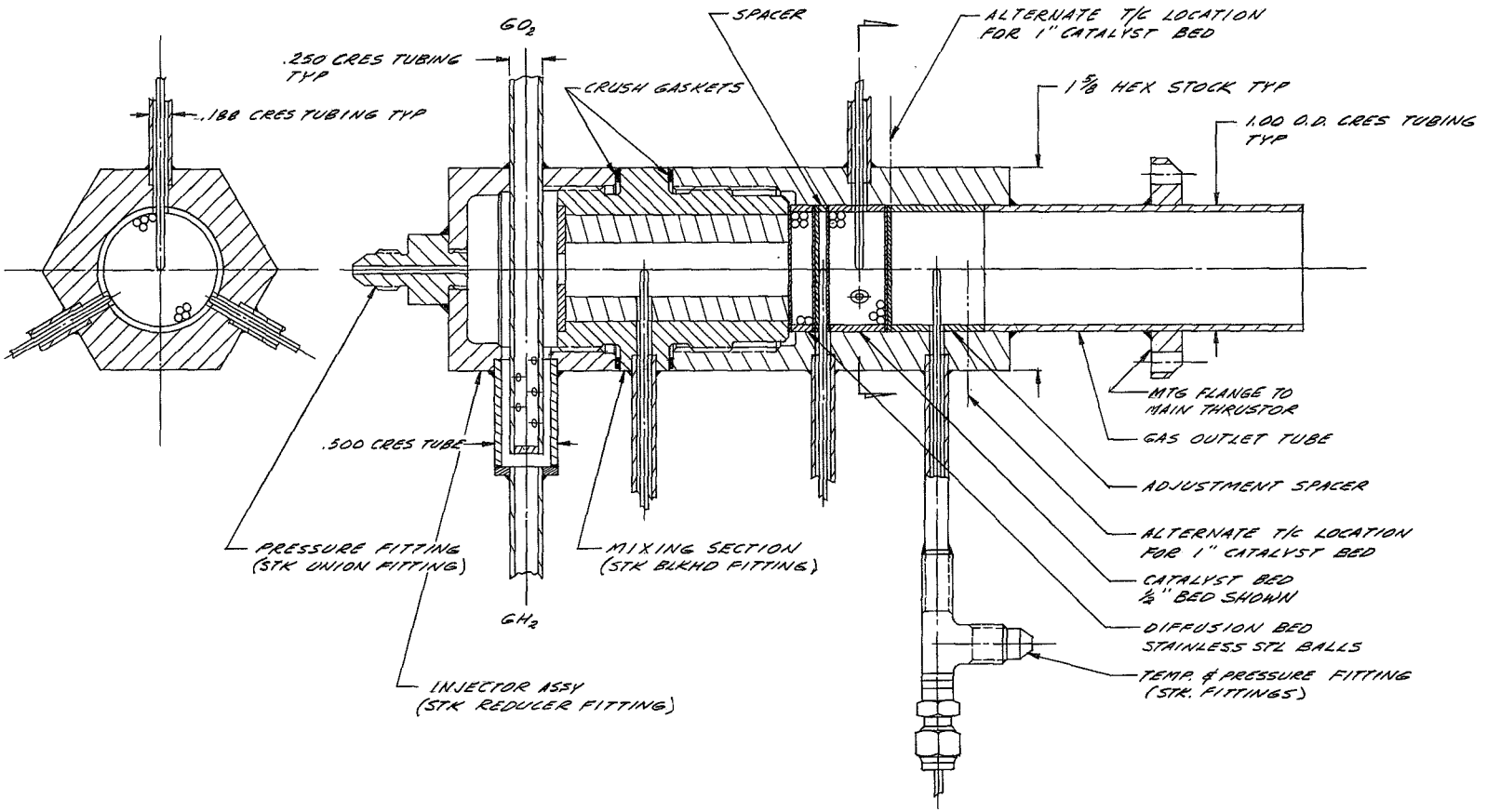

Figure 31. Catalytic Reactor Igniter—Low Chamber Pressure Thruster

Reactor instrumentation ports were provided at the locations shown in Figure 31. Both pressure and temperature measurements were taken at each location within the mixing zone, diffusion zone, catalyst bed, and downstream chamber by means of the tee fitting configurations illustrated. Additional temperature measurements were taken radially and circumferentially within the catalyst bed, as shown in the section view at left. Bare-wire tipped Chromel/Alumel thermocouple probes were used for increased thermal response.

The completed low pressure reactor assembly is shown in Figure 32. A disassembled view of the same reactor is presented in Figure 33. From left to right, the components are: (1) reactor body and exit tube, (2) catalyst bed cartridge, (3) catalyst (Engelhard MFSA shown), (4) catalyst retaining screen (welded to cartridge after loading), (5) diffusion zone spacer, (6) diffusion bed cartridge, (7) stainless steel balls, (8) retaining screen, (9) mixing section, and (10) injector assembly. The reactor readily accommodated catalyst beds of various lengths and diameters, and the replaceable inserts within the mixing section facilitated modifications during the test program.

4.1.2 High Pressure Reactor Igniter

The design concept for the high chamber pressure thruster igniter was identical to Figure 31, except that the overall size was reduced to one-half inch (1.27 cm) fitting and tube sizes. The same provisions for pressure and temperature instrumentation and variation of catalyst bed configurations were also incorporated in this hardware.

The reactor assembly is illustrated in Figure 34, and a disassembled view is shown in Figure 35. From left to right, the components are: (1) reactor body and exit tube, (2) spacer (changed to accommodate catalyst beds of varied lengths), (3) catalyst bed cartridge, (4) catalyst (Shell 405 ABSG shown), (5) catalyst retaining screen, (6) diffusion zone spacer, (7) diffusion bed cartridge, (8) stainless steel balls, (9) retaining screen, (10) mixing section, and (11) injector assembly. Numerous catalyst bed configurations were prepared for testing, as described in subsequent sections of this report.

4.2 TEST INSTALLATION AND PROCEDURES

All testing was conducted at the TRW Systems Inglewood Test Site, C-2 altitude test stand. The stand steam ejection system has a 120,000 feet (36580 m) simulated altitude capability. The ignition effects of a higher vacuum level, nominally 10^{-5} mm Hg, were investigated by employment of an auxiliary high vacuum chamber and associated pumping equipment, as described in the following paragraphs.

4.2.1 Test Stand Installation

The altitude test stand installation of the low chamber pressure thruster igniter is shown in Figure 36. This photograph, taken with the steam ejection system vacuum cover retracted, shows the low pressure

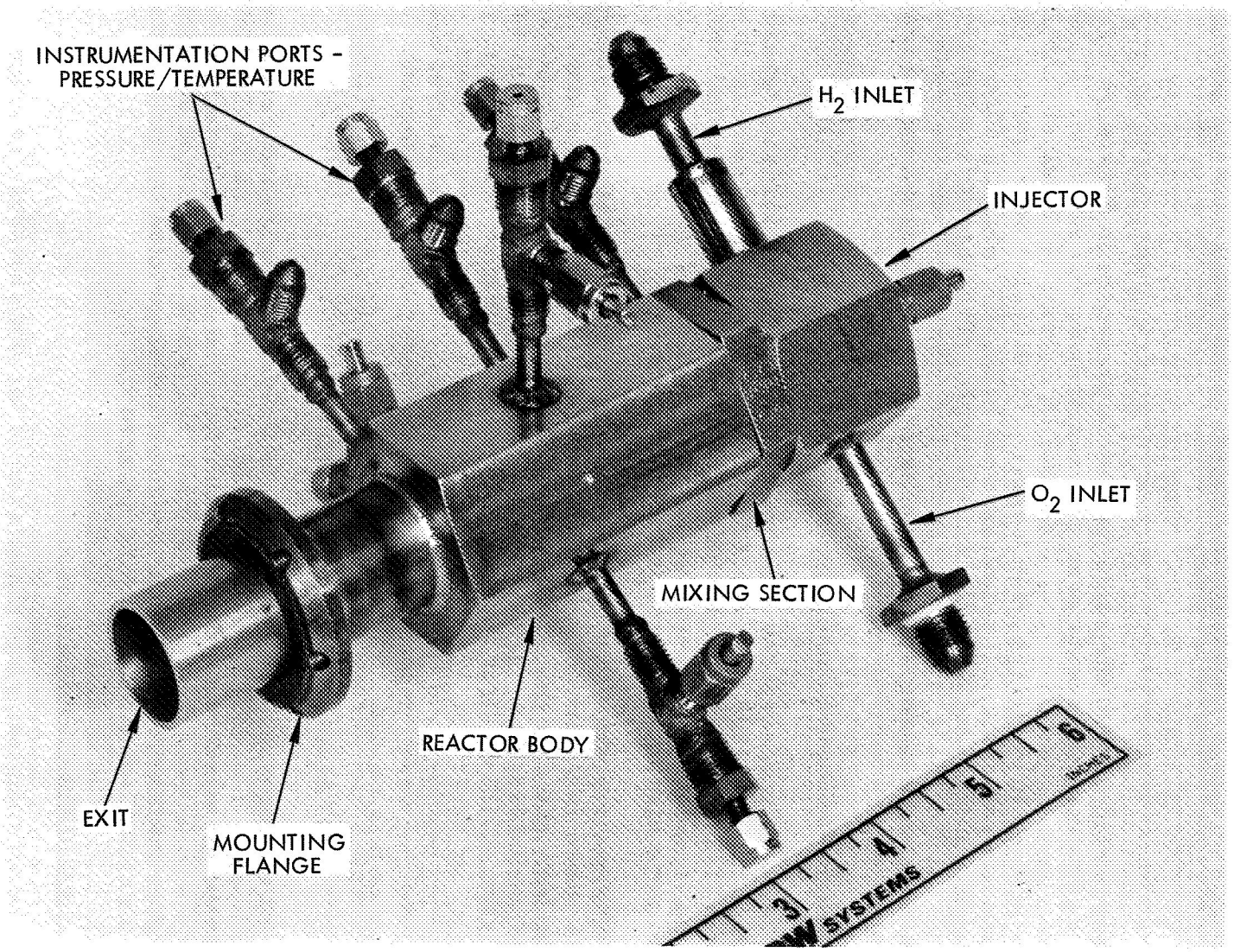

Figure 32. Catalytic Reactor Igniter Assembly—Low Chamber Pressure Thruster

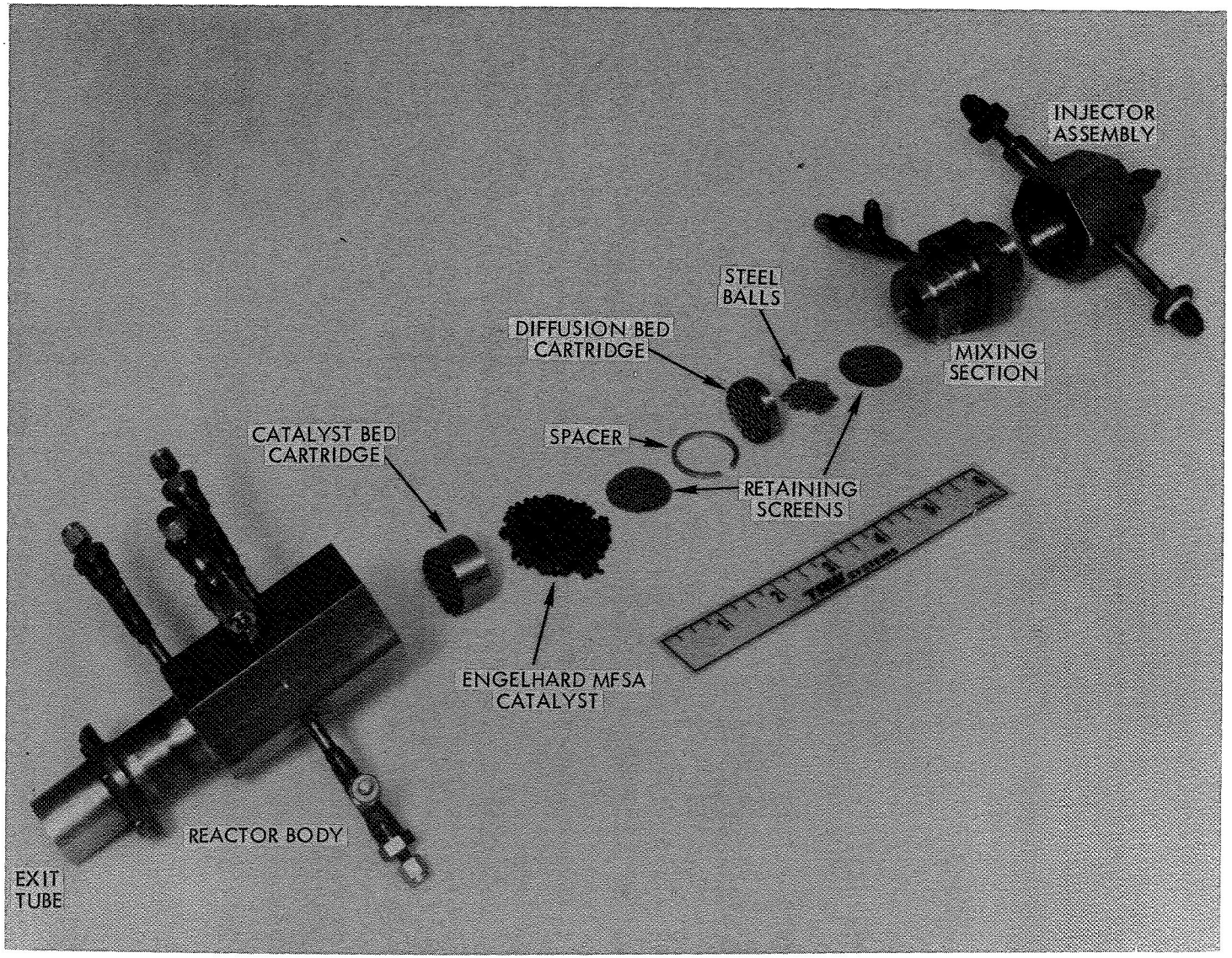

Figure 33. Disassembled Catalytic Reactor Igniter — Low Chamber Pressure Thruster

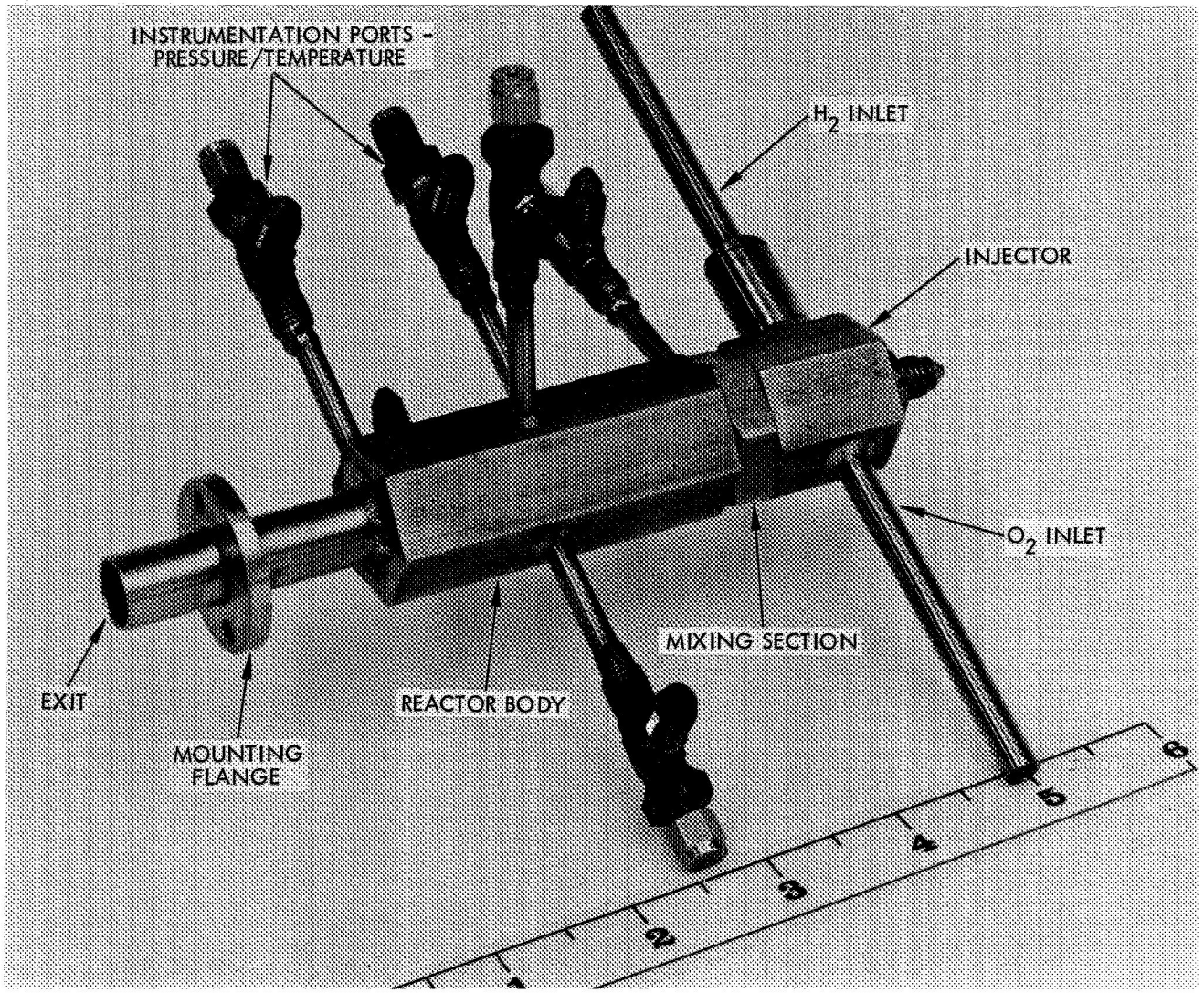

Figure 34. Catalytic Reactor Igniter Assembly—High Chamber Pressure Thruster

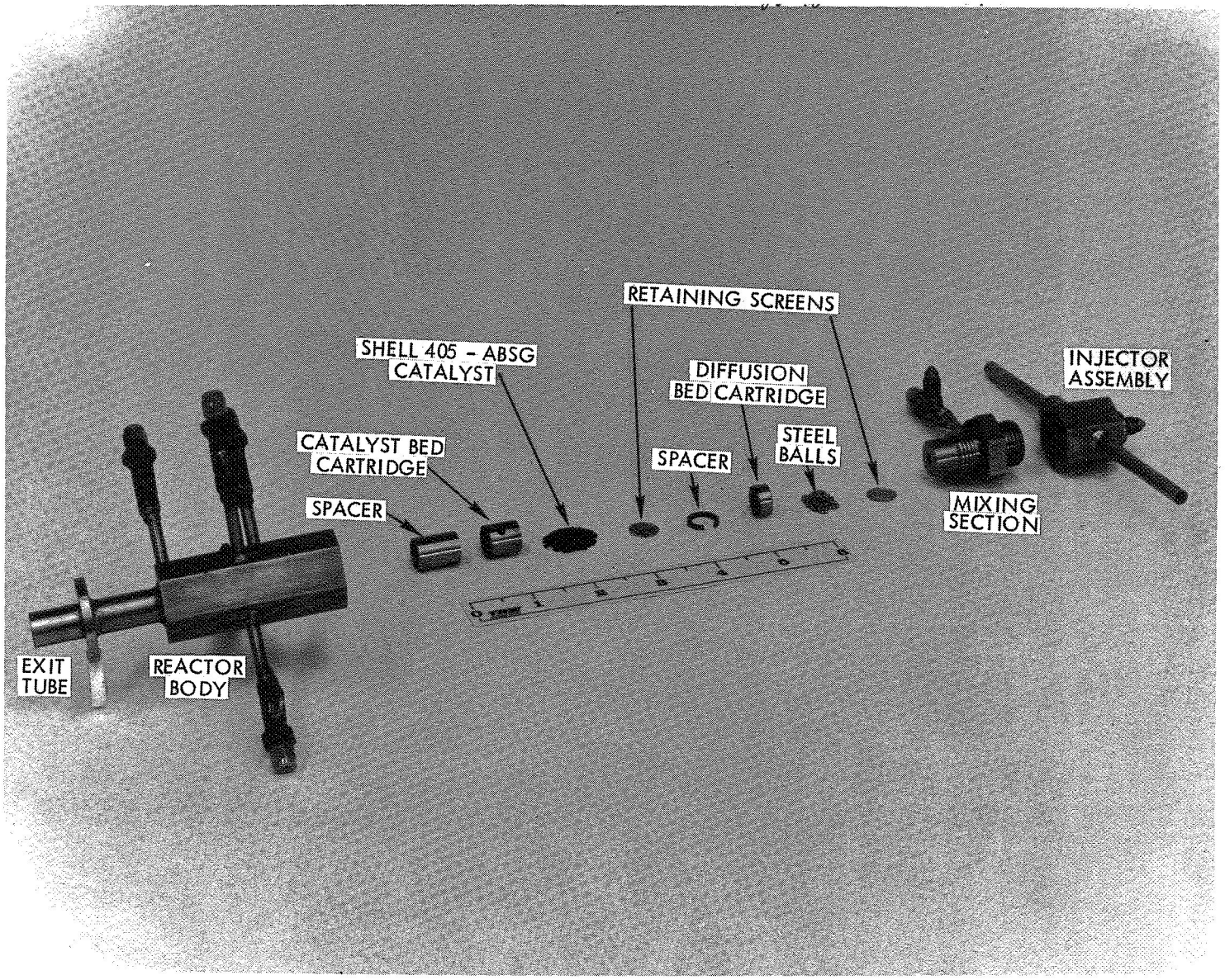

Figure 35. Disassembled Catalytic Reactor Igniter – High Chamber Pressure Thruster

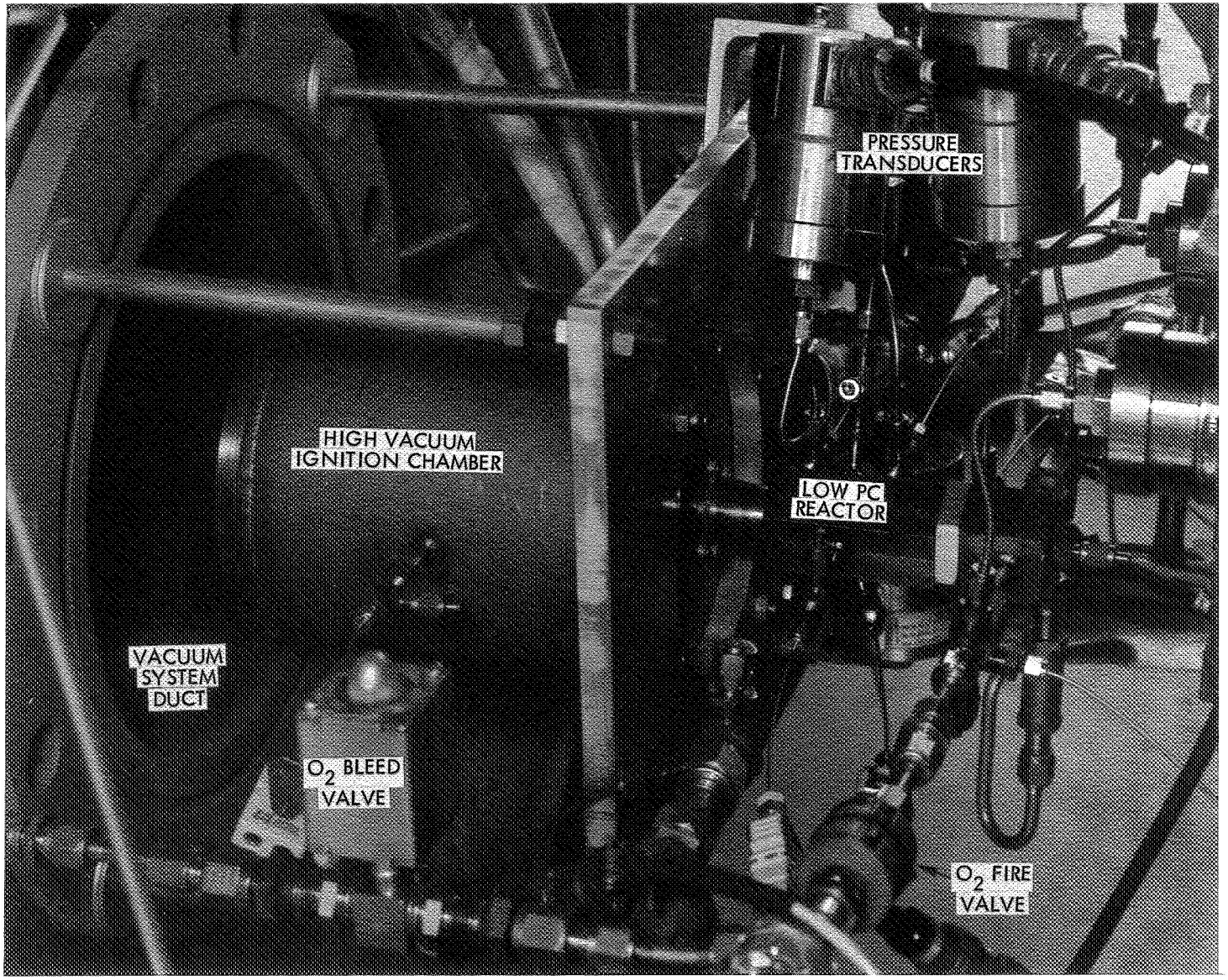

Figure 36. Altitude Test Stand Installation—Low P_c Catalytic Reactor and Auxiliary High Vacuum Ignition Chamber (H_2 feed system not shown, but identical to O_2 system)

catalytic reactor assembly mounted to the auxiliary high vacuum ignition chamber. The auxiliary chamber was used to attain the high vacuum, nominally 10^{-5} mm Hg, level for selected ignition tests. The cell vacuum level, 0.06 psia (413.7 N/m^2) nominal, was provided by the existing steam ejection system.

The auxiliary vacuum chamber (Figure 36, left) had an opening in the downstream end sealed by a flapper plate hinged at the top. High vacuum ignitions were performed by pumping down the auxiliary chamber to the 10^{-5} mm Hg level while the remainder of the cell was held at the vacuum level provided by the steam ejection system. Immediately after reactor flow was initiated, the flapper opened; however, the cell vacuum level was sufficient to maintain sonic flow at the reactor exit, and downstream pressures were no longer critical.

Figure 37 is an overall view of the altitude stand showing the auxiliary high vacuum pumping console. This unit contained a mechanical roughing pump and a diffusion pump capable of achieving a pressure level of 10^{-6} mm Hg, and was connected to the reactor downstream auxiliary vacuum chamber shown in the right background of Figure 37 and in the close-up view of Figure 36. An Alphatron vacuum gage shown in the line at the top of the console was used to monitor pump performance, and an ion gage (not visible in the photograph) was installed near the high vacuum chamber to measure actual pressures just prior to ignition. The large cell cover shown in the left background of Figure 37 was rolled forward to enclose the entire stand installation prior to all firings.

Figure 38 is a photograph of the high pressure reactor auxiliary vacuum chamber. The hinged flapper plate sealed against the "O" ring while the chamber was pumped down. The springs shown were added to each auxiliary chamber to maintain the vacuum seal after the steam ejection system had reduced the external pressure to 0.06 psia (413.7 N/m^2). These springs were positioned to provide sealing force, yet allowing opening of the flapper with minimal pressure rise after onset of propellant flow. Once the flapper opened, the springs also served to retract the plate away from the opening, as shown. This technique allowed the attainment of vacuum levels of 10^{-5} mm Hg. In addition, the auxiliary chamber exits had the same cross-sectional areas as the main thrust chamber throats, thus providing the same reactor downstream pressure levels that existed when the igniters were fired in the complete thruster assemblies.

4.2.2 Reactor Test Procedures

The test procedures for the reactor experiments were selected to insure maximum activity of the catalysts evaluated. Based upon the conclusions of the laboratory catalyst activity investigations listed in Section 3.3, the following techniques were employed to remove and exclude oxygen from the catalyst surface:

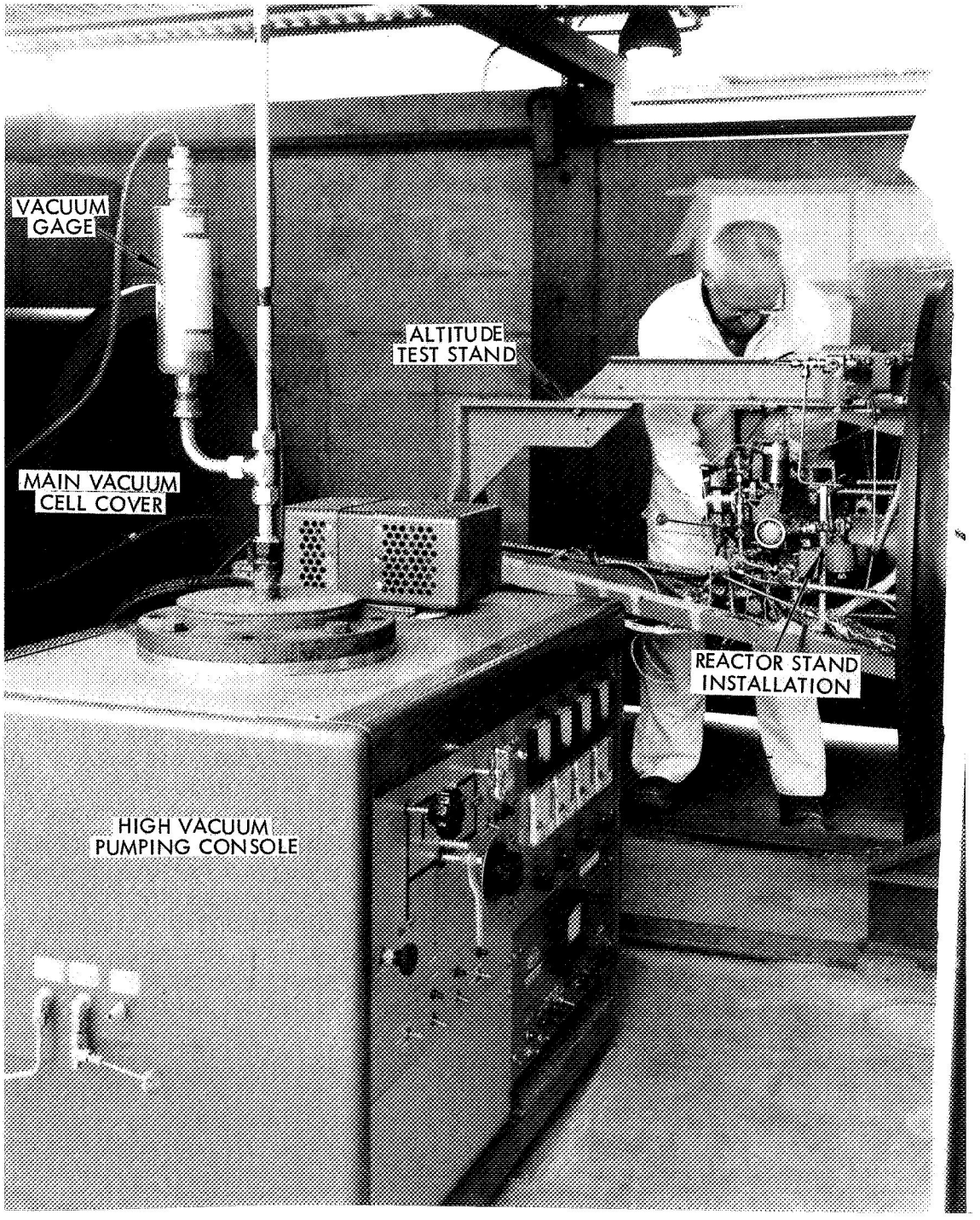

Figure 37. Auxiliary Vacuum Pump Installation For Catalytic Reactor High Vacuum Ignition Tests (10^{-5} mm Hg.)

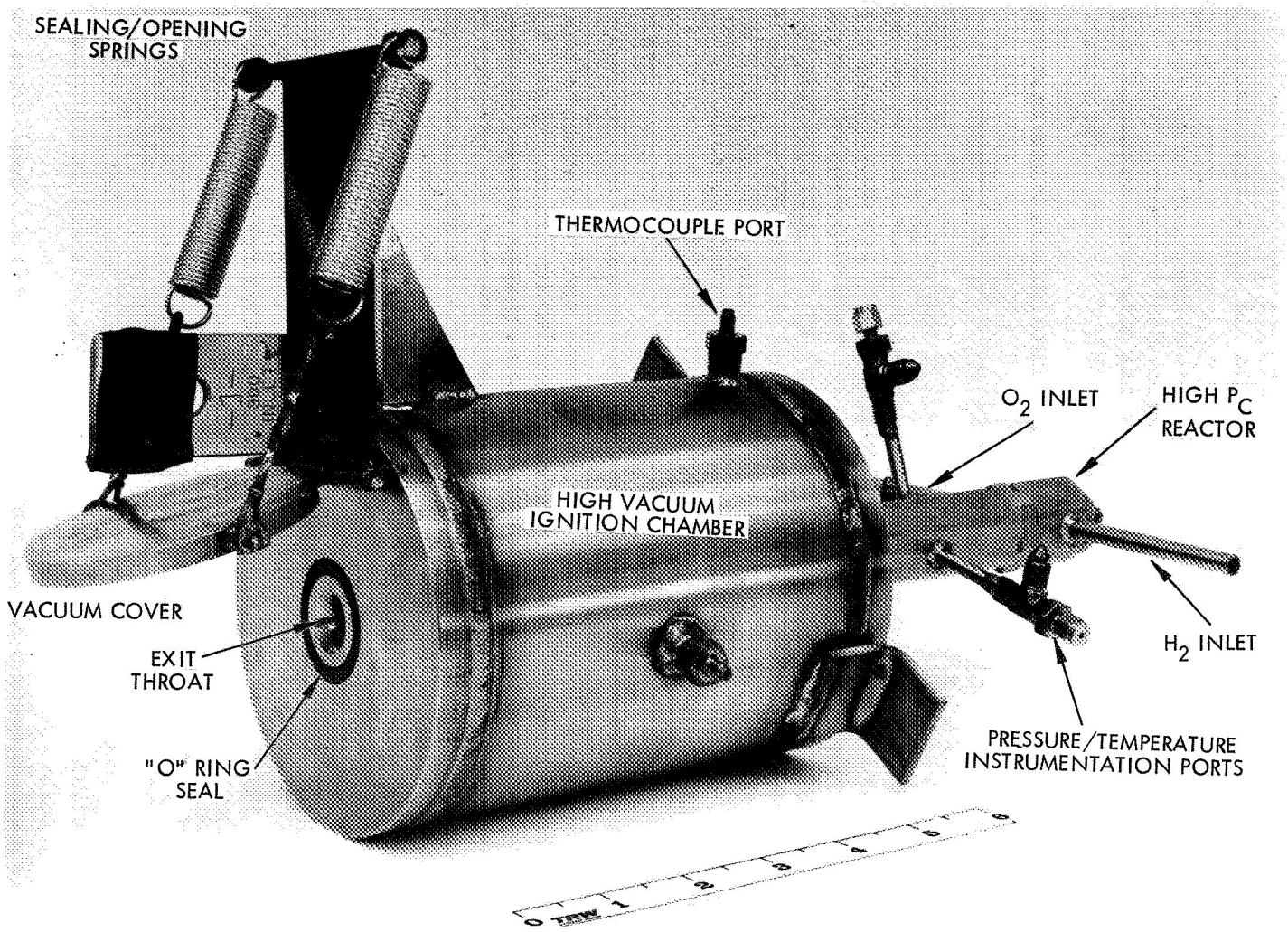

Figure 38. Auxiliary High Vacuum Ignition Chamber and Low P_c Catalytic Reactor

- All catalytic reactor firings were conducted under vacuum conditions with a hydrogen lead (nominally 10 milliseconds).

- Tests were terminated with a hydrogen lag, then purged with hydrogen to enhance catalyst activity by preabsorbing hydrogen on the catalyst surface.

- Low temperature ignition tests were preceded by operating the catalyst at elevated temperatures (pretreatment) to remove any absorbed oxygen, thus enhancing catalyst activity.

The approved test matrix for the catalytic reactor tests is presented in Table 13.

4.3 EXPERIMENTAL RESULTS

A total of 288 reactor test firings were conducted to evaluate the ignition characteristics of the Shell 405-ABSG and Engelhard MFSA catalysts at two vacuum ignition levels. Data from these tests are listed in Tables 14 and 15. The ignition effects of catalyst bed length, propellant and bed temperatures, and helium dilution of propellants were investigated. The following sections discuss the experimental data obtained with each pressure level reactor, and present the recommendations for catalyst selection based upon evaluation of overall results.

4.3.1 Reactor Test Data

The experimental data obtained from the low pressure and high pressure catalytic reactor tests are summarized in Tables 14 and 15, respectively. The three catalyst formulations evaluated were: (1) Shell 405-ABSG, 14-18 mesh, (2) Engelhard MFSA 1/16 inch (0.159 cm) spherical, and (3) a mixture of both the Shell 405-ABSG and Engelhard MFSA catalysts, as recommended after analysis of the laboratory catalyst activity experimental results. The low pressure reactor tests listed in Table 14 are described as follows:

Tests 737-755: Initial tests were conducted with a 0.870-inch (2.21 cm) diameter by 0.50-inch (1.27 cm) long Shell 405 bed. Igniter response and effluent temperatures were determined with ambient propellants at flow rates from 2.5 to 10 percent of nominal thruster flow rates.

Tests 756-762: These tests were performed to evaluate a 0.25-inch (0.637 cm) long Shell catalyst bed. Reduced effluent temperatures of ~1250°F (950°K) indicated this length bed was insufficient to support complete reaction with ambient temperature propellants at the flow rates tested.

Tests 763-768: Using the same catalyst bed, tests were performed with -250°F (117°K) propellants. Quenching of the reaction occurred on runs 766-768 with this bed length when flow rates were increased above 5 percent of nominal thruster flows.

Table 13. Catalytic Reactor Tests Minimum Test Matrix—Each Catalyst

Series I—Low Pressure Reactor Tests

Matrix Element* No.	Vacuum Level** H, L	Propellant Temp. °F (°K)	Bed Temp. °F (°K)	He in O_2 Dilution % He	He in H_2 Dilution % He	Bed Length L1, L2
1	L	70 (294)	70 (294)	0	0	L1
2	H	"	"	"	"	"
3	L	"	"	25	10	"
4	"	"	"	5	5	"
5	"	"	"	25		"
6	"	-100 (200)	-100 (200)	0	0	"
7	"	"	"	25	10	"
8	"	-250 (117)	-250 (117)	0	0	"
9	"	"	"	25	10	"
10	"	"	"	5	5	"
11-20	Repeat 1-10 above with increased catalyst bed length					L2

Series II—High Pressure Reactor

21-40 Repeat elements 1-20 above for high pressure reactor.

---

*One or more tests were conducted for each matrix element.

**Two different vacuum levels more maintained for ignition only: "L" indicates the lower vacuum level as provided by the latitude cell stream ejection system, and "H" indicates the higher vacuum ignition level to be attained by diffusion pumping of a sealed volume at the reactor exit. After onset of propellant flow, a sonic condition existed, and maintaining the higher vacuum level was not necessary.

Table 14. Low Pressure Reactor Test Data

Run No.	P Bed Inlet psia	P Bed Inlet kN/m^2	P_{CD} psia	P_{CD} kN/m^2	$\dot{W}_T$ lb/sec	$\dot{W}_T$ kg/sec	M.R. O/F	Max TE °F	Max TE °K	Response Time sec to .95 TE	Comments
C2-737	16.1	111.0	(a)		.0022	.00103	.992	1631	1162	4.89	
738	18.5	127.6	(a)		.00273	.00123	.993	1645	1169	3.47	
739	23.9	164.8	(a)		.00377	.00171	.999	1637	1165	2.74	
740	31.3	215.8	(a)		.00535	.00243	1.012	1637	1165	2.45	
741	15.2	104.8	(a)		.00221	.00100	.983	1643	1168	4.22	
742	6.4	44.1	(a)		.00069	.00032	1.070	1546	1114	9.92	
747	35.7	246.1	.856	5.9	.00560	.00254	1.007	1719	1210	3.13	Shell 405 ABSG, 14-18 mesh catalyst bed, .870 in. (2.21 cm) dia by .50 in. (1.27 cm) long, pure ambient propellants
748	21.2	146.2	.370	2.6	.00290	.00132	.965	1709	1205	4.19	
749	36.0	248.2	.856	5.9	.00555	.00252	1.014	1756	1231	2.71	
750	20.3	140.0	(a)		.00291	.00132	.972	1758	1232	(a)	
751	20.6	142.0	.537	3.7	.00291	.00132	.967	1757	1231	4.34	
752	31.9	219.9	.887	6.1	.00545	.00247	1.018	1736	1220	3.73	
753	32.4	223.4	1.000	6.9	.00544	.00247	1.014	1743	1224	3.09	
754	18.8	129.6	.523	3.6	.00277	.00126	.980	1687	1193	4.71	
755	9.8	67.6	.278	1.9	.00130	.00059	.828	1477	1076	7.52	
756	8.5	58.6	.543	3.7	.00280	.00127	.999	1252	951	(a)	
757	8.5	58.6	.533	3.7	.00279	.00127	.995	1321	989	4.96	
758	14.8	102.0	.944	6.5	.00535	.00243	1.031	1234	941	2.72	Shell 405 ABSG catalyst bed, .25 in. (.637 cm) long, pure ambient propellants
759	4.4	30.3	.264	1.8	.00128	.00058	.837	1267	959	5.58	
760	3.0	20.7	.187	1.3	.00081	.00037	.798	1215	930	10.82	
761	8.4	57.9	.540	3.7	.00283	.00128	1.011	1267	959	4.38	
762	8.5	58.6	.546	3.8	.00284	.00129	1.001	1312	984	4.62	
763	4.5	31.0	.278	1.9	.00137	.00062	.845	1184	913	7.44	Catalyst bed same as above, pure, -250°K (117°K) propellants bed initially at ambient temperature
764	7.4	51.0	.447	3.1	.00261	.00118	1.123	1301	978	(a)	
765	7.1	49.0	.446	3.1	.00267	.00121	1.077	1045	836	3.69	
766-68	Ignition and quench										
769	15.2	104.8	1.010	7.0	.00545	.00247	1.037	1107	870	5.15	
770	15.1	104.1	1.046	7.2	.00545	.00247	1.039	1049	838	6.53	
771	8.2	56.5	.641	4.4	.00277	.00126	.986	1159	899	16.93	
772	4.2	29.0	.294	2.0	.00124	.00056	.925	1317	987	24.14	Engelhard MFSA, .063 in. (.153 cm) dia. catalyst. bed length .50 in. (1.27 cm), pure ambient propellants
773	6.2	42.7	.547	3.8	.00282	.00128	1.011	588	582	35.96	
774	6.2	42.7	.541	3.7	.00281	.00127	1.012	687	637	16.14	
775	11.4	78.6	1.046	7.2	.00548	.00249	1.034	514	541	11.59	
776	3.2	22.1	.293	2.0	.00124	.00056	.935	991	806	21.60	
777	18.7	128.9	15.586	107.5	.00503	.00228	.855	1192	918	(a)	
778	24.6	169.6	20.753	143.1	.00549	.00249	1.019	1861	1289	9.51	
779	24.7	170.3	20.739	143.0	.00541	.00245	.995	1866	1292	2.93	Catalyst bed same as above, igniter throat added, D_t = .268 in. (.60 cm)
780	25.4	175.1	21.401	147.6	.00551	.00250	1.032	1891	1306	2.80	
781	13.5	93.1	10.834	74.7	.00287	.00130	1.020	1873	1296	4.24	
782	6.0	41.4	4.610	31.8	.00129	.00059	.877	1542	1112	9.20	
783	5.0	34.5	3.865	26.6	.00101	.00046	1.431	2048	1393	6.81	
784	5.2	35.9	4.107	28.3	.00115	.00052	1.105	1714	1208	6.91	Same configuration, propellants at -250°F (117°K), ambient bed—ignition and quench
785	11.0	75.8	9.352	64.5	.00238	.00108	1.371	2045	1391	2.94	
786	18.9	130.3	16.599	114.4	.00400	.00181	.720	942	779	15.91	
787	4.8	33.1	3.936	27.1	.00115	.00052	1.167	1450	1061	7.04	

[a] Data invalid.

Table 14. Low Pressure Reactor Test Data (Continued)

Run No.	P Bed Inlet psia	P Bed Inlet kN/m^2	P_{CD} psia	P_{CD} kN/m^2	$\dot{W}_T$ lb/sec	$\dot{W}_T$ kg/sec	M.R. O/F	Max TE °F	Max TE °K	Response Time sec to .95 TE	Comments
788	14.8	102.0	.334	2.3	.00282	.00128	1.012	1707	1204	5.33	Engelhard MFSA catalyst, bed length 1.0 in. (2.54 cm), no igniter throat, pure ambient propellants.
789	14.9	102.7	.336	2.3	.00284	.00129	1.003	1723	1213	5.27	
790	25.8	177.9	.713	4.9	.00542	.00246	1.003	1690	1194	3.38	
791	26.0	179.3	.722	5.0	.00541	.00245	1.014	1707	1204	3.33	
792	7.0	48.3	.145	1.0	.00122	.00055	.874	1552	1118	9.91	
793	6.6	45.5	.279	1.9	.00265	.00120	1.092	1287	970	3.69	Same configuration propellants at -250°F (117°K), ambient bed—no sustained reaction.
794	4.0	27.6	.165	1.1	.00224	.00102	.590	174	352	12.79	
795	3.9	26.9	.170	1.2	.00234	.00106	.676	247	393	21.00	
796	4.3	29.6	.190	1.3	.00237	.00107	.641	288	415	7.71	
797	18.7	128.9	11.241	77.5	.00279	.00127	1.003	1812	1262	4.47	Engelhard MFSA catalyst, 1.0 in. (2.54 cm) long, igniter throat D_t = .268 in. (.68 cm), pure ambient propellants
798	18.8	129.6	11.298	77.9	.00280	.00127	1.000	1823	1268	4.18	
799	7.1	49.0	3.830	26.4	.00113	.00051	.755	1654	1174	7.80	
800	34.2	235.8	22.243	153.4	.00539	.00244	1.034	1862	1290	2.55	
801	16.8	115.8	9.996	68.9	.00145	.00066	.966	1804	1258	3.95	Same configuration, pure propellants and bed at -100°F (200°K)
802	16.1	111.0	10.043	69.2	.00147	.00067	.935	1689	1194	5.21	
803	15.5	106.9	9.95	68.6	.00148	.00067	.953	1738	1221	7.15	
804	27.0	186.2	18.93	130.5	.00288	.00131	.948	1683	1190	3.89	
805	6.5	44.8	3.83	26.4	.00062	.00028	.853	1563	1124	10.83	
806	4.9	33.8	3.31	22.8	.00105	.00048	.982	49	283	2.40	-100°F (200°K), 25%He-O_2, pure H_2
807	6.9	47.6	4.34	29.9	.00095	.00043	.763	1597	1143	25.85	-100°F (200°K), pure O_2, 10% He-H_2
808	10.6	73.1	7.25	50.0	.00160	.00073	.970	772	684	6.80	25% He-O_2, pure H_2
809	10.4	71.7	6.82	47.0	.00143	.00065	1.232	1092	862	6.20	
810	11.1	76.5	7.46	51.5	.00159	.00072	1.035	877	743	5.25	25% He-O_2, 10% He-H_2
811	17.5	120.7	10.618	73.2	.00156	.00071	1.000	1948	1338	4.61	Pure O_2, 10% He-H_2
812	16.4	113.1	10.169	70.1	.00147	.00067	.943	1897	1309	3.93	-250°F (117°K) pure propellants, ambient bed
813	5.3	36.5	3.694	25.5	.00157	.00071	.952	No ignition		-	-250°F (117°K) propellants and bed
814	30.1	207.5	.545	3.8	.00277	.00126	1.016	1640	1166	5.57	Shell 405 ABSG catalyst, 1.0 in. (2.54 cm) bed length, pure ambient propellants
815	25.7	177.2	.475	3.3	.00260	.00118	.894	1644	1169	5.09	
816	43.8	302.0	1.012	7.0	.00430	.00195	1.047	1713	1207	3.66	
817	15.6	107.6	.184	1.3	.00128	.00058	.973	1542	1112	9.45	
818	52.1	359.2	1.600	11.0	.00540	.00245	1.011	1700	1200	3.46	
819	16.0	110.3	.538	3.7	.00250	.00113	.776	837	720	5.63	25% He-O_2, pure H_2
820	24.8	171.0	.729	5.0	.00257	.00117	.832	1690	1194	5.41	Pure O_2, 10% He-H_2
821	20.7	142.7	.644	4.4	.00285	.00129	1.019	893	751	5.16	-250°F(117°K), 25% He-O_2, pure H_2
822	29.4	202.7	.879	6.1	.00283	.00128	.984	1745	1225	4.78	Same configuration, pure propellants at -250°F (117°K)
823	13.1	90.3	.385	2.7	.00142	.00064	.759	1213	929	16.96	
824	15.0	103.4	.581	4.0	.00306	.00139	.807	1321	989	10.40	
825	46.6	321.3	1.587	10.9	.00545	.00247	.977	1664	1180	4.00	
826	7.0	48.3	.197	1.4	.00143	.00065	.971	No ignition		-	-250°F (117°K), 25%He-O_2, pure O_2
827	26.7	184.1	.811	5.6	.00301	.00137	.904	1519	1099	6.04	-250°F (117°K), pure O_2, 10% He-H_2
828	8.6	59.3	.264	1.8	.00293	.00133	.925	No ignition		-	-250°F (117°K), 25% He-O_2, 10% He-H_2

Table 14. Low Pressure Reactor Test Data (Continued)

Run No.	P Bed Inlet psia	P Bed Inlet kN/m²	P_{CD} psia	P_{CD} kN/m²	$\dot{W}_T$ lb/sec	$\dot{W}_T$ kg/sec	M.R. O/F	Max TE °F	Max TE °K	Response Time sec to .95 TE	Comments
829	10.1	69.6	8.671	59.8	.00108	.00049	.741	1554	1119	9.41	Engelhard MFSA catalyst bed, 1.0 inch (2.54 cm) long, igniter throat D_t = .170 in (.43 cm)
830	9.1	62.7	7.965	54.9	.00089	.00040	.421	1574	1130	8.43	
831	31.7	218.6	28.267	194.9	.00284	.00129	.970	1557	1120	4.10	
832	9.5	65.5	8.421	58.1	.00126	.00057	1.028	758	676	7.23	25%He-O_2, pure H_2
833	21.3	146.9	19.565	134.9	.00282	.00128	.982	769	683	3.77	
834	10.4	71.7	8.809	60.7	.00111	.00050	.747	1495	1086	8.34	Pure O_2, 10%He-H_2
835	9.6	66.2	8.472	58.4	.00124	.00056	1.048	791	695	7.89	25%He-O_2, 10%He-H_2
836	13.2	91.0	11.277	77.8	.00138	.00063	.763	1409	1038	7.13	
837	5.4	37.2	5.181	35.7	.00073	.00033	.690	No Ignition		--	-250°F (117°K) pure propellants
838	10.2	70.3	9.589	66.1	.00150	.00068	.762	No Ignition		--	
839	10.3	71.0	7.947	54.8	.00093	.00042	.522	1619	1155	6.70	Shell 405-ABSG catalyst bed, .50 in. (1.27 cm) long, igniter throat D_t = .170 in. (.43 cm)
840	12.2	84.1	9.223	63.6	.00111	.00050	.809	1599	1144	5.79	
841	33.8	233.0	28.008	193.1	.00278	.00126	.986	1755	1230	3.16	
842	9.6	66.2	7.612	52.5	.00117	.00053	1.004	862	734	5.64	25%He-O_2, pure H_2
843	22.1	152.4	18.829	129.8	.00278	.00126	.953	737	665	2.18	
844	15.4	106.2	11.548	79.6	.00122	.00055	.956	1636	1164	5.98	Pure O_2, 10%He-H_2
845	11.0	75.8	8.749	60.3	.00127	.00058	1.051	856	731	5.60	25%He-O_2, pure H_2
846	15.5	106.9	11.797	81.3	.00157	.00071	.673	1626	1159	5.46	-250°F (117°K) propellants
847	14.1	97.2	11.426	78.7	.00164	.00074	.628	1342	1001	10.07	
848	10.8	74.5	9.580	66.1	.00198	.00090	.498	No Ignition		--	-250°F (117°K) propellants and bed
849	9.3	64.1	7.473	51.5	.00102	.00046	.295	1167	904	3.72	Ambient propellants and bed
850	30.7	211.7	26.157	180.3	.00332	.00151	.704	1551	1117	4.16	-250°F (117°K), pure propellants
851	5.9	40.7	5.173	35.7	.00155	.00070	.695	No Ignition		--	-250°F (117°K), 25%He-O_2, pure H_2
852	12.9	88.9	10.639	73.4	.00143	.00065	.686	1248	949	9.22	-250°F (117°K), pure O_2, 10%He-H_2
853	5.9	40.7	5.131	35.4	.00151	.00068	.753	No Ignition		--	-250°F (117°K), 25%He-O_2, 10%He-H_2
998	11.0	75.8	8.523	58.8	.00101	.00046	.692	1699	1199	9.81	Mixed catalyst bed—.50 in. (1.27 cm) shell 405-ABSG upstream .50 in. (1.27 cm) Engelhard MFSA downstream, pure ambient propellants
999	14.8	102.0	11.049	76.2	.00122	.00055	1.089	1809	1260	7.80	
1000	25.5	175.8	20.812	143.5	.00221	.00100	1.004	1783	1246	4.77	
1001	31.3	215.8	25.836	178.1	.00280	.00127	.989	1842	1279	3.92	
1002	23.3	160.6	20.321	140.1	.00295	.00134	1.087	927	770	3.13	25%He-O_2, pure H_2
1003	23.3	160.6	20.384	140.5	.00297	.00135	1.078	911	761	3.97	
1004	28.3	263.4	23.839	164.4	.00284	.00129	.990	1586	1136	4.30	5%He-O_2, pure H_2
1005	12.0	82.7	9.685	66.8	.00120	.00054	.897	1695	1197	8.20	-100°F (200°K), pure propellants
1006	10.7	73.8	8.822	60.8	.00120	.00054	.922	1536	1109	7.91	-100°F (200°K), 5%He-O_2, pure H_2
1007	7.1	49.0	6.573	45.3	.00104	.00047	.684	912	762	6.23	-100°F (200°K), 25%He-O_2, pure H_2
1008	13.4	92.4	10.988	75.8	.00132	.00060	.831	1497	1987	7.15	
1009	11.0	75.8	9.448	65.1	.00118	.00054	.773	1522	1101	8.83	
1010	29.8	205.5	26.457	182.4	.00305	.00138	.886	1528	1104	15.18	-250°F (117°K), pure propellants
1011	10.8	74.5	10.444	72.0	.00296	.00134	.858	No Ignition		--	
1012	10.5	72.4	9.423	65.0	.00121	.00055	.764	1524	1102	14.22	
1013	10.6	73.1	10.293	71.0	.00140	.00063	.938	1235	941	17.05	-250°F (117°K), 5%He-O_2, pure H_2
1014	4.1	28.3	4.610	31.8	.00140	.00063	.967	No Ignition		--	-250°F (117°K), 25%He-O_2, pure H_2
1015	4.8	33.1	5.086	35.1	.00209	.00095	1.925	No Ignition		--	
1016	15.2	104.8	12.886	88.8	.00216	.00098	2.156	1512	1095	13.62	
1017	50.9	350.9	44.090	304.0	.00485	.00220	.895	1788	1249	3.52	Pure ambient propellants
1018	12.6	86.9	11.816	81.5	.00135	.00061	.907	1679	1188	7.18	

Table 15. High Pressure Reactor Test Data

Run No.	P Bed Inlet psia	P Bed Inlet kN/m^2	PCD psia	PCD kN/m^2	$\dot{W}T$ lb/sec	$\dot{W}T$ kg/sec	M.R. O/F	Maximum TE °F	Maximum TE °K	Response Time sec to .95 TE	Comments
854	93.0	641.2	4.518	31.2	.00298	.00135	.835	1567	1126	2.45	Shell 405 ABSG, 14-18 mesh catalyst, .430 in. (1.09 cm) by 1.0 in. (2.54 cm) long, pure ambient propellants
855	101.3	698.4	4.861	33.5	.00307	.00139	.883	1671	1184	3.72	
856	168.0	1158.3	9.621	66.3	.00582	.00264	.897	1734	1219	1.47	
857	44.8	308.9	1.848	12.7	.00126	.00057	.775	1501	1089	4.92	
858	67.3	464.0	3.691	25.4	.00300	.00136	.876	832	718	1.76	25% He - O_2 pure H_2
859	50.1	345.4	3.139	21.6	.00310	.00141	.882	373	463	1.95	50% He - O_2 pure H_2
860	104.4	719.8	4.628	31.9	.00287	.00130	.920	1675	1186	2.13	Pure O_2, 10% He - H_2
861	33.7	232.4	1.534	10.6	.00133	.00060	.960	794	696	3.34	25% He - O_2, 10% He - H_2
862	68.7	473.7	3.634	25.1	.00278	.00126	.871	838	721	1.47	
863	45.5	313.7	1.848	12.7	.00138	.00063	.720	1300	978	3.61	Same catalyst configuration as above -250°F (117°K) pure propellants, mixture ratio below 0.8 O/F
864	15.7	108.2	1.254	8.6	.00129	.00059	.610	No Ignition			
865	43.8	302.0	1.787	12.3	.00136	.00062	.739	1228	938	4.27	
866	90.7	625.4	4.780	33.0	.00323	.00146	.792	1474	1074	9.86	
867	57.6	397.1	2.786	19.2	.00310	.00141	.707	No Ignition			
868	81.6	562.6	5.374	37.1	.00543	.00246	.777	No Ignition			
869	42.5	293.0	2.474	17.1	.00293	.00133	.867	No Ignition			-250°F (117°K). 25% He - O_2, pure H_2
870	80.9	557.8	4.328	29.8	.00308	.00140	.854	1570	1128	3.06	-250°F (117°K), pure O_2, 10% He - H_2
871	47.9	330.3	3.352	23.1	.00264	.00120	.622	832	718	1.66	-250°F (117°K). 25% He - O_2, 10% He - H_2
872	100.7	694.3	4.857	33.5	.00320	.00145	.836	1618	1154	4.68	Same catalyst configuration pure ambient propellants
873	101.8	701.9	4.713	32.5	.00301	.00137	.857	1621	1156	1.97	
874	102.4	706.0	4.720	32.5	.00300	.00136	.858	1620	1155	1.91	
875	Run Data Invalid										
876	139.6	962.5	100.365	692.0	.00396	.00180	1.045	1654	1174	6.02	Same catalyst configuration increase M.R., pure ambient propellants, igniter throat added, D_t = .090 in. (.22 cm)
877	140.2	966.7	100.573	693.4	.00393	.00178	1.020	1639	1166	4.18	
878	63.8	439.9	41.545	286.4	.00175	.00079	.995	1390	1022	4.16	
879	99.0	682.6	72.443	499.5	.00407	.00185	.955	844	724	6.02	25% He - O_2, pure H_2
880	77.2	532.3	58.012	400.0	.00412	.00187	.968	376	464	4.18	50% He - O_2, pure H_2
881	69.8	481.3	51.201	353.0	.00374	.00170	1.340	507	537	4.16	
882	101.3	698.4	74.146	511.2	.00411	.00186	.959	874	741	2.11	25% He - O_2, 5% He - H_2
883	111.4	768.0	80.257	553.4	.00442	.00200	1.116	1003	813	1.21	
884	139.0	958.4	96.330	664.2	.00404	.00183	.974	1587	1137	2.04	Pure O_2, 5% He - H_2
885	103.6	714.3	69.564	479.6	.00328	.00149	1.051	1853	1285	2.18	Shell 405 ABSG catalyst, bed length 1.0 in. (2.54 cm), pure propellants at -250°F (117°K), mixture ratio and flow rate excursions
886	112.1	772.9	80.273	553.5	.00362	.00164	.998	1740	1222	4.97	
887	25.4	175.1	19.901	137.2	.00170	.00077	.643	No Ignition			
888	18.8	129.6	14.503	100.0	.00190	.00086	.592	No Ignition			
889	24.8	171.0	19.196	132.4	.00195	.00088	.826	No Ignition			
890	125.6	866.0	88.758	612.0	.00393	.00178	1.010	1626	1159	2.22	
891	53.3	367.4	42.550	293.4	.00360	.00163	.742	No Ignition		-	
892	124.8	860.5	88.355	609.2	.00355	.00161	.994	1596	1142	3.07	
893	52.1	359.2	41.201	284.1	.00333	.00151	.889	No Ignition		-	-250°F (117°K), 25% He - O_2, pure H_2
894	39.4	271.7	30.549	210.6	.00210	.00095	.955	No Ignition		-	
895	127.0	875.6	92.005	634.4	.00403	.00183	.967	1594	1141	4.21	Pure O_2, 5% He - H_2
896	39.9	275.1	31.234	215.4	.00219	.00099	.887	No Ignition		-	25% He - O_2, 5% He - H_2

Table 15. High Pressure Reactor Test Data (Continued)

Run No.	P Bed Inlet psia	P Bed Inlet kN/m^2	PCD psia	PCD kN/m^2	$\dot{W}T$ lb/sec	$\dot{W}T$ kg/sec	M.R. O/F	Maximum TE °F	Maximum TE °K	Response Time sec to .95 TE	Comments
897	45.3	312.3	4.603	31.7	.00282	.00128	1.017	1597	1143	3.78	Engelhard NFSA, .063 in. (.153 cm) dia catalyst, bed length 1.0 in. (2.54 cm), pure ambient propellants, no igniter throat.
898	45.2	311.6	4.580	31.6	.00281	.00127	1.015	1592	1140	2.80	
899	83.1	573.0	9.188	63.3	.00542	.00246	1.016	1607	1148	1.95	
900	21.7	149.6	1.914	13.2	.00125	.00057	1.001	1560	1122	4.75	
901	24.7	170.3	3.025	20.9	.00291	.00132	1.041	No Ignition		-	25% He - O_2, pure H_2
902	25.4	175.1	3.107	21.4	.00318	.00144	1.236	No Ignition		-	
903	24.1	166.2	2.933	20.2	.00285	.00129	1.011	No Ignition		-	25% He - O_2, 5% He - H_2
904	43.6	300.6	4.442	30.6	.00263	.00119	1.172	1864	1291	6.84	Pure O_2, 5% He - H_2
905	44.5	306.8	4.695	32.4	.00283	.00128	.999	1579	1133	2.98	Pure ambient propellants
906	43.1	297.2	4.429	30.5	.00282	.00128	1.024	1572	1129	3.09	
907	42.7	294.4	4.466	30.8	.00281	.00127	1.014	1574	1130	2.74	
908	37.9	261.3	3.923	27.0	.00239	.00108	.883	1592	1140	2.80	-250°F (117°K) propellants, ambient bed
909	7.8	53.8	1.077	7.4	.00094	.00043	.776	No Ignition		-	-250°F (117°K) propellants and bed
910	35.0	241.3	3.968	27.4	.00269	.00122	.999	1448	1060	4.09	-100°F (200°K), pure propellant
911	20.9	144.1	2.698	18.6	.00264	.00120	.981	No Ignition		-	
912	8.2	56.5	1.236	8.5	.00120	.00054	1.093	No Ignition		-	
913	19.3	133.1	1.642	11.3	.00118	.00054	1.154	1732	1218	9.65	
914	108.0	744.6	100.087	690.1	.00284	.00129	1.031	1807	1259	2.23	Engelhard MFSA catalyst bed length 1.0 in. (2.54 cm), pure ambient propellants, igniter throat added
915	107.9	743.9	99.959	689.2	.00291	.00132	.980	1758	1232	2.65	
916	45.9	316.5	41.701	287.5	.00125	.00057	1.020	1653	1174	3.43	
917	67.0	462.0	63.500	437.8	.00288	.00131	1.081	678	632	2.71	25% He-O_2, pure H_2
918	73.4	506.1	69.506	479.3	.00309	.00140	1.243	838	721	2.47	
919	66.4	457.8	63.187	435.7	.00285	.00129	1.030	657	620	6.98	25% He - O_2, 5% He - H_2
920	95.8	660.5	88.428	609.7	.00283	.00128	1.019	1478	1076	2.50	5% He - O_2, 5% He - H_2
921	106.7	735.7	98.519	679.3	.00279	.00127	.989	1773	1240	2.26	Pure O_2, 5% He - H_2
922	Run invalid - no H_2 flow										
923	105.0	724.0	97.516	672.4	.00273	.00124	1.067	1891	1306	2.11	-100°F (200°K) propellants, ambient bed
924	106.2	732.2	99.372	685.2	.00279	.00127	1.027	1810	1261	3.35	-100°F (200°K) propellants and bed
925	44.3	305.4	40.934	282.2	.00124	.00056	1.074	1662	1179	4.67	
926	44.5	306.8	41.759	287.9	.00234	.00106	.884	No Ignition		-	-100°F (200°K), 25% He - O_2, pure H_2
927	47.2	325.4	44.023	303.5	.00324	.00147	1.338	No Ignition		-	
928	46.9	323.4	43.710	301.4	.00337	.00153	1.446	No Ignition		-	-100°F (200°K) 25% He - O_2, 5% He - O_2
929	46.4	319.9	43.278	298.4	.00290	.00132	1.111	No Ignition		-	
930	40.0	275.8	37.389	257.8	.00248	.00112	1.352	No Ignition		-	-100°F (200°K) pure O_2
931	47.0	324.1	43.892	302.6	.00261	.00118	.964	No Ignition		-	-100°F (200°K) pure propellants
932	102.6	707.4	95.447	658.1	.00393	.00178	1.010	1711	1206	1.62	Ambient propellants and bed
933	44.6	307.5	39.594	273.0	.00173	.00078	1.006	1691	1195	2.99	-250°F (117°K) propellants, ambient bed
934	15.1	104.1	15.121	104.3	.00089	.00040	.985	No Ignition		-	-250°F (117°K) propellants and bed
935	28.6	197.2	27.410	189.0	.00179	.00081	1.049	No Ignition		-	

Table 15. High Pressure Reactor Test Data (Continued)

Run No.	P Bed Inlet psia	P Bed Inlet kN/m^2	PCD psia	PCD kN/m^2	$\dot{W}T$ lb/sec	$\dot{W}T$ kg/sec	M.R. O/F	Maximum TE °F	Maximum TE °K	Response Time sec to .95 TE	Comments
936	106.8	736.4	91.097	628.1	.00284	.00129	1.076	1566	1126	2.45	Mixed catalyst bed - .50 in. (1.27 cm) Shell 405 ABSG upstream .50 in. (1.27 cm) Engelhard MFSA downstream pure ambient propellant, igniter throat added
937	105.9	730.2	90.532	624.2	.00280	.00127	1.062	1551	1117	2.11	
938	105.0	724.0	89.825	619.3	.00278	.00126	1.070	1558	1121	2.07	
939	47.4	326.8	39.128	269.8	.00128	.00058	1.049	1438	1054	3.27	
940	48.7	335.8	39.803	274.4	.00128	.00058	1.044	1420	1044	3.19	
941	35.9	247.5	30.273	208.7	.00131	.00059	1.130	797	698	2.27	25% He - O_2, pure H_2
942	35.2	242.7	30.044	207.1	.00131	.00059	1.108	715	653	2.92	
943	95.7	659.8	83.210	573.7	.00285	.00129	1.072	1287	970	2.26	5% He - O_2, pure H_2, ambient
944	99.7	687.4	82.230	567.0	.00274	.00124	1.093	1481	1078	6.05	5% He - O_2, pure H_2, -250°F (117°K)
945	49.3	339.9	34.345	236.8	.00201	.00091	.888	No Ignition		-	-250°F (117°K), pure propellants
946	91.7	632.2	77.436	533.9	.00274	.00124	1.131	1450	1061	2.93	
947	41.6	296.8	30.020	207.0	.00130	.00059	.994	507	537	16.45	
948	43.3	298.5	33.556	231.4	.00126	.00057	1.046	1072	851	11.58	
949	86.0	593.0	75.170	518.3	.00276	.00125	1.122	No Ignition		-	-250°F (117°K) 5% He - O_2, pure H_2
950	89.8	619.2	74.261	512.0	.00303	.00137	1.467	1343	1001	7.09	
951	63.7	439.2	4.223	29.1	.00278	.00126	1.001	1415	1041	2.15	Shell 405 ABSG catalyst, .50 in. (1.27 cm) bed length, pure ambient propellants, no igniter throat
952	64.1	442.0	4.286	29.6	.00280	.00127	1.001	1435	1053	1.97	
953	64.2	442.6	4.276	29.5	.00280	.00127	1.004	1431	1050	1.79	
954	114.7	790.8	8.425	58.1	.00530	.00240	.997	1468	1071	1.84	
955	31.7	218.6	1.809	12.5	.00125	.00057	1.037	1442	1056	2.92	
956	21.8	150.3	1.556	10.7	.00122	.00055	.996	719	655	2.23	25% He - O_2, pure H_2
957	44.3	305.4	3.523	24.2	.00310	.00140	1.259	636	609	1.91	
958	65.3	450.2	4.302	29.7	.00307	.00139	1.241	1470	1072	1.96	5% He - O_2, pure H_2
959	60.8	419.2	3.694	25.5	.00247	.00112	1.192	1718	1210	1.94	-250°F (117°K), pure propellants
960	46.8	322.7	3.563	24.6	.00275	.00125	1.029	875	741	5.71	
961	98.8	681.2	5.886	40.6	.00522	.00237	1.038	325	436	4.44	
962	24.8	171.0	1.420	9.8	.00111	.00050	1.184	1369	1016	12.60	
963	9.6	66.2	.836	5.8	.00089	.00040	1.056	No Ignition		-	-250°F (117°K), 25% He - O_2, pure H_2
964	10.2	70.3	.989	6.8	.00112	.00050	1.048	No Ignition		-	-250°F (117°K), 5% He - O_2, pure H_2
965	10.5	72.4	.996	6.9	.00111	.00050	1.015	No Ignition		-	-250°F (117°K), pure propellant
966	25.6	176.5	1.380	9.5	.00112	.00051	1.198	1423	1046	6.01	
967	104.5	720.5	87.840	605.6	.00278	.00126	1.019	1460	1066	1.97	Same catalyst configuration, pure ambient propellants, igniter throat added
968	104.2	718.4	87.300	601.9	.00276	.00125	1.013	1449	1060	1.96	
969	104.9	723.3	88.205	608.2	.00278	.00126	1.018	1467	1070	1.98	
970	46.0	317.2	36.349	250.6	.00119	.00054	1.092	1385	1025	2.97	
971	33.4	230.3	27.509	189.7	.00117	.00053	1.063	664	624	2.18	25% He - O_2, pure H_2
972	80.2	553.0	68.420	471.7	.00287	.00130	1.054	644	613	1.77	
973	96.7	666.7	81.218	560.0	.00283	.00128	1.028	1213	929	1.96	5% He - O_2, pure H_2
974	96.3	664.0	78.820	543.4	.00247	.00112	1.237	1808	1260	1.96	-250°F (117°K) propellants ambient bed
975	90.0	620.5	74.605	514.4	.00275	.00125	1.033	1308	982	4.88	-250°F (117°K) propellants and bed
976	35.3	243.4	28.282	195.0	.00126	.00057	.934	381	467	8.18	
977	41.7	287.5	33.373	230.1	.00220	.00100	1.106	No Ignition		-	-250°F (117°K), 25% He - O_2, pure H_2
978	42.5	293.0	34.065	234.9	.00209	.00095	1.051	No Ignition		-	-250°F (117°K), 5% He - O_2, pure H_2

Table 15. High Pressure Reactor Test Data (Continued)

Run No.	P Bed Inlet psia	P Bed Inlet kN/m^2	PCD psia	PCD kN/m^2	$\dot{W}T$ lb/sec	$\dot{W}T$ kg/sec	M.R. O/F	Maximum TE °F	Maximum TE °K	Response Time sec to .95 TE	Comments
979	84.7	584.0	81.925	564.9	.00285	.00129	.994	1377	1020	1.98	Engelhard MFSA catalyst, .50 in (1.27 cm) bed length, pure ambient propellants, igniter throat added, D_t = .090 in. (.22 cm)
980	84.6	583.3	81.781	563.9	.00280	.00127	1.023	1467	1070	1.76	
981	84.4	581.9	81.625	562.8	.00279	.00127	1.020	1470	1072	1.48	
982	40.9	282.0	39.798	274.4	.00122	.00055	1.122	1718	1210	2.42	
983	41.4	285.4	40.304	277.9	.00122	.00055	1.122	1731	1217	2.36	
984	57.4	395.8	55.626	383.5	.00286	.00130	1.078	325	436	.96	
985	88.6	610.9	85.570	590.0	.00421	.00191	2.036	1164	902	2.61	25% He - O_2, pure H_2
986	83.3	574.3	80.330	553.9	.00391	.00177	2.549	1495	1086	1.82	
987	77.7	535.7	75.082	517.8	.00282	.00128	1.040	1201	923	2.28	5% He - O_2, pure H_2
988	51.0	351.6	49.379	340.4	.00291	.00132	1.121	146	336	Quenched	
989	58.6	404.0	56.630	390.4	.00381	.00173	2.330	268	404	1.14	50% He - O_2, pure H_2
990	94.0	648.1	92.159	635.4	.00179	.00081	.568	2153	1451	Quenched	-250°F (117°K) propellants, ambient bed
991	20.9	144.1	16.574	114.3	.00132	.00060	.913	No Ignition		-	-250°F (117°K) propellants, and bed
992	77.2	532.3	75.222	518.6	.00273	.00124	1.045	1483	1079	1.94	
993	73.1	504.0	71.241	491.2	.00276	.00125	1.025	1270	961	3.35	-100°F (200°K) pure propellants
994	32.5	224.1	31.879	219.8	.00119	.00054	1.034	1292	973	4.36	
995	38.5	265.4	37.761	260.3	.00263	.00119	1.038	No Ignition		-	-100°F (200°K), 25% He - O_2, pure H_2
996	39.4	271.7	38.641	266.4	.00246	.00112	.992	No Ignition		-	-100°F (200°K), 5% He - O_2, pure H_2
997	88.0	606.7	86.875	599.0	.00279	.00127	2.102	2204	1480	2.61	-100°F (200°K), 5% He - O_2, pure H_2

Tests 769-776: Engelhard MFSA catalyst was evaluated with ambient temperature propellants. Response times increased and effluent temperatures decreased compared to the Shell catalyst tests. Note that bed inlet pressures during these tests were less than 50 percent of the bed inlet pressures measured during the Shell catalyst tests 747-755.

Tests 777-782: Repeated above tests with a 0.268-inch (0.681 cm) diameter igniter throat added to increase bed pressures, which improved response and increased effluent temperatures at same mixture ratios as tests 769-776.

Tests 783-787: Tested Engelhard catalyst with -250°F (117°K) propellants and bed initially at ambient. Reaction was initiated, but quenched as flow continued and bed temperatures were reduced at the upstream end of the catalyst bed.

Tests 788-792: Evaluations of 1.0-inch (2.54 cm) long bed of Engelhard catalyst. Satisfactory response and temperatures were attained without an igniter throat, as catalyst bed drop was sufficient to increase bed inlet pressure.

Tests 793-796: Quenching occurred when the same catalyst bed was tested with propellants at -250°F (117°K), as predicted from the laboratory catalyst investigation results.

Tests 797-800: Added igniter throat, thus increasing pressures, improved response compared to tests 788-792.

Tests 801-807: Same configuration, satisfactory ignitions attained with 100°F (200°K) propellants, and helium dilutions of 25 percent He-O_2 and 10 percent He-H_2.

Tests 808-811: Ignitions attained with helium dilutions as high as 25 percent He-O_2 and 10 percent He-H_2 with ambient temperature propellants.

Tests 812-813: Engelhard catalyst tests with -250°F (117°K) propellants — ignition with ambient bed but not with catalyst bed prechilled to -250°F (117°K), as expected from earlier results.

Tests 814-818: Tests with Shell catalyst, 1.0-inch (2.54 cm) bed length, flow rate excursion with pure, ambient propellants resulted in satisfactory ignitions.

Tests 819-821: Ignition attained with 25 percent He-O_2 and 10 percent He-H_2, with ambient and -250°F (117°K) propellants.

Tests 822-828: Ignitions with Shell catalyst attained with -250°F (117°K) bed and propellants, except at 25 percent He-O_2 dilution.

Tests 829-835: Tests with Engelhard catalyst and igniter throat. Ignitions attained with pure and 25 percent $He-O_2$, 10 percent $He-H_2$ dilute propellants.

Tests 836-838: Same catalyst bed, no ignition with -250°F (117°K) propellants, except initial reaction with ambient bed.

Tests 839-853: Evaluations of 0.50-inch (1.27 cm) long Shell catalyst bed with igniter throat. Ignition attained at -250°F (117°K) except for test 848 (low MR), and tests with 25 percent $He-O_2$ dilution, verifying the results of runs 822-828.

Tests 988-1018: Tests performed with a mixed bed of Shell and Engelhard catalysts. Ignitions attained at -100°F (200°K) and with helium dilutions to 25 percent $He-O_2$, but no ignitions with higher flow rates and -250°F (117°K) propellants, indicating that the bed length was insufficient for reaction at these conditions.

Results of the high pressure catalytic reactor tests listed in Table 15 were as follows:

Tests 854-862: Ignitions were attained with a 1.0-inch (2.54 cm) long Shell catalyst bed at propellant dilutions to 50 percent $He-O_2$ and 10 percent $He-H_2$.

Tests 863-871: Same catalyst bed tested with -250°F (117°K) pure and dilute propellants— ignitions not consistent at reduced mixture ratios, indicating that higher mixture ratios are required at these propellant temperatures.

Tests 872-875: Tests with ambient propellants and reduced mixture ratios resulted in satisfactory ignitions.

Tests 876-884: Igniter throat of 0.090-inch (0.216 cm) diameter added, same catalyst configuration—ignitions attained with ambient propellants and dilutions to 50 percent $He-O_2$.

Tests 885-896: Mixture ratio and flow rate excursions with -250°F (117°K) propellants, no ignitions attained at MR of 0.826 or below with pure propellants, or with 25 percent $He-O_2$.

Tests 897-913: Engelhard catalyst evaluations, 1.0-inch (2.54 cm) bed length, no igniter throat. Ignitions attained at ambient with dilutions to 25 percent $He-O_2$ and propellant and bed temperatures of -100°F (200°K) but not at -250°F (117°K).

Tests 914-935: Same Engelhard catalyst bed, but 0.090-inch (0.216 cm) diameter igniter throat added. Reactor response improved 25 percent compared to tests 897-913 but limits of ignition remained unchanged with respect to propellant dilutions and temperatures.

Tests 936-950: Mixed bed tests, 0.50-inch (1.27 cm) of each (Shell and Engelhard) catalyst with igniter throat. Marginal ignitions with -250°F (117°K) propellants with response times as long as 16 seconds.

Tests 951-966. Shell catalyst bed, 0.50-inch (1.27 cm) long, no igniter throat. Ignitions attained with pure propellants at -250°F (117°K), but not with dilute conditioned propellants with this bed length, indicating the need for increased bed lengths.

Tests 967-978: Same catalyst configuration, igniter throat added. No significant change in response or ignition limits compared to tests 951-966.

Tests 979-997: Engelhard catalyst, 0.50-inch (1.27 cm) bed length, igniter throat added. Satisfactory ignitions attained with dilutions of 50 percent $He-O_2$ with ambient propellants, pure -100°F (200°K) propellants, but not at -250°F (117°K).

Typical computer plotted temperature data from these tests are presented and discussed in the following data evaluation. Additional plots of all valid thermal response data from the reactor tests listed in Tables 14 and 15 have been included in Appendix B of this report.

4.3.2 Reactor Test Data Evaluation

Analysis and evaluation of the reactor test data were performed to establish the effects of variations of catalyst bed configuration and operating conditions on reactor response characteristics. The results of these evaluations are discussed in the following sections.

4.3.2.1 Response Effects of Propellant Flow Rate

Some of the experimental results obtained from low pressure reactor tests using Shell 405 ABSG 14-18 mesh catalyst are presented in Figure 39. The data plotted in the figure is from a series of igniter tests made with varied total propellant flow rates through a fixed 0.50-inch (1.27 cm.) long catalyst bed configuration. Previous ignition energy level tests had indicated that main thruster ignition could be attained with a range of igniter flow rates from 2 to 10 percent of main injector flows, provided the effluent temperature was above the autoignition temperature of the mixed propellants. The curves in Figure 39 indicate that the same final effluent temperature - (TE) was attained after approximately five seconds of reactor operation independent of flow rates; however, the minimum time required to achieve steady-state effluent temperature increased as the flow rate through the catalyst bed was reduced. The catalyst bed temperatures responded nearly identically for each flow rate and are shown as a single curve (T_{BED}).

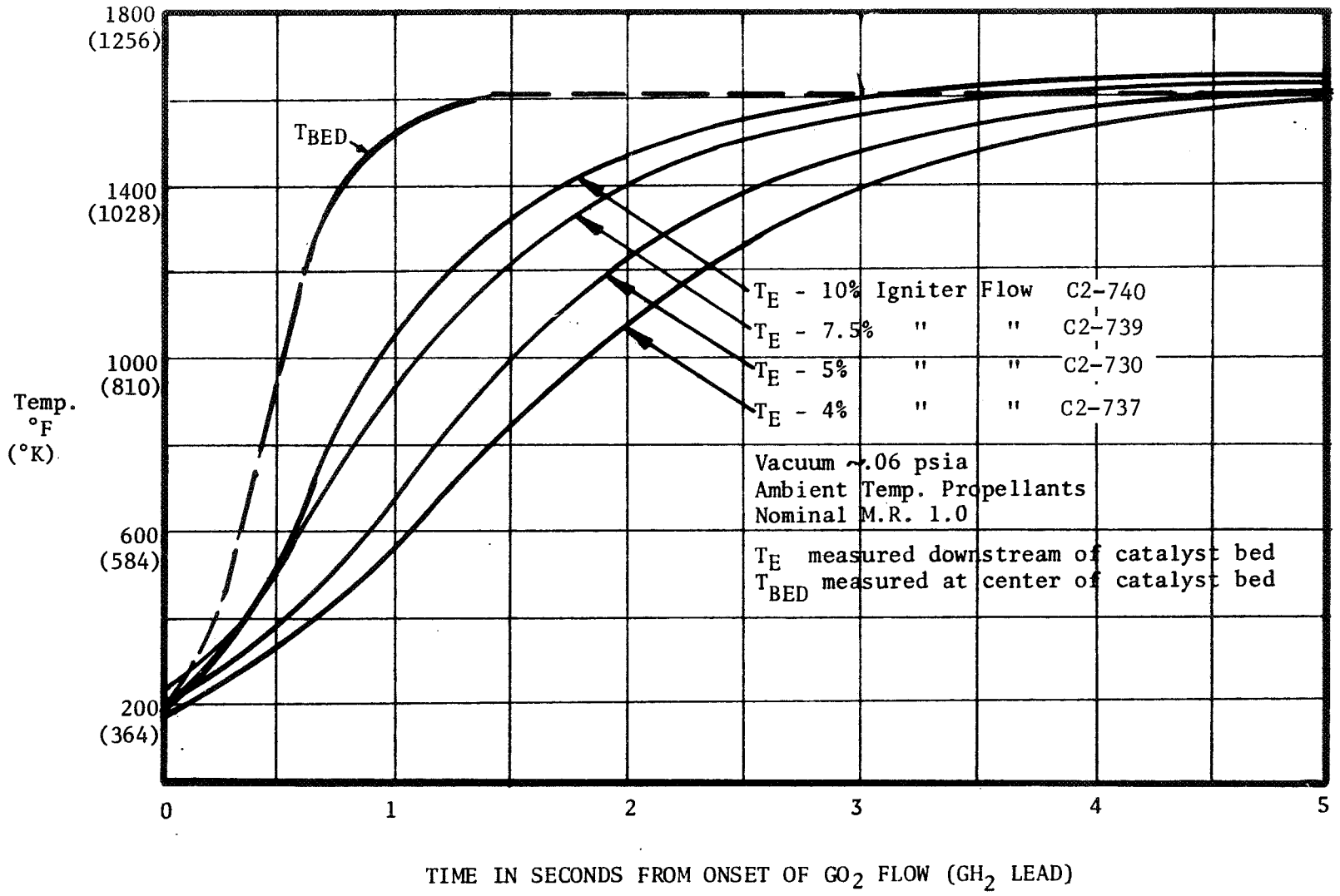

Figure 39. Low Pressure Reactor Test Results—Flow Rate Excursions with Shell 405 ABSG Catalyst

Results of these tests indicated that, for the particular catalyst bed configuration tested, delay time in attaining the effluent temperature required for main thruster ignition could be reduced by increasing igniter flow rates. However, the increased flow rates result in higher pressure drops across the catalyst bed and increased supply pressure requirements. Bed inlet pressures for a range of igniter flow rates through different bed lengths of Shell 405-ABSG catalyst are presented in Figure 40. The specified contractual propellant supply pressure of 16 psia (110 kN/m^2), as noted in the figure, limits the maximum flow rate for each catalyst bed length.

4.3.2.2 Response Effects of Catalyst Bed Length

Figure 41 is a correlation of thermal response data from reactor ignition tests with three different bed lengths of Shell 405-ABSG catalyst. Each of these tests was performed at propellant flow rates corresponding to the 16 psia (110kN/m^2) maximum inlet pressure available for the low pressure system. Normalized temperatures (T/T_o) were plotted to compare thermal response independently of final reaction temperatures. The curves in Figure 41 indicate that a longer catalyst bed resulted in increased time required to reach near steady-state (0.95 T_o) temperatures compared to a shorter bed (same diameter and propellant feed pressure). These results were anticipated, since increasing the mass of catalyst also increases the bed thermal lag due to greater heat capacity of the bed. Highest response is indicated for the one-quarter inch bed, although this length was not sufficient for complete reaction of the propellants.

4.3.2.3 Response Effects of Vacuum Ignition Level

Thermal response data from successive tests at two vacuum ignition levels are presented in Figure 42. Data points from back-to-back high pressure reactor runs at each vacuum level show excellent repeatability and indicate that the higher vacuum level had no significant effect on ignition delay and response. The lower set of curves in Figure 42, plotted from 0.25-inch (0.635 cm) bed data, indicates more variation in run-to-run thermal response than the 1.0-inch (2.54 cm) bed data, apparently because the shorter bed was not sufficient for complete reaction of the propellants. Although the final bed exit temperature obtained for the 10^{-5} mm Hg vacuum ignition test is somewhat lower than for the 0.06 psia (413.7 N/m^2) test, effect of vacuum level at ignition does not appear to be significant from this data. Two ignition tests at the same vacuum level also vary in thermal response with the short catalyst bed, as shown in the figure.

4.3.2.4 Response Effects of Reaction Pressure

Initial low pressure reactor tests were performed with a 0.50-inch (1.27 cm) catalyst bed length and a "throatless" igniter exit. The data plotted in Figure 43 reveals that the average steady-state catalyst bed reaction pressures without an exit throat for the Engelhard MFSA 1/16 inch (0.16 cm) spherical catalyst were less than 50 percent of the bed pressures measured for a Shell 405-ABSG, 14-18 mesh catalyst bed of the same diameter and length.

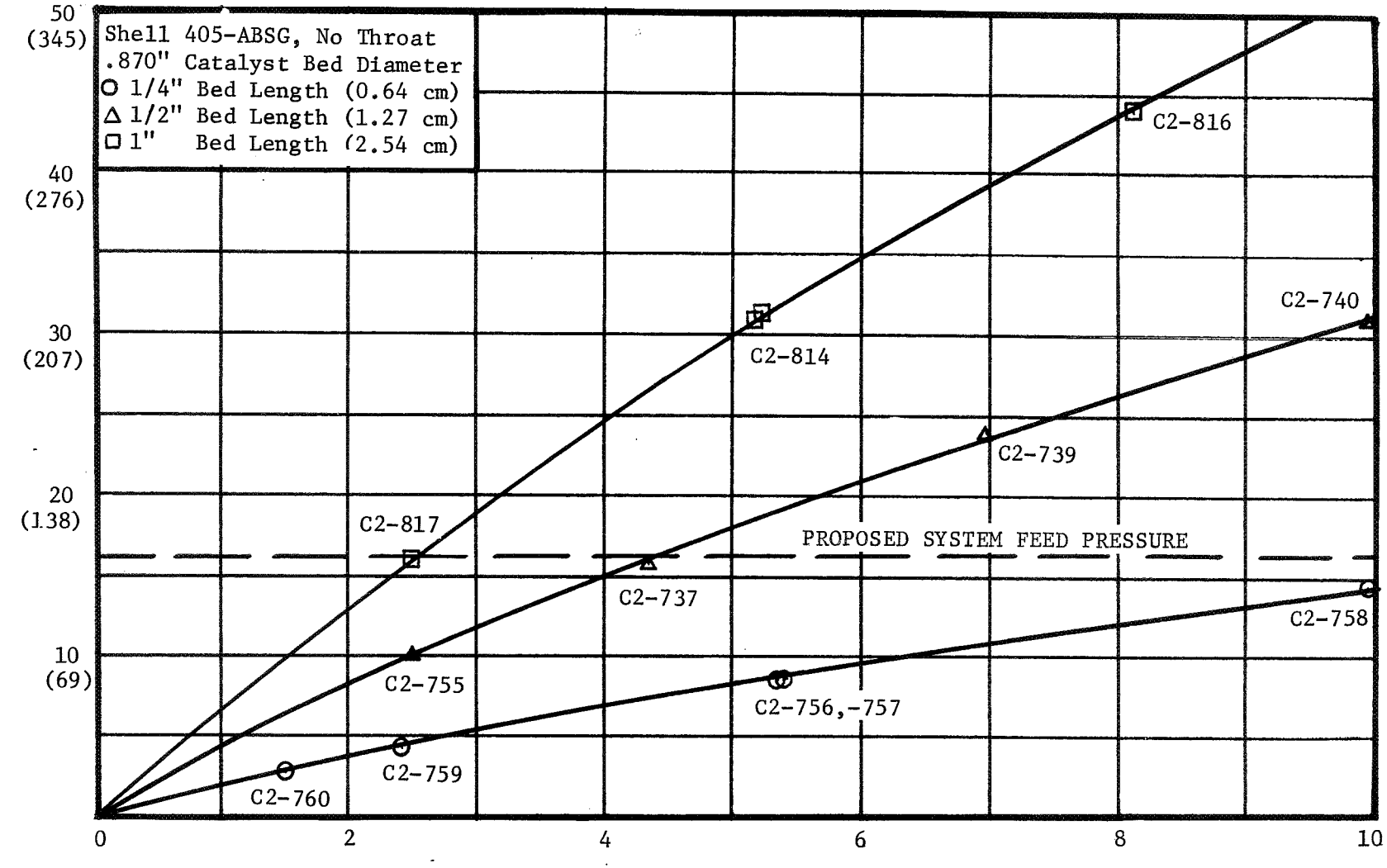

Figure 40. Low Pressure Reactor Bed Inlet Pressures at Varied Flow Rates—Shell 405 ABSG Catalyst

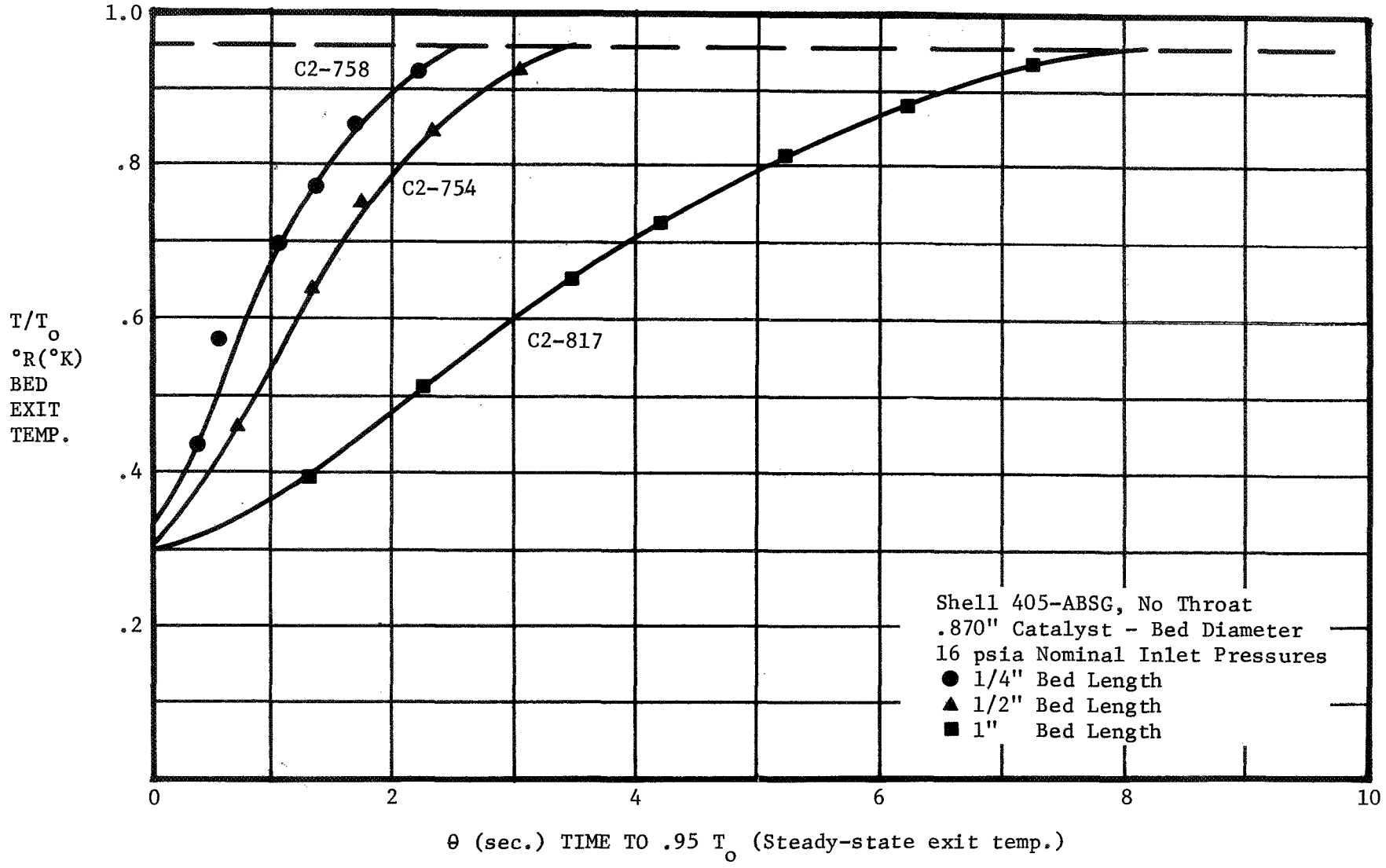

Figure 41. Low Pressure Reactor Thermal Response Data Correlation for Shell 405 ABSG Catalyst Beds of Varied Lengths

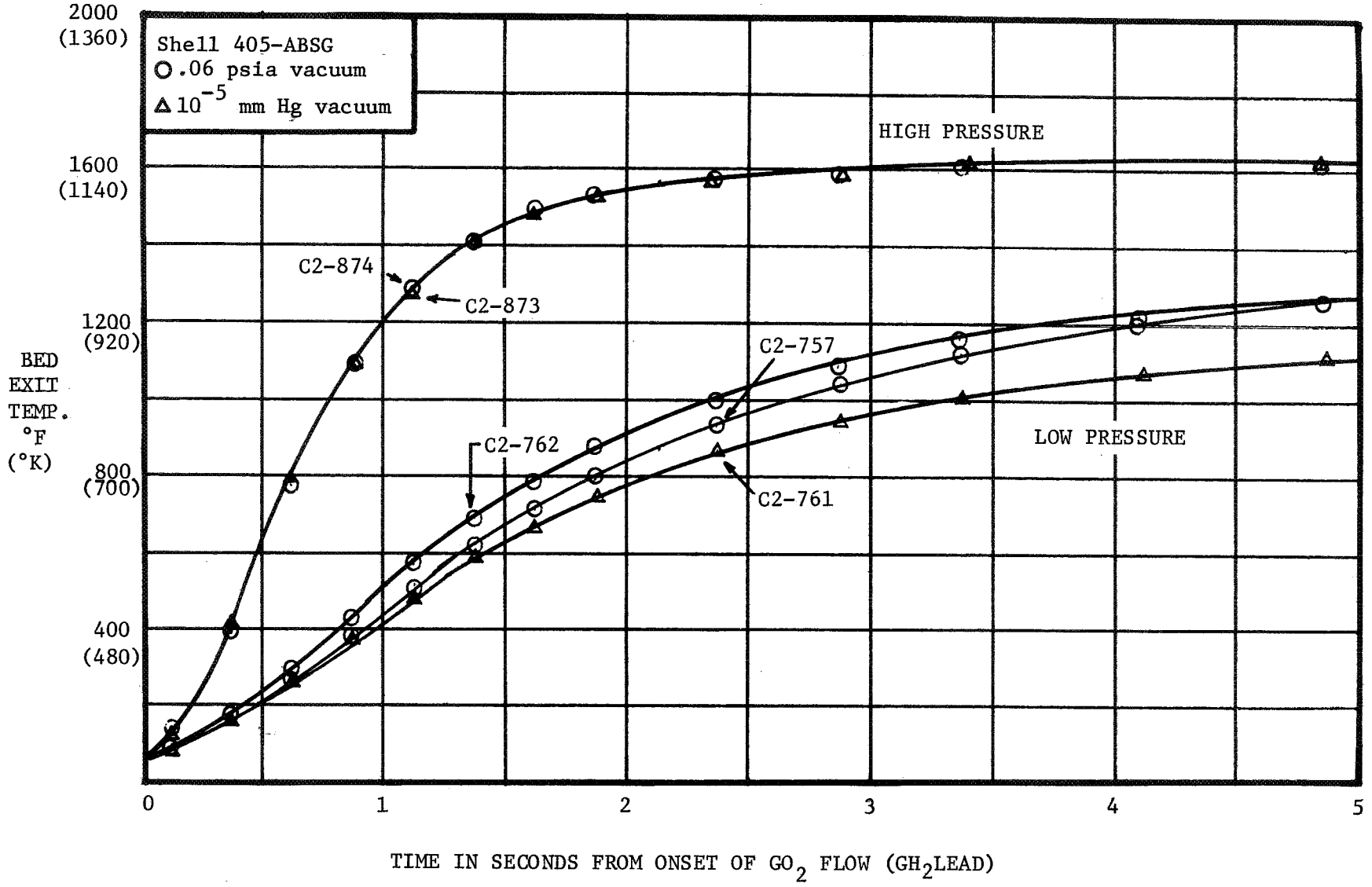

Figure 42. Reactor Thermal Response at Two Vacuum Ignition Levels— Shell 405 ABSG Catalyst

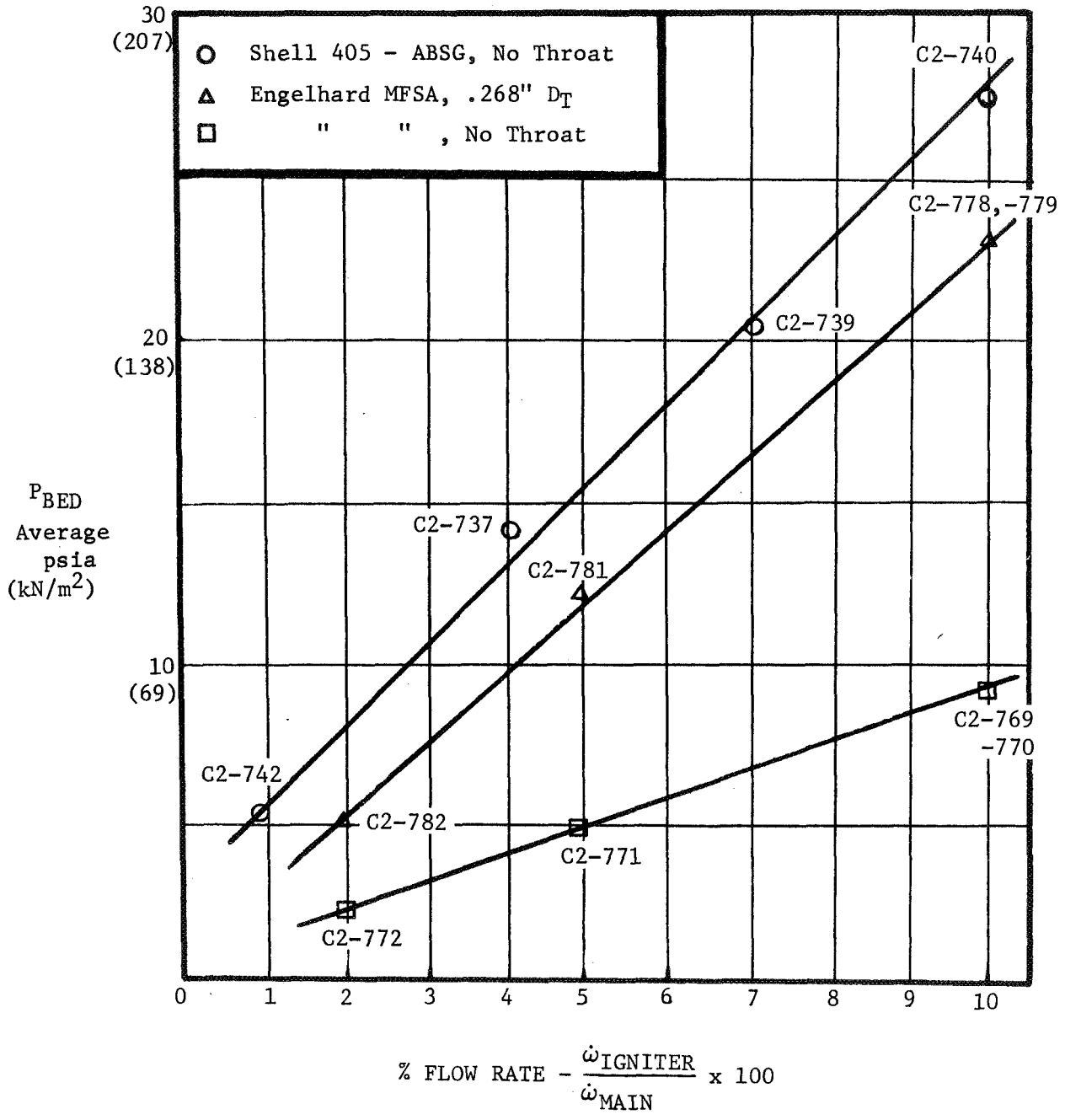

Figure 43. Low Pressure Reactor Bed Pressures—Shell 405 ABSG and Engelhard MFSA Catalyst

In order to compare the reaction rates of both catalyst types at similar pressures, a throat insert was fabricated and installed in the igniter exit, as depicted in Figure 44. The throat diameter was sized to provide an igniter chamber pressure equal to the main thruster P_c at a nominal igniter flow rate of 5 percent of main thruster flow. The resulting average bed pressures (center curve, Figure 43) are only slightly lower than the corresponding bed pressures of the Shell catalyst with no throat.

Correlation of low pressure reactor thermal response data obtained from tests with identical bed configurations of Shell 405-ABSG and Engelhard MFSA catalysts is presented in Figure 45. The figure legend identifies the curves for the different bed pressures, attained by varying the igniter flow rates. The Engelhard catalyst tests incorporated the throat insert to raise the bed pressures to levels comparable to the Shell catalyst experiments. The results indicate that at these initial temperatures and pressures, both catalyst types are nearly identical in thermal response. Also, a marked increase in response time with decreased pressure for each catalyst is indicated in Figure 45.

4.3.2.5 Response Effects of Low Temperature Propellants

Low temperature data correlations are presented in Figures 46 to 48 for each catalyst formulation. Figures 46 and 47 compare the response of the Engelhard MFSA catalyst at ambient temperature and -75°F (214°K), respectively. Each of these figures also compares the thermal response times at different flow rates, as indicated.

Figure 48 compares the thermal response of a Shell 405-ABSG catalyst bed at initial temperatures from ambient to -230°F (128°K). The response time at -230°F (128°K) is double the time required to reach near steady-state temperatures from 72°F (296°K), about 5 seconds compared to 2-1/2 seconds. Of particular interest is the fact that the thermal response at -150°F (172°K) is nearly equal to the ambient temperature bed response.

Typical computer plotted data from this experimental series are shown in Figures 49 through 57. Location of the thermocouples and flow rates are noted on each plot. Additional data are included in Appendix B.

Figures 49 to 51 indicate the effects of varied flow rates with a 0.50-inch (1.27 cm) bed of Shell 405-ABSG at ambient temperature conditions. Note the marked decrease in response as flow rates are reduced from 10 to 2 percent of nominal thruster flows.

Figures 52 to 54 present low temperature response data obtained with the Shell 405-ABSG catalyst. Comparison of upstream bed thermocouples, T_{b1}, and T_{b4}, in Figures 52 and 53 indicate that reaction occurs further downstream in the 1.0-inch (2.54 cm) catalyst bed as flow rates are increased from 2 percent to 5 percent of nominal thruster flows. A subsequent test at 10 percent flow rates resulted in no sustained reaction. Low temperature reactions were also attained with a 0.50-inch (1.27 cm) long Shell catalyst bed, as indicated by Figure 54.

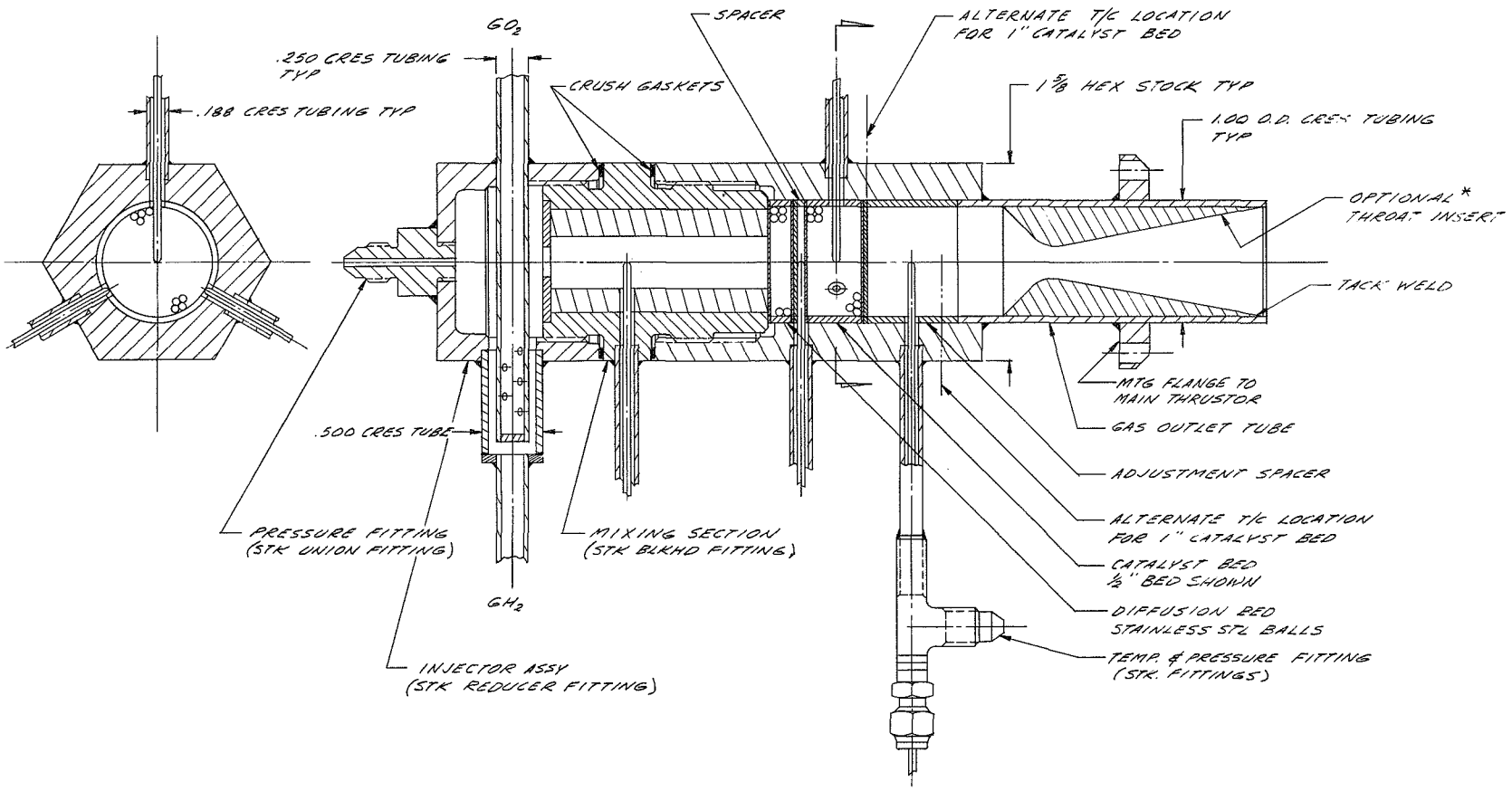

Figure 44. Catalytic Reactor Igniter—Low Pressure Thruster

*Modified to include removable throat insert.

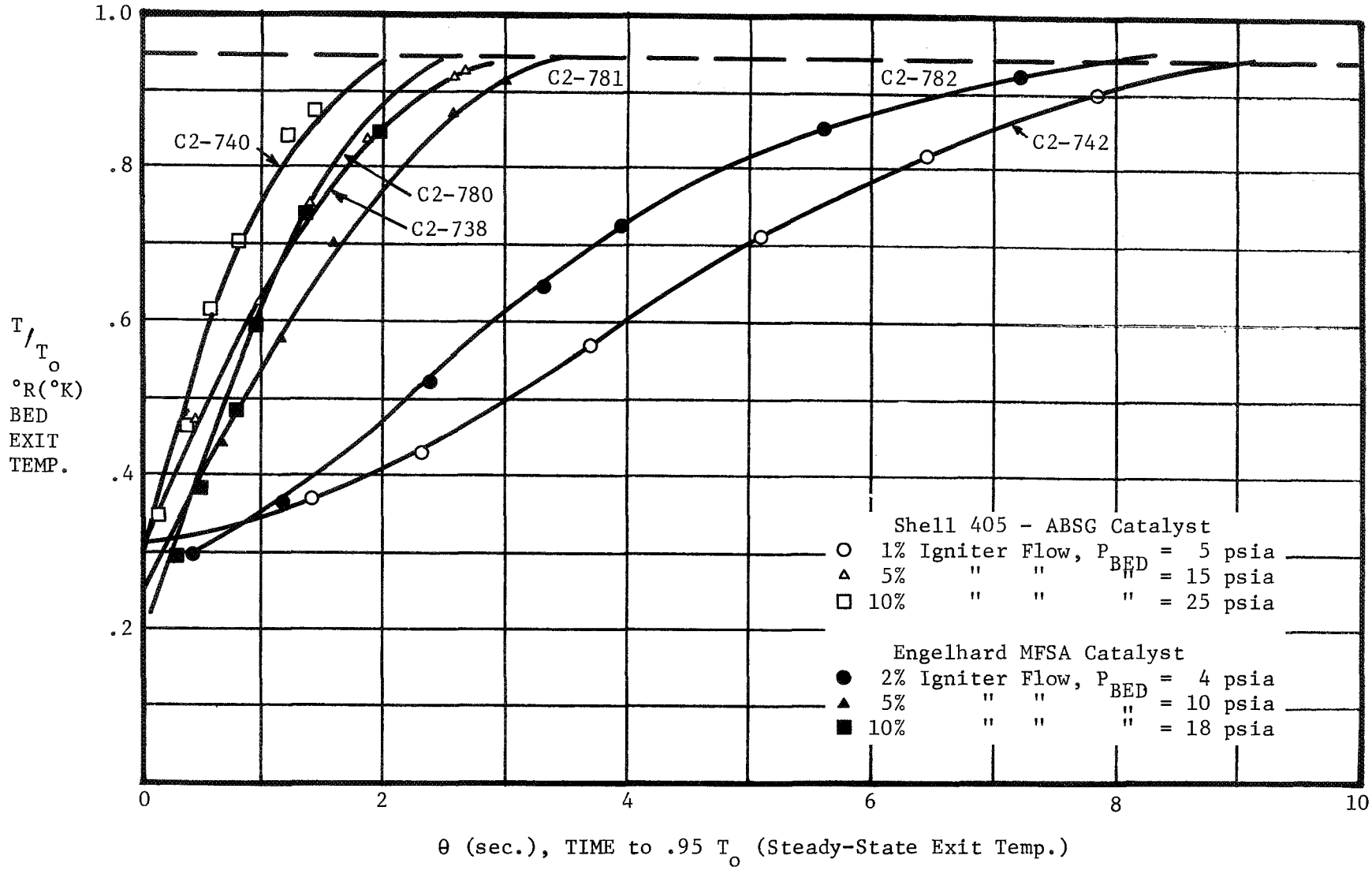

Figure 45. Low Pressure Reactor Data Correlation—Shell 405 ABSG and Engelhard MFSA Catalysts

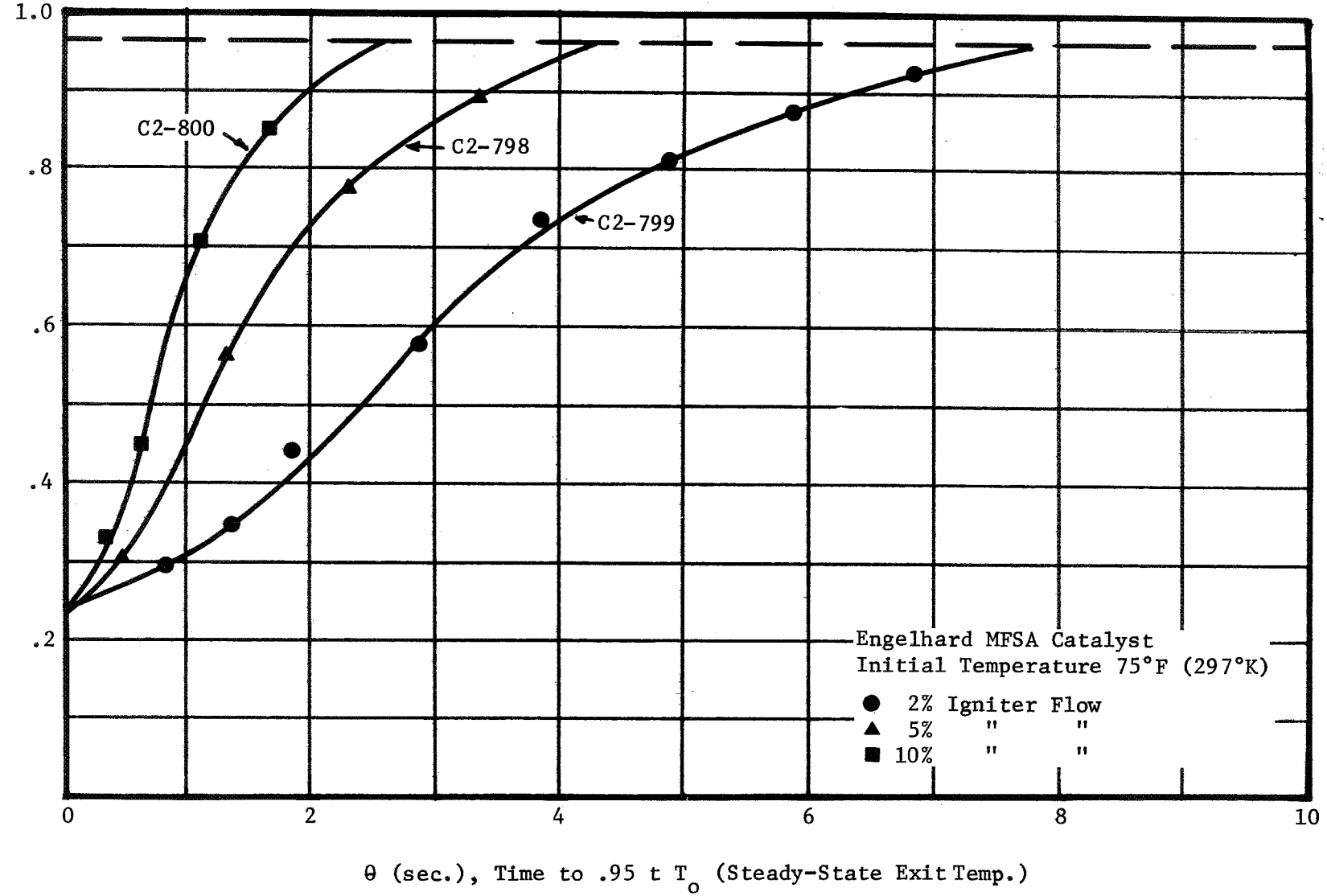

Figure 46. Low Pressure Reactor Data Correlation—Engelhard MFSA Catalyst, 1 in. (2.54 cm) Bed Length

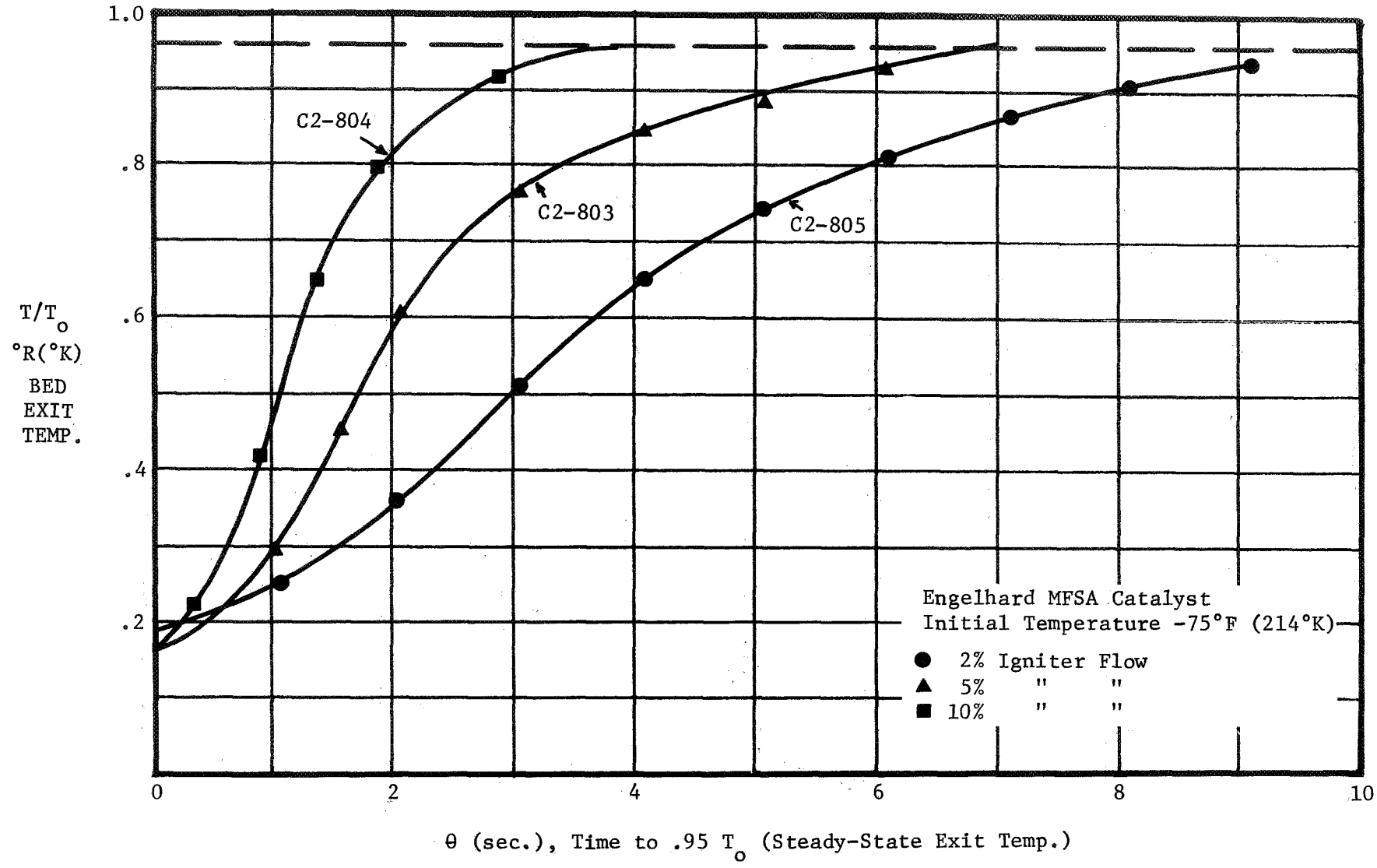

Figure 47. Low Pressure Reactor Data Correlation—Engelhard MFSA Catalyst

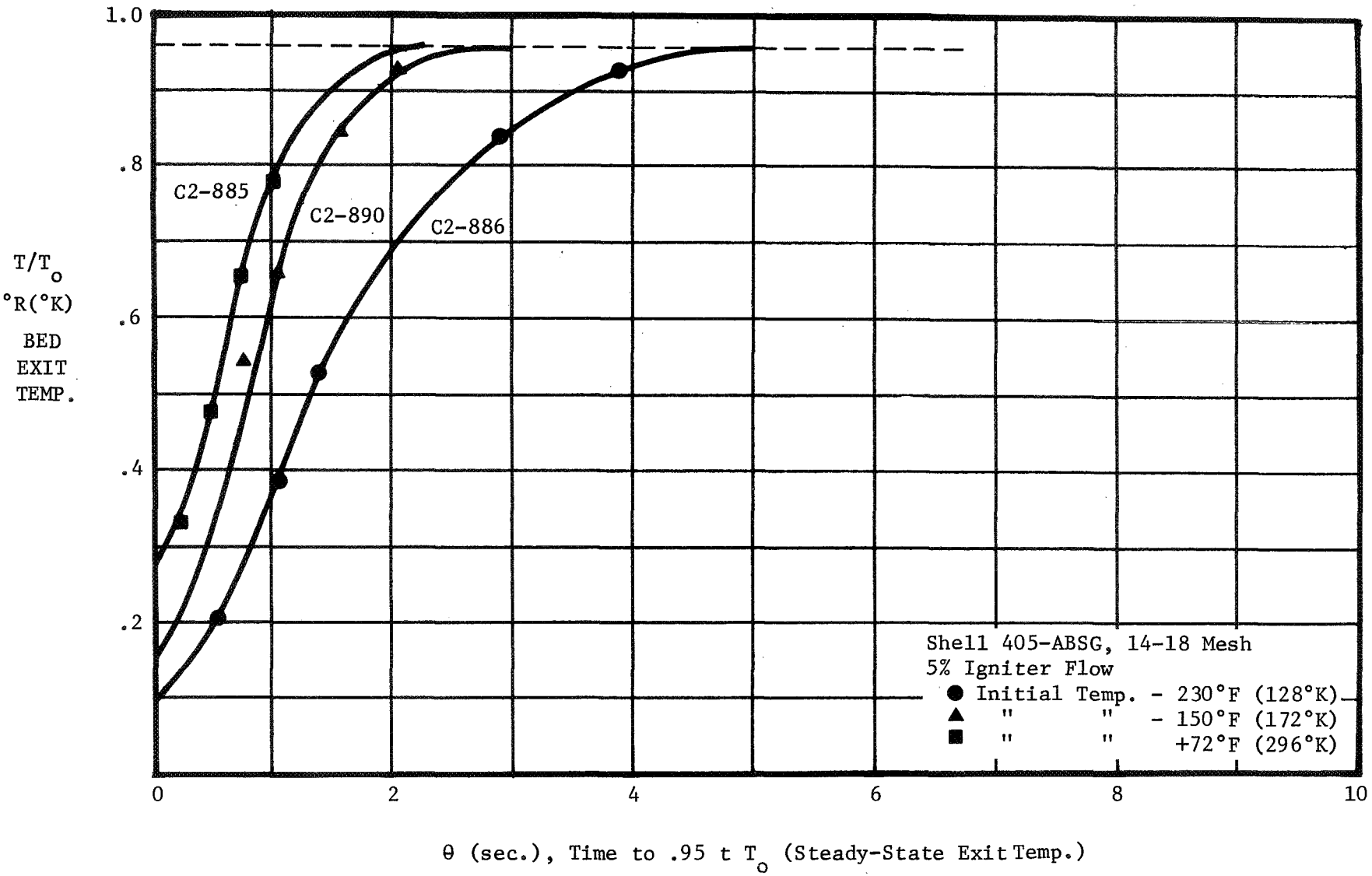

Figure 48. High Pressure Reactor Data Correlation—Shell 405 ABSG Catalyst, 1 in. (2.54 cm) Bed Length

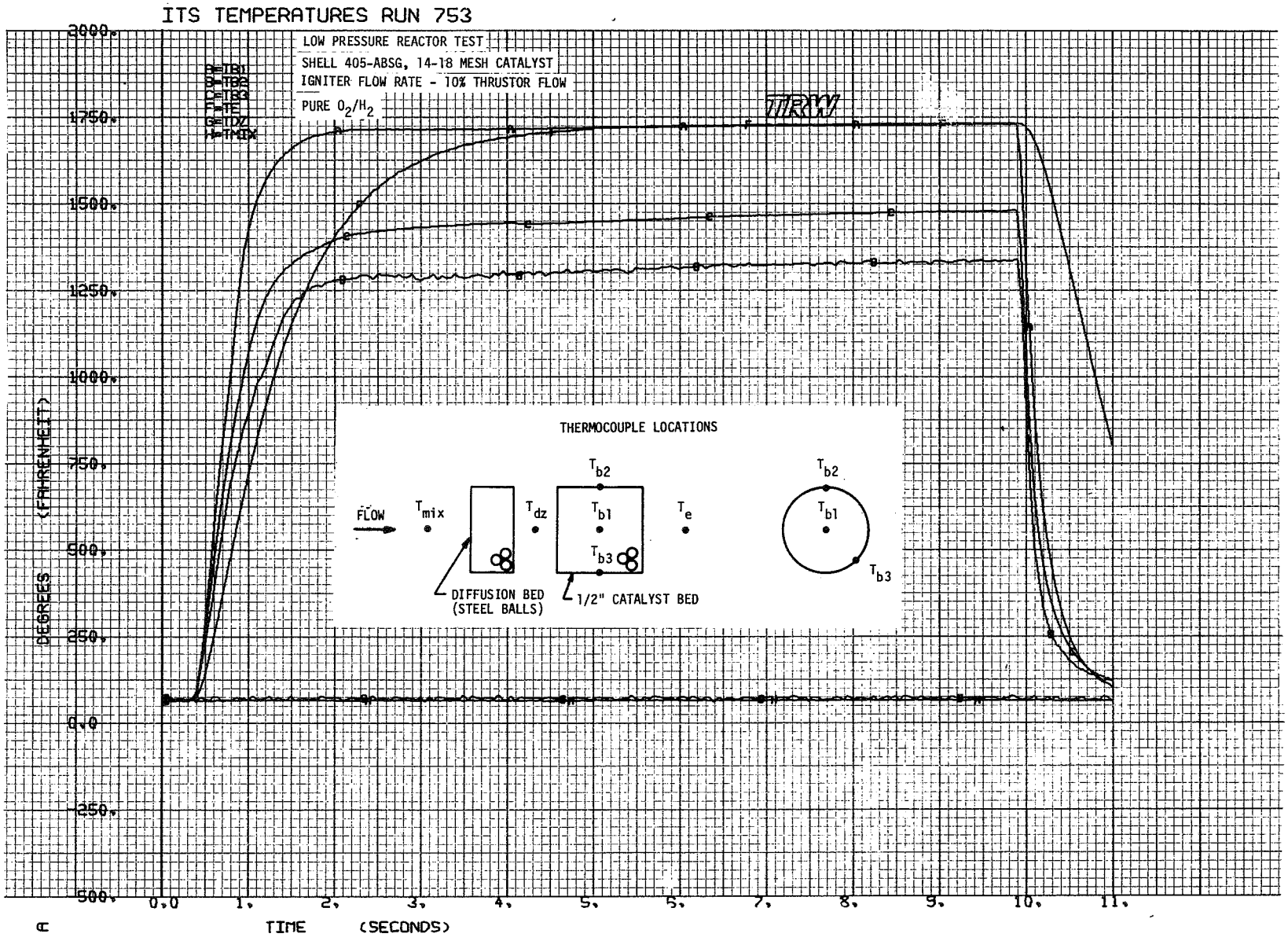

Figure 49. Catalyst Bed Temperatures—Run 753

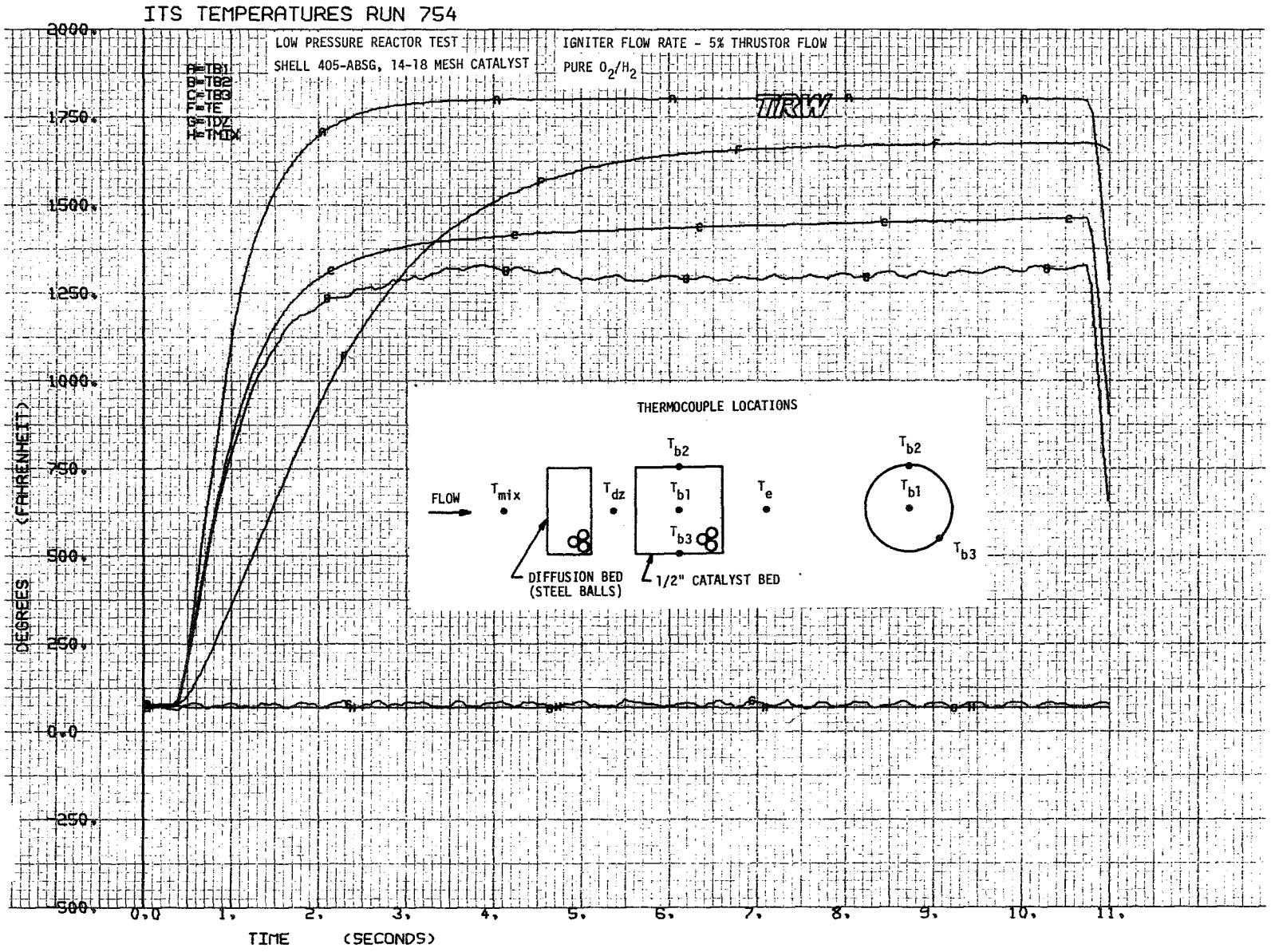

Figure 50. Catalyst Bed Temperatures—Run 754

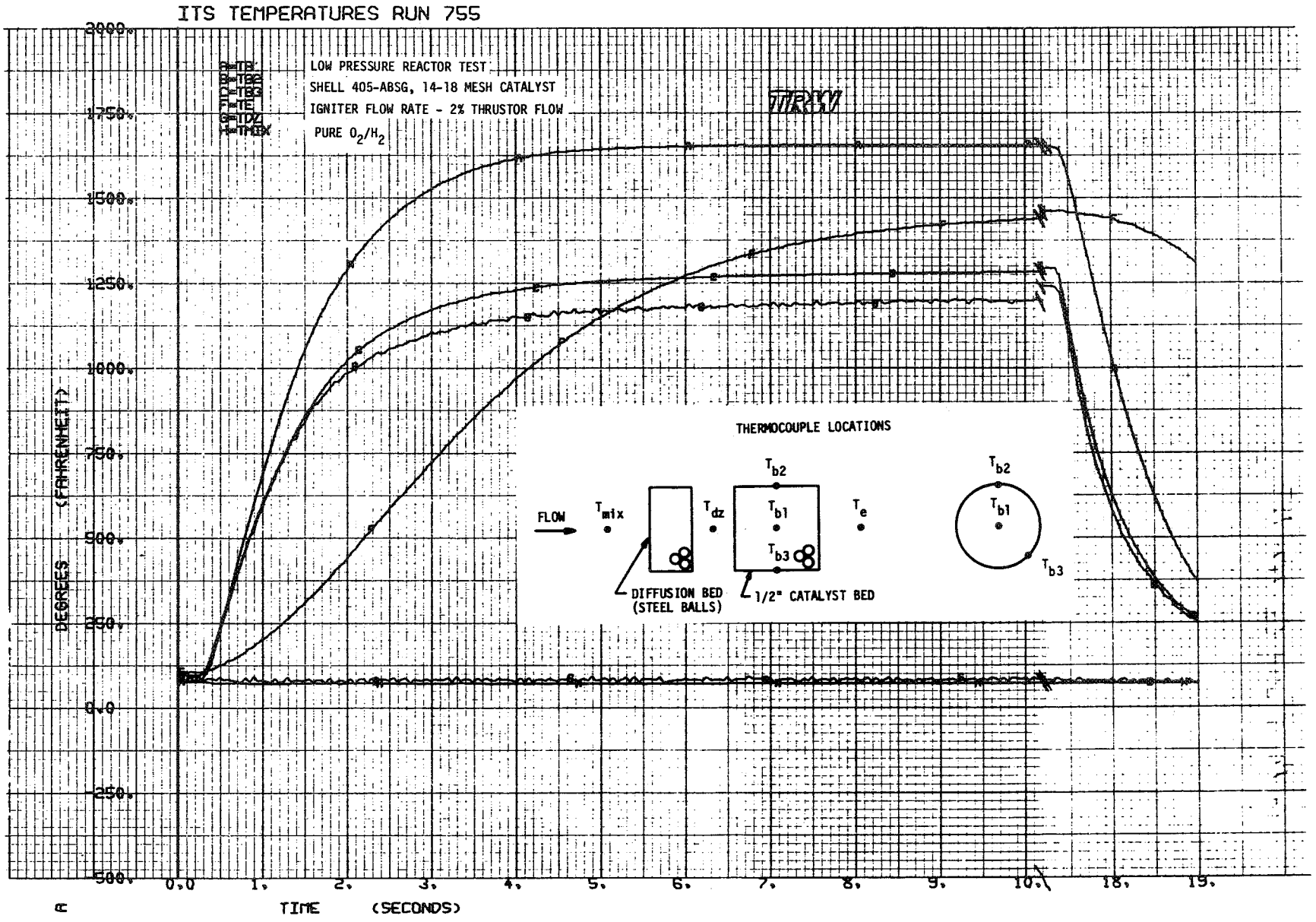

Figure 51. Catalyst Bed Temperatures—Run 755

ITS TEMPERATURES RUN 823

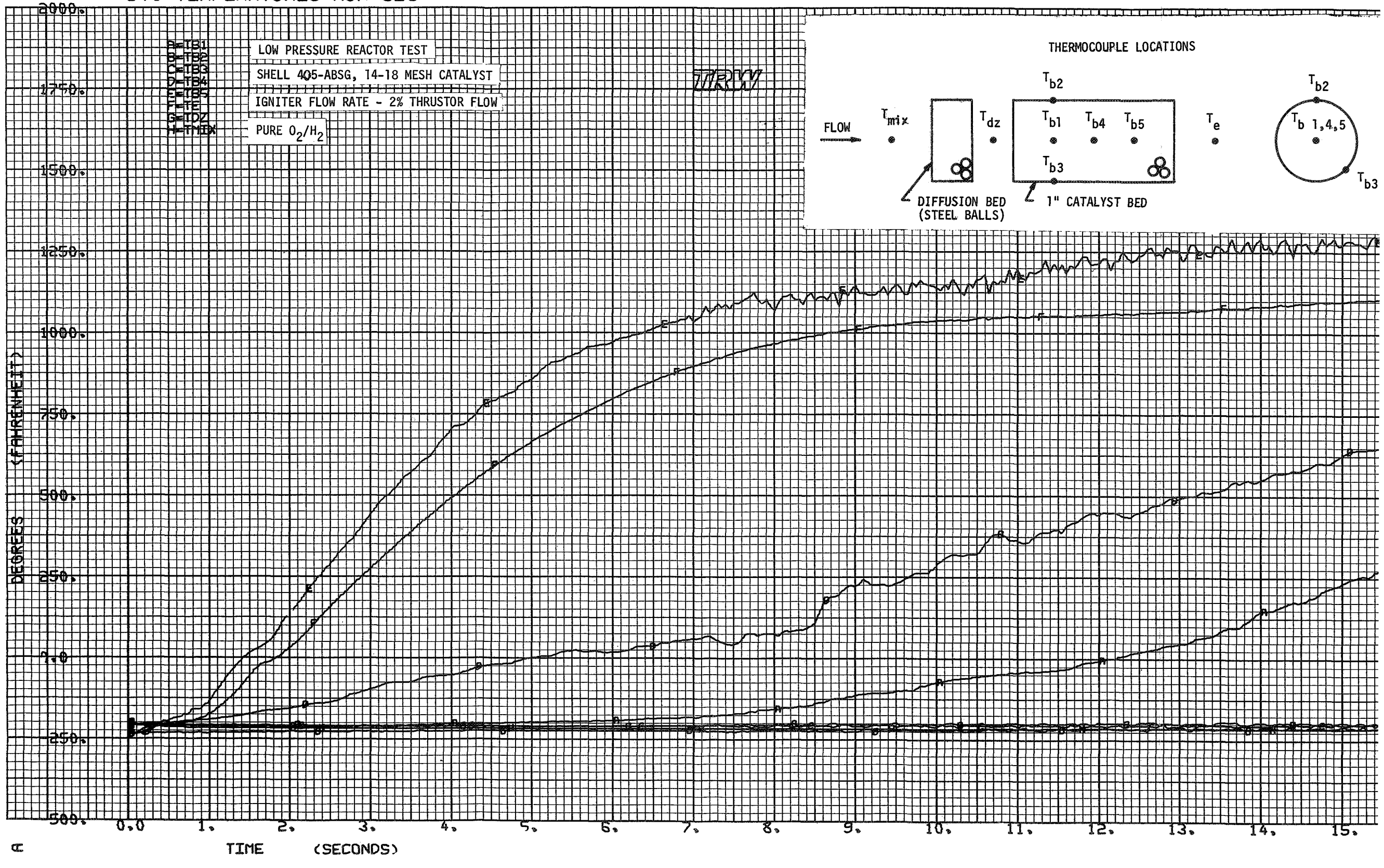

Figure 52

TEMPERATURES RUN 823

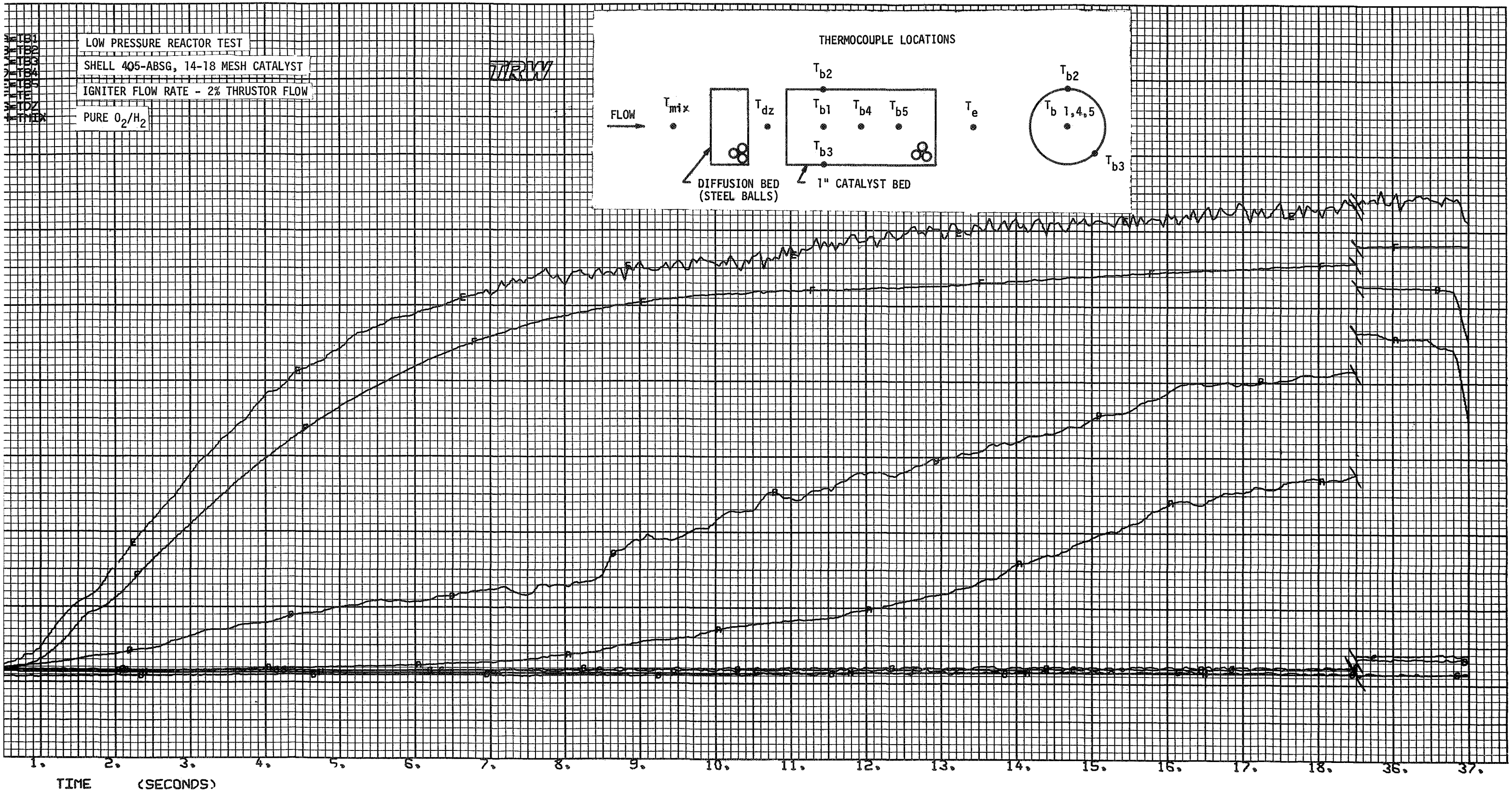

Figure 52. Catalyst Bed Temperatures—Run 823

ITS TEMPERATURES RUN 824

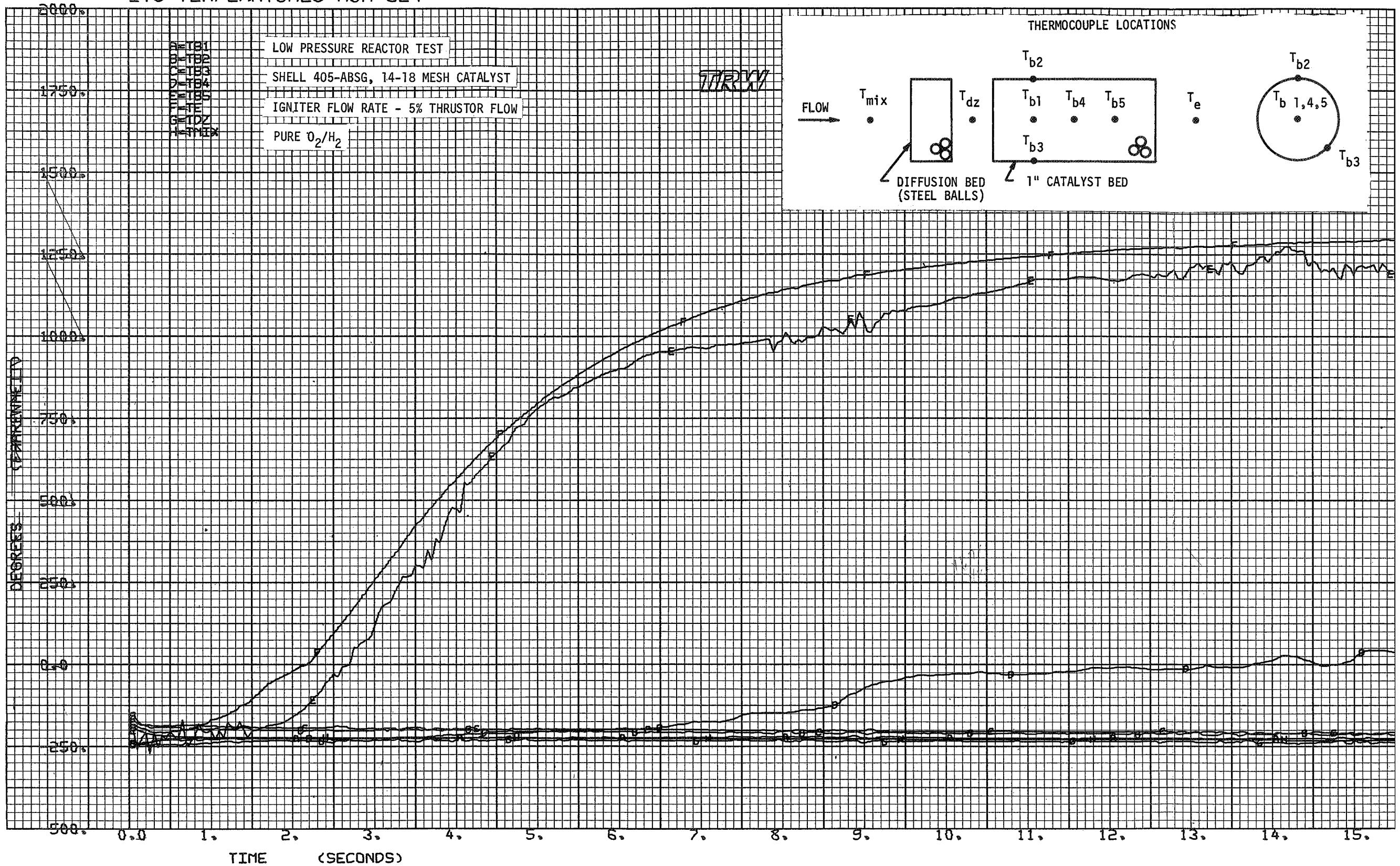

Figure

TEMPERATURES RUN 824

LOW PRESSURE REACTOR TEST

SHELL 405-ABSG, 14-18 MESH CATALYST

IGNITER FLOW RATE - 5% THRUSTOR FLOW

PURE O_2/H_2

TRW

THERMOCOUPLE LOCATIONS

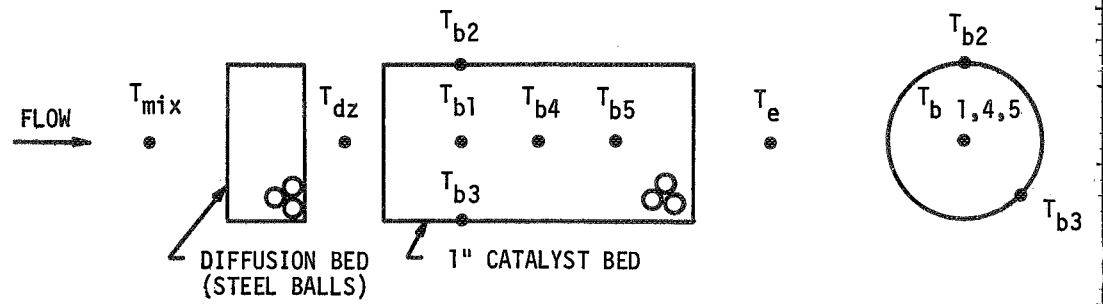

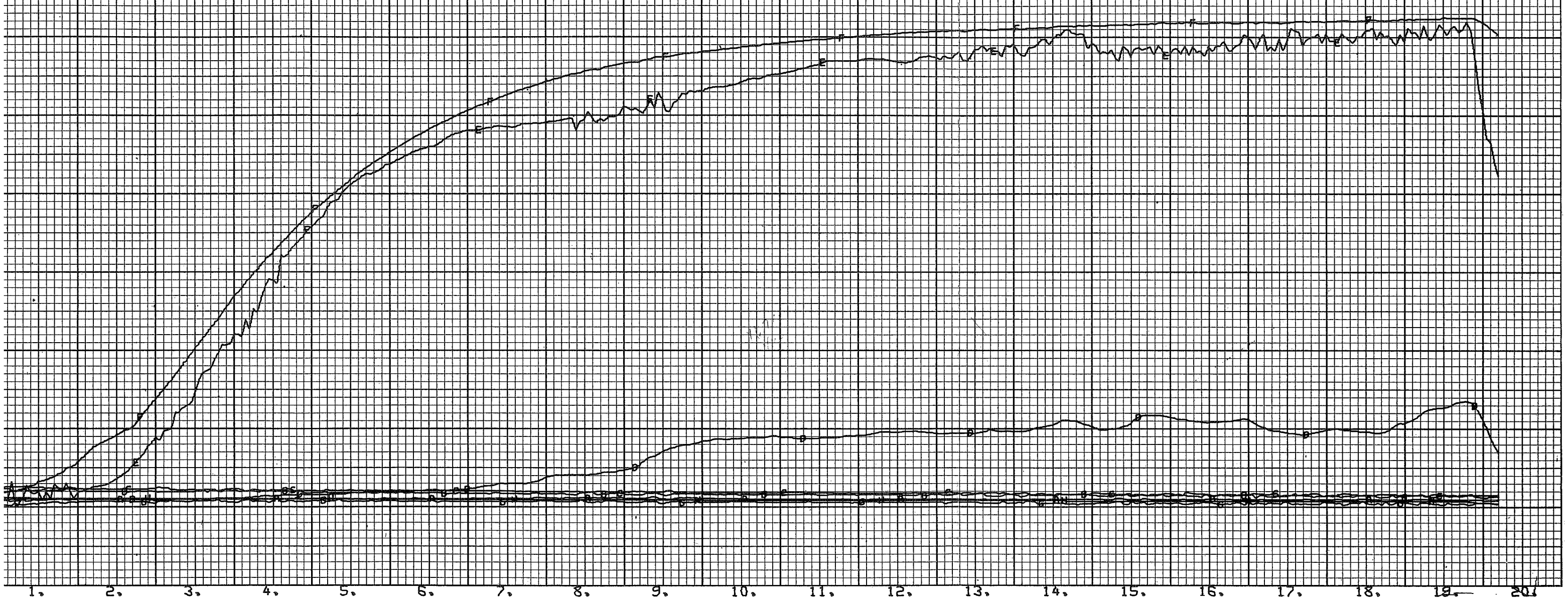

Figure 53. Catalyst Bed Temperatures—Run 824

2

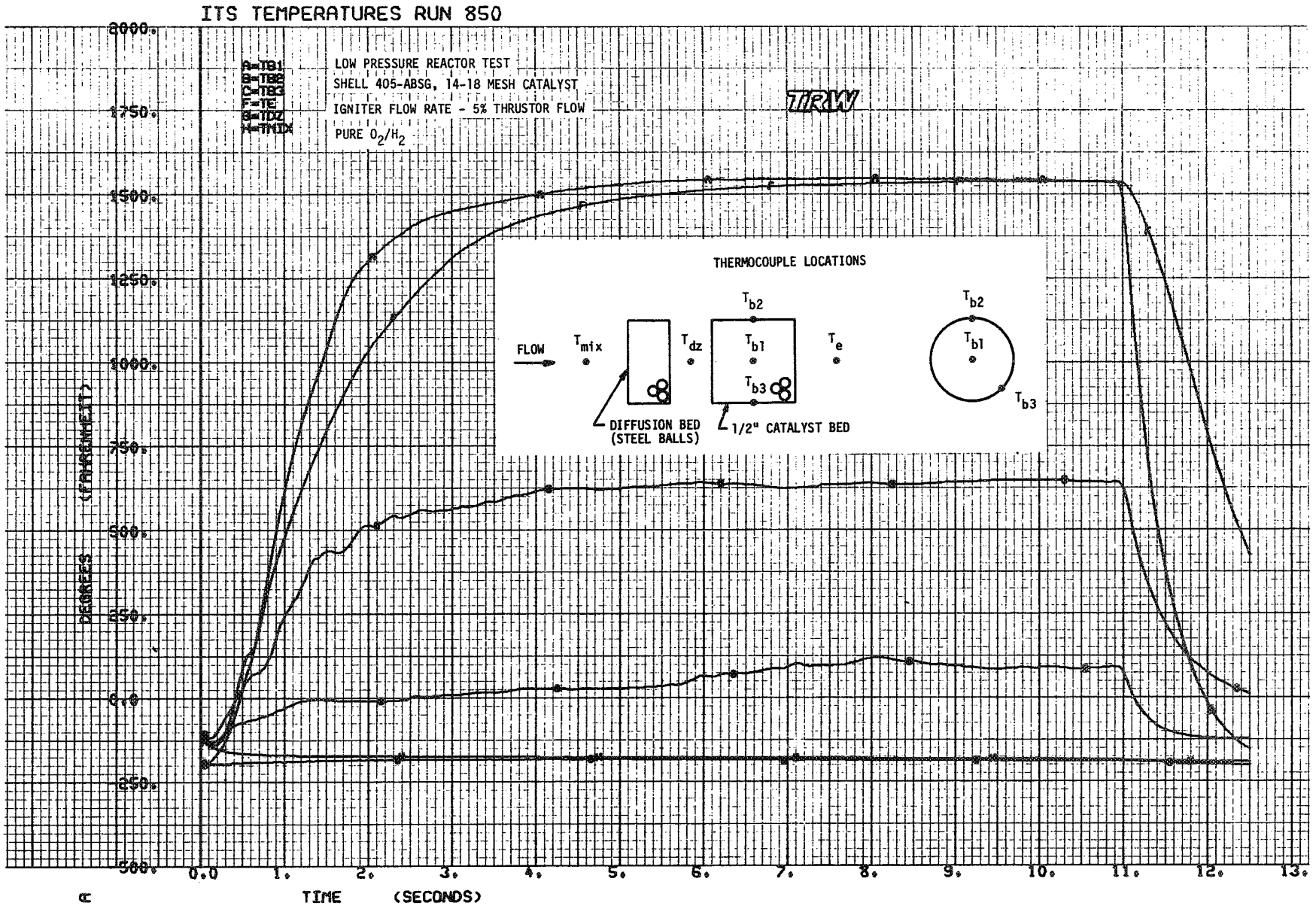

Figure 54. Catalyst Bed Temperatures—Run 850

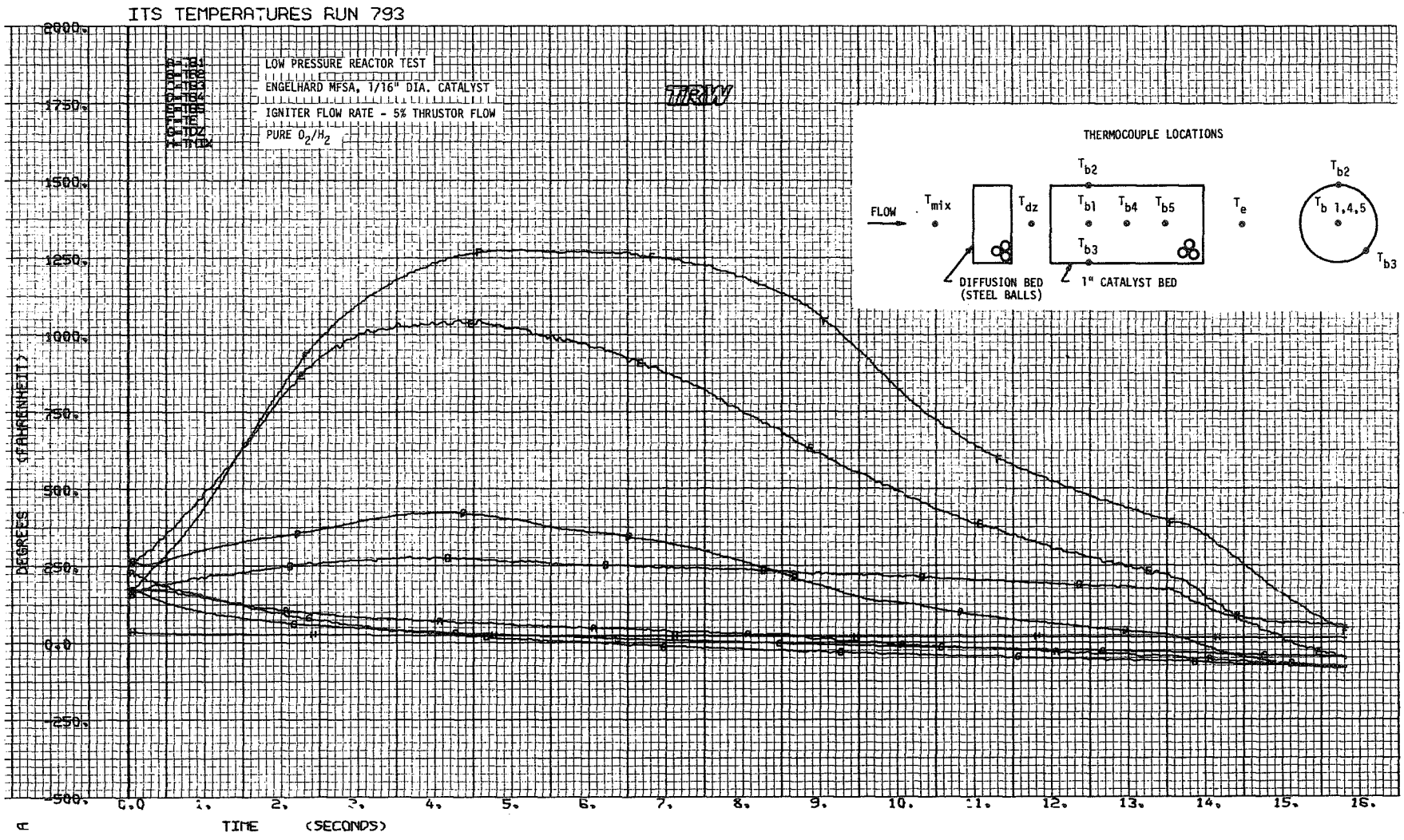

Figure 55. Catalyst Bed Temperatures—Run 793

ITS TEMPERATURES RUN 925

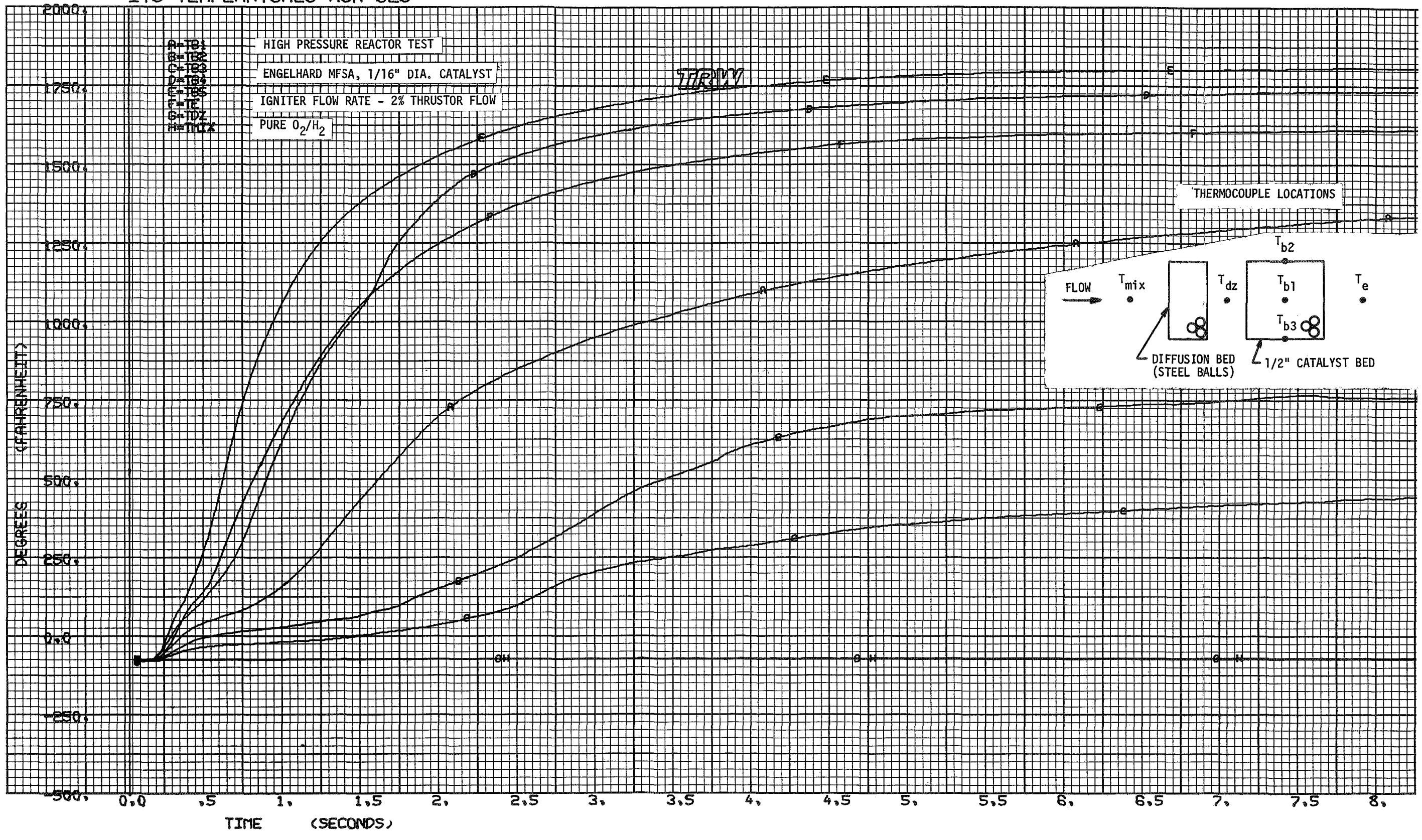

Figur

/

ATURES RUN 925

- HIGH PRESSURE REACTOR TEST
- ENGELHARD MFSA, 1/16" DIA. CATALYST
- IGNITER FLOW RATE - 2% THRUSTOR FLOW
- PURE O_2/H_2

TRW

THERMOCOUPLE LOCATIONS

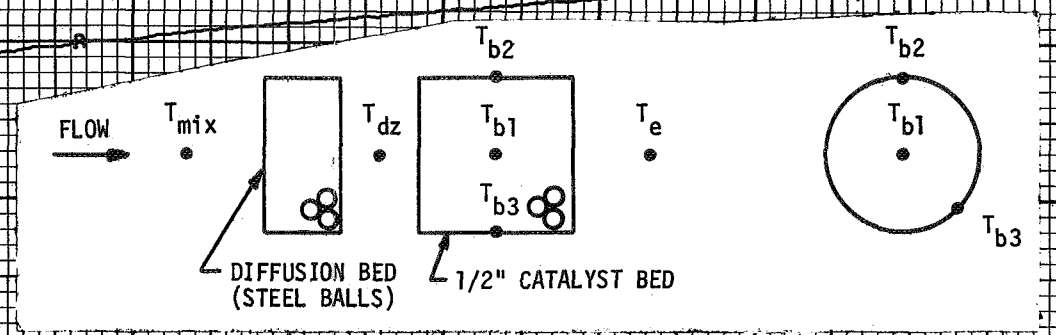

1, 1,5 2, 2,5 3, 3,5 4, 4,5 5, 5,5 6, 6,5 7, 7,5 8, 8,5 9, 17, 17,5 18,

1E (SECONDS)

Figure 56. Catalyst Bed Temperatures—Run 925

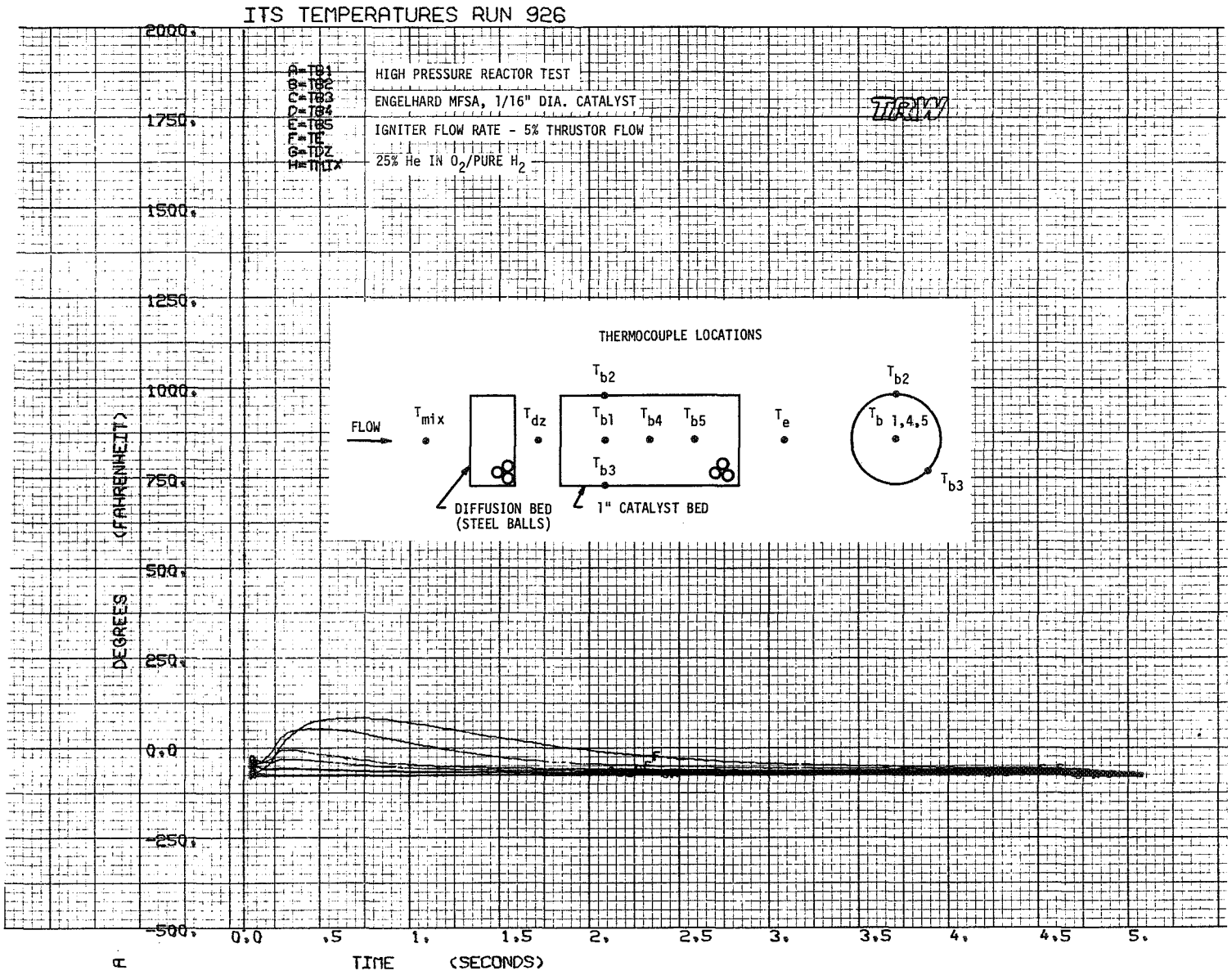

Figure 57. Catalyst Bed Temperatures—Run 926

No reactions were achieved with the Engelhard MFSA catalyst when both initial catalyst bed and propellant temperatures were below - 100°F (200°K). Initial reaction would occur when lower temperature propellants first contacted an ambient bed of Engelhard catalyst, but eventual "flameout" would result, as shown in Figure 55. However repeatable ignitions with Engelhard catalyst were attained at all temperatures above -100°F (200°F) with pure propellants. Figure 56 presents typical data indicating sustained reaction at -75°F (214°K) with a 0.50-inch (1.27 cm) bed of Engelhard MFSA 1/16 inch (0.16 cm) catalyst.

4.3.2.6 Response Effects of Propellant Helium Dilution

Effects of helium dilution of propellants on ignition with each catalyst formulation were also investigated by using supply containers of certified mixed gases. Dilutions by weight of 5, 25, and 50 percent He in O_2 and 5 and 10 percent He in H_2 were evaluated. At ambient temperatures, reaction was sustained with maximum He-O_2 dilutions of 25 percent at low pressure and 50 percent with the high pressure igniter. However, at low temperatures, reaction was significantly affected by helium dilution of the oxygen supply, as indicated by Figure 57. Helium dilutions of as high as 10 percent by weight in the hydrogen proved to have little effect on the reaction with either catalyst, except that higher reaction temperatures were attained because of the resultant increase in O_2/H_2 mixture ratio.

4.3.2.7 Mixed Catalyst Bed Evaluations

In addition to the evaluation of the Shell 405-ABSG and Engelhard MFSA catalysts over the range of operating conditions described, a series of tests at each pressure level was performed with a mixed bed including both catalyst types. These bed configurations consisted of 0.50 inch (1.27 cm) of Shell catalyst upstream of 0.50 inch (1.27 cm) of Engelhard catalyst, separated by a screen to prevent migration. Mixed beds were tested as a means of attaining the low temperature ignition capability of the Shell catalyst and increased reaction rates at temperatures above -100°F (200°K), but no advantages were observed compared to a homogeneous bed of Shell 405-ABSG catalyst.

4.3.3 Summary and Recommendations

A summary of the catalytic reactor experimental results is presented in Table 16. The test conditions which resulted in reactor ignition, as listed in the table, define the limits of operation for each catalyst formulation at the pressure levels evaluated. Also, as indicated by the reactor tests and laboratory investigations, exposure of the catalysts to high vacuum environments prior to ignition had no significant effect on the reaction rate or low temperature ignition capability.

Based upon these experimental results, one catalyst formulation and one vacuum level were recommended for combined thruster/igniter testing. Since no effects of high vacuum exposure were evident, subsequent tests

were performed at steam system vacuum levels of 120,000 feet (36580 m) simulated altitude. Shell 405-ABSG 14-18 mesh catalyst was recommended for all subsequent testing for the following reasons:

- Reaction was achieved at -250°F (117°K) with the Shell 405-ABSG catalyst, while the Engelhard MFSA catalyst did not sustain reaction below -100°F (200°K).

- Engelhard MFSA catalyst, or a mixed bed of the Shell and Engelhard catalysts, did not exhibit any increased activity at elevated temperature, or any other observable advantages, compared to a homogeneous bed of Shell 405-ABSG catalyst.

Table 16. Reactor Test Summary

Test Conditions Resulting in Reactor Ignition
(Shell 405-ABSG and Engelhard MFSA Catalysts)

	Low Pressure Igniter		High Pressure Igniter	
	Shell	Engelhard	Shell	Engelhard
Mininum propellant and bed temperatures	-250°F (117°K)	-100°F (200°K)	-250°F (117°K)	-100°F (200°K)
Igniter flow rate (% of thruster flow)	2-10%	2-10%	2-10%	2-10%
Helium dilution in oxygen (max wt %)	25% @ ambient not @ -250°F (117°K)	25% @ ambient not @ -100°F (200°K)	50% @ ambient not @ -250°F(117°K)	50% @ ambient not @ -100°F(200°K)
Helium dilution in hydrogen (max wt %)	10% @ ambient 10% @ -250°F(117°K)	10% @ ambient 10% @ -100°F(200°K)	10% @ ambient 10% A -250°F(117°K)	5%(1) @ ambient not @ -100°F(200°K)
Catalyst bed lengths attaining complete reaction	1/2(2) - 1" (1.27-2.54 cm)	1/2 - 1" (1.27-2.54 cm)	1/2 - 1" (1.27-2.54 cm)	1/2 - 1" (1.27-2.54 cm)

(1) 10% $He-H_2$ was not available when this test was performed, thus 5% $He-O_2$ was the maximum dilution tested.

(2) A 1/4" (.64 cm) long Shell catalyst bed was tested, and incomplete reaction resulted. Subsequent tests of 1/4" beds were eliminated from the test series.

5. COMBINED THRUSTER/IGNITER TESTS

A series of 484 test firings was conducted during this phase of the program to investigate the thruster/igniter interactions and overall thruster operating characteristics. The specific objectives of this task effort were as follows:

- Design and fabricate a complete thruster for each chamber pressure
- Determine minumum igniter energy level requirements for satisfactory ignition of each thruster
- Evaluate catalyst bed geometry effects on thruster/igniter response
- Establish steady-state baseline performance for each thruster
- Conduct pulse mode tests with -250°F (117°K) conditioned propellants

The following report sections describe in detail the thruster hardware, and discuss the various types of test firings conducted and the experimental results.

5.1 THRUSTER HARDWARE DESCRIPTION

A complete injector and thrust chamber assembly was designed and fabricated for each chamber pressure level, 10 and 100 psia (69 and 690 kN/m^2). The basic thruster hardware is described in this section; modifications to the hardware appear in the discussion of the test series during which the changes were performed.

5.1.1 Thruster Injectors and Ignition Chambers

The design concept for the low pressure injector is shown in Figure 58, and is typical of both main thruster injectors. In the basic configuration, gaseous propellants were injected through continuous annular orifices into the combustion chamber. These orifices were independently adjustable by means of calibrated flat shims, as shown. This adjustment capability allowed optimization of both absolute and relative propellant injection velocities.

Additional injection techniques, such as impinging doublets of any number, could also be evaluated with the same basic injector by removing the adjustment shims and bottoming the annular orifices after milling slots in the metering surfaces of the injector sleeve (Figure 58). The sleeve was designed for ease of fabrication to allow a number of orifice configurations to be readily evaluated, if desired.

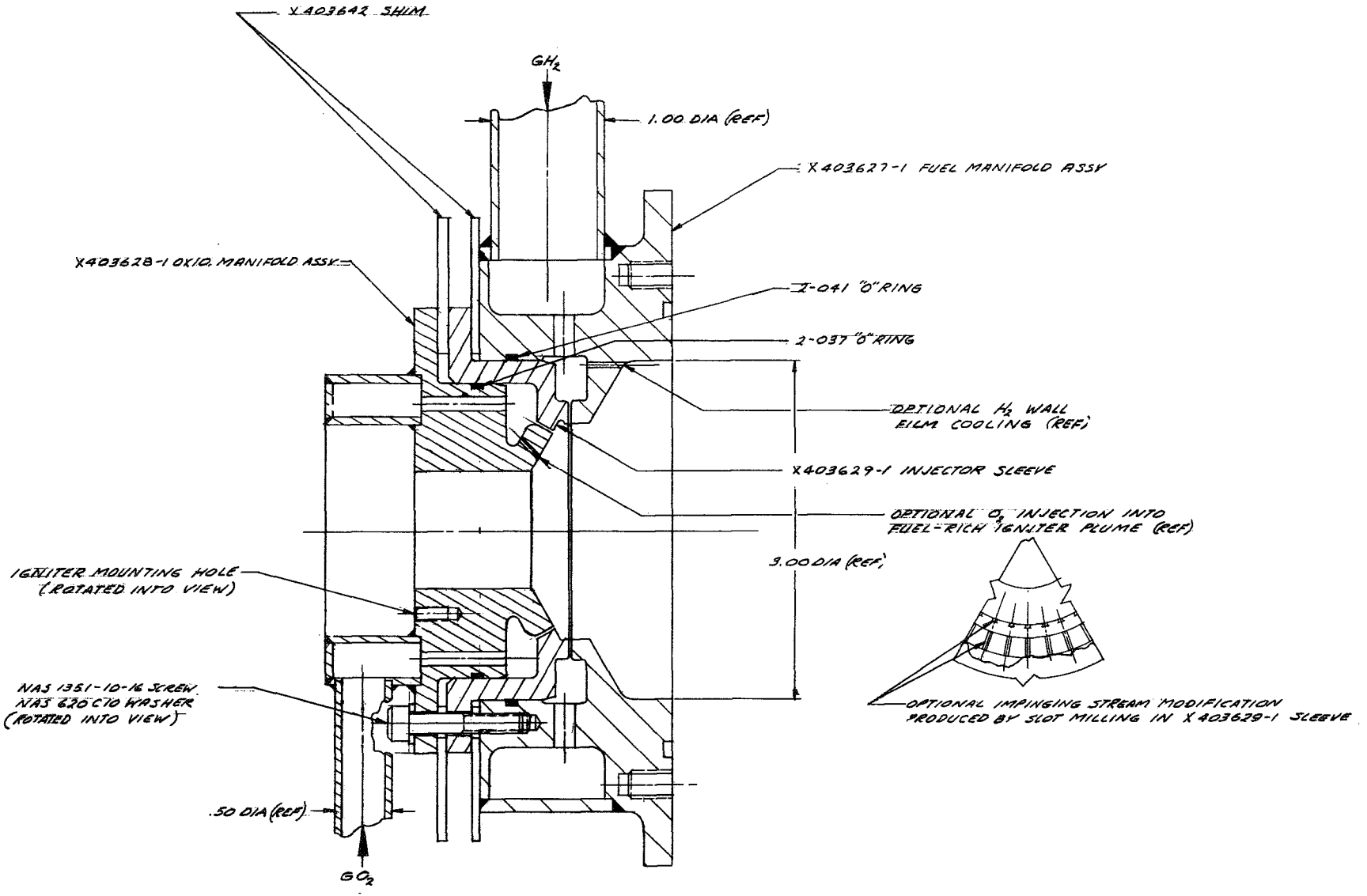

Figure 58. Main Injector Assembly—Low Chamber Pressure Thruster

Because both propellants were injected as gases, the usual required pressure drops for liquid injectors did not apply. Instead, velocity criteria were of primary consideration in determining injection area requirements. The injection Mach numbers for the two pressure levels of operation are given below, assuming equal pressure drops for both propellants.

P_c = 10 psia (69 kN/m^2)		P_c = 100 psia (690 kN/m^2)	
ΔP	M	ΔP	M
psi (kN/m^2)		psi (kN/m^2)	
1 (6.9)	0.37	5 (34.5)	0.27
2 (13.8)	0.52	10 (68.9)	0.37
3 (20.7)	0.63	15 (103.4)	0.46
4 (27.6)	0.71	20 (137.9)	0.52
5 (34.5)	0.78	25 (172.4)	0.57

At propellant inlet temperatures of -250°F (117°K) the velocities for these ΔP levels range from 1000 to 2120 ft/sec (305 to 646 m/sec) for gaseous hydrogen at the low pressure operation to 735 to 1550 ft/sec (224 to 472 m/sec) at the higher pressure. The gaseous oxygen injection velocities range from 170 to 359 ft/sec (52 to 109 m/sec) at the low pressure and 124 to 252 ft/sec (38 to 77 m/sec) at 100 psia (690 kN/m^2) operation. It is evident that sizeable injection velocities are achieved with little pressure drop. Initial injection Mach numbers of 0.6 were selected for each propellant for both thrusters, resulting in injection pressure drops of nominally 3 psi (20.7 kN/m^2) for the low pressure injector and 25 psi (172.4 kN/m^2) for the high pressure thruster injector.

The catalytic igniter was mounted in the center of the injector and thermally isolated from the main injector by an insulating seal. The gaseous oxygen was injected nearest the center of the chamber, to provide an oxidizer-rich environment for optimum reaction with the fuel-rich (O_2/H_2 mixture ratio 1:1) igniter plume. Additional pure oxygen was injected directly into the igniter plume to facilitate ignition by drilling the optional orifices into the oxidizer manifold, as shown in Figure 58.

An annular undercut about 0.050 inch (0.127 cm) deep was made immediately upstream of the gaseous hydrogen injection orifice as a means of controlling injector recirculation gas flow to minimize heat transfer to the gaseous oxygen injection area. Injection of the hydrogen between the main oxygen orifice and the chamber wall provided a favorable fuel-rich wall environment to minimize heat transfer to the chamber. The hydrogen feed manifold was designed so that additional hydrogen could be injected for chamber cooling by drilling orifices as indicated in Figure 58.

The completed injectors for each pressure level are shown in Figure 59, with the low pressure injector on the left. The adjustable annular oxidizer (inner gap) and fuel (outer gap) injection orifices can be seen in the figure. Also shown are the center inlet ports for the igniters and the seal rings and mounting bolt holes for the thrust chambers.

The disassembled injectors for the 10 and 100 psia (69 and 690 kN/m^2) thrusters are shown in Figures 60 and 61, respectively. From left to right, the detail parts for each are: (1) fuel manifold assembly, (2) fuel injection orifice adjustment shims, (3) injector sleeve, (4) oxidizer orifice shims, (5) oxidizer manifold assembly, and (6) assembly screws and washers. No interpropellant welds or seals were used in either injector; any weld or seal leakage would vent externally of the injector or thrust chamber.

The first set of thrust chamber hardware was designed for the ignition energy level tests. Although these firings were all performed under vacuum conditions, no thrust measurements were to be taken, thus no altitude nozzle extensions were required. Workhorse thrust chambers were fabricated with steel sections and copper nozzles for each pressure level.

Figure 62 is a view of both thrusters disassembled. The component parts of each thruster, left to right, are: (1) retaining ring, (2) nozzle section, (3) chamber sections, and (4) injector assembly. Seal gaskets and assembly bolts are not shown in this figure.

Both thruster assemblies are shown in Figure 63, with the low pressure thruster on the left. The larger propellant line on each thruster is the gaseous hydrogen inlet, and the smaller line is the gaseous oxygen inlet. Pressure ports were provided in each propellant manifold to measure injection pressures. Each thrust chamber had two sections to provide the variable chamber volumes required for testing. Chamber pressure instrumentation ports were incorporated into the downstream chamber section of each thruster. The lucite rod shown extending from the high pressure thrust chamber is a view "window" to allow use of an IR detector to indicate main thruster ignition. Four rows of holes 90 degrees apart were drilled in each copper nozzle section. Chromel/alumel thermocouple junctions were peened into these holes to provide capability of both axial and circumferential heat flux determination in the nozzle convergence and throat areas.

5.1.2 Altitude Thrust Chambers

Baseline performance tests required the determination of impulse response and the measurement of altitude thrust and specific impulse. Nozzle expansion ratios of 40:1 were specified for the performance tests. Design of altitude thrust chambers incorporated test experience obtained with the workhorse chamber hardware used for the ignition test series.

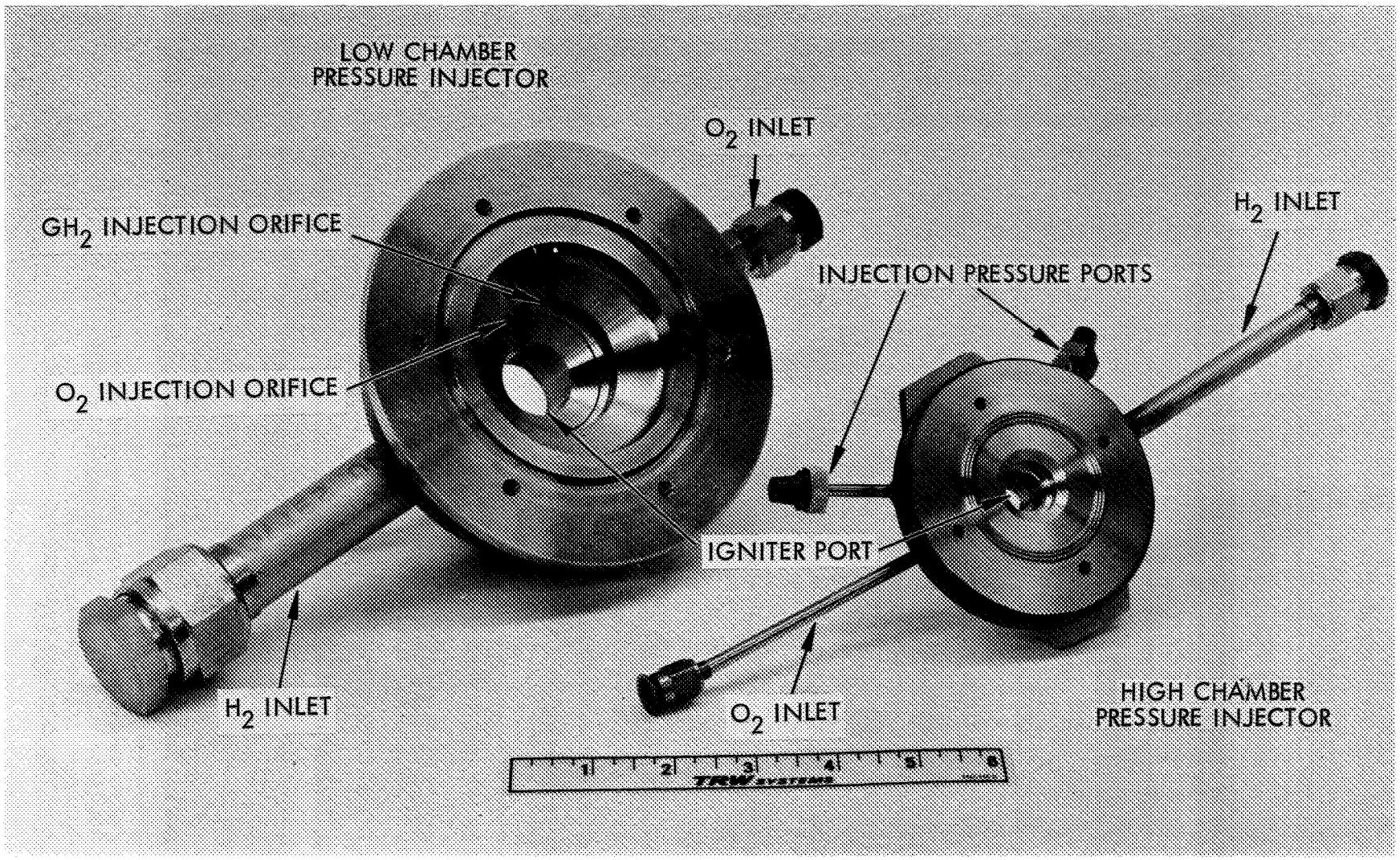

Figure 59. Thruster Injector Assemblies

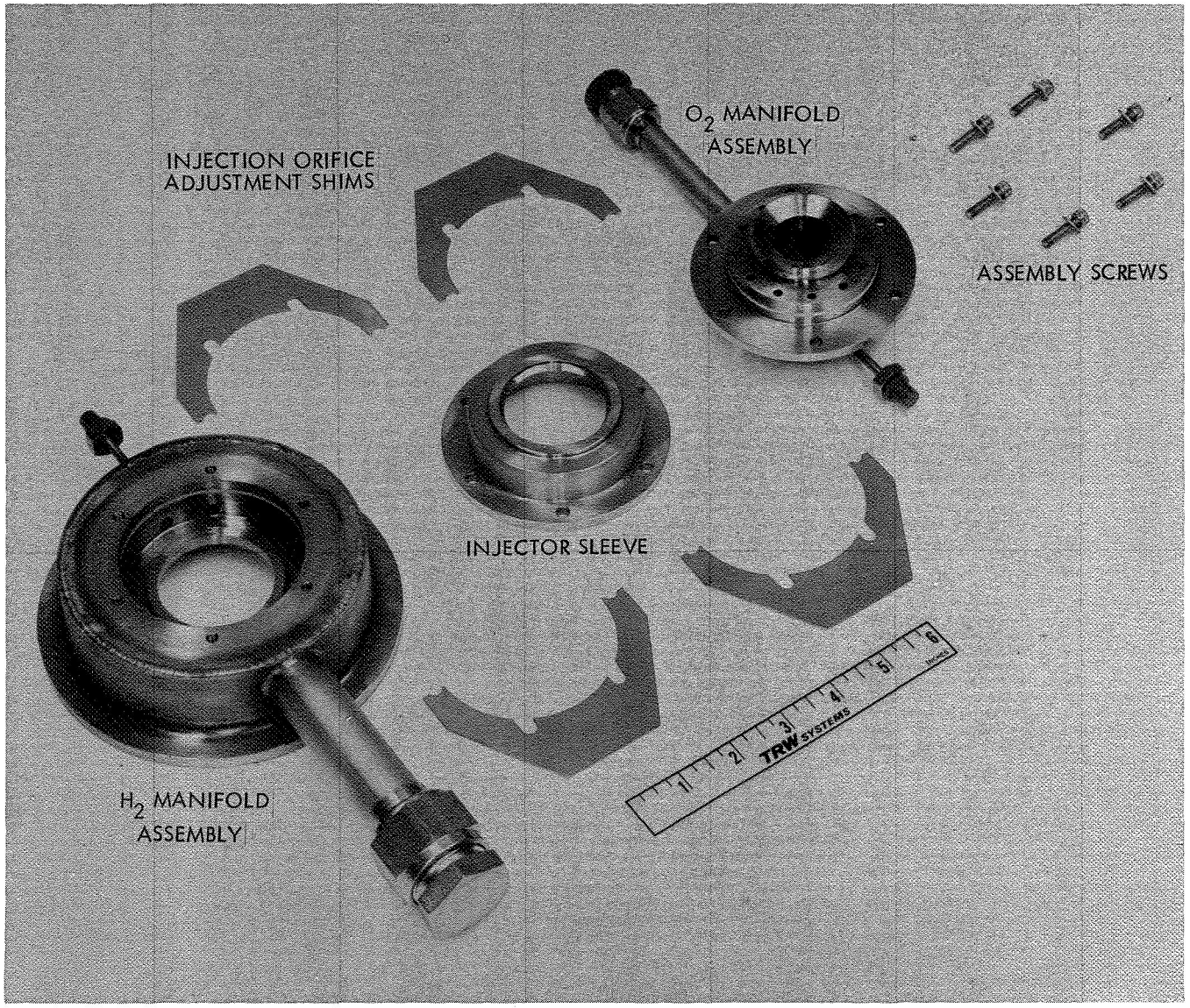

Figure 60. Disassembled Injector — Low Chamber Pressure Thruster

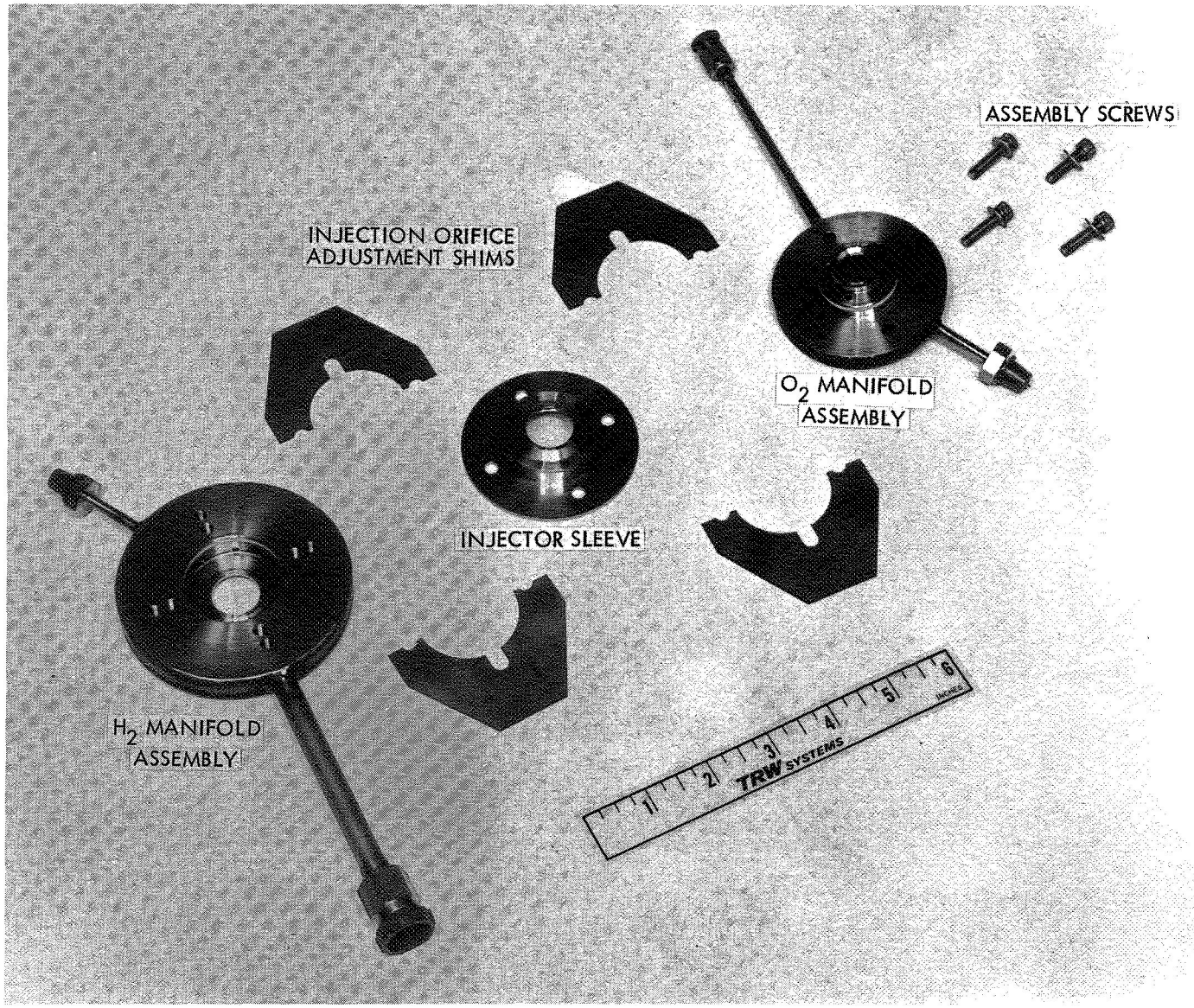

Figure 61. Disassembled Injector—High Chamber Pressure Thruster

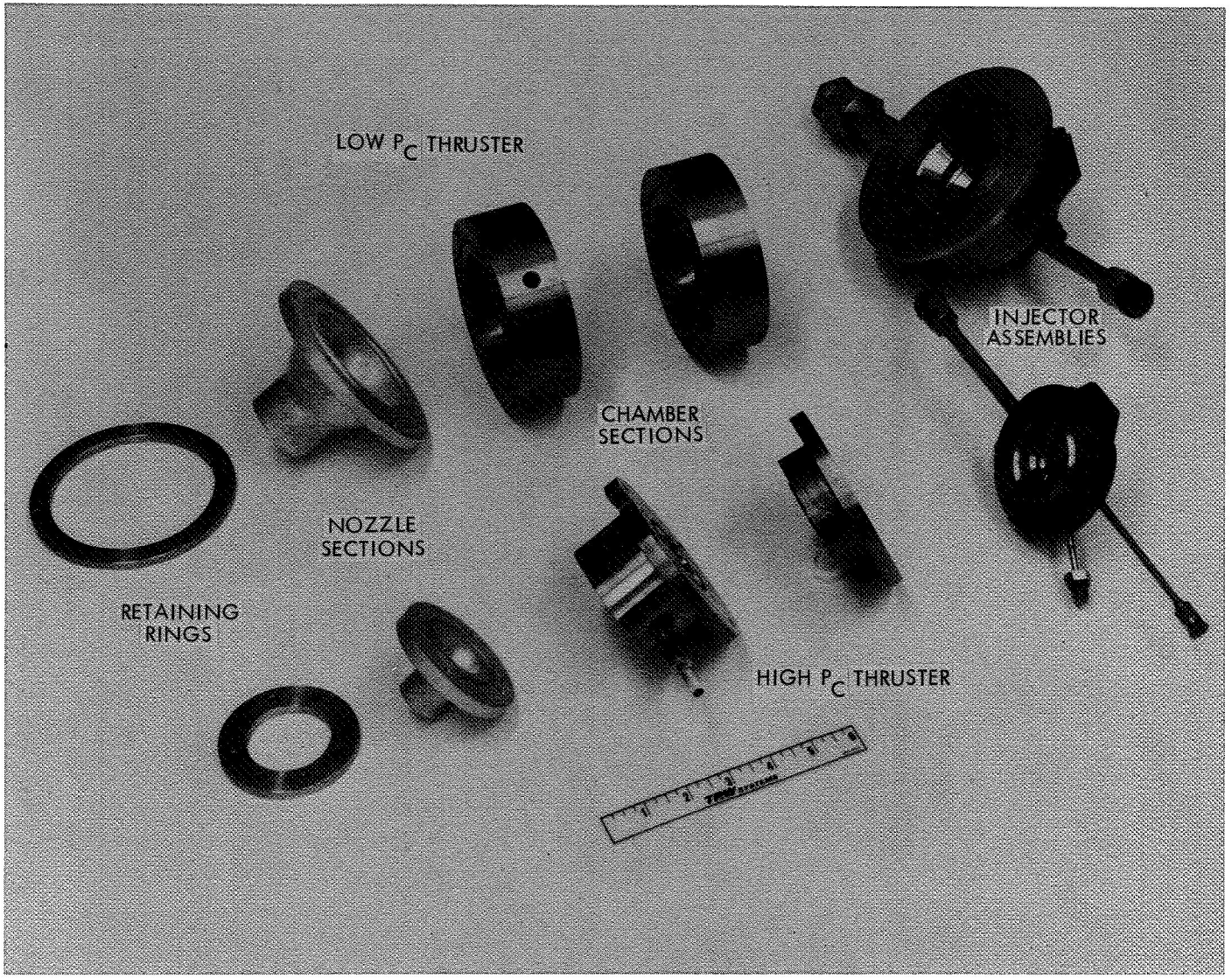

Figure 62. Disassembled Main Thrusters

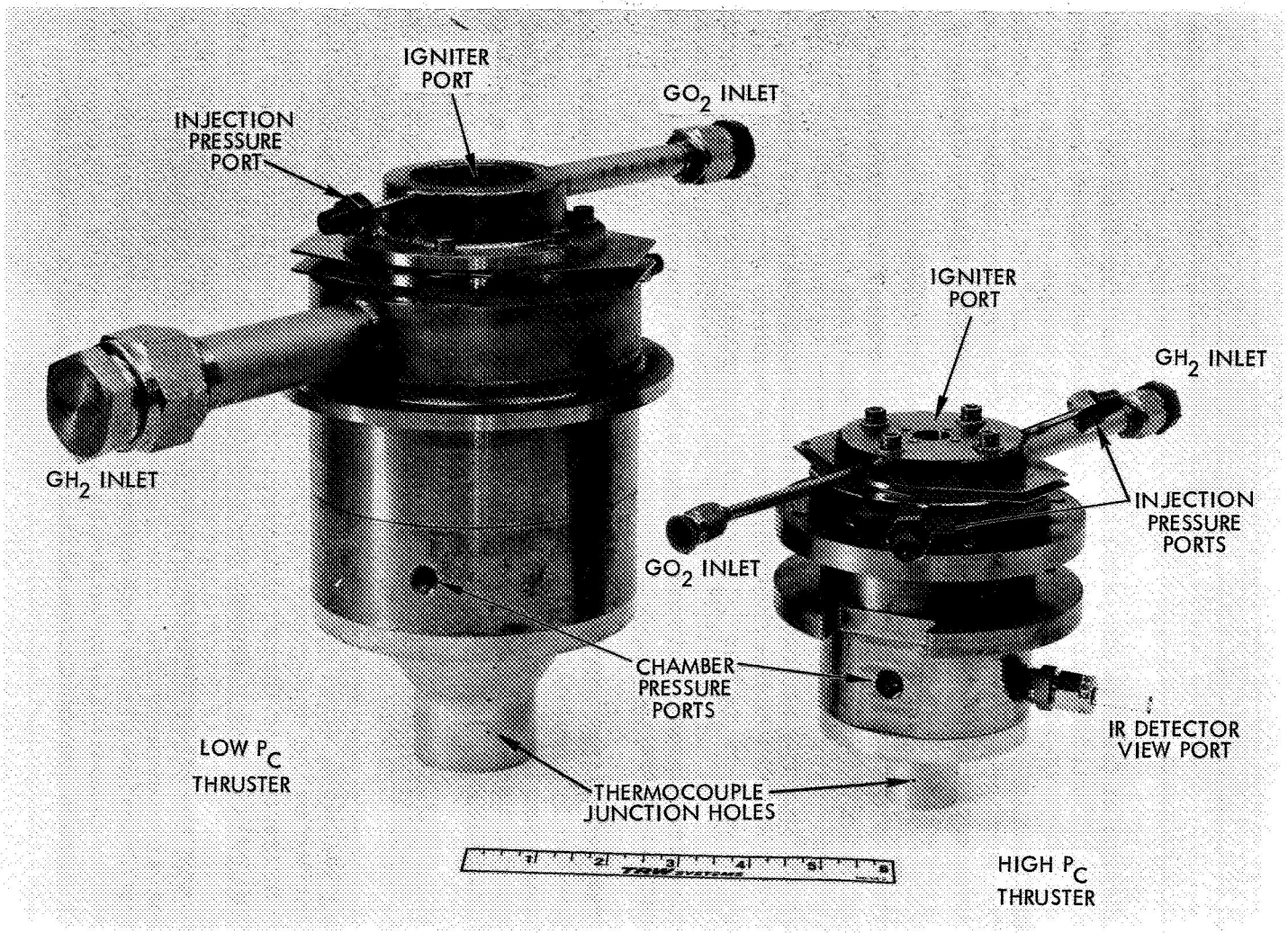

Figure 63. Main Thruster Assemblies

The altitude chamber design for the high chamber pressure thruster is shown in Figure 64. The combustion chamber and 40:1 area ratio nozzle were machined into a single piece of copper stock. The heat sink capability of the copper was more than adequate to attain the required 20-second run durations. Redundant chamber pressure instrumentation ports were provided in the chamber walls. The separate chamber sections used in the ignition tests were compatible with the diameters and seals of the altitude chamber hardware, and were utilized to perform chamber L* variation tests.

Design of the low pressure altitude thrust chamber is presented in Figure 65. The chamber assembly consisted of a copper heat sink chamber and a stainless steel nozzle assembly. The nozzle skirt was fabricated by spin-forming of a welded metal cone. The nozzle was then welded to a flange, and the assembly was bolted to the copper chamber. Stainless steel split back-up plates were utilized to insure uniform loading of the crush gasket seals.

Both of the altitude chamber nozzle contours were machined as constant radii. Design and performance analyses had shown that for thrust chambers of this size, a Rao optimum contour could be approximated by constant throat and nozzle radii without significant performance losses. In fact, for small nozzles, the difference between the Rao optimum contour and a constant radius is often within normal machining tolerances. A single nozzle radius greatly reduces the time and expense of preparing machining templates, and this design technique was utilized for all altitude test hardware during this program.

The completed altitude thrust chambers for each pressure level are shown in Figure 66, along with the mating injectors. The low pressure thrust chamber hardware, near the top of the photograph, consisted of a chamber and nozzle assembly. Shown below is the one-piece high pressure thrust chamber.

Both altitude thruster assemblies are shown in Figure 67. The igniters for each thruster are not included in this photograph. Major components of the low pressure thruster, at the left, were bolted together, utilizing stainless steel split back-up plates. The high pressure injector was attached to the one-piece chamber by cap screws threaded into steel inserts in the copper thrust chamber. Crush gaskets were used to pressure seal both thrust chamber assemblies. Each thruster was provided with two chamber pressure measurement ports (one visible in Figures 66 and 67, and the other directly opposite). Chromel/alumel thermocouple junctions were peened into holes drilled in the copper chambers prior to initiation of test to obtain both outer and inner wall temperatures for heat flux determination. Thermocouples were also welded to the low pressure thruster nozzle extension for additional thermal data acquisition.

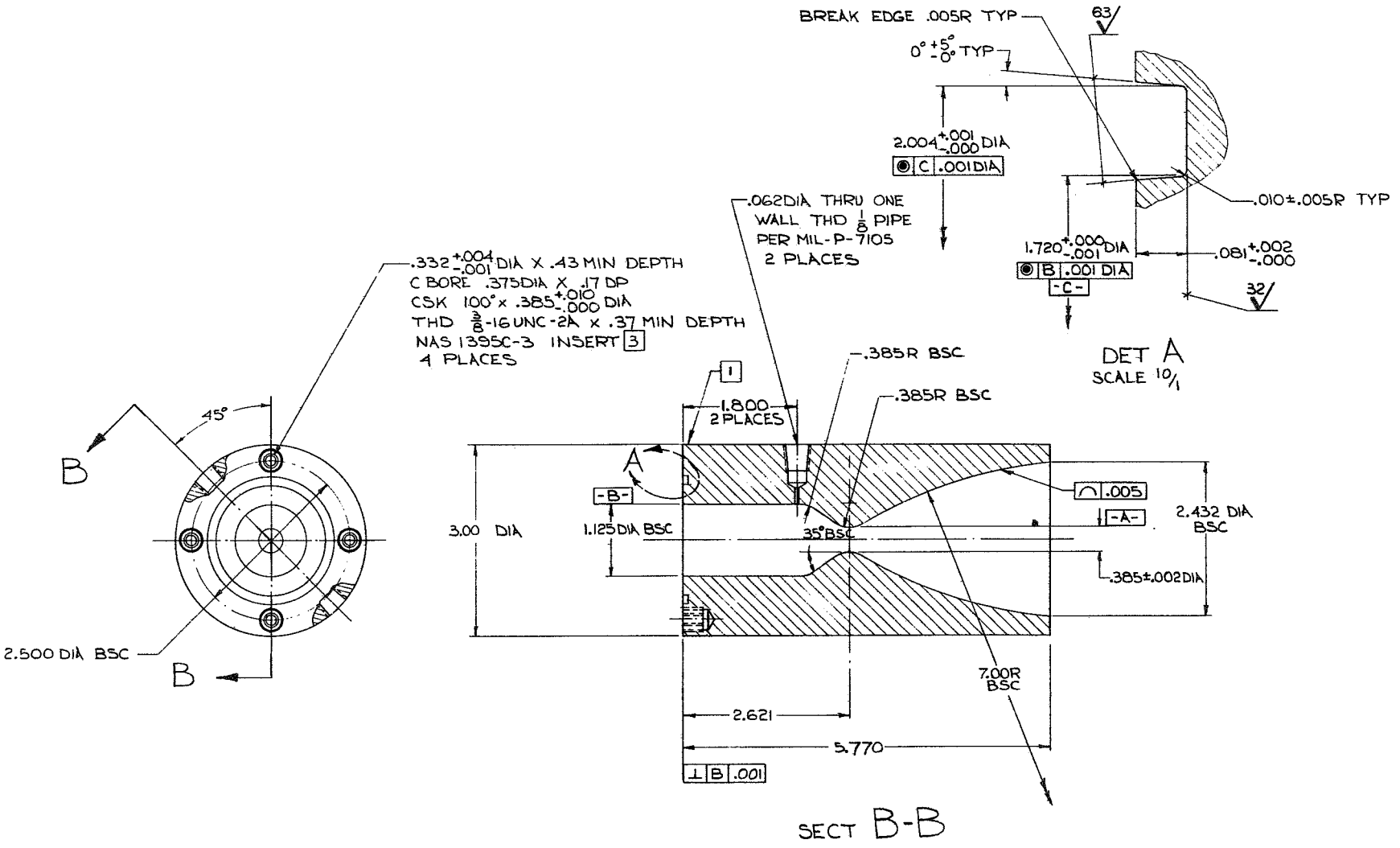

Figure 64. Altitude Thrust Chamber (Copper Heat Sink)—High Pressure Thruster

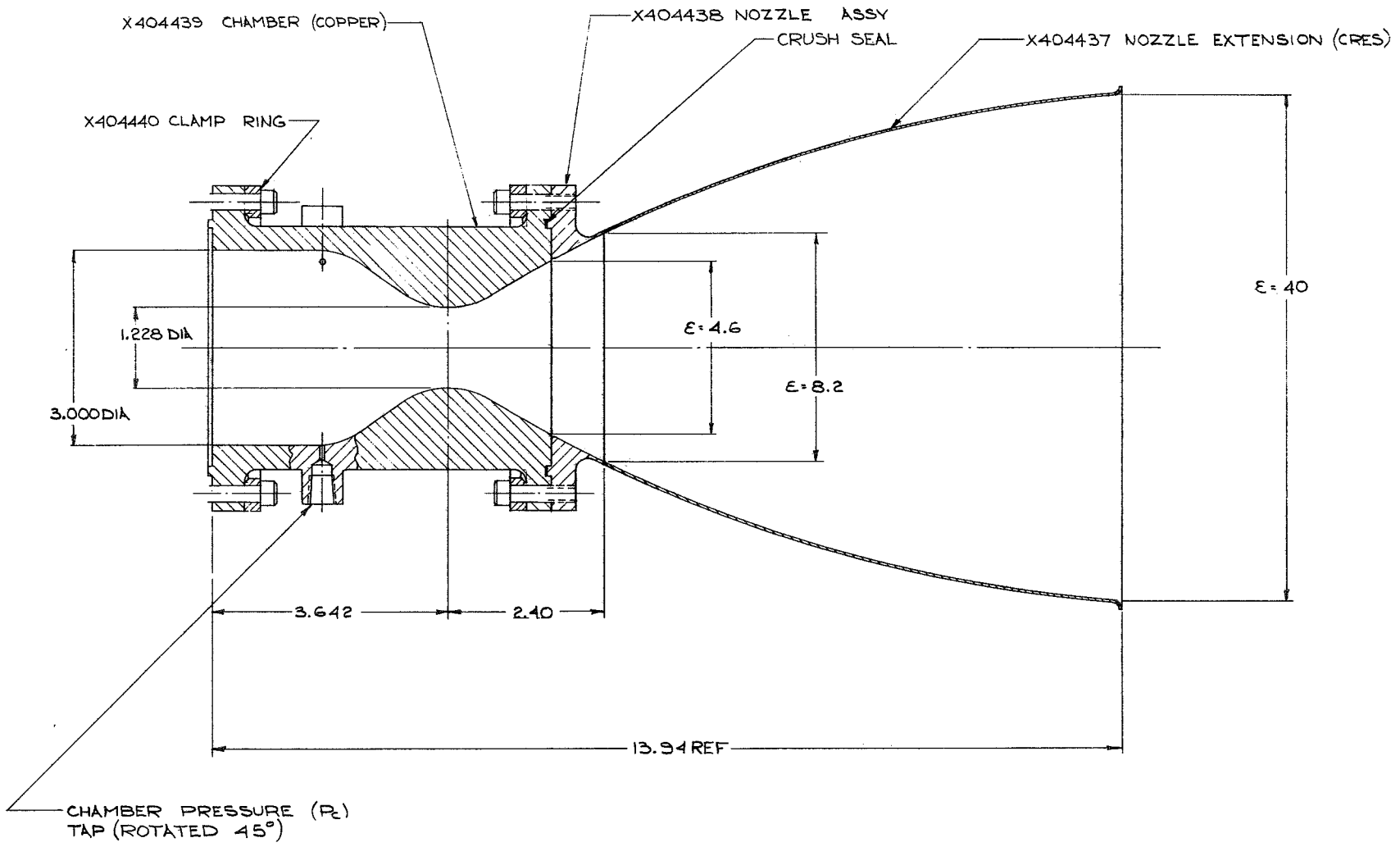

Figure 65. Altitude Thrust Chamber Assembly—Low Pressure Thruster

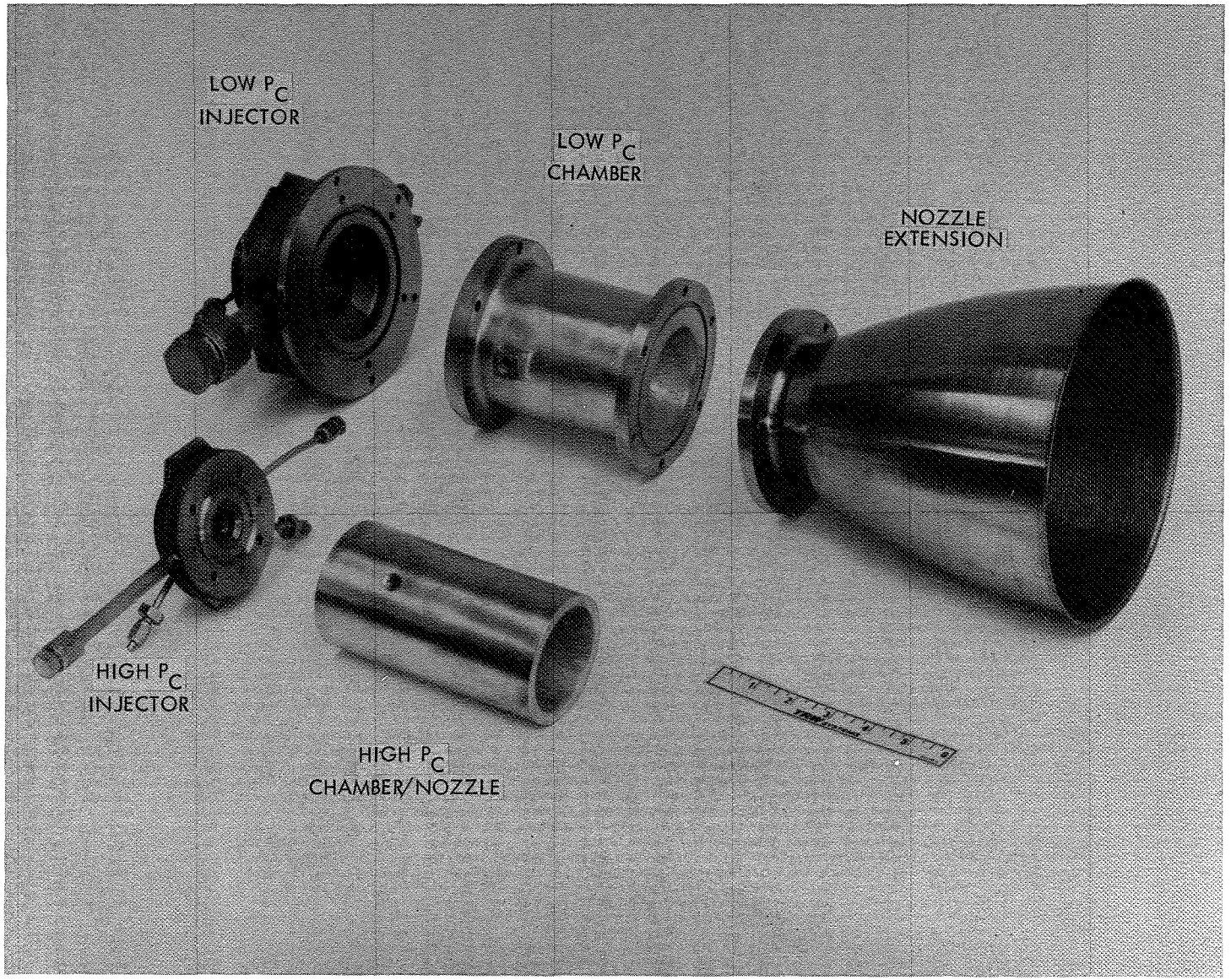

Figure 66. Disassembled Main Thrusters — 40:1 Expansion Ratio Altitude Nozzles

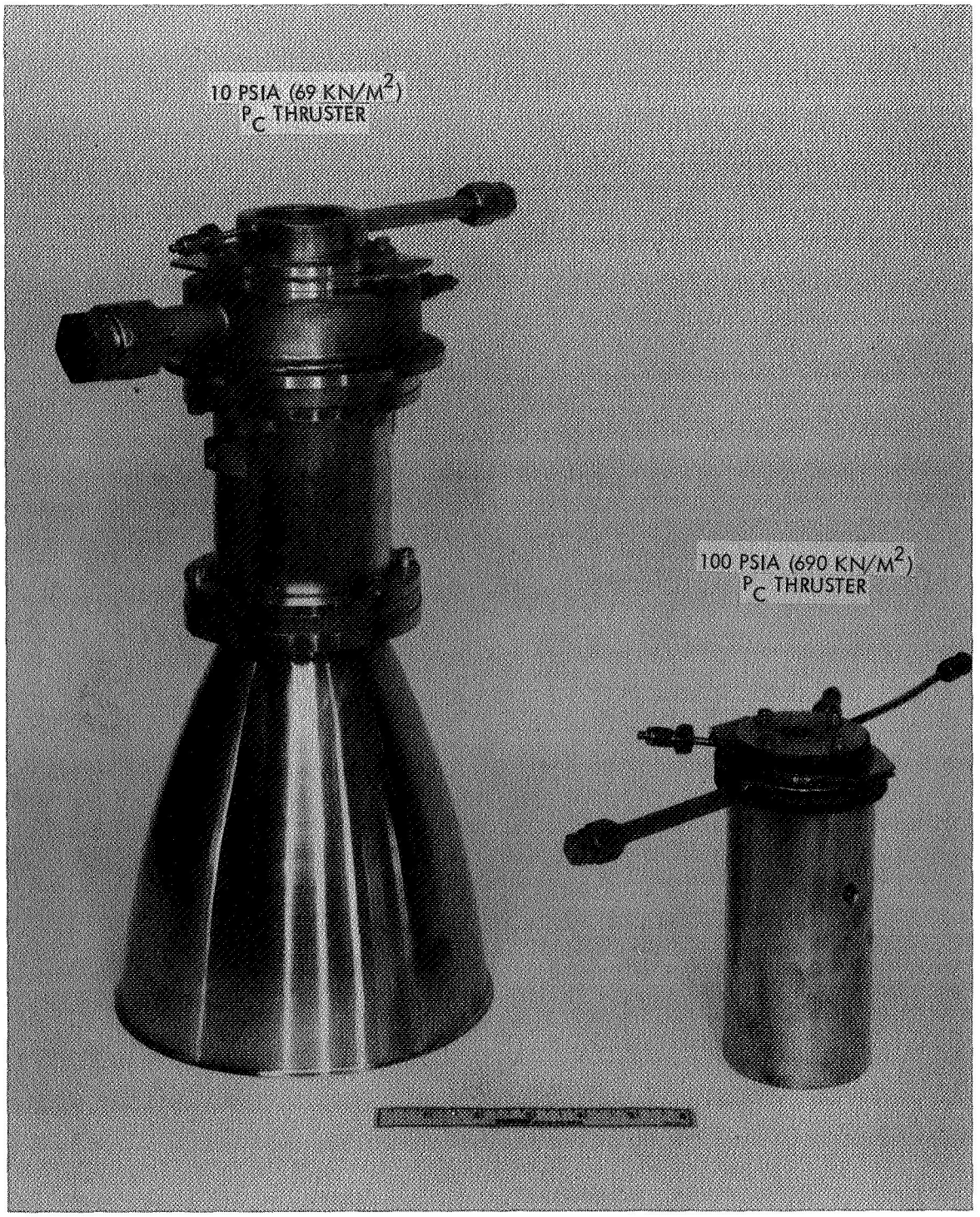

Figure 67. Main Thruster Assemblies — Altitude Nozzles

5.2 IGNITION ENERGY LEVEL TESTS

Thruster/igniter tests were performed to characterize the energy level requirements for ignition of a nominal 20 lbf (89N) O_2/H_2 thruster. The objectives of this test series were:

- Conduct ignition test firings to establish minimum igniter flow rates and effluent temperatures required to insure main thruster ignition at each pressure level.
- Determine the effect on ignition energy requirements and ignition delay caused by variables such as thrust chamber volume, propellant temperatures and dilutions, and lead or lag of igniter/thruster valves.

The following paragraphs describe the test installation and procedures employed, and discuss the experimental results obtained.

5.2.1 Test Description

The propellant supply and conditioning system used for all thruster/igniter testing is shown in Figure 68. (H_2 system shown—O_2 system basically the same). The C-2 altitude test stand installation for the low chamber pressure thruster is shown in Figure 69. This photograph, taken with the vacuum cover retracted, shows the thruster, propellant fire valves, and the propellant bleed valves used to condition propellants and to insure pure propellant flow for ignition tests.

Figure 70 is a closeup view showing the high pressure thruster injector and thrust chamber, and the workhorse igniter attached to the center of the main injector. Stand installation of both chamber pressure thrusters utilized the same propellant feed system and valves, and required only the changing of pressure transducers for the higher pressure operation.

Workhorse igniter hardware was used for this test series to establish design criteria for the reactors described in Section 4.1 of this report. The thruster hardware is described in detail in Section 5.1.

The igniter assembly used for the low chamber pressure ignition tests, shown in Figure 71, was constructed from standard stainless steel fittings and tubing for ease of modification. A single instrumentation port downstream of the catalyst bed was used for both pressure and temperature measurement, as shown in the illustration. A similar port was added to the upstream mixing tube for positive detection of flashback.

Figure 72 shows the workhorse high pressure igniter assembly used for these tests. Disassembled components of the igniter are shown in Figure 73. From left to right, the details are: (1) combustion chamber and nozzle, (2) bed holder with pressure and temperature instrumentation, (3) catalyst bed retaining screen and sleeve, (4) catalyst, (5) diffusion bed

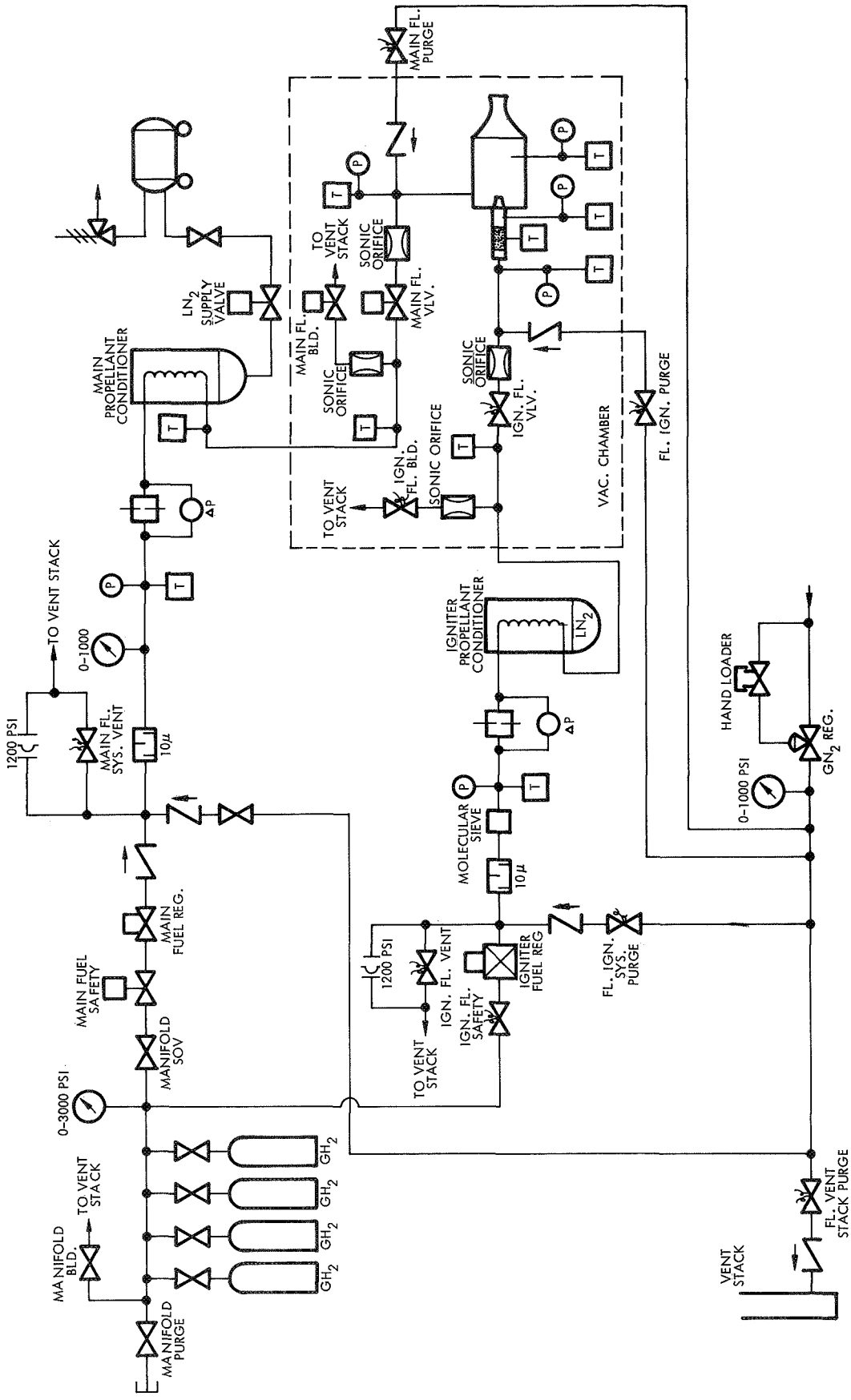

Figure 68. H_2/O_2 Thruster Facility Schematic , GH_2

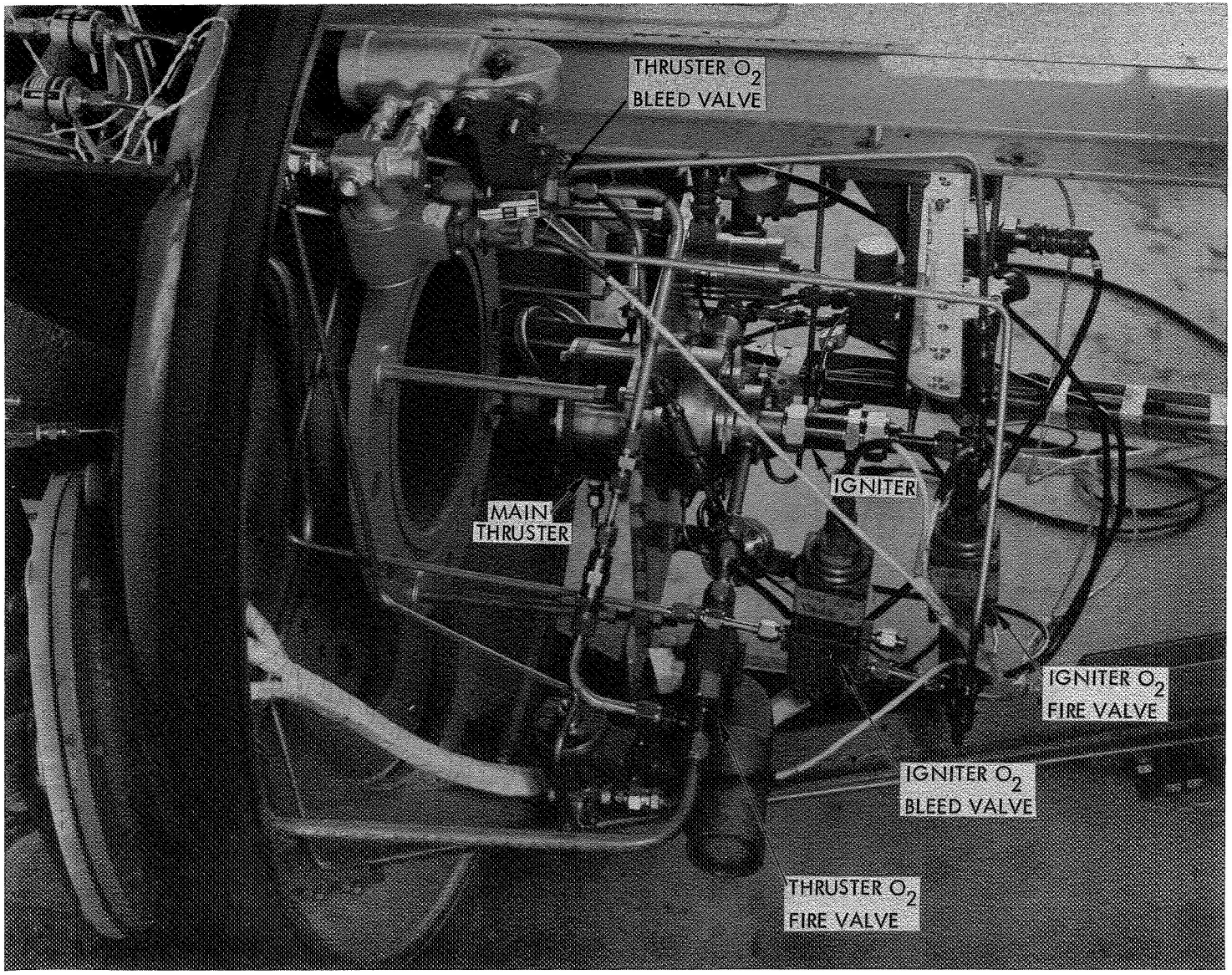

Figure 69. Altitude Test Stand Installation — Low Chamber Pressure Thruster

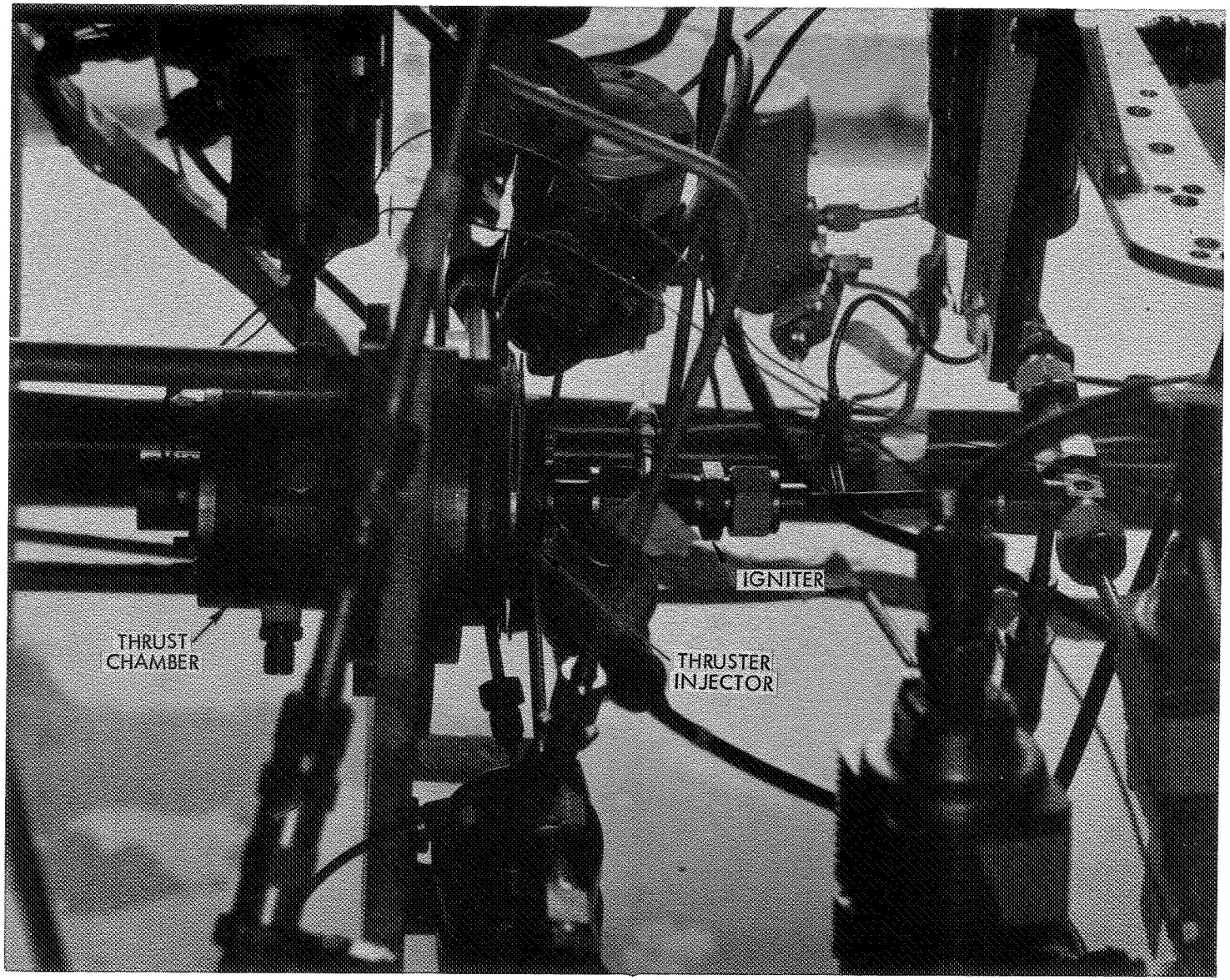

Figure 70. Altitude Thrust Stand Installation – High Chamber Pressure Thruster/Igniter

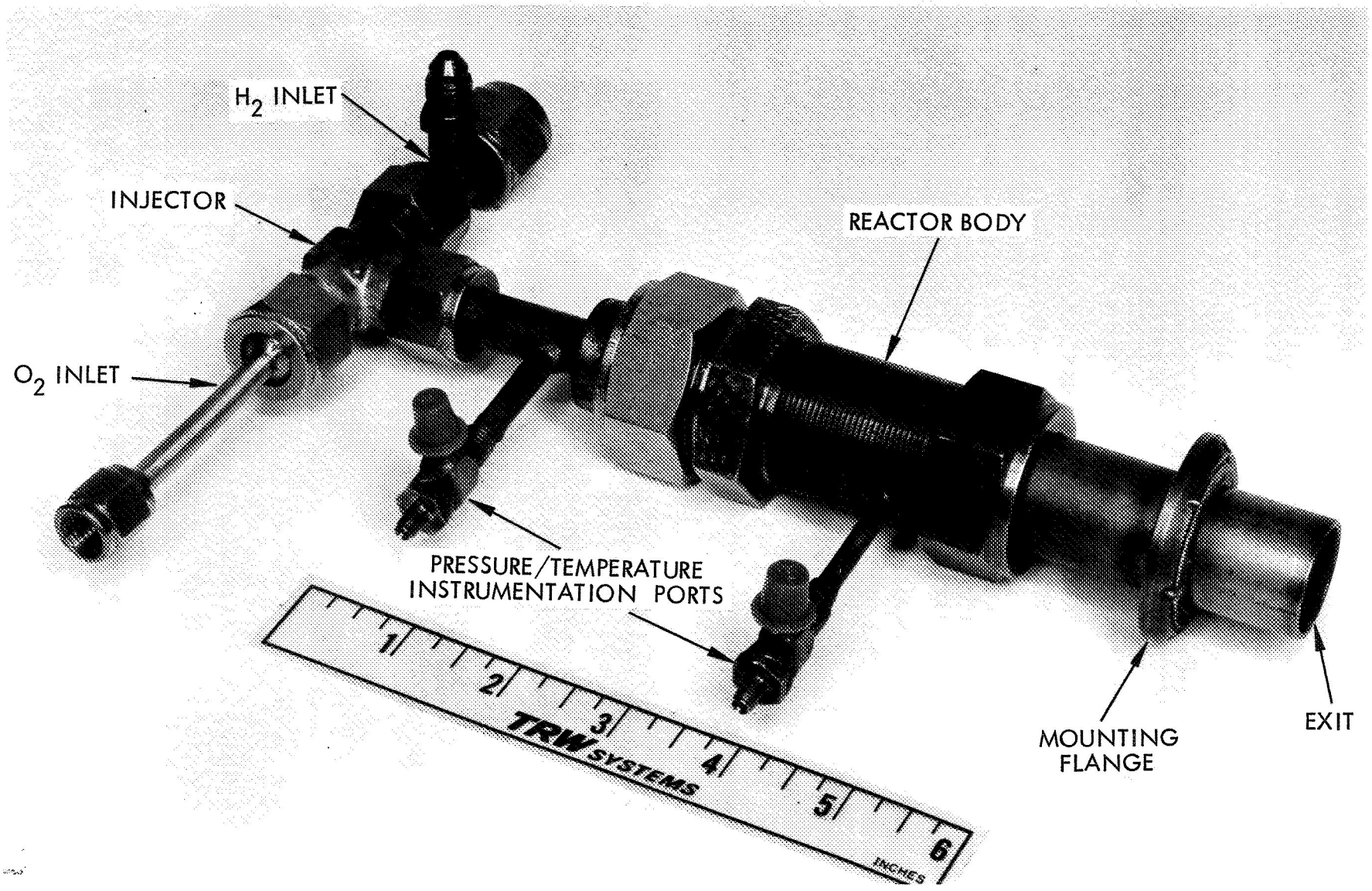

Figure 71. Workhorse Igniter Assembly—Low Pressure Thruster

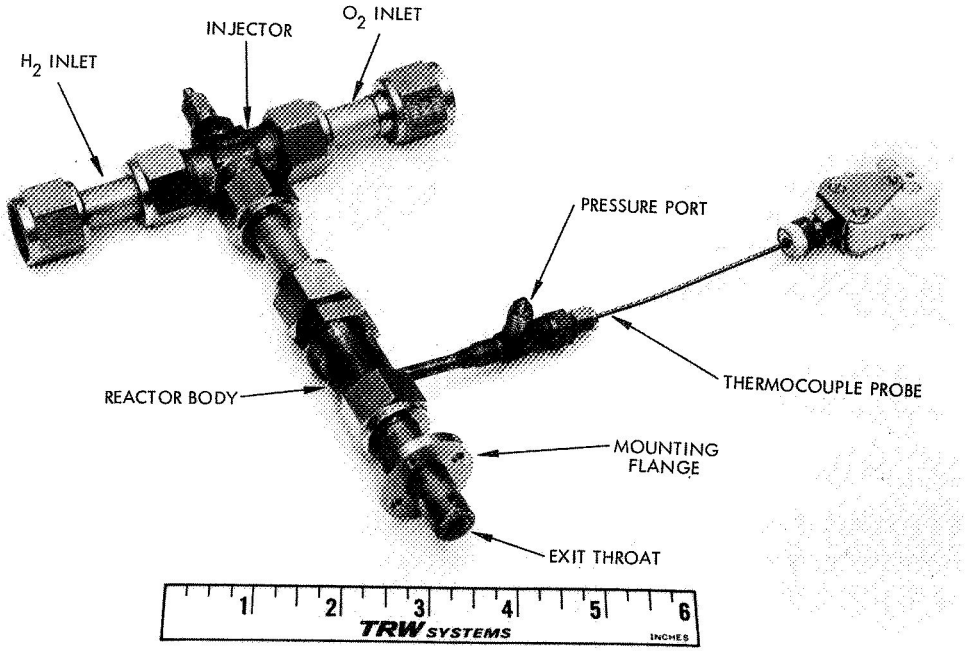

Figure 72. Workhorse Igniter Assembly— High Pressure Thruster

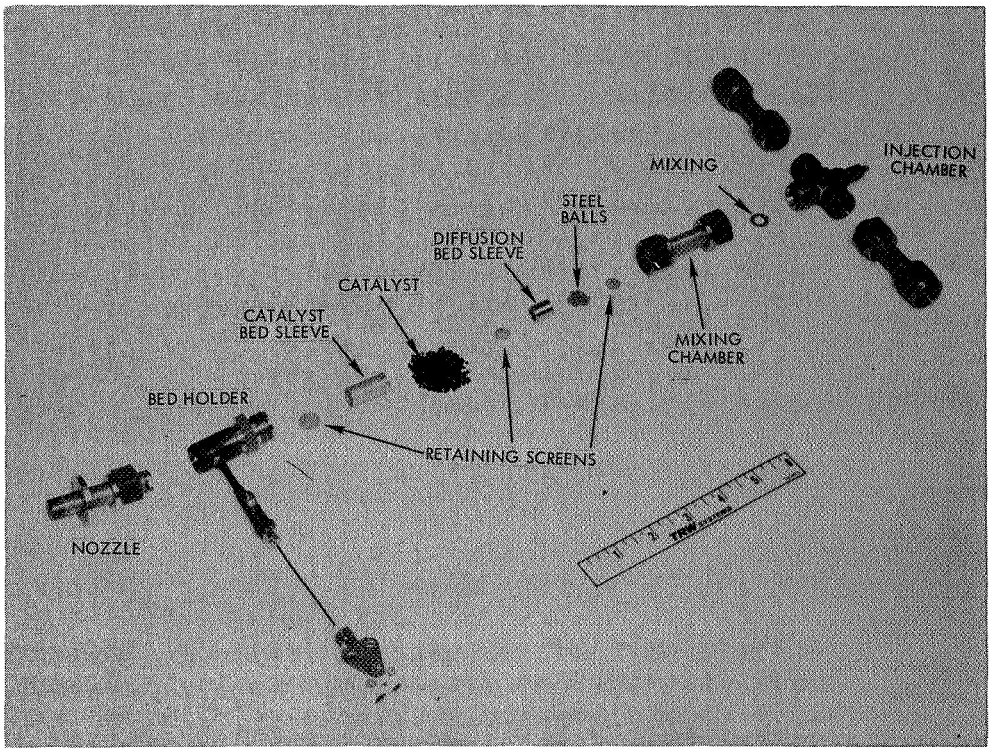

Figure 73. Disassembled Workhorse Igniter— High Pressure Thruster

retaining screen and sleeve, (6) steel ball diffusion bed, (7) upstream retaining screen, (8) mixing chamber, (9) mixing orifice, and (10) injection chamber and inlet lines. The use of standard tubing and fittings for the igniter allowed rapid and very inexpensive changes in catalyst bed configurations and propellant mixing velocities.

The approved test matrix for performance of the ignition energy level tests is presented in Table 17. Ignition limits at each chamber pressure level were determined by varying the igniter flow rate and/or effluent temperature.

5.2.2 Discussion of Results

All thruster ignition energy level test results are summarized in Table 18, except for checkout tests of the igniters only. Descriptions of the thruster ignition tests follow.

Test 449: Main thruster ignition was achieved on the first test at 100 psia (690 kN/m^2) chamber pressure. However, flashback of the combustion flame front upstream through the igniter occurred. No damage to the injector itself was observed. A reduction in diameter of the igniter mixing volume was made to prevent recurrence of flashback by increasing throughput velocities to greatly exceed the theoretical flame velocity.

Tests 466-470: Ignition of the 10 psia (69 kN/m^2) thruster was not attained on initial tests with a 0.228-inch (0.579 cm) diameter igniter throat, even with igniter flow rates as high as 50 percent of thruster flow.

The evolution of the final low pressure igniter exit configuration is illustrated, left to right, in Figure 74. The throat section at the left was designed with an extended exit to avoid combustion gas recirculation. The next igniter configuration (center of Figure 74) was fabricated by machining out the throat and welding a screen and deflector plate to the end of the open 1-inch (2.54 cm) OD igniter exit tube. The intent of this modification was to deflect the igniter effluent gas radially outward to intersect and react with the main thruster propellant streams.

The final igniter exit design was the most successful and the simplest to fabricate of the configurations tested. Shown at the right in Figure 74, this igniter tip is a squared-off standard 1-inch (2.54 cm) OD stainless tube. Compared to the igniter throat of the initial design, this open tube provided a flow of lower-velocity fuel-rich igniter reaction gases nearer to both the primary sheet and secondary orifice oxygen injection streams of the main thruster, which appeared to promote ignition. Use of a "throatless" igniter also allowed operation of the igniter at lower propellant supply pressures, which was an essential goal of the 10 psia (69 kN/m^2) chamber pressure thruster development. The igniter tip shown in the photograph (Figure 74, right) was used for all of the low pressure ignition tests, plus numerous igniter-only firings, and remained in excellent condition.

Table 17. Minimum Test Matrix—Igniter Energy Level Tests

Matrix Element* No.	Chamber Pressure psia (kN/m^2)	Igniter Flow %**	Propellant Temp. °F (°K)	He in O_2 Dilution % He	He in H_2 Dilution % He	Igniter Flow Lead/Lag	Chamber Length L1, L2
1	100 (690)	10	70 (294)	0	0	lead	L1
2	"	"	"	"	"	lag	"
3	"	5	"	"	"	lead	"
4	"	2	"	"	"	"	"
5	"	5	"	50	10	"	"
6	"	"	"	10	5	"	"
7	"	"	"	25	0	"	"
8	"	"	"	"	"	"	L2
9	"	"	"	0	0	"	"
10-18	10 (69)	Repeat 1-9 for 10 psia (69 KN/m^2) Pc thruster					
19	10 (69)	5	-250 (117)	0	0	lead	L1
20	"	"	"	50	10	"	"
21	"	"	"	10	5	"	"
22	"	"	"	25	0	"	"
23	"	"	-100 (200)	"	"	"	"
24	"	"	"	50	10	"	"
25-30	100 (690)	Repeat 19-24 for 100 psia (690 kN/m^2) Pc thruster					

* One or more tests were conducted for each matrix element

** Igniter flow rate expressed as percentage of main thruster flow.

Table 18. Ignition Energy Level Test Data

Run No	P_c Measured psia	P_c Measured kN/m^2	Chamber L* in	Chamber L* cm	He-O_2 % He	He-H_2 % He	$\dot{\omega}$ Igniter % T	T Effluent °F	T Effluent °K	Comments
C2-449	121.0	834.0	30	76.2	0	0	10.1	1571	1128	Initial high P_c configuration - flashback
466-70	No Ignition		30	76.2	0	0	10-50	>1800	>1255	Initial low P_c configuration - exit throat
474	12.8	88.2	30	76.2	0	0	10.1	1841	1278	
476	12.8	88.2	30	76.2	0	0	9.4	1803	1257	Low P_c igniter modification - screen/deflector over exit
494	13.2	91.0	30	76.2	0	0	8.9	1822	1268	
504	12.6	86.9	30	76.2	0	0	6.4	1790	1250	
505-10	No Ignition		30	76.2	0	0	5-10	<1730	<1216	Lower igniter effluent temperature.
511	13.4	92.4	30	76.2	0	0	9.3	1750	1228	Increased TE to attain ignition
525	12.9	88.9	20	76.2	0	0	10.0	1892	1306	
526	12.6	86.9	20	50.8	0	0	8.1	1871	1295	
527	11.2	77.2	20	50.8	0	0	6.0	1880	1300	
528	11.9	82.0	20	50.8	0	0	5.3	1893	1307	Low P_c thruster ignition energy level survey, open tube igniter exit/secondary O_2 injection configuration — thruster ignition attained at igniter flow rates from 1 to 10% of thruster flow, except when TE <1750°F (1228°K)
529	No Ignition		20	50.8	0	0	2.8	1721	1211	
530	11.6	80.0	30	76.2	0	0	3.0	1896	1309	
531	No Ignition		30	76.2	0	0	1.9	1688	1193	
532	11.4	78.6	30	76.2	0	0	2.0	1872	1295	
533	11.9	82.0	30	76.2	0	0	1.5	1765	1236	
534	11.4	78.6	30	76.2	0	0	1.1	1751	1228	
547	No Ignition		30	76.2	0	0	5.4	1791	1250	
548	10.5	72.4	30	76.2	0	0	5.8	1886	1303	
549	10.7	73.8	30	76.2	0	0	5.6	1892	1306	Low P_c ignition tests with -100°F (200°K) propellants
555	10.4	71.7	30	76.2	0	0	5.5	1864	1291	
561	10.4	71.7	30	76.2	0	0	5.6	1882	1301	
562	No Ignition		30	76.2	0	0	9.4	1820	1266	
567	10.0	68.9	30	76.2	0	0	5.7	1951	1339	Low P_c ignition tests with -250°F (117°K) propellants
568	No Ignition		30	76.2	0	0	3.1	1859	1288	
574-75	No Ignition		30	76.2	50	0	3-5	>1800	>1255	
576	10.0	68.9	30	76.2	5	0	5.2	1892	1306	
577	10.2	70.3	30	76.2	5	0	2.9	1871	1295	
578-82	No Ignition		30	76.2	25	0	1-10	>1800	>1255	Low P_c thruster propellant dilution effects survey - certified premixed helium dilutions of O_2 and/or H_2 - thruster ignition at all dilutions except 25 and 50% He in O_2
585	11.5	79.3	30	76.2	0	10	5.1	1837	1276	
588	10.3	71.0	30	76.2	5	10	5.3	1881	1300	
590-92	No Ignition		30	76.2	25	10	2-10	>1870	>1294	
610	11.0	75.8	30	76.2	0	5	5.0	1839	1277	
618	134.0	924.0	30	76.2	0	0	5.2	1722	1212	
619	139.0	958.0	30	76.2	0	0	7.8	1751	1228	
620	140.0	965.0	30	76.2	0	0	10.1	1795	1253	
621	133.0	917.0	30	76.2	0	0	5.3	1637	1165	High P_c thruster ignition energy level survey, open tube igniter configuration thruster ignition attained at $\dot{\omega}_I$ from 2 to 10 of $\dot{\omega}_T$ at TE >1250°F (950°K)
622	131.0	903.0	30	76.2	0	0	2.1	1311	984	
623	133.0	917.0	30	76.2	0	0	5.1	1326	992	
624	135.0	931.0	30	76.2	0	0	5.0	1252	951	
625	No Ignition		30	76.2	0	0	4.6	1143	890	

Table 18. Ignition Energy Level Test Data (Continued)

Run No.	P_c Measured psia	P_c Measured kN/m^2	Chamber L* in	Chamber L* cm	He-O_2 % He	He-H_2 % He	$\dot{\omega}$ Igniter % T	T Effluent °F	T Effluent °K	Comments
649-51	No Ignition		20	50.8	50	0	5-10	>1700	>1200	
652-55	No Ignition		20	50.8	50	10	5-10	>1700	>1200	
656	131.0	903.0	20	50.8	0	10	5.0	1711	1206	
658	138.0	951.0	20	50.8	0	10	10.2	1793	1251	
659	93.0	641.0	20	50.8	25	10	10.0	1781	1245	
660	90.0	621.0	20	50.8	25	10	5.1	1770	1239	
664	89.0	614.0	20	50.8	25	0	5.0	1752	1229	
666	95.0	655.0	20	50.8	25	0	10.2	1798	1254	
667	117.0	807.0	20	50.8	5	0	5.3	1783	1229	
668	122.0	841.0	20	50.8	5	0	10.3	1795	1253	
669	120.0	827.0	20	50.8	5	10	5.1	1781	1245	
670	123.0	848.0	20	50.8	5	10	10.5	1763	1235	High P_c thruster propellant dilution effects survey - certified premixed helium dilutions of O_2 and/or H_2 - thruster ignition at all dilutions except 50% He in O_2
671	130.0	896.0	20	50.8	0	5	5.0	1717	1209	
672	138.0	951.0	20	50.8	0	5	10.0	1794	1252	
679	127.0	876.0	30	76.2	0	5	2.1	1721	1211	
680	130.0	896.0	30	76.2	0	10	2.0	1726	1214	
681	114.0	786.0	30	76.2	5	10	2.2	1749	1227	
682	118.0	814.0	30	76.2	5	0	2.1	1717	1209	
683	No Ignition		30	76.2	50	10	2.3	1614	1152	
684	No Ignition		30	76.2	50	0	2.2	1592	1140	
685	88.0	607.0	30	76.2	25	0	2.0	1559	1121	
686	89.0	614.0	30	76.2	25	0	2.2	1822	1268	
687	90.0	621.0	30	76.2	25	10	2.0	1437	1054	
688	90.0	621.0	30	76.2	25	10	2.2	1767	1237	
689	110.0	758.0	30	76.2	0	0	2.1	1812	1262	
690	116.0	800.0	30	76.2	0	0	2.4	1433	1051	
692	116.0	800.0	30	76.2	0	0	5.8	1722	1212	
694	129.0	889.0	30	76.2	0	0	9.9	1767	1237	High P_c ignition tests with -250°F (117°K) propellants
695	133.0	917.0	30	76.2	0	0	8.8	1434	1052	
696	No Ignition		30	76.2	0	0	7.9	1307	982	
700	124.0	855.0	30	76.2	0	0	5.0	1771	1239	
704	136.0	938.0	30	76.2	0	0	9.8	1730	1216	
705	134.0	924.0	30	76.2	0	0	8.0	1463	1068	
709	126.0	869.0	30	76.2	0	0	2.1	1437	1054	High P_c ignition tests with -100°F (200°K) propellants
710	126.0	869.0	30	76.2	0	0	1.9	1351	1006	
715	No Ignition		30	76.2	0	0	10.1	1275	964	
716	142.0	979.0	30	76.2	0	0	10.1	1776	1242	IR detection evaluation

Figure 74. Workhorse Igniter Exit Configurations—Low Pressure Thruster Ignition Energy Tests

Tests 474-504: Successful ignitions were attained by removing the igniter throat and adding a screen/deflector over the exit (center, Figure 74). Igniter flow rates were varied from 6.4 to 9.4 percent of thruster flow rate.

Tests 505-511: No ignitions were achieved with the same configuration when igniter effluent temperatures were below 1730°F (1216°K). Ignition was attained at TE = 1750°F (1228°K).

Tests 525-534: Satisfactory ignitions were attained at all effluent temperatures above 1750°F (1228°F) with igniter flow rates from 1 to 10 percent of thruster flow. The open tube igniter exit configuration (Figure 74, right) was incorporated for these tests, in conjunction with the optional secondary oxidizer injection orifices (described in Section 5.1.1). Four 0.090-inch (0.229 cm) diameter holes were drilled into the main oxidizer manifold at a 45-degree angle with the center axis to inject 10 percent of the oxygen into the fuel-rich igniter plume upstream of main propellant sheet impingement. This modification was intended to raise the local mixture ratio and resulting temperature of the igniter effluent gases prior to reaction with the main propellants. The secondary oxygen injection orifices can be seen in Figure 75 as four equally spaced holes in the annular area between the center igniter tube exit and the main oxidizer injection gap.

Tests 547-555: Low pressure thruster ignitions were attained with -100°F (200°K) propellants at effluent temperatures above 1791°F (1250°K). Lower effluent temperature resulted in no ignition on test 547.

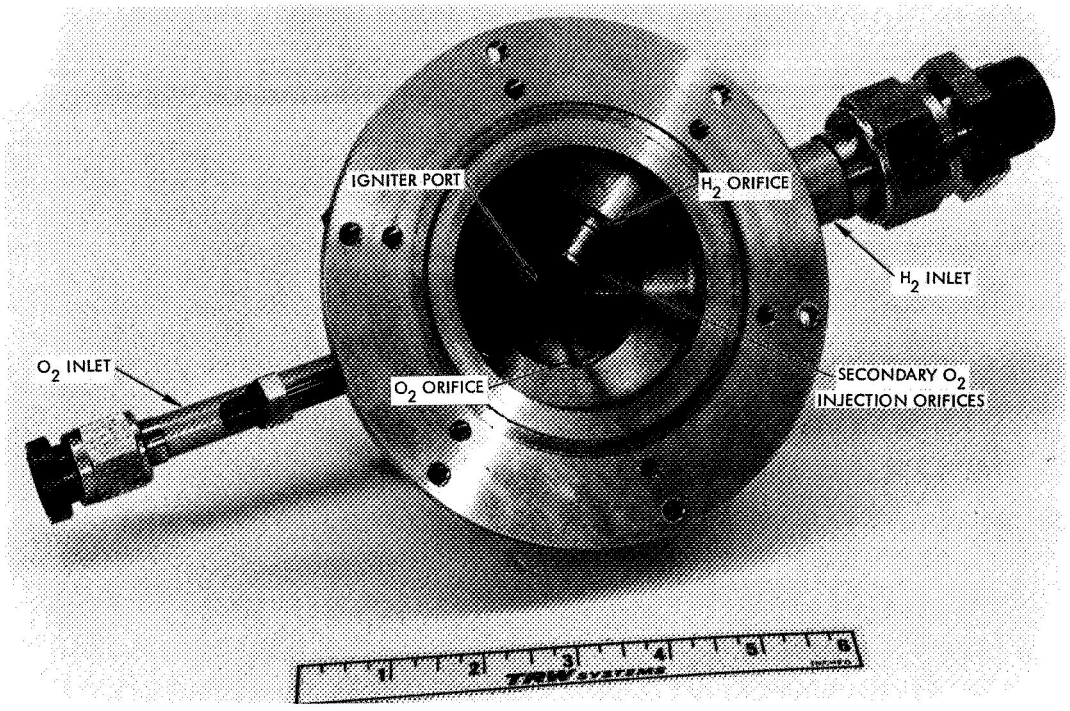

Figure 75. Injector Face of Low Pressure Thruster Modified to Include Secondary Oxygen Injection Orifices

Tests 561-568: Ignition with -250°F (117°K) propellants was attained on runs 561 and 567, where effluent temperatures were 1859°F (1288°K) or higher. No ignitions occurred at lower effluent temperatures (tests 562, 568).

Tests 574-610: Low pressure thruster dilute propellant tests resulted in no ignition with helium dilutions of 25 percent or more in the main oxygen supply.

Tests 618-625: High pressure thruster ignitions were attained with ambient temperature propellants at all igniter flow rates from 2 to 10 percent of total thruster flow rate, but only at effluent temperatures above 1250°F (950°K).

Tests 649-688: High pressure thruster ignitions were attained with helium diluted main propellants except with 50 percent helium in oxygen.

Tests 689-696: Ignition with -250°F (117°K) propellants required increasing effluent temperatures to over 1430°F (1050°K).

Tests 700-715: Propellant temperature of -100°F (200°K) also required higher effluent temperatures for ignition, compared to ambient temperature propellant tests (618-625).

Test 716: This test was conducted to evaluate the use of an IR detector cell to indicate main thruster ignition response. Results of this test are described in the following data evaluation.

5.2.3 Data Evaluation and Analysis

After both pressure level thrusters had been modified to incorporate secondary oxidizer injection and "open tube" igniter exits, successful ignitions were achieved over a range of igniter flow rates from 2 to 10 percent of thruster flows.

Figures 76 and 77 were traced from oscillograph recordings of typical ignition tests at each chamber pressure level. These records show that main thruster ignition was attained upon onset of main hydrogen flow (an oxidizer lead of 0.035 second was employed for the tests shown), as indicated by the main injection pressure and chamber pressure traces. Shown in Figure 76 is the output of an IR detector cell directed through a "window" in the thrust chamber, which further verified the occurrence of main thruster ignition. Minimum igniter effluent temperatures required for ignition of ambient temperature main propellents were found to be 1250°F (950°K) for the high pressure thruster and 1750°F (1228°K) for the low pressure thruster. Repeatable ignitions with no delays were achieved even at igniter flow rates as low as 1 percent of thruster flow, as long as these minimum temperature requirements were met.

These experimental results appeared to be inconsistant with the concept of a minimum energy ignition requirement, since the energy, or enthalpy input, is a function of the igniter flow rate as well as the effluent temperature.

The enthalpy rate difference above the autoignition temperature of 1100°F (922°K) is:

$$\dot{H}_{AI} = \dot{W}_{igniter}\, C_p\, (T_{effluent} - T_{AI}) \qquad (3)$$

Although ignitions were attained at $\dot{W}_I$ from 2 to 10 percent of thruster $\dot{W}_T$, at the same minimum T_E, the energy inputs are quite different:

$$.02\ \dot{W}_T\, C_p\, (T_E - T_{AI}) << .10\ \dot{W}_T\, C_p\, (T_E - T_{AI}) \qquad (4)$$

where the $\dot{W}_T$, C_p, and $(T_E - T_{AI})$ terms are equal on each side of the equation. It is expected that igniter flow rates could be reduced to a point where ignition would not occur even at very high effluent temperatures. However, for the conditions experimentally evaluated during this program, the primary requirement for ignition was found to be a minimum igniter effluent temperature rather than an energy limit.

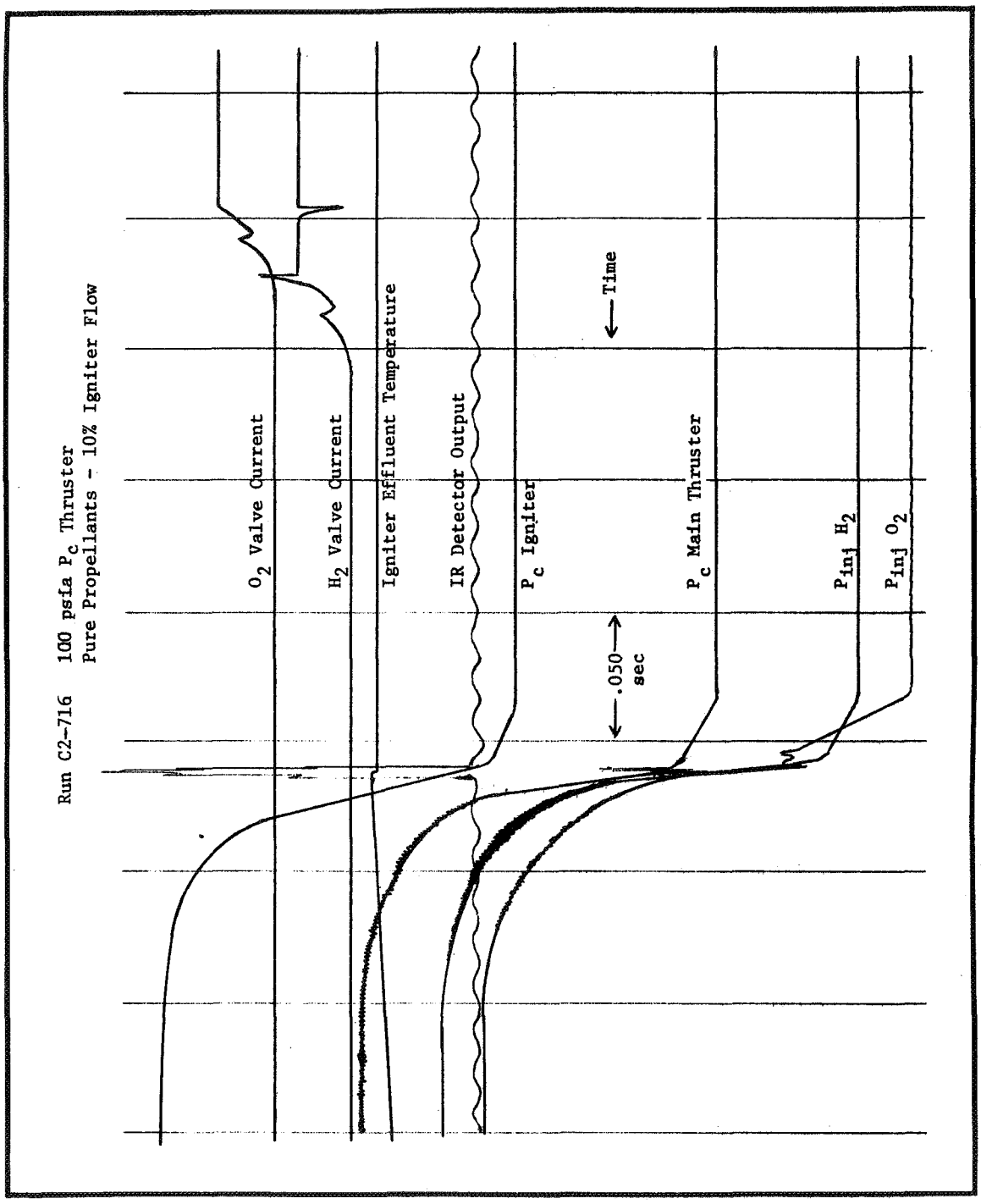

Figure 76. Oscillograph Recording of High Pressure Thruster Ignition

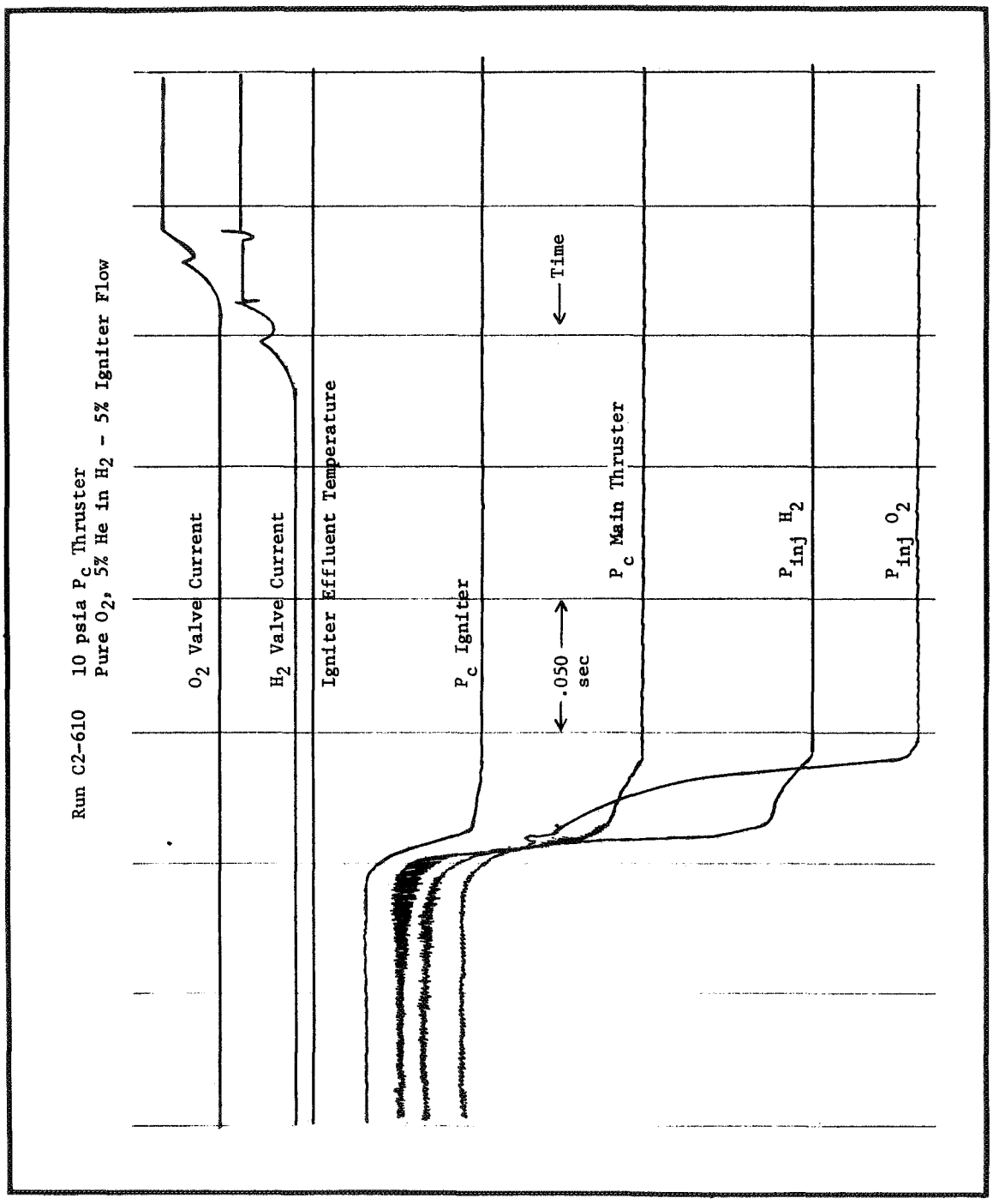

Figure 77. Oscillograph Recording of Low Pressure Thruster Ignition

The geometry of the igniter exit and main injector configurations was also determined to be critical in attaining thruster ignitions. In analyzing the effects of the secondary oxidizer injection modification, the mixing model shown in Figure 78 was utilized. The model indicates that injection of pure oxygen into the fuel-rich (mixture ratio 1:1) effluent gases increases the local resultant gas temperatures as high as 3800° to 5000°F (2367° to 3033°K) upstream of the main propellant injection point. These temperatures are the theoretical O_2-H_2 combustion temperatures assuming complete reaction of the secondary oxygen flow with the igniter effluent gas over the 2 to 10 percent igniter flow rates, as illustrated in Figure 79. This figure indicates that maximum local combustion temperatures (stoichiometric mixture ratio) occurred with igniter flow rates of 1 to 2 percent of thruster flow reacting with 10 percent of the main oxygen injected through the secondary oxidizer orifices. The dotted curve in Figure 79 reveals that increasing the secondary oxygen injection flow to 20 percent would result in maximum local reaction temperatures with ~4 percent igniter flow rates.

Figure 80 presents the resultant chamber gas temperatures prior to ignition calculated from the following enthalpy balance assuming uniform mixing of the igniter effluent and main injector oxygen and hydrogen flows:

$$\dot{W}_{Igniter}\, C_{pI}\, (T_{Effluent} - T_{Mix}) + \dot{W}_{O_2}\, C_{PO_2}\, (T_{O_2} - T_{Mix}) + \dot{W}_{H_2}\, C_{pH_2}\, (T_{H_2} - T_{Mix}) = 0 \qquad (5)$$

The lower curve in Figure 80 indicates the resultant temperatures (T_{Mix}) of the chamber gases for various igniter flow rates. The upper curves were also calculated from Equation (5), but are based on the assumption that all of the igniter effluent and secondary oxygen flows react before mixing completely with the main thruster propellants. These resultant temperatures are significantly higher than the gas mixture temperatures with no secondary oxygen flow, but are still well below the autoignition temperature of ~1100°F (922°K). It was therefore concluded that if mixing of the igniter effluent and main thruster gases occurs at a rate greater than the rate of reaction (thus allowing homogenous mixing) no ignition can be attained.

The injector/igniter configurations employed during this experimental effort achieved successful ignitions over a wide range of propellant temperatures. The effect of propellant inlet temperatures on the minimum igniter effluent temperatures is shown in Figure 81. The higher effluent temperature requirement for ignition of the low pressure thruster was later experimentally determined to be a pressure effect by operating the high pressure thruster at pressures as low as 12 psia (83 kN/m^2).

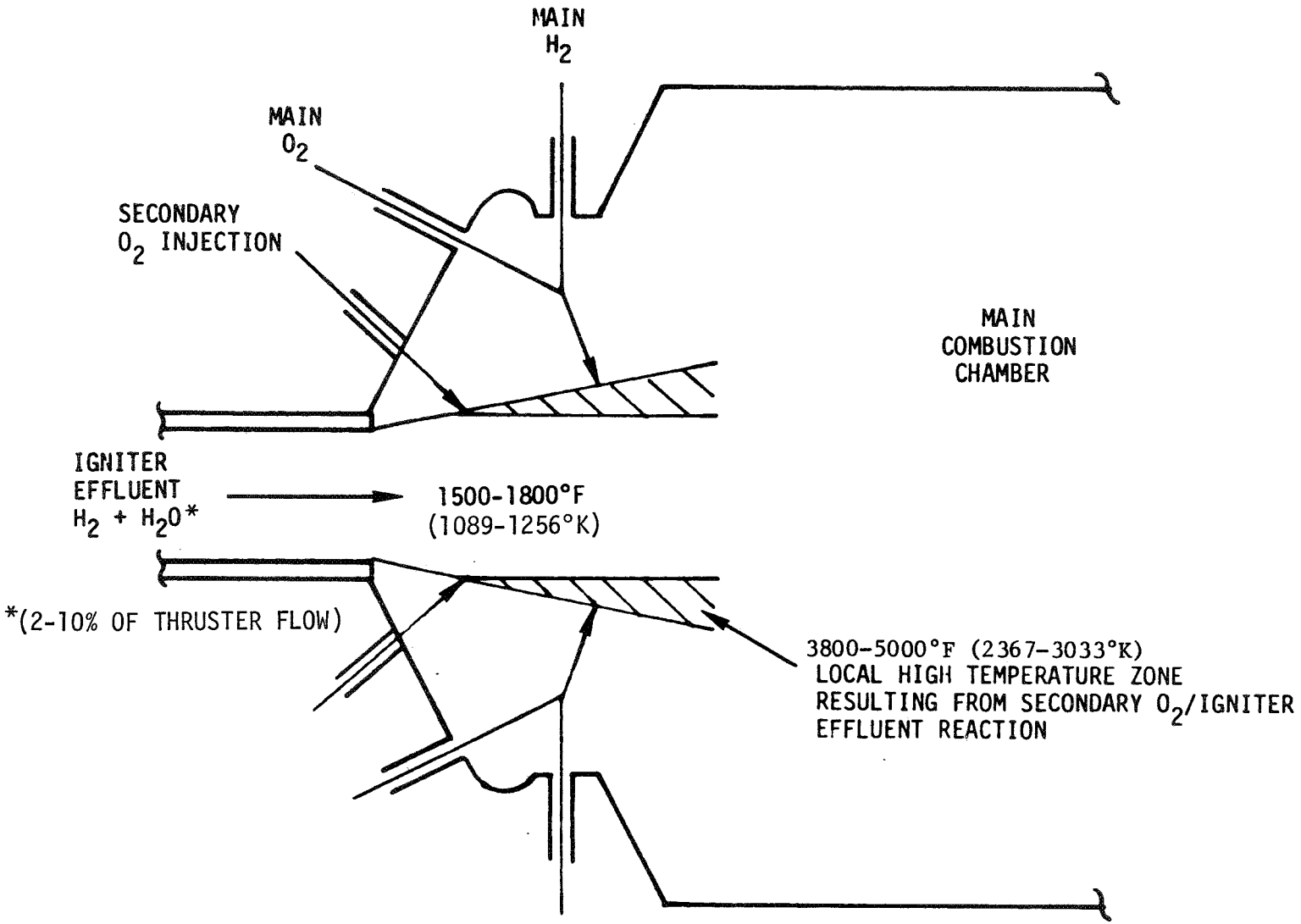

Figure 78. Igniter/Thruster Propellant Mixing Model—Secondary Oxygen Injection

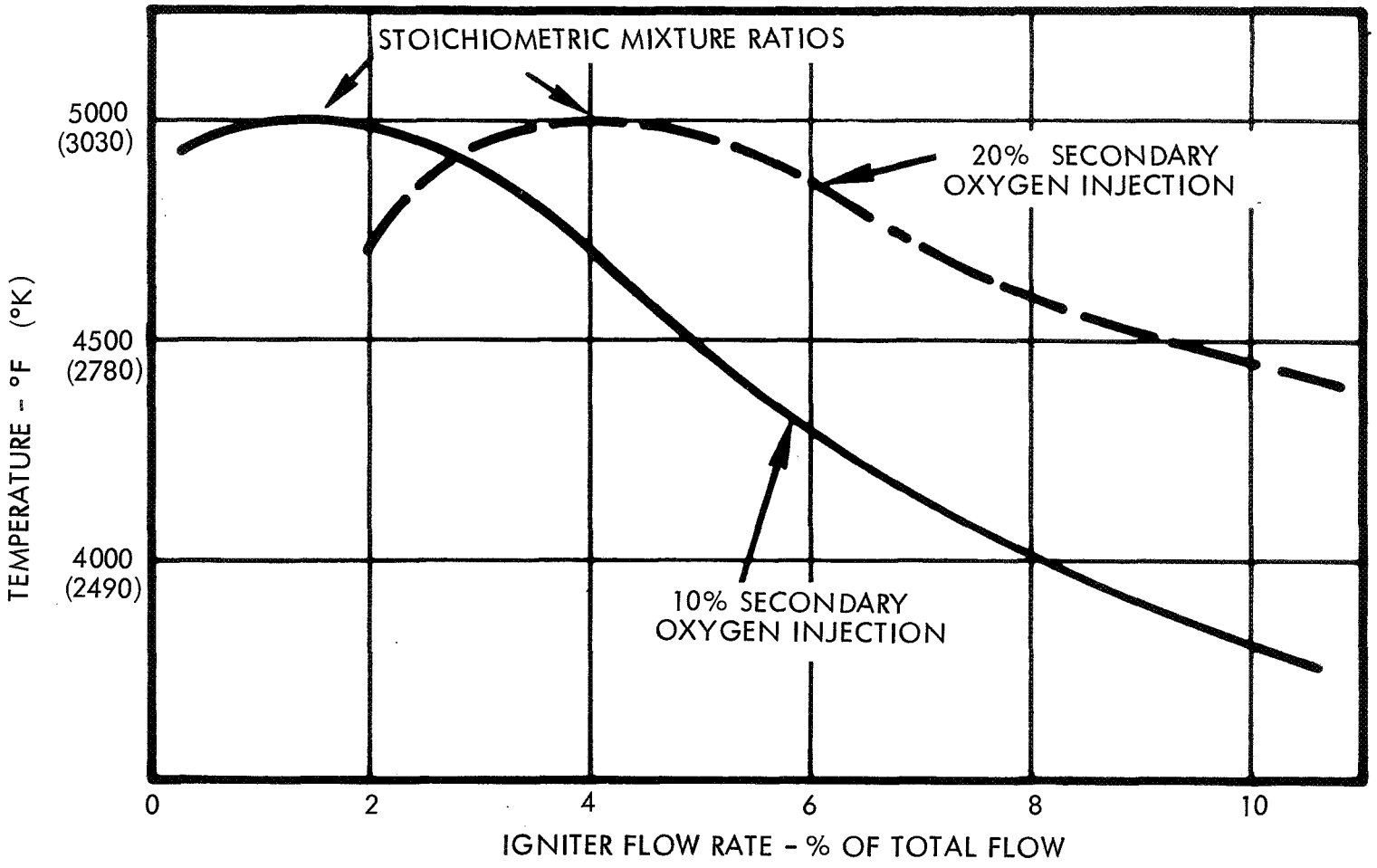

Figure 79. Local Combustion Temperature for Igniter Effluent/Secondary Oxygen Reaction

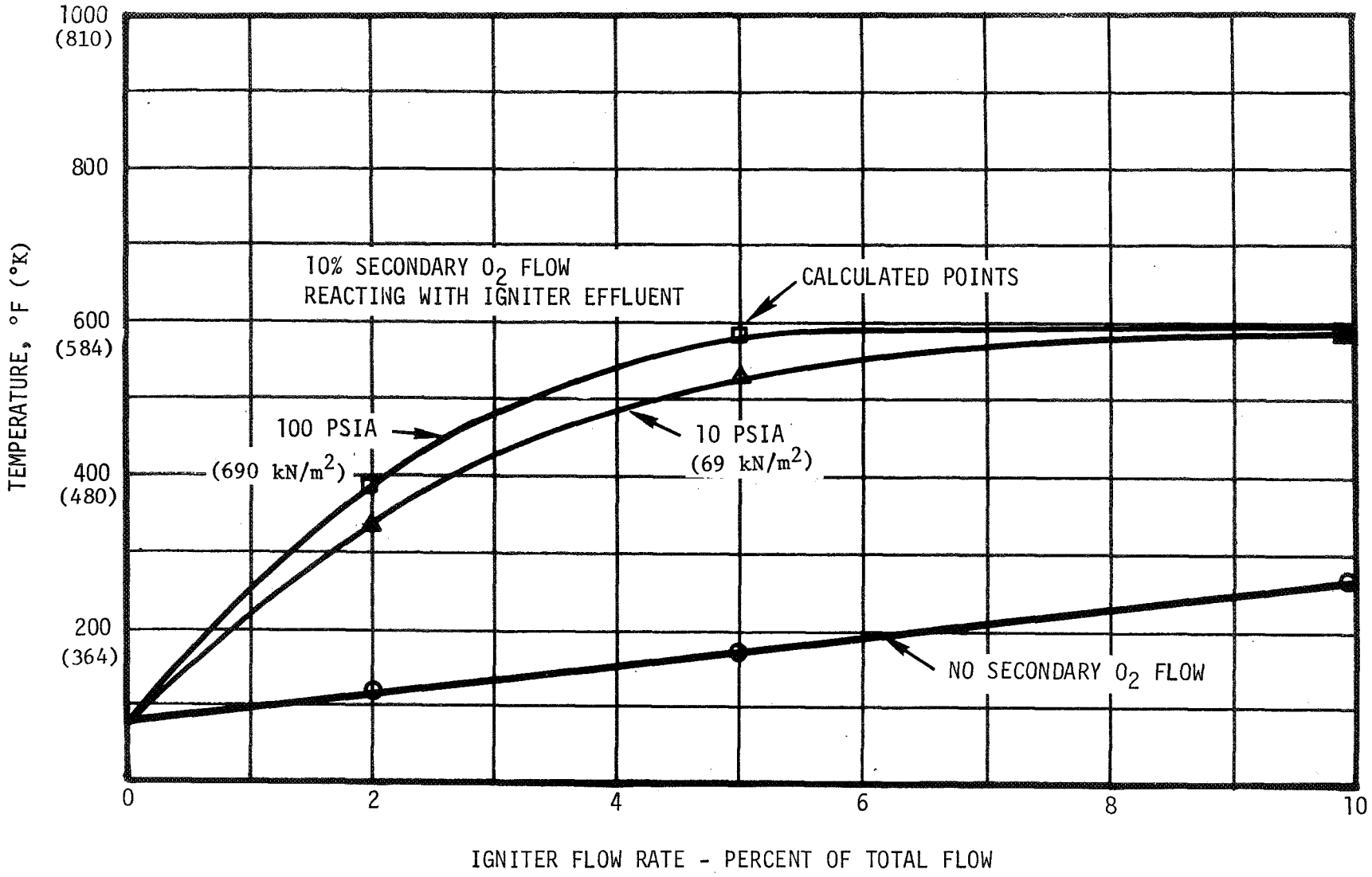

Figure 80. Resultant Chamber Gas Temperature Calculated From Enthalpy Balance Assuming Homogeneous Mixing

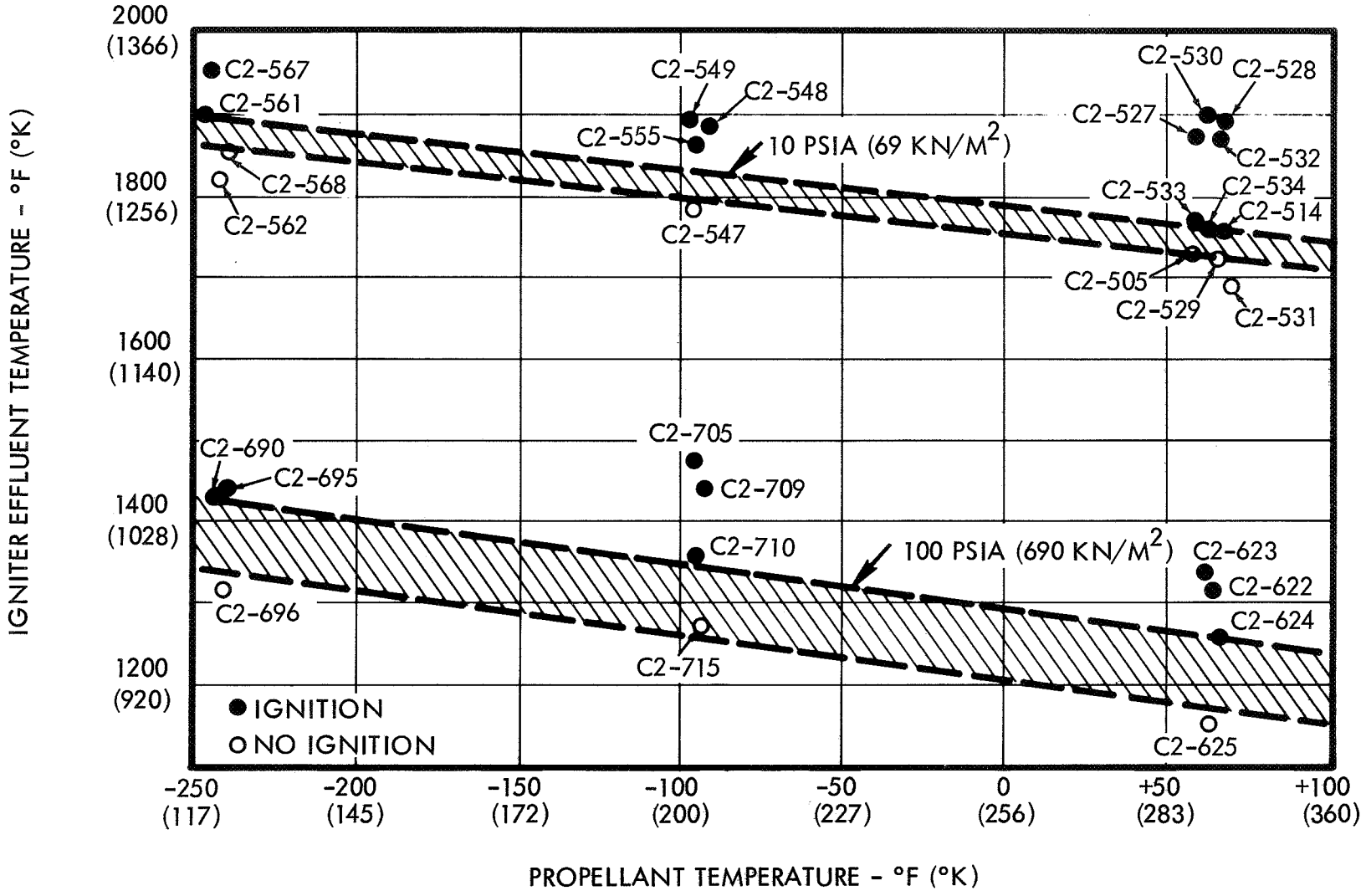

Figure 81. Igniter Effluent Temperatures Required for Ignition

The igniter effluent temperatures of 1800°F (1256°K) required for ignition at these pressures were nearly identical to the temperatures required for ignition of the low pressure thruster. Tests of each pressure level thruster with two different chamber characteristic lengths, L* of 20 and 30 inches (50.8 and 76.2 cm), revealed no effects of chamber volume on ignition characteristics. Ignitions were attained with oxidizer/fuel propellant valve leads from 10 to 35 milliseconds.

A summary of all thruster/igniter test conditions resulting in ignition during this test series is presented in Table 19. The primary requirement for thruster ignition was experimentally determined to be a minimum igniter effluent temperature for each thruster pressure level, as listed in Table 19. Ignition was not attained with helium in oxygen dilutions of 25 or 50 percent by weight for the low pressure tests, or with 50 percent He-O_2 at the higher pressure. The helium-hydrogen dilutions tested, 5 and 10 percent by weight, were ignitable at both pressure levels. Ignitions were achieved with each thruster at propellant temperatures as low as -250°F (117°K) and at igniter flow rates from 2 to 10 percent of total thruster flow.

The ignition energy level test series defined the requirements for thruster ignition at each chamber pressure level, and determined the effects of propellant temperature and dilution on ignition limits. These experimental results provided the necessary design criteria for the catalytic reactor igniters used for all subsequent testing during the program.

5.3 IGNITER BED OPTIMIZATION TESTS

The next thruster/igniter test series was conducted to investigate the effects of catalyst bed design variations on the overall thruster operating characteristics. Specific objectives of the test series were:

- Perform thruster/igniter test firings to establish the ignition delay and impulse response times for various catalyst bed L/D ratios and downstream volumes.
- Determine the optimum catalyst bed configuration for each pressure level thruster at selected propellant inlet conditions (temperature and helium dilutions).

The test installation, hardware configurations, and experimental results are presented and discussed in the following sections.

5.3.1 Test Description

The altitude thrust chambers (40:1 nozzle expansion ratios) described in Section 5.1.2 were first used during this test series. Thrust measurements were taken to determine impulse response times. The thruster and igniter hardware used for these tests was described in detail in Sections 5.1.1 and 4.1, respectively.

Table 19. Summary of Igniter Energy Level Tests

Test Conditions Resulting in Main Thruster Ignition

	Low P_c Thruster	High P_c Thruster
Minimum igniter effluent temperature	1750°F (1228°K)	1250°F (950°K)
Igniter flow rates (% of thruster flow)	1* - 10%	2 - 10%
Helium dilution in oxygen (wt. %)	5%	5, 25%
Helium dilution in hydrogen (wt. %)	5, 10%	5, 10%
Propellant inlet temperatures	70, -100, -250°F (294, 200, 117°K)	70, -100, -250°F (294, 200, 117°K)

*The 1% flow resulted during a test intended for 2% igniter flow rates. No 1% igniter flow tests were performed at the high P_c level.

Test stand installation of the 10 psia (69 kN/m^2) chamber pressure altitude thruster/igniter is illustrated in Figure 82. The thrust mount was a rigid frame supported from above by thin metal flexures. The suspended mass of the stand was limited to the thruster itself, minimal aluminum supporting structure, and only those pressure transducers requiring close-coupling to achieve maximum response. The all-welded cryogenic fire valves were mounted to the fixed portion of the stand and connected to the injector through mesh-sheathed metallic bellows flex lines, as shown in the photograph. By these techniques of minimizing the spring mass of the system, high frequency response thrust measurements were achieved. The same thrust stand and propellant feed system was utilized for the 100 psia (690 kN/m^2) hardware.

The load cell remote calibration apparatus is shown in Figure 83. Calibrated weights (certified to be within 1 gram of nominal) were supported by a motor-driven platform. Four weights wired together enabled step calibration of the load cell at any time before and/or after firings while simulated altitude conditions were maintained.

Each of the catalyst bed configurations tested at the low chamber pressure level are displayed in Figure 84. The three catalyst cartridges at left contained 0.870-inch (2.21 cm) diameter beds of 0.25, 0.50, and 1.0 inch (0.635, 1.27, and 2.54 cm) lengths.

Second from right is a reduced diameter bed cartridge, 0.620-inch (1.575 cm) diameter, which provided a catalyst bed of one-half the cross-sectional area previously tested. Spacers are welded to each end of this cartridge to center the bed within the igniter body. The final configuration (extreme right, Figure 83) was the longest catalyst bed evaluated, 1.48 inches (3.76 cm). Screens were welded over each end of the cartridges to retain the catalyst.

Shown in the background of Figure 84 are the diffusion zone spacer (slotted to admit a thermocouple probe), stainless steel ball diffusion bed, and additional spacers used to retain the shorter catalyst cartridges within the igniter housing. The ball diffusion bed, incorporated in the initial reactor design to prevent flashback by increasing local velocity and by flame quenching, was not used with the 1.48-inch (3.76 cm) long catalyst bed. No flashback occurred, however, indicating that the flow velocity through the igniter mixing section was sufficiently above the flame velocity to preclude flashback. An additional purpose of the diffusion bed was to enhance propellant mixing prior to catalyst bed reaction. No bed streaking or other indication of insufficient mixing was observed without this bed, further signifying that it may be possible to eliminate the diffusion bed with the existing igniter design.

The high pressure catalyst bed configurations tested are illustrated in Figure 85. Shown from left to right in the foreground of the photograph are the catalyst cartridges for the 0.50-inch (1.27 cm) long nominal and reduced diameter beds, and the 1.0- and 1.5-inch (2.54 and 3.81 cm) long nominal diameter beds. The nominal catalyst bed diameter for the 100 psia

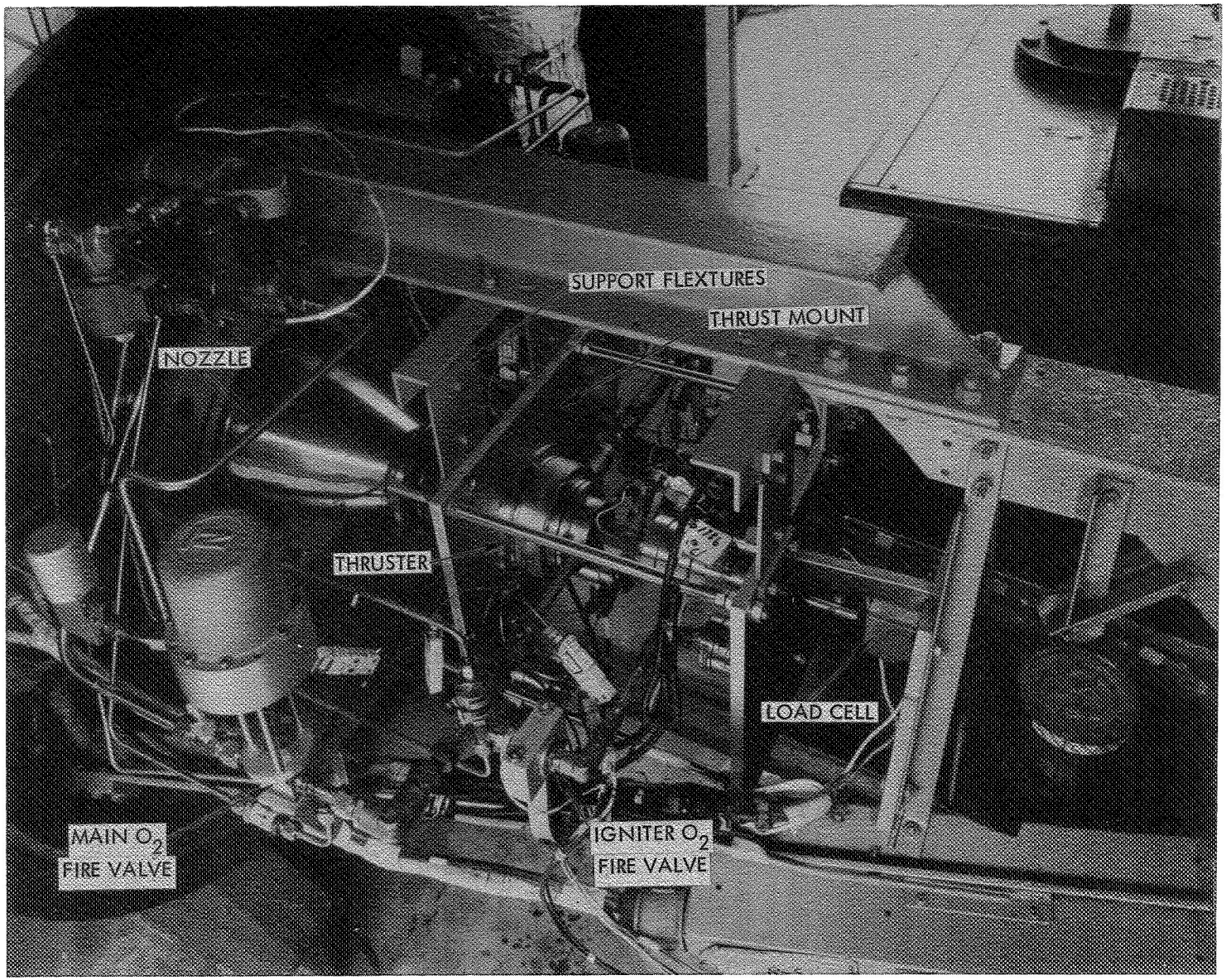

Figure 82. Overall Altitude Test Stand Installation – Low Pressure Thruster/Igniter

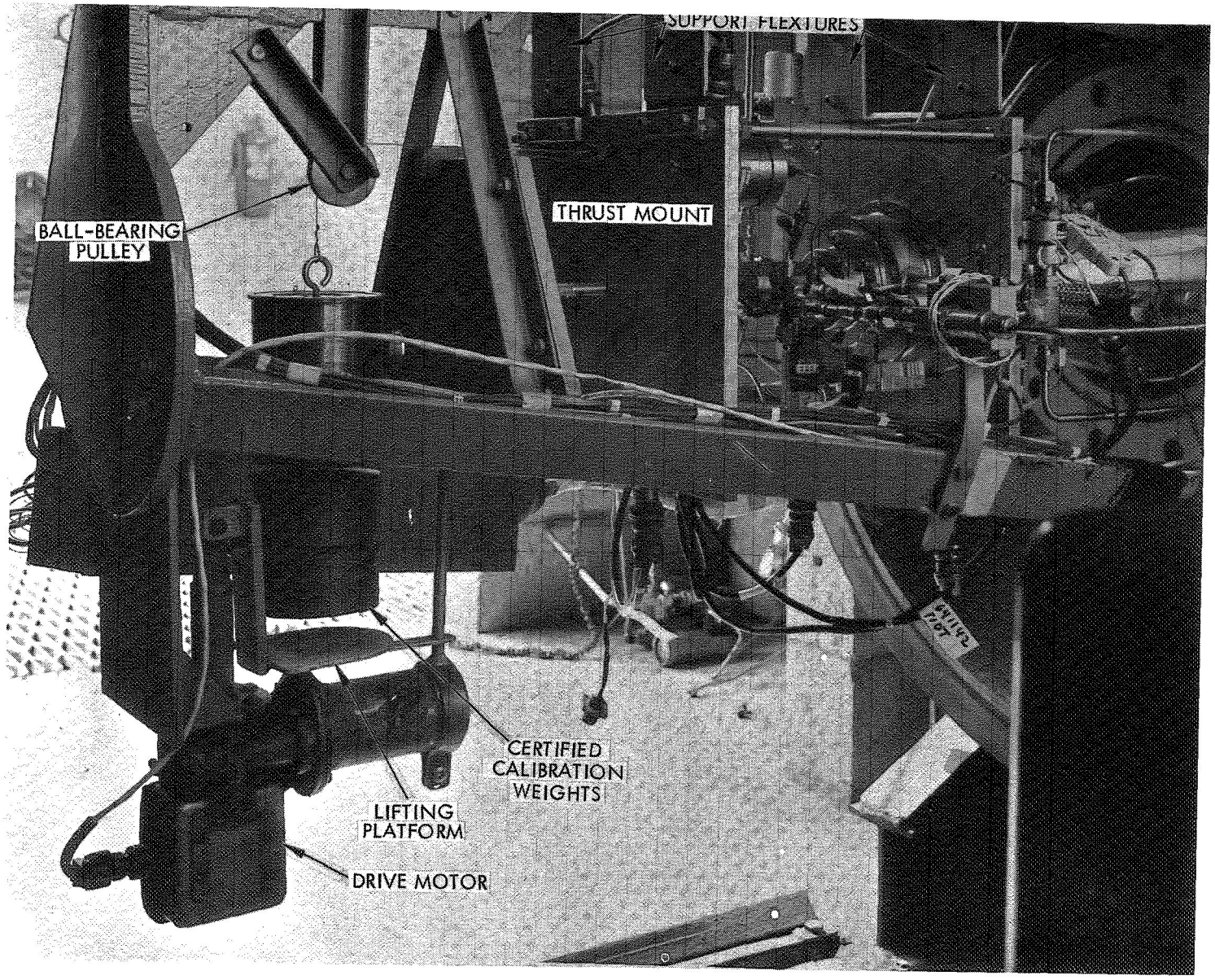

Figure 83. Motor-Driven Remote Calibration Apparatus - Altitude Thrust Measurement Stand

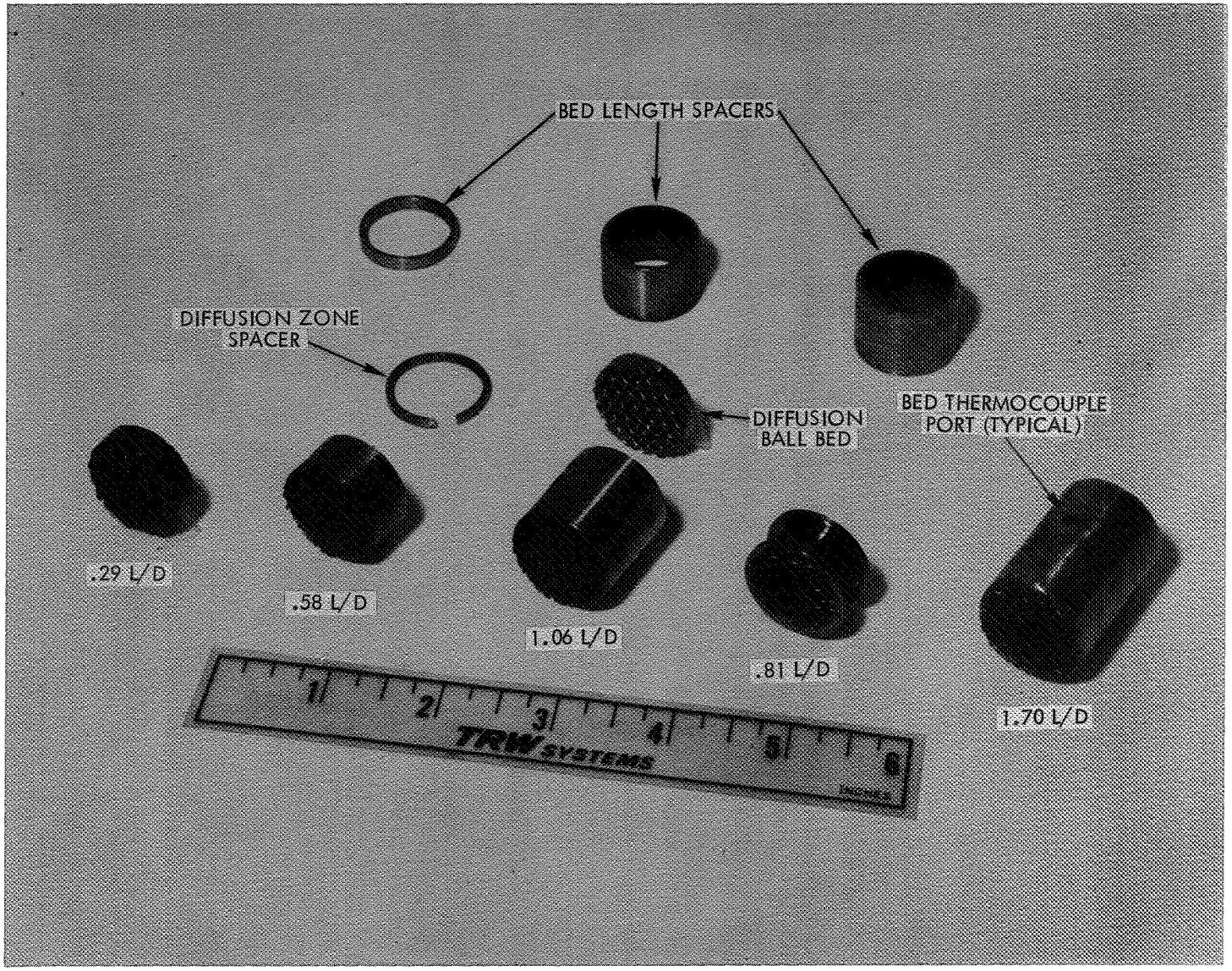

Figure 84. Low Pressure Igniter Catalyst Bed Configurations

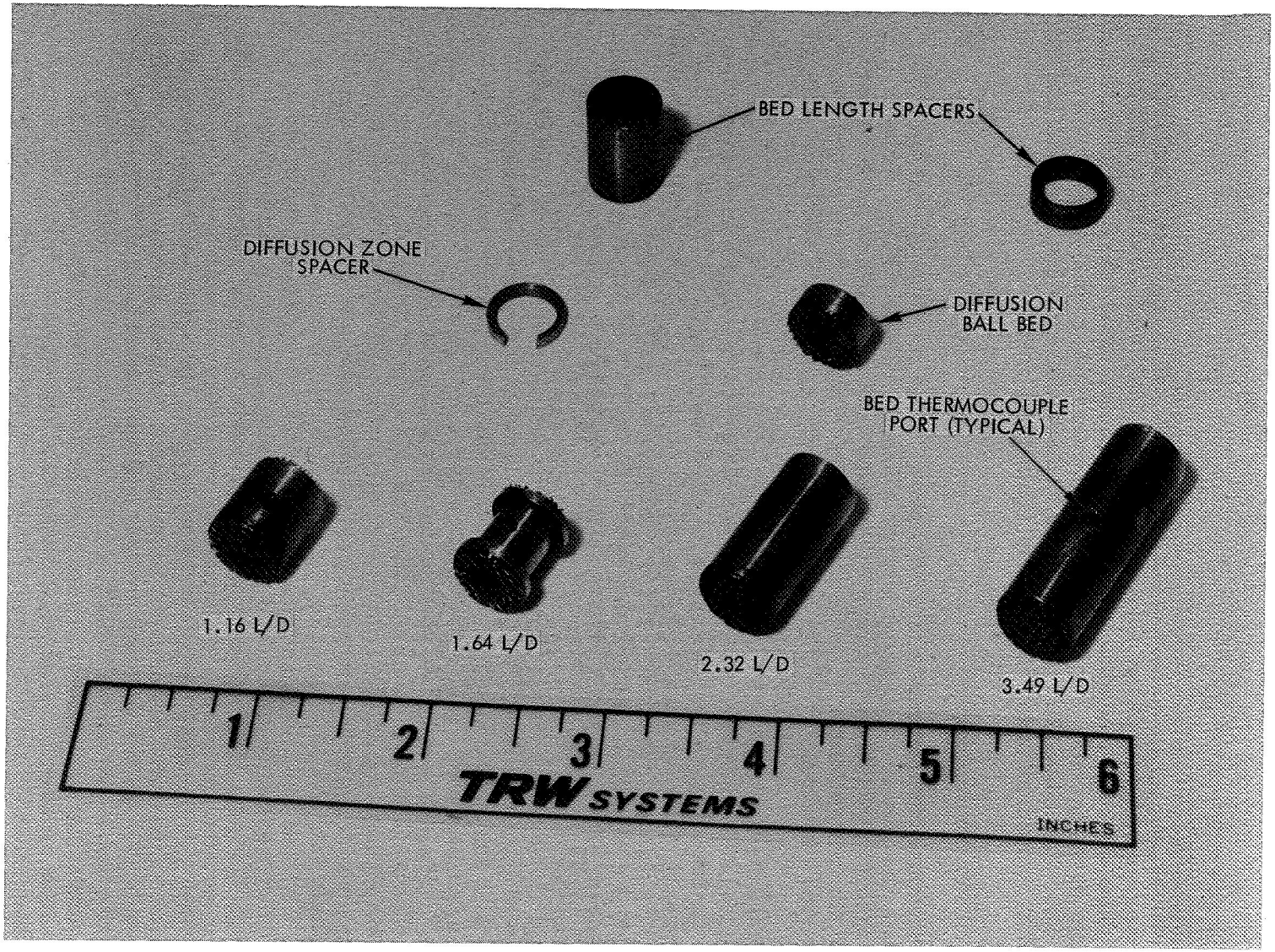

Figure 85. High Pressure Igniter Catalyst Bed Configurations

igniter is 0.430-inch (1.09 cm). The reduced diameter cartridge, 0.305-inch (0.775 cm), provided a catalyst bed of one-half the cross-sectional area for test evaluation. The 1.5-inch (3.81 cm) long catalyst bed was tested without the ball diffusion bed with no igniter flashback or other adverse effects.

Catalyst bed optimization tests with each pressure level thruster were performed at propellant temperatures of +70° and -250°F (294° and 117°K). The effects of helium diluted main propellants were also evaluated during this test series. The approved test matrix for this task is presented in Table 20. The Shell 405 ABSG catalyst formulation was selected for these tests, based on previous results (Section 4.3.3).

5.3.2 Discussion of Results

Additional low pressure thruster tests were performed during this series with the modified injector design shown in Figure 86. Separate stream injection of the main oxygen flow was intended to promote better mixing of the propellants. The modified injector stainless steel sleeve and a 36-slot aluminum oxidizer injection orifice ring are shown in Figure 87.

Figure 88 shows the injector face with the slotted oxidizer injection orifice ring installed. The hydrogen is injected radially inward as a full annular sheet. The four drilled secondary oxygen injection orifices can be seen equally spaced about the center igniter exit tube. The continuous sheet oxidizer injection orifice configuration is shown for comparison in Figure 89.

Cold flows using gaseous nitrogen and helium were made with both the separate oxidizer stream and full annular low pressure injectors, and also with the high pressure injector. Double-exposure holographic interferograms of these flows are shown and compared in Figure 90. These interferograms are analogous to topographical maps, in that each line is indicative of a change in composition of the gas, just as each line on a topographical map signifies a change in elevation. Therefore, the flows in (b) and (c) of Figure 90 are interpreted to be more homogeneous or better mixed than the flow in (a). Based on these interferograms, which indicated that the gas mixing characteristics of the multiple oxidizer stream low pressure injector was more nearly similar to the higher performing 100 psia (690 kN/m^2) injector, tests were performed to evaluate the modified injector. Ignition was not achieved with this injector configuration presumably because the hydrogen, injected radially inward as shown in Figure 85, penetrated between the oxygen streams too readily and quenched the igniter effluent before ignition could occur. The fact that ignition would not occur with the improved propellant mixing tends to substantiate the conclusion presented earlier in Section 5.2.3: that ignition would be precluded if the mixing rate exceeds the reaction rate of the igniter/main thruster gases. The continuous sheet injection configuration was used for all subsequent low pressure thruster tests.

Table 20. Task IVB—Igniter Bed Optimization Tests

Matrix Element* No.	Chamber Pressure Level	Propellant & Bed Temp. °F (°K)	He in O_2 Dilution % He	He in H_2 Dilution % He	Catalyst Bed L/D 1, 2, 3	Downstream Volume L* 1, 2
1	Low	70 (294)	0	0	1	1
2	Low	-250 (117)	0	0	1	1
3	Low	70 (294)	25	10	1	1
4	Low	70 (294)	25	0	1	1
5	Low	70 (294)	0	0	2	1
6	Low	-250 (117)	0	0	2	1
7	Low	70 (294)	25	10	2	1
8	Low	70 (294)	0	0	3	1
9	Low	-250 (117)	0	0	3	1
10	Low	70 (294)	25	10	3	1
11	Low	70 (294)	0	0	1	2
12	Low	-250 (117)	0	0	1	2
13-24	Repeat 14-20 for high Pc level thruster					

*One or more tests were conducted for each matrix element.

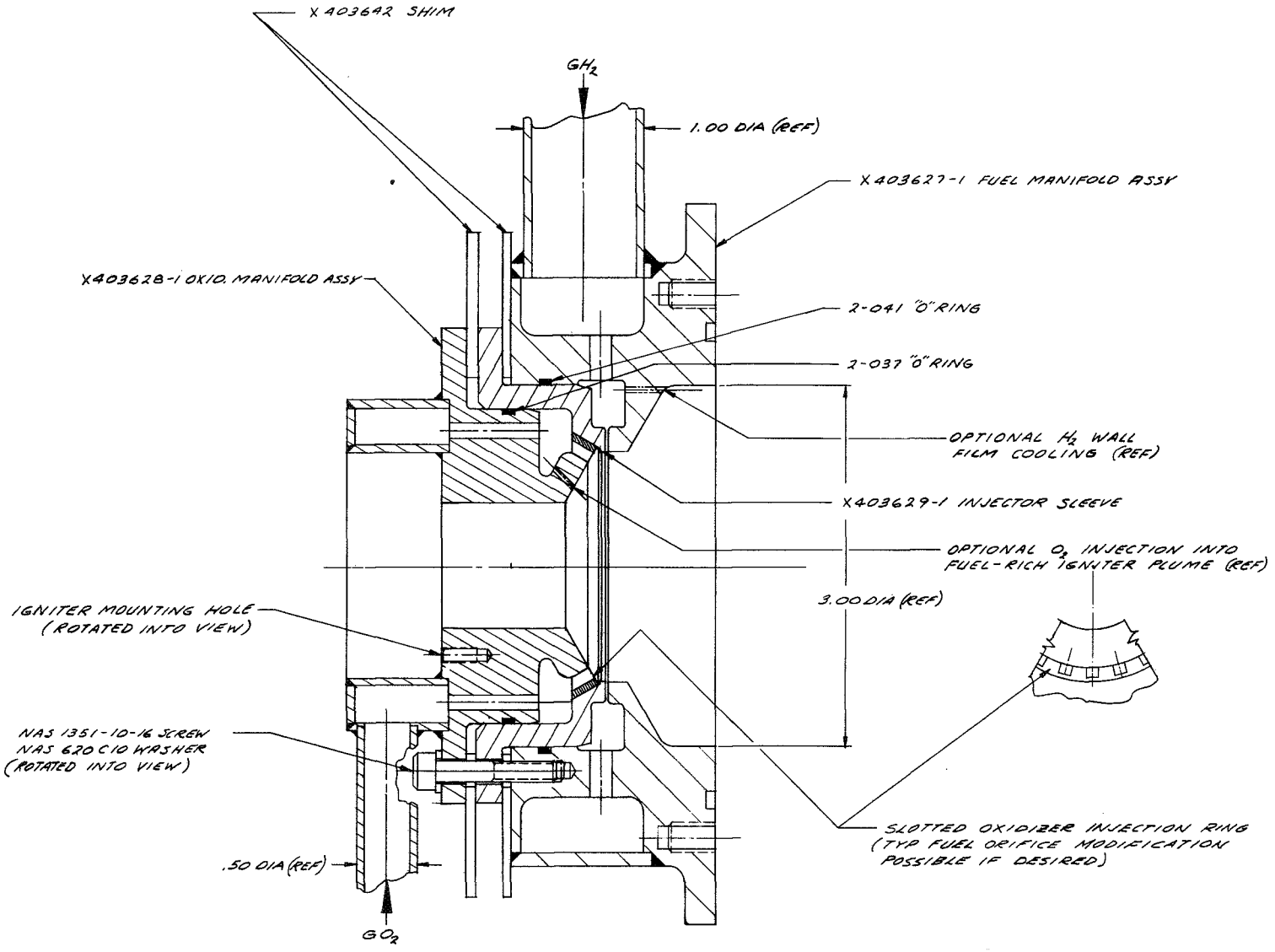

Figure 86. Main Injector Assembly—Low Chamber Pressure Thruster (Modified to include slotted oxidizer injection orifices)

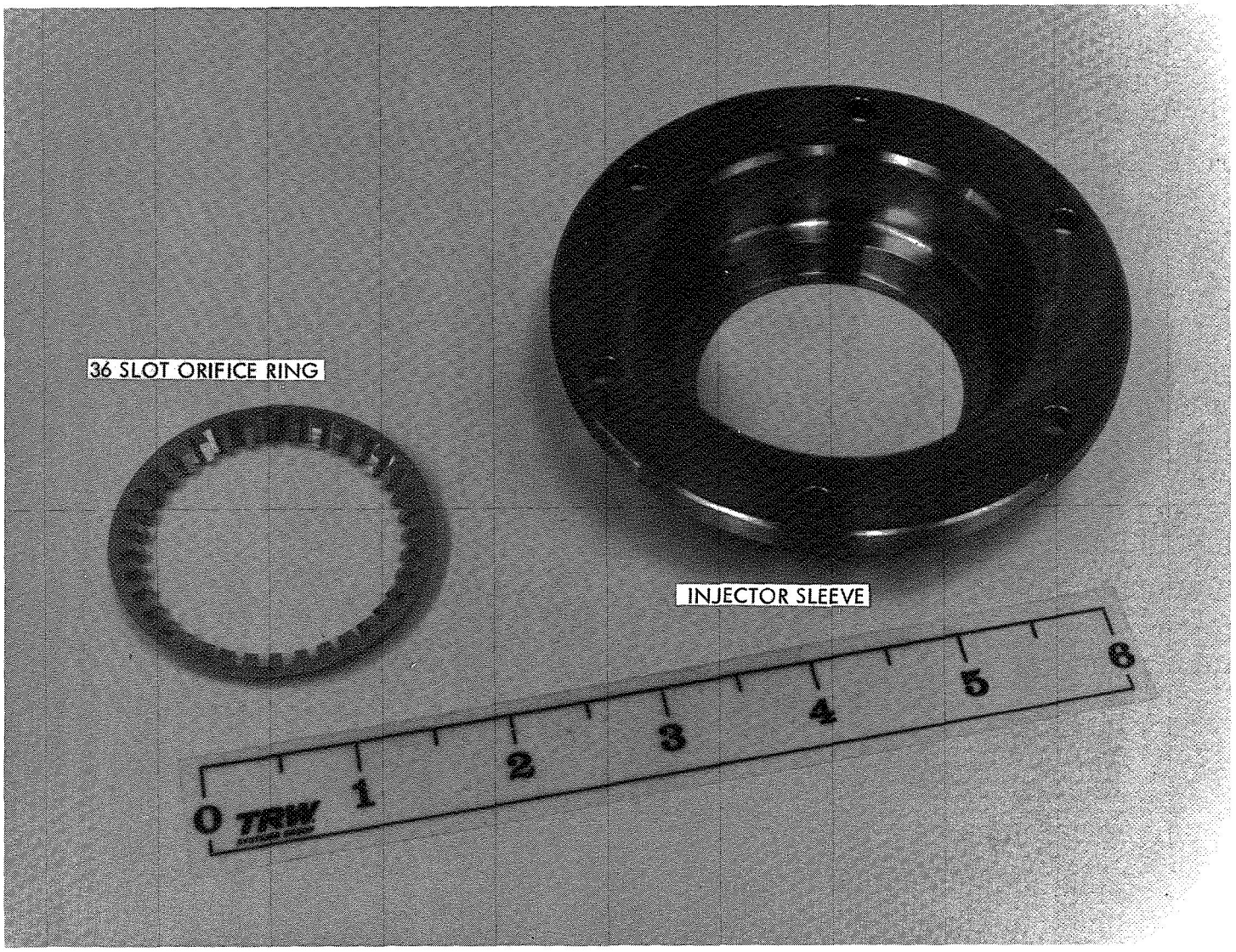

Figure 87. Serrated Oxidizer Injection Orifice Ring and Modified Sleeve

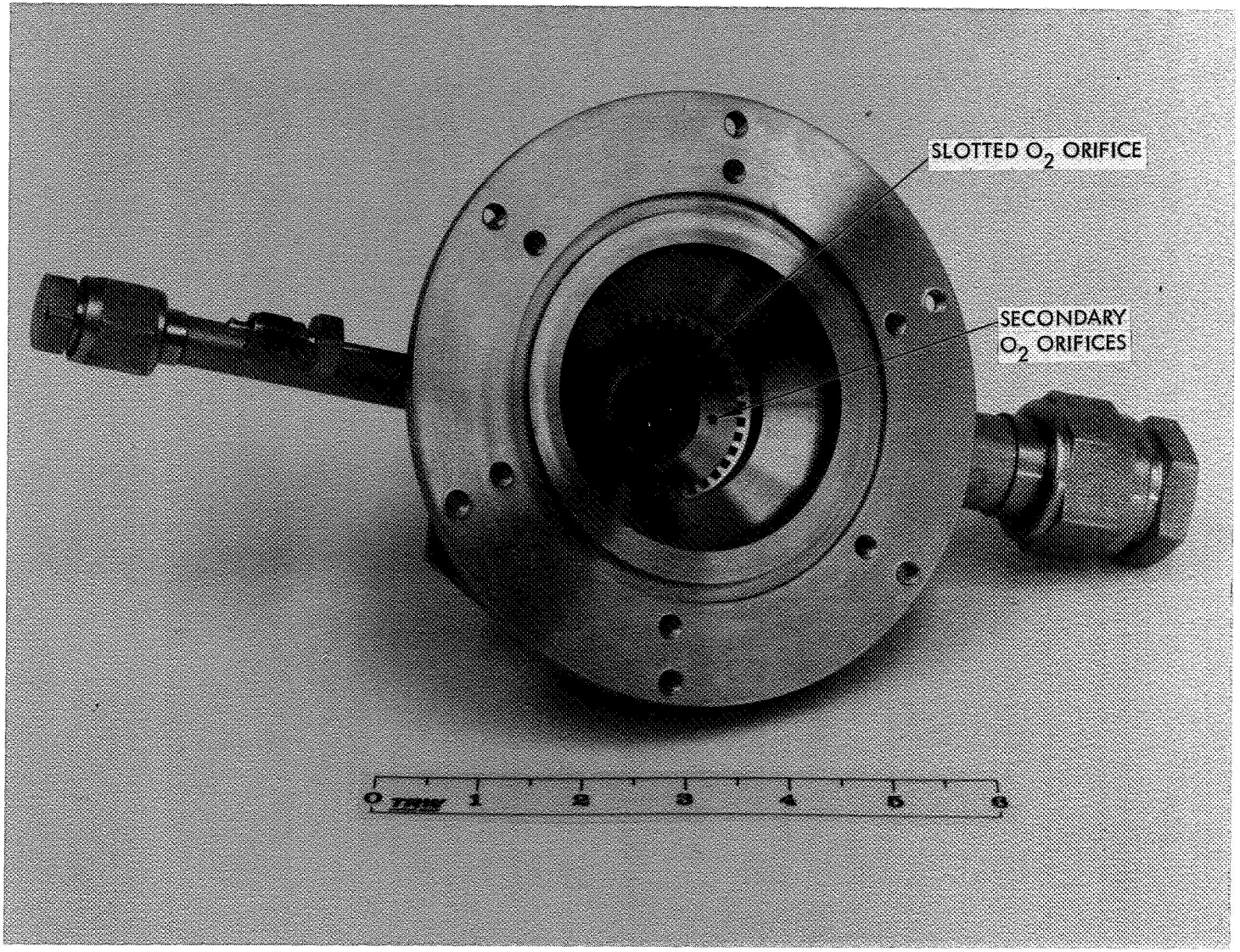

Figure 88. Stream Injection Oxidizer Orifice Configuration

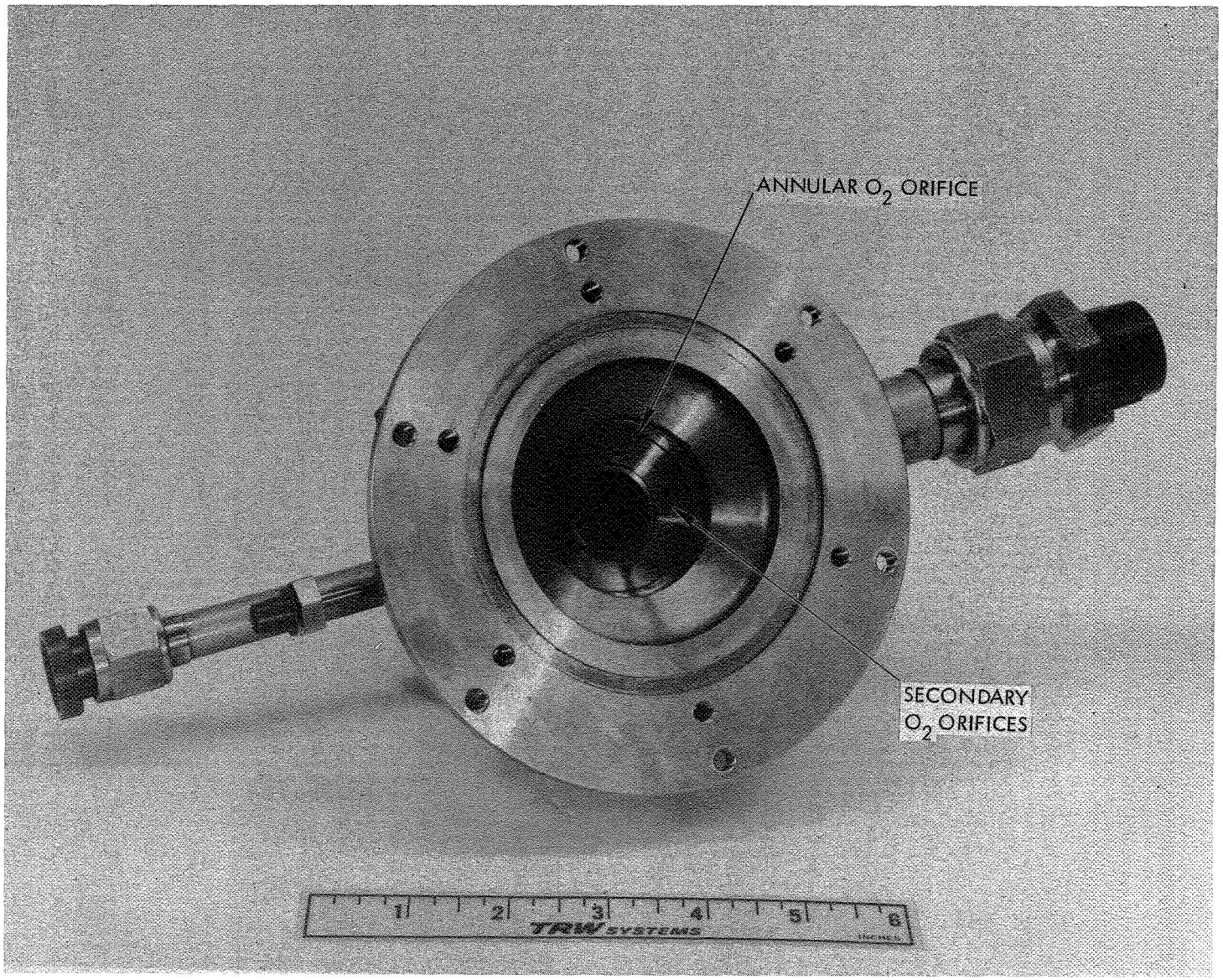

Figure 89. Continuous Sheet Oxidizer Injection Configuration

(a) 10 psia P_c Thruster Injector

Full Annular gap injection orifices for both propellants (nominal gap thickness .050")

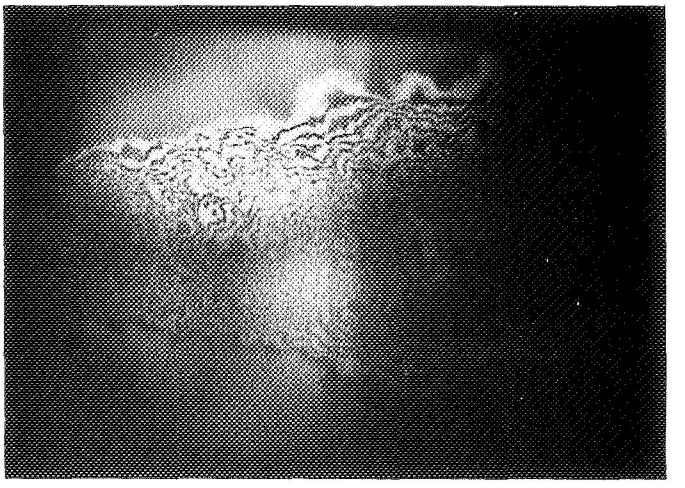

Flow →

(b) 10 psia P_c Thruster Injector

Same as (a) above, except center oxidizer injection gap changed to a ring of 36 rectangular orifices of equivalent flow area. No change in fuel injection orifice from (a).

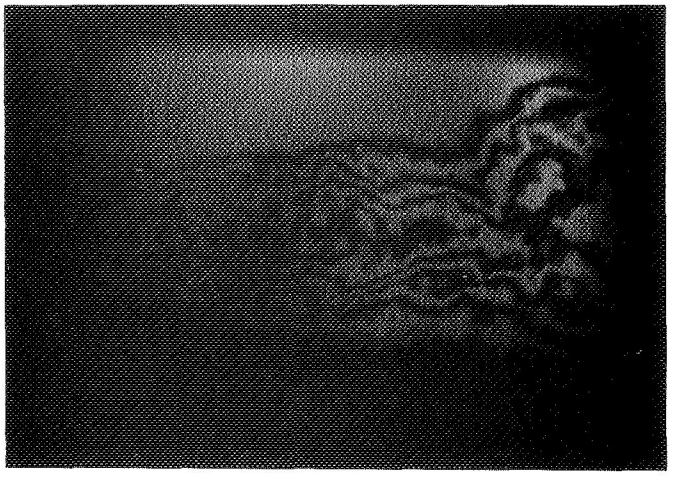

Flow →

(c) 100 psia P_c Thruster Injector

Full annular gap injection orifices for both propellants (nominal gap thickness .015")

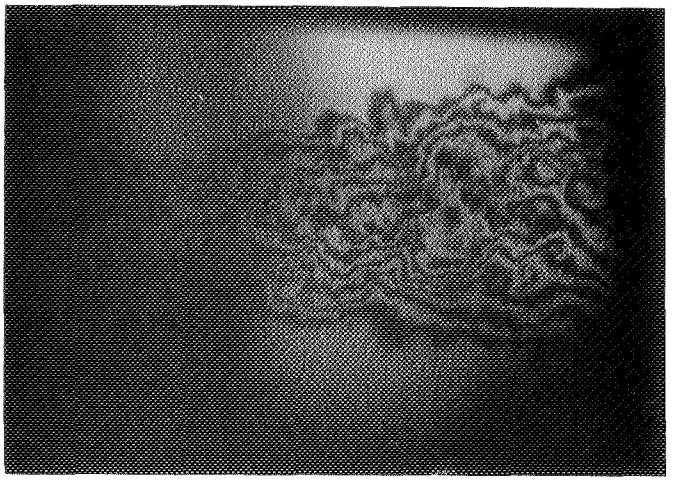

Flow →

Figure 90. Double-Exposure Holographic Interferograms of GO_2/GH_2 Injectors Using GH_2/GHe as Simulant Flow Mediums — Both Gases Flowing Simultaneously

Test data from the bed optimization series is presented in Table 21. Descriptions of these tests are as follows:

Tests 1024-1030: No ignitions were attained with the 36-slot low P_c injector configuration shown in Figure 88, as described previously.

Test 1031: Low chamber pressure injector configuration was changed to continuous sheet oxidizer injection (Figure 89). No ignition was attained at an effluent temperature of 1648°F (1171°K).

Test 1032-1034: Same configuration was used, successful ignitions were attained at effluent temperatures as low as 1639°F (1166°K) when igniter flow rate was reduced to 2 percent of thruster flow (test 1034).

Test 1035-1038): No ignitions of the low P_c thruster were achieved with an igniter throat of 0.170 inch (0.432 cm) diameter added.

Tests 1039-1046: A reduced diameter catalyst bed, 0.620 inch (1.58 cm) diameter was evaluated, and no significant change in response times was observed, compared to tests 1032-1034.

Tests 1047-1052: A longer catalyst bed, 1.48 inch (3.76 cm) by 0.870-inch (2.21 cm) diameter, was evaluated. Effluent temperatures of over 1927°F (1326°K) were required for ignition with pure, ambient temperature propellants. No ignitions were attained with dilutions of 25 percent helium in oxygen.

Tests 1053-1056: Reduced chamber length tests were conducted, repeating tests 1032-1034. No significant effects of reduced chamber volume on thruster ignition characteristics were evident.

Tests 1057-1061: High chamber pressure thruster ignitions were attained with a 0.430-inch (1.09 cm) diameter by 0.50-inch (1.27 cm) long catalyst bed at igniter effluent temperatures as low as 1234°F (941°K).

Tests 1062-1069: Reduced diameter catalyst bed tests resulted in no ignition at effluent temperatures below 1500°F (1089°K).

Tests 1070-1079: High P_c thruster tests with a 1.50-inch (3.81 cm) long catalyst bed resulted in an 80 percent increase in igniter response times compared to tests 1060-1061. No ignitions were attained with dilutions of 25 percent helium in oxygen.

Tests 1080-1090: Reduced chamber tests indicated that increased effluent temperatures of over 1700°F (1200°K) were required for ignition as P_c was decreased to 12.1 psia (83.4 kN/m^2).

Figure 91 is a correlation of the bed response data from Table 21. This log-log data plot indicates that igniter response time generally decreased as the square of the igniter flow rate for each fixed bed configuration, and increased as nearly the one-half power of the catalyst bed

Table 21. Igniter Bed Optimization Test Data

Run No.	P_c Measured psia	P_c Measured kN/m^2	$\dot{W}_T$ lbs/sec	$\dot{W}_T$ kg/sec	M.R. O/F	Chamber L* in.	Chamber L* cm	Cat. Bed L/D	$\dot{W}$ Igniter lbs/sec	$\dot{W}$ Igniter kg/sec	T Effluent °F	T Effluent °K	Response Time sec to .95 TE	Comments
C2-1024-30	No ignition - slotted oxidizer injection orifice													36 slot injector configuration
1031	No ignition - reduced igniter effluent temperature													TE = 1648°F (1171°K), $W_I = 5\%\ W_T$
1032	10.4	71.7	.0564	.0256	2.62	30	76.2	.58	.00278	.00126	1841	1278	4.66	Pure ambient propellants catalyst bed .870 in. (2.21 cm) dia by .50 in. (1.27 cm) long
1033	10.5	72.4	.0558	.0253	2.52	30	76.2	.58	.00523	.00237	1920	1322	3.18	
1034	10.3	71.0	.0565	.0256	2.59	30	76.2	.58	.00125	.00057	1639	1166	6.19	
1035-38	No ignition - igniter throat added for these tests.													Igniter D_t = .170 in. (.432 cm)
1039	10.8	74.5	.0566	.0257	2.56	30	76.2	.81	.00124	.00056	1833	1274	5.63	Pure ambient propellants, catalyst bed .620 in. (1.58 cm) dia by .50 in. (1.27 cm)
1040	10.7	74.5	.0570	.0259	2.54	30	76.2	.81	.00125	.00057	1786	1248	6.24	
1041	No ignition - reduced igniter effluent temperature													TE = 1167°F (904°K)
1042	11.0	75.8	.0579	.0263	2.48	30	76.2	.81	.00123	.00056	1732	1218	6.20	Repeat of C2-1040
1043	No ignition - reduced igniter effluent temperature													TE = 1689°F (1194°K)
1044	10.7	73.8	.0586	.0266	2.71	30	76.2	.81	.00304	.00138	1751	1228	4.81	Pure ambient propellant
1045	10.0	68.9	.0530	.0240	3.13	30	76.2	.81	.00126	.00057	1998	1365	5.36	Pure propellants, -250°F (117°K)
1046	No ignition - reduced igniter effluent temperature to 1826°F (1270°K)													
1047-49	No ignition - reduced igniter effluent temperatures below 1927°F (1326°K)													Pure ambient propellant, catalyst bed .870 in. (2.21 cm) dia by 1.48 in. (3.76 cm) long
1050	11.1	76.5	.0598	.0271	2.47	30	76.2	1.70	.00509	.00231	1969	1349	5.38	
1051	No ignition - 25.25% He - O_2, 9.46% He - H_2													Dilute propellant tests, catalyst bed L/D = 1.70
1052	No ignition - 25.25% He - O_2, pure H_2													
1053	10.3	71.0	.0569	.0258	2.59	20	50.8	.58	.00282	.00128	1805	1258	5.69	Reduced chamber length tests 870 in. (2.21 cm) dia by .50 in. (1.27 cm) long catalyst bed
1054	10.1	69.6	.0586	.0266	3.01	20	50.8	.58	.00284	.00129	1906	1259	4.87	
1055	10.0	68.9	.0573	.0260	3.09	20	50.8	.58	.00122	.00055	1696	1198	7.11	
1056	9.9	68.3	.0560	.0254	2.62	20	50.8	.58	.00276	.00125	1852	1284	4.96	
1057	117.0	805.0	.0574	.0260	2.679	30	76.2	1.16	.00278	.00126	1590	1139	2.84	Pure propellant except as noted, catalyst bed .430 in. (1.09 cm) dia by .50 in. (1.27 cm) long
1058	108.0	745.0	.0527	.0239	2.535	30	76.2	1.16	.00499	.00226	1494	1085	1.97	
1059	No ignition - dilute propellants 25.25% He - O_2, 9.46% He - H_2													
1060	104.0	720.0	.0505	.0229	2.752	30	76.2	1.16	.00282	.00128	1737	1220	1.89	
1061	(lost tranducer)		.0500	.0227	2.525	30	76.2	1.16	.00288	.00131	1234	941	1.94	
1062	103.0	711.0	.0501	.0227	2.534	30	76.2	1.64	.00282	.00128	1709	1205	2.86	Catalyst bed .305 in. (775 cm) dia by .50 (1.27 cm) long
1063-67	No ignition - reduced igniter effluent temperatures below 1500°F (1089°K)													
1068	106.0	728.0	.0514	.0233	2.606	30	76.2	1.64	.00272	.00123	1913	1318	2.33	
1069	No ignition - igniter effluent temperature 1700°F (1200°K)													
1070	101.0	698.0	.0503	.0228	2.600	30	76.2	3.49	.00279	.00127	1589	1138	3.38	Catalyst bed .430 in. (1.09 cm) dia by 1.50 in. (3.81 cm) long
1071	101.0	698.0	.0509	.0231	2.549	30	76.2	3.49	.00281	.00127	1599	1144	3.42	
1072	103.0	707.0	.0513	.0233	2.561	30	76.2	3.49	.00286	.00130	1736	1220	3.34	
1073-76	No ignition - dilute propellants 25.98% He - O_2, 9.40% He - H_2													
1077	101.0	698.0	.0504	.0229	2.495	30	76.2	3.49	.00281	.00127	1665	1180	3.48	
1078	101.0	698.0	.0500	.0227	2.505	30	76.2	3.49	.00213	.00097	1574	1130	3.77	
1079	100.0	690.9	.0493	.0224	2.538	30	76.2	3.49	.00174	.00079	1466	1070	3.89	
1080	99.2	684.0	.0501	.0227	2.459	20	50.8	1.16	.00283	.00128	1571	1128	2.00	Reduced chamber length and chamber pressure tests with same catalyst bed configuration as C2-1057-61
1081	48.7	335.8	.0258	.0117	2.371	20	50.8	1.16	.00147	.00067	1759	1233	2.88	
1082	No ignition - effluent temperature 1591°F (1139°K)													
1083	26.2	180.6	.0149	.0068	2.485	20	50.8	1.16	.00136	.00062	1764	1235	3.18	
1084-88	No ignition - igniter effluent temperatures below 1700°F (1200°K)													
1089	12.1	83.4	.0083	.0038	2.302	20	50.8	1.16	.00048	.00022	1790	1250	4.80	
1090	100.0	689.5	.0506	.0230	2.528	20	50.8	1.16	.00277	.00126	1462	1068	1.98	

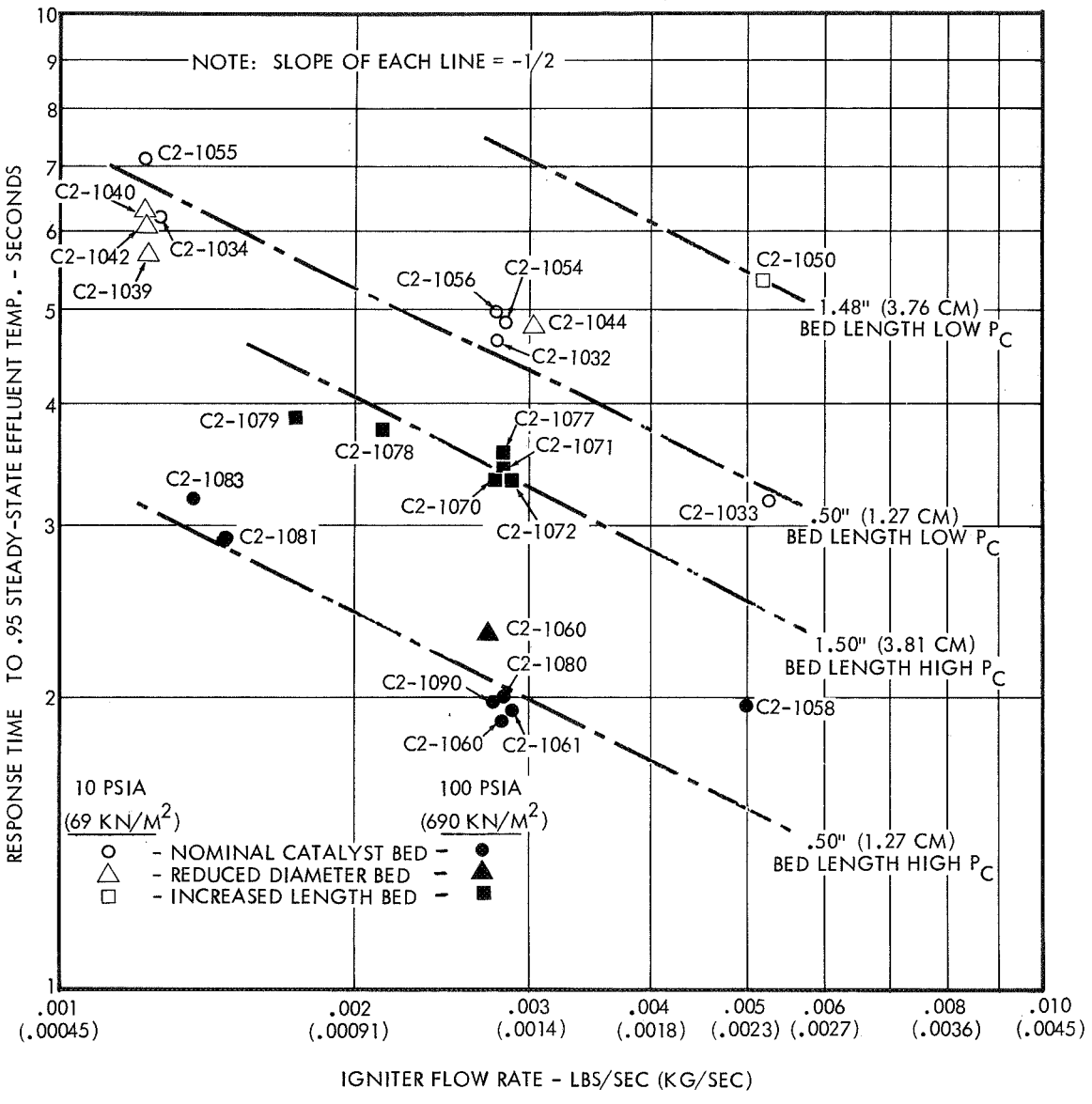

Figure 91. Correlation of Igniter Bed Optimization Data— Thermal Response Versus Flow Rate

length for a fixed igniter flow rate at each P_c level. The thermal response of the bed would be expected to increase linearly with the mass of catalyst (or length, for beds of the same diameter), however, the increased average bed pressure caused by the higher pressure drop across the longer catalyst bed causing the loss of response time to be less would be predicted based upon bed mass differences only. No decrease in response time is evident for the reduced diameter beds at either pressure level, although the mass of catalyst in each case is approximately one-half that of the nominal diameter bed of the same length.

Igniter response time versus igniter flow rate per unit of catalyst bed cross-sectional area is presented in Figure 92. This correlation reveals that the nominal catalyst bed data at both pressure levels fall on a straight line on a log-log plot, and that response times decrease as the square of $\dot{w}_{igniter}/A_{bed}$, similar to Figure 91. Increased length catalyst beds at each pressure level resulted in longer igniter thermal response times compared to the nominal beds, with the reduced diameter bed data falling in between, as shown in Figure 92.

A summary of the catalyst bed optimization test results in presented in Table 22. Three different bed configurations were evaluated at each thruster chamber pressure level to investigate the effects of diameter changes and bed length on the overall thruster response time. Ignition of the thrusters at onset of main propellant flows was achieved with each of the configurations tested. However, as indicated in Table 22, the longer catalyst beds exhibited increased delay times (Figures 91 and 92) and higher temperatures within the catalyst bed in achieving the minimum effluent temperature required for thruster ignition. A higher igniter effluent temperature was required for main thruster ignition at both pressure levels with the reduced diameter catalyst beds. Best overall performance in each case was attained with the shorter, nominal diameter bed configurations, 0.870 inch (2.21 cm) and 0.430 inch (1.09 cm).

5.4 BASELINE PERFORMANCE TESTS

Thruster/igniter baseline performance tests were conducted at each chamber pressure level. The objectives of these tests were as follows:

- Establish baseline thruster/igniter response characteristics
- Measure steady-state altitude performance (thrust, C*, and specific impulse)

Based on the results of the bed optimization test series, a fixed igniter bed and thruster configuration was selected for the baseline tests at each pressure level. These configurations, test conditions, and experimental results are described in the following paragraphs.

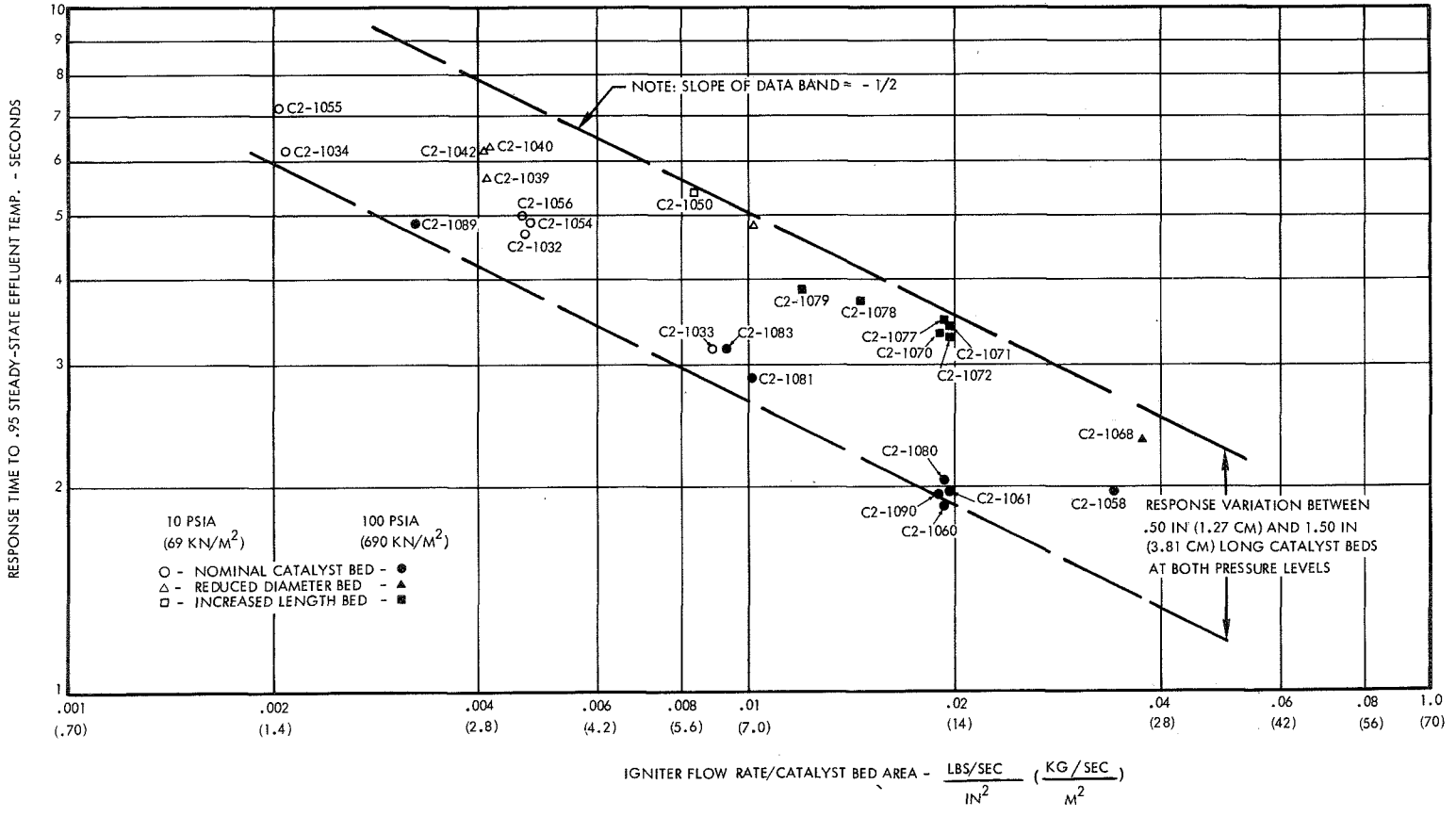

Figure 92. Correlation of Igniter Bed Optimization Data— Thermal Response Versus Flow Rate/Bed Area

Table 22. Summary of Experimental Results—Igniter Bed Optimization Tests

Chamber Pressure	Catalyst Bed Configuration			Results
	Length	Diameter	L/D	
10 psia (69 kN/m^2)	.50" (1.27 cm)	.870" (2.21 cm)	.58	Good thermal response, lowest effluent temperature required for thruster ignition.
↓	.50 (1.27)	.620 (1.575)	.81	Higher effluent temperature required for thruster ignition.
	1.48 (3.76)	.870 (2.21)	1.70	Longest thermal lag, higher bed temperatures required for thruster ignition.
100 psia (690kN/m^2)	.50 (1.27)	.430 (1.09)	1.16	Good thermal response, lowest effluent temperature required for thruster ignition.
↓	.50 (1.27)	.305 (.775)	1.64	Higher effluent temperatures required for thruster ignition.
	1.50 (3.81)	.430 (1.09)	3.49	Longest thermal lag, higher bed temperatures required for thruster ignition.

5.4.1 Description of Test Conditions

Baseline performance tests were performed at the following propellant inlet conditions:

- Propellant temperatures - +70°, -100°, -250°F (294°, 200°, 117°K)
- Helium dilution in oxygen - 0, 5, 25 percent by weight
- Helium dilution in hydrogen - 0, 5, 10 percent by weight

Tests with 50 percent He-O_2 were deleted from this test series, since ignition had not been achieved in previous tests with this dilution. Ignition could potentially have been attained with these amounts of He in O_2 by greatly increasing the O_2/H_2 mixture ratio. However, an overall thruster mixture ratio of 2.5 was specified for all testing under this contract.

The thruster/igniter configurations selected for the baseline performance tests are defined in Table 23. The 1.0-inch (2.54 cm) catalyst bed length was selected after analysis of the catalytic reactor test results, which indicated that this length was superior for low temperature and dilute propellant reaction. The open-tube (no throat) igniter tip configuration was also selected for the baseline test series.

Table 23. Baseline Thruster Configurations

	Low Pressure Thruster	High Pressure Thruster
• Igniter bed diameter	0.870 inch (2.21 cm)	0.430 inch (1.09 cm)
• Igniter bed length	1.00 inch (2.54 cm)	1.00 inch (2.54 cm)
• Throat diameter	1.228 inch (3.119 cm)	0.385 inch (0.978 cm)
• Chamber L*	30 inch (76.2 cm)	30 inch (76.2 cm)
• Nozzle expansion ratio	40:1	40:1

5.4.2 Discussion of Results

Baseline performance test results for each chamber pressure level thruster are presented in Table 24. The methods used to determine and correct performance are discussed in detail in Appendix C. Figure 93 indicates the correlation between the corrected combustion efficiencies determined by thrust and chamber pressure measurements.

Table 24. Baseline Performance Summary

Run No.	P_c psia	P_c kN/m²	$\dot{W}_T$ lbs/sec	$\dot{W}_T$ kg/sec	M.R. O/F	C* corr. ft/sec	C* corr. m/sec	F vac. corr. lbs	F vac. corr. N	I_{sp} corr. lbf sec/lbm	I_{sp} corr. Nsec/kg	η_{C^*F} %	$\eta_{C^*P_c}$ %	Comments
C2-1102	102.5	706.7	.0510	.0232	2.67	7693	2345	21.49	95.59	409.0	4011	.9238	.9155	Pure ambient propellants, nominal injector gaps[1]
1103	105.6	728.1	.0515	.0234	2.62	7680	2341	21.86	97.24	411.9	4039	.9305	.9140	
1104	101.0	696.4	.0507	.0230	2.60	7648	2331	21.03	93.55	402.5	3947	.9093	.9101	
1105	99.8	701.9	.0509	.0231	2.56	7659	2334	21.46	95.46	409.2	4013	.9243	.9115	
1111	100.2	690.9	.0507	.0230	2.65	7658	2334	21.58	95.99	413.2	4052	.9333	.9144	Pure ambient propellants, O_2 inj.gap~.009 in(.023cm) H_2 inj.gap~.016 in(.041 cm)
1112	107.0	737.7	.0525	.0238	2.65	7874	2400	22.60	100.53	417.2	4091	.9423	.9370	
1113	101.0	696.4	.0511	.0232	2.57	7606	2318	21.81	97.02	414.2	4062	.9357	.9052	
1117	100.0	689.5	.0513	.0233	2.62	7531	2295	20.70	92.08	403.4	3956	.9112	.8962	5.0% He-O_2/pure H_2, ambient[1]
1118	100.0	689.5	.0512	.0232	2.45	7508	2288	20.53	91.32	401.0	3932	.9058	.8935	5.0% He-O_2/9.3%He-H_2, " [1]
1132	101.7	701.2	.0509	.0231	2.62	7830	2387	21.12	93.95	415.0	4070	.9374	.9318	Pure ambient propellants,[1]
1133	101.8	701.9	.0501	.0227	2.52	7959	2426	21.09	93.81	421.0	4129	.9510	.9472	
1134	101.7	701.2	.0496	.0225	2.59	8032	2448	20.78	92.43	419.0	4109	.9464	.9558	
1152	96.4	664.7	.0482	.0218	2.56	7707	2349	19.29	85.81	400.2	3925	.9204	.9338	Pure propellants, 100°F(200°K)[1]
1161	91.8	633.1	.0473	.0215	2.55	7488	2282	18.81	83.67	397.6	3899	.9295	.9222	Pure propellants, 250°F(117°K)[1]
1167	10.9	75.2	.0591	.0268	2.44	7020	2140	21.63	96.22	366.1	3590	.8421	.8552	Pure ambient propellants, nominal injector gaps[2]
1168	10.5	72.4	.0561	.0254	2.70	7120	2170	20.70	92.08	368.9	3618	.8490	.8473	
1181	11.1	76.5	.0569	.0258	2.48	7482	2280	22.16	98.57	389.5	3820	.8949	.8904	Pure ambient propellants, fuel injection gap .028 in (.071 cm)
1183	11.7	80.7	.0589	.0267	2.50	7659	2334	23.41	104.13	397.4	3897	.9150	.9115	
1185	10.7	73.8	.0555	.0252	2.53	7323	2332	21.21	94.35	382.2	3748	.8912	.8715	Pure ambient propellants, fuel injection gap .032 in (.081 cm)
1193	9.4	64.8	.0506	.0229	2.33	7262	2213	19.03	84.65	376.1	3688	.8864	.8943	Pure propellants, ~250°F(117°K) fuel injection gap .032 in. (.081 cm)

[1] Nominal high pressure injector gaps - .011 in (.028 cm) O_2, .016 in (.041 cm) H_2

[2] Nominal low pressure injector gaps - .044 in (.112 cm) O_2, .053 in (.135 cm) H_2

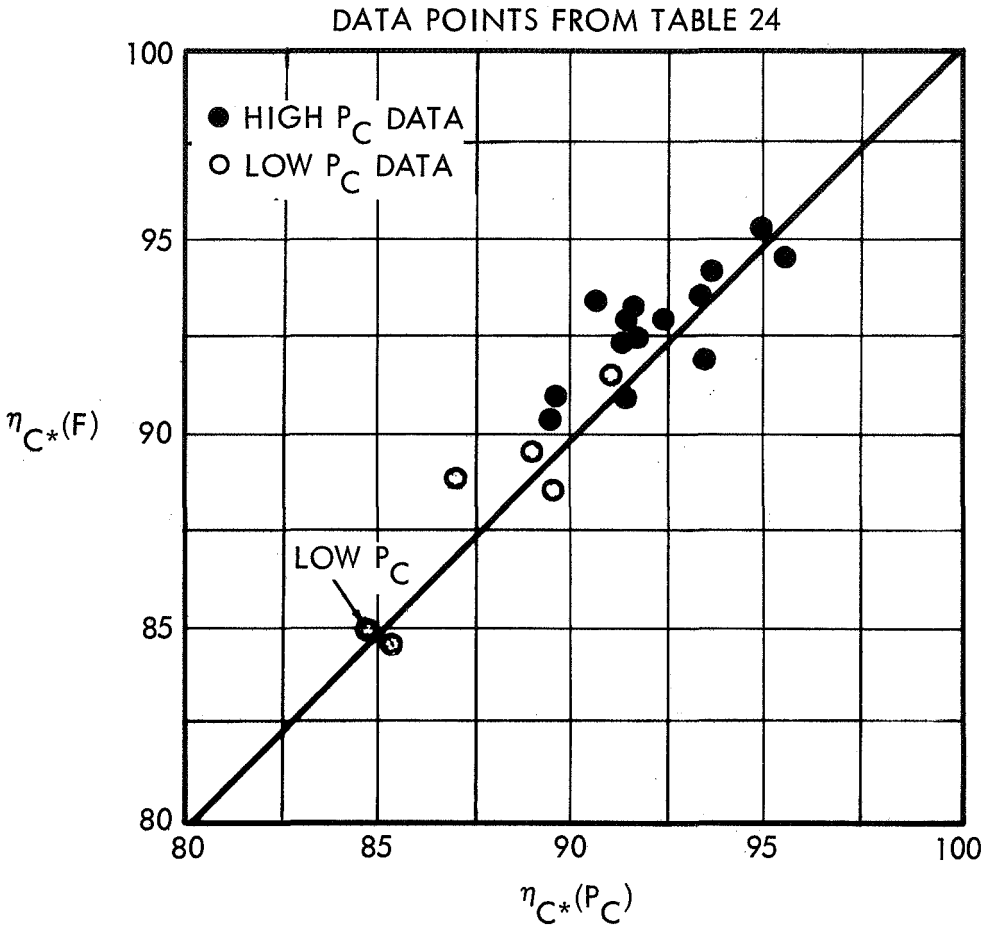

Figure 93. Comparison of Thrust and Chamber Pressure C* Measurements

Since attainment of maximum thruster performance was not an objective of this investigation, no extensive optimization of injection velocities or relative momentum ratios was conducted. However, a limited number of baseline tests were performed at different fuel injection orifice gaps (each thruster injector incorporated gap adjustment capability, as described in Section 5.1.1).

Descriptions of the baseline tests follow.

Test 1102-1105: High chamber pressure tests were performed to determine repeatability of steady-state measured performance, both C* and specific impulse. These tests were performed with ambient temperature propellants at nominal oxidizer and fuel injection gaps of 0.011 inch (0.028 cm) and 0.016 inch (0.041 cm), respectively.

Tests 1111-1113: These tests were conducted to determine the performance effects of varying the propellant momentum ratio by changing the oxidizer injection gap from 0.011 to 0.009 inch (0.028 to 0.023 cm). Both I_{sp} and C* increased approximately 1.5 percent compared to tests 1102-1105.

Tests 1117-1118: High chamber pressure baseline tests were performed with helium diluted propellants. Dilutions of 5 percent $He-O_2$ resulted in a 2 percent performance degradation compared to tests 1102-1105 with pure propellants and identical injection gaps.

Tests 1132-1134: These high P_c baseline tests were performed with pure ambient temperature propellants and nominal injection gaps. Performance results based on thrust and pressure measurements showed good agreement (note η_{C*F}, η_{C*P_c} columns).

Tests 1152-1161: Propellants were conditioned to -100°F (200°K) and -250°F (117°K) for these baseline tests. Measured performance was 4 to 8 percent lower than ambient tests 1132-1134, but was over 92 percent of theoretical performance at these propellant temperatures.

Tests 1167-1168: Initial low chamber pressure baseline performance tests were conducted with pure ambient propellants and oxidizer and fuel injection gaps of 0.044 inch (0.112 cm) and 0.053 inch (0.135 cm), respectively. Measured performance was nominally 85 percent of theoretical equilibrium C*.

Tests 1181-1183: Fuel injection velocities were increased for these tests by reducing the fuel injection gap to 0.028 inch (0.071 cm), resulting in a 5 percent increase in measured thruster performance.

Test 1185: A test was conducted at an intermediate fuel gap of 0.034 inch (0.081 cm) to determine performance effects. Performance decreased approximately 2 percent compared to tests 1181-1183.

Test 1193: This low chamber baseline test was performed with propellants at -250°F (117°K). Measured performance was 89 percent of equilibrium C* for these propellant temperatures.

Figures 94 and 95 compare the high chamber baseline performance results with theoretical performance for these propellants. Figures 96 and 97 indicate the variation in impulse and C* performance with injector pressure ratios.

Low chamber pressure baseline performance data are presented in Figures 98 and 99, along with theoretical performance values for this P_c level. Performance as a function of injection pressure ratios (Figures 100 and 101) also indicates increased impulse and C* performance as oxidizer/fuel injection pressure ratios were reduced.

5.4.3 Performance Summary

A summary of the baseline performance, including the effect of increased fuel injection velocities on performance of the low pressure thruster, is presented in Table 25. Measured vacuum performance is included for tests conducted with propellants at ambient and -250°F (117°K). Thruster ignition was attained with helium-oxygen dilutions of 5 percent by weight, but not with 25 percent helium dilution of the oxygen supply. Helium-hydrogen dilutions of 5 and 10 percent by weight were ignitable at both chamber pressure levels.

5.5 THRUSTER PULSE MODE TESTS

The purpose of this test series was to determine the pulse mode performance characteristics of each thruster/igniter configuration. The specific objectives of the test series were:

- Perform pulse mode test firings to establish performance and response times for each pressure level thruster
- Determine the effects on the thrust profile caused by varying the propellant lead/lag durations
- Evaluate the effects of modifying the pulse mode duty cycles ("on" time versus "off" time)

The thruster/igniter configurations selected for the baseline performance tests were also used for this test series. The approved test matrix for these tests is presented in Table 26.

5.5.1 Test Description

The thruster pulse mode tests were performed with pure hydrogen-oxygen propellants conditioned to -250°F (117°K) and the igniter catalyst bed initially at ambient temperature. Required duty cycles of 200 msec on/100 msec off were performed for each pressure level thruster. Two additional pulse duty cycles were evaluated for each thruster: 100 msec

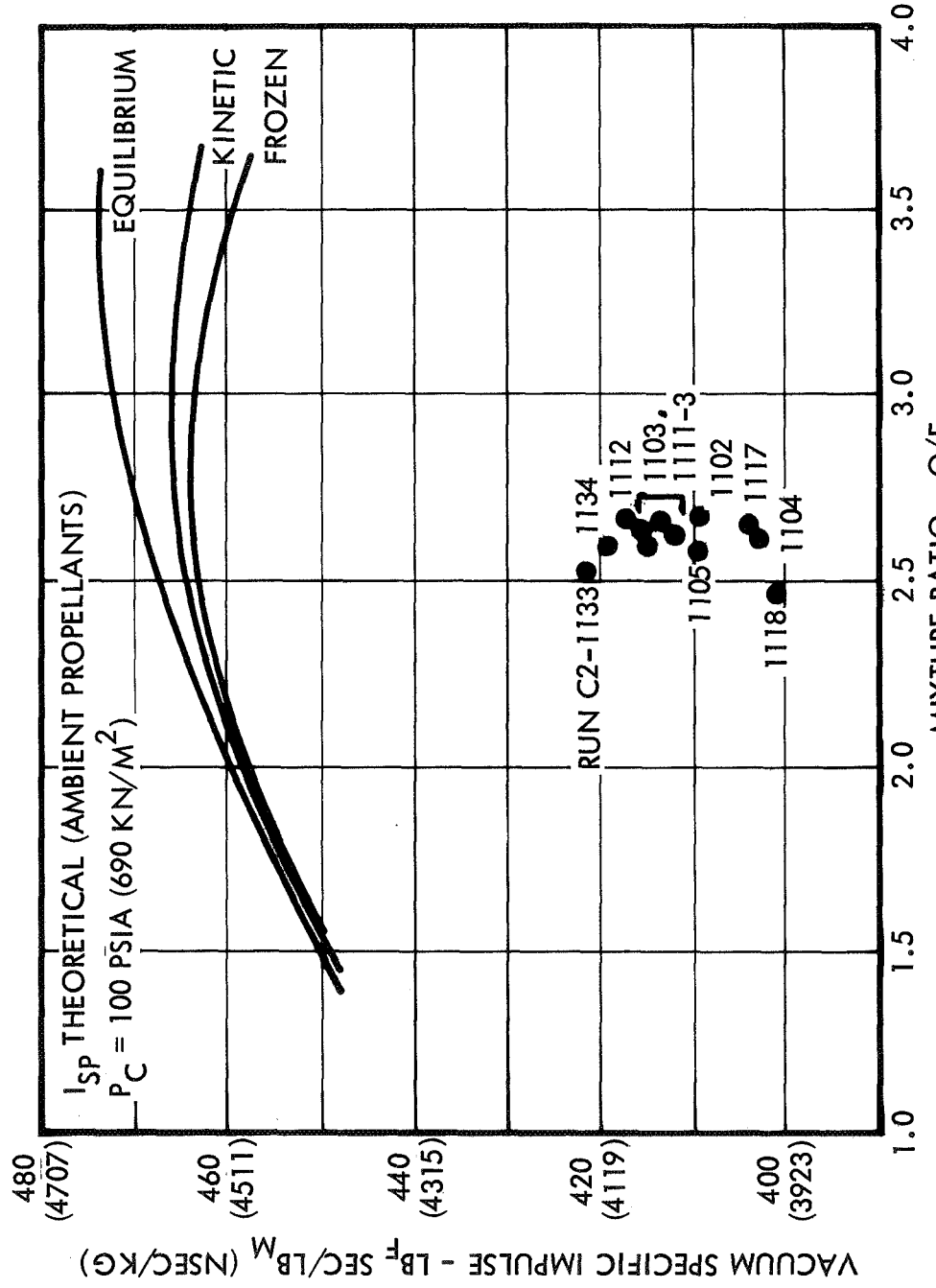

Figure 94. Baseline Impulse Performance—High P_c Thruster

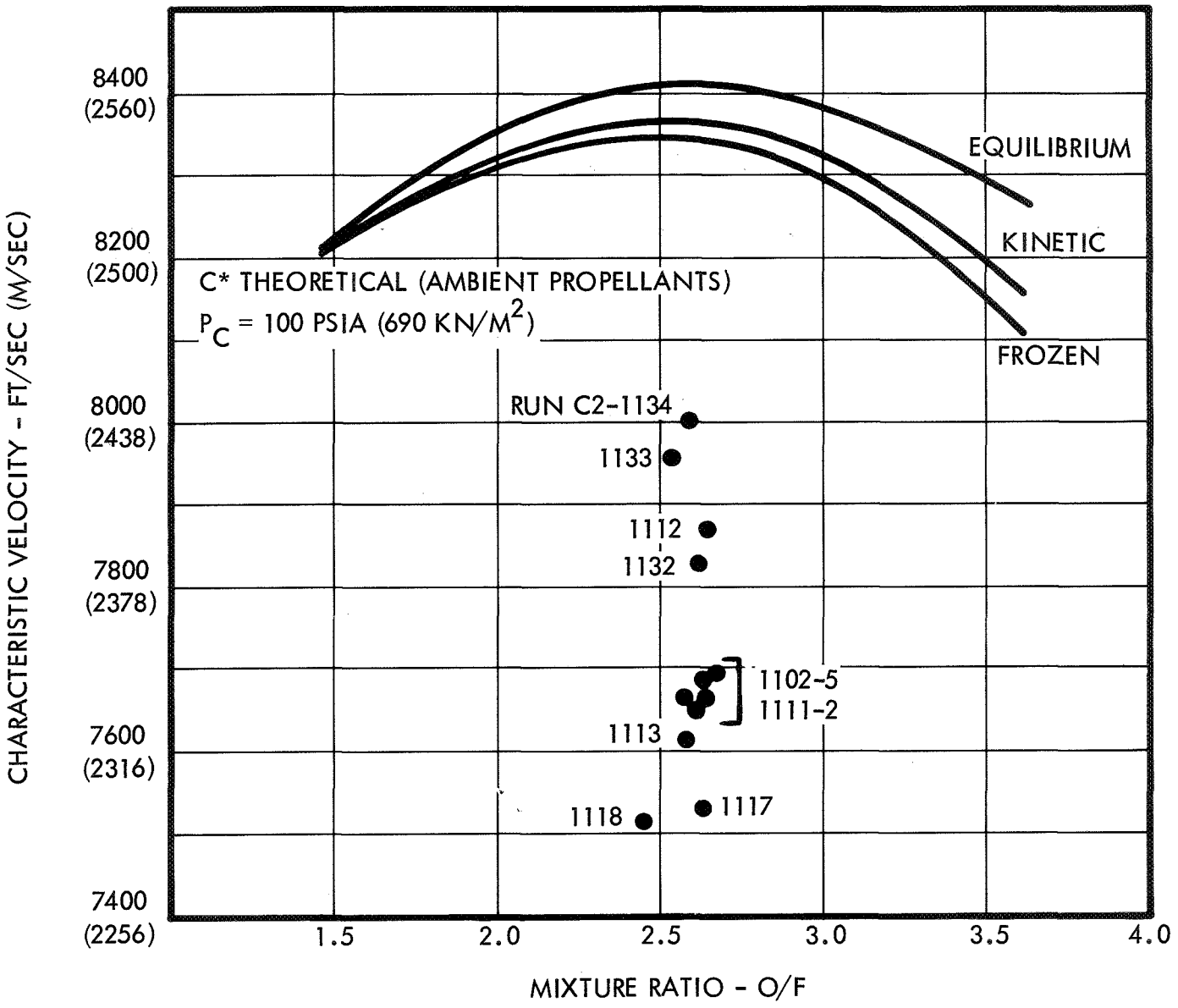

Figure 95. Baseline C* Performance—High P_c Thruster

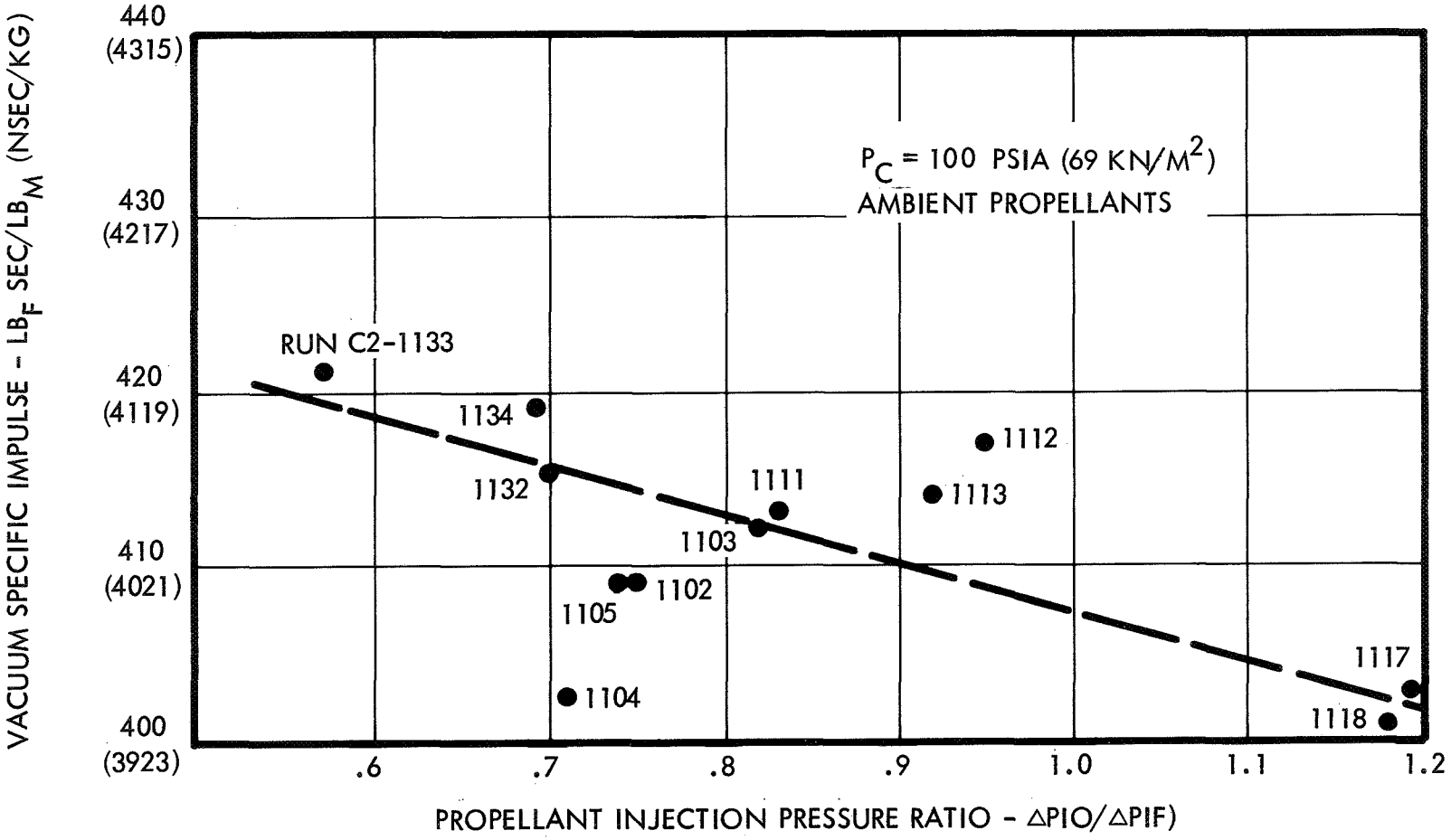

Figure 96. Effect of Injection Pressure Ratio on Impulse Performance—High P_c Baseline Tests

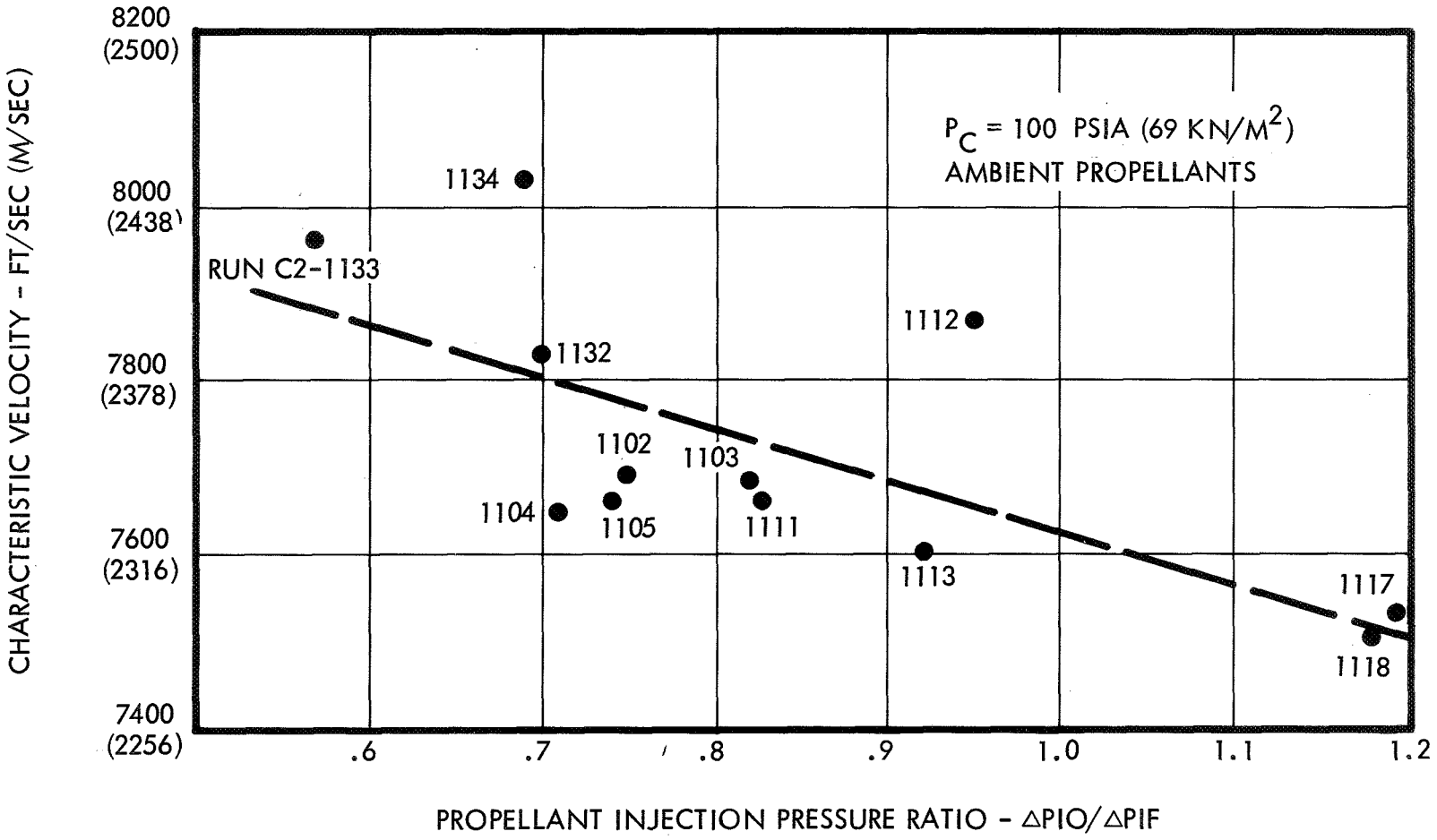

Figure 97. Effect of Injection Pressure Ratio on C* Performance — High P_c Baseline Tests

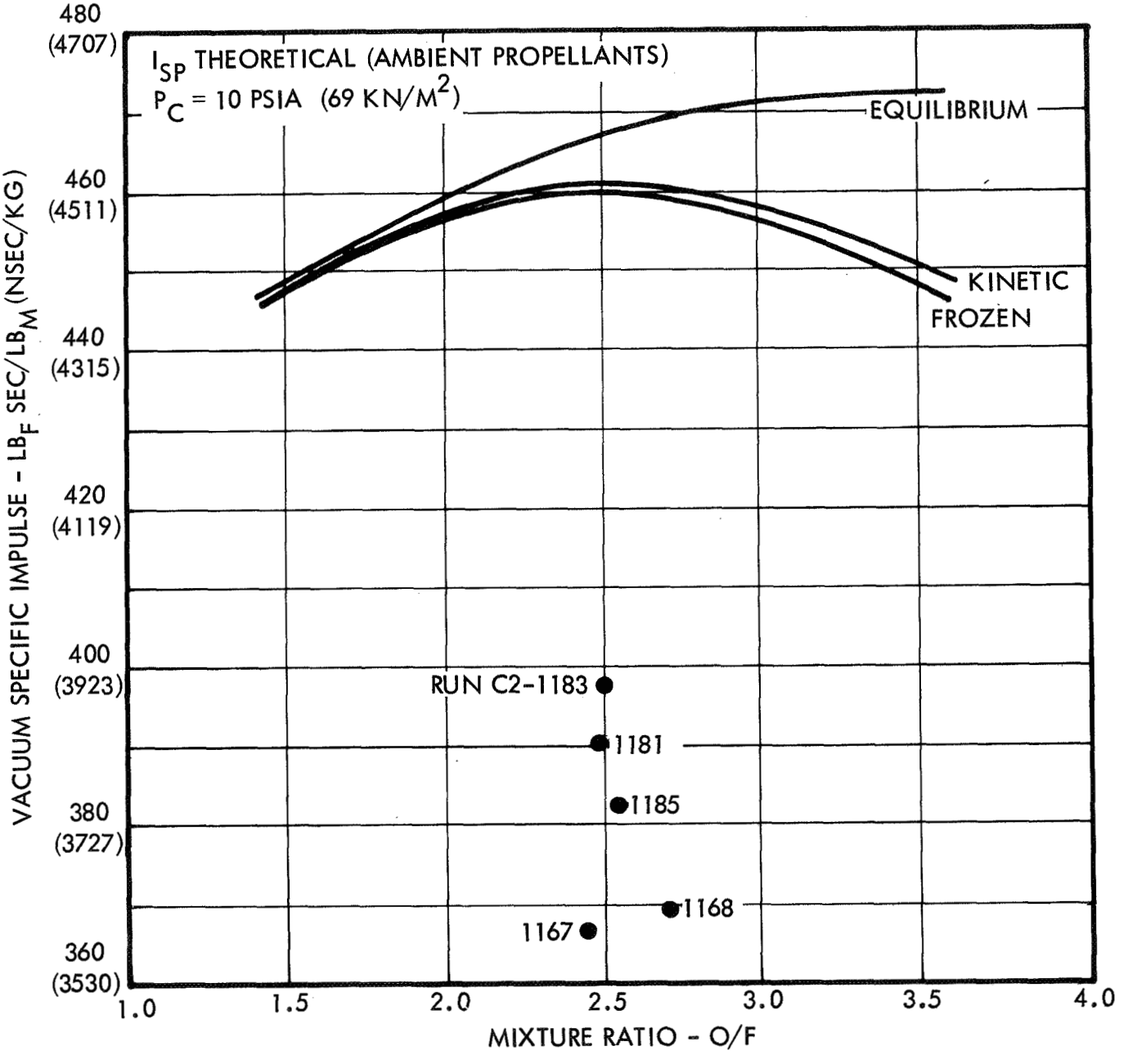

Figure 98. Baseline Impulse Performance—Low P_c Thruster

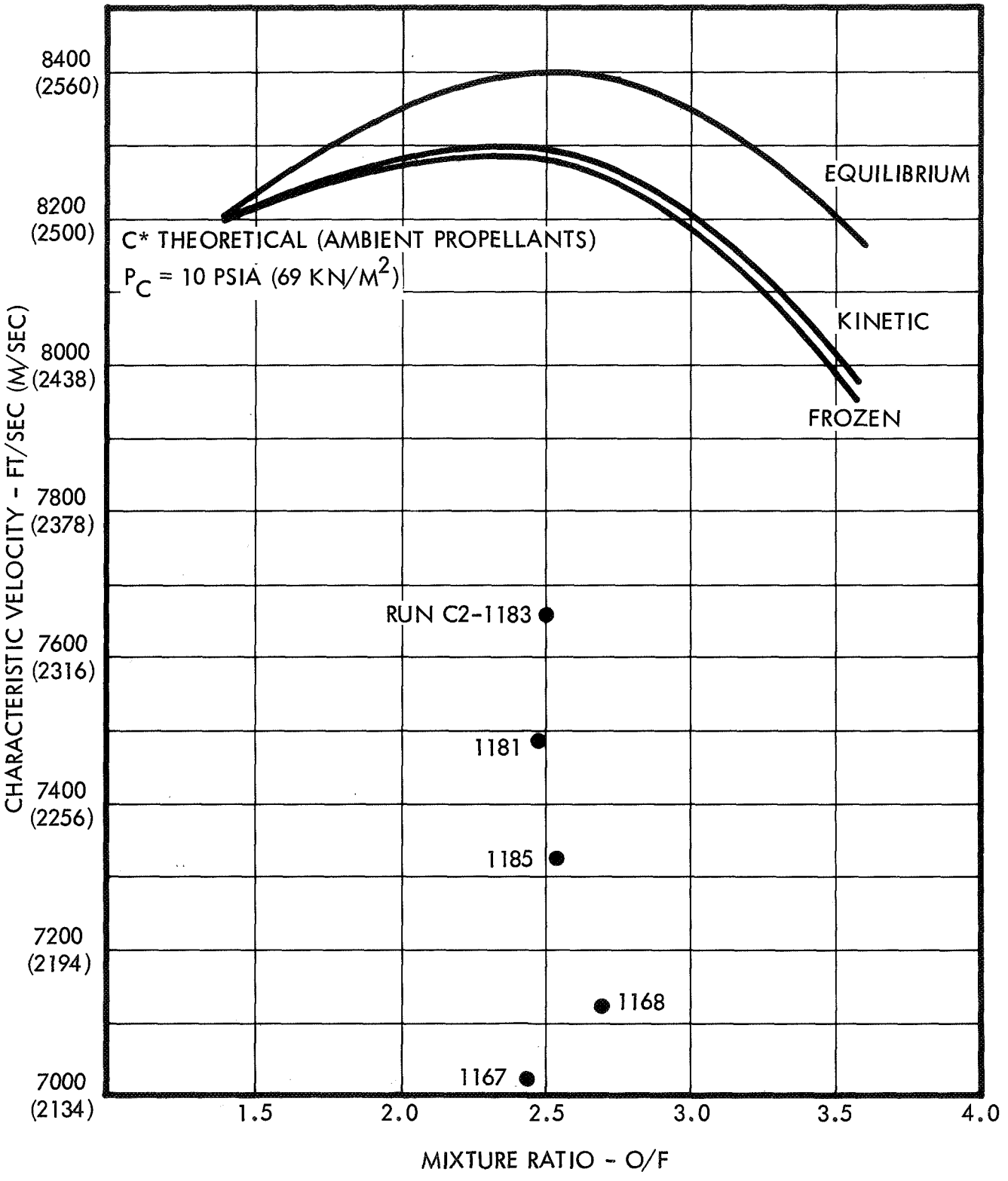

Figure 99. Baseline C* Performance—Low P_c Thruster

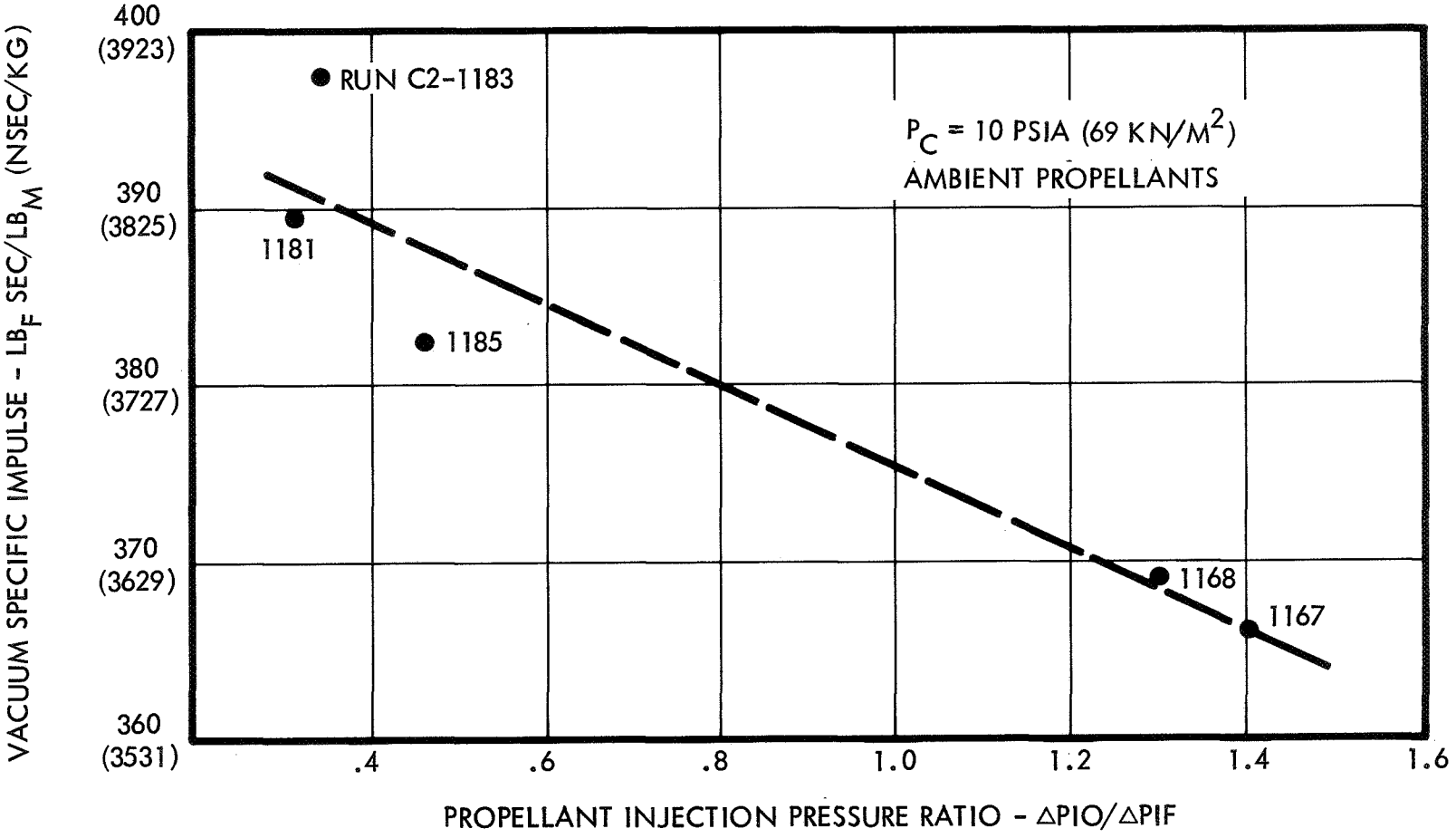

Figure 100. Effect of Injection Pressure on Impulse Performance— Low P_c Baseline Tests

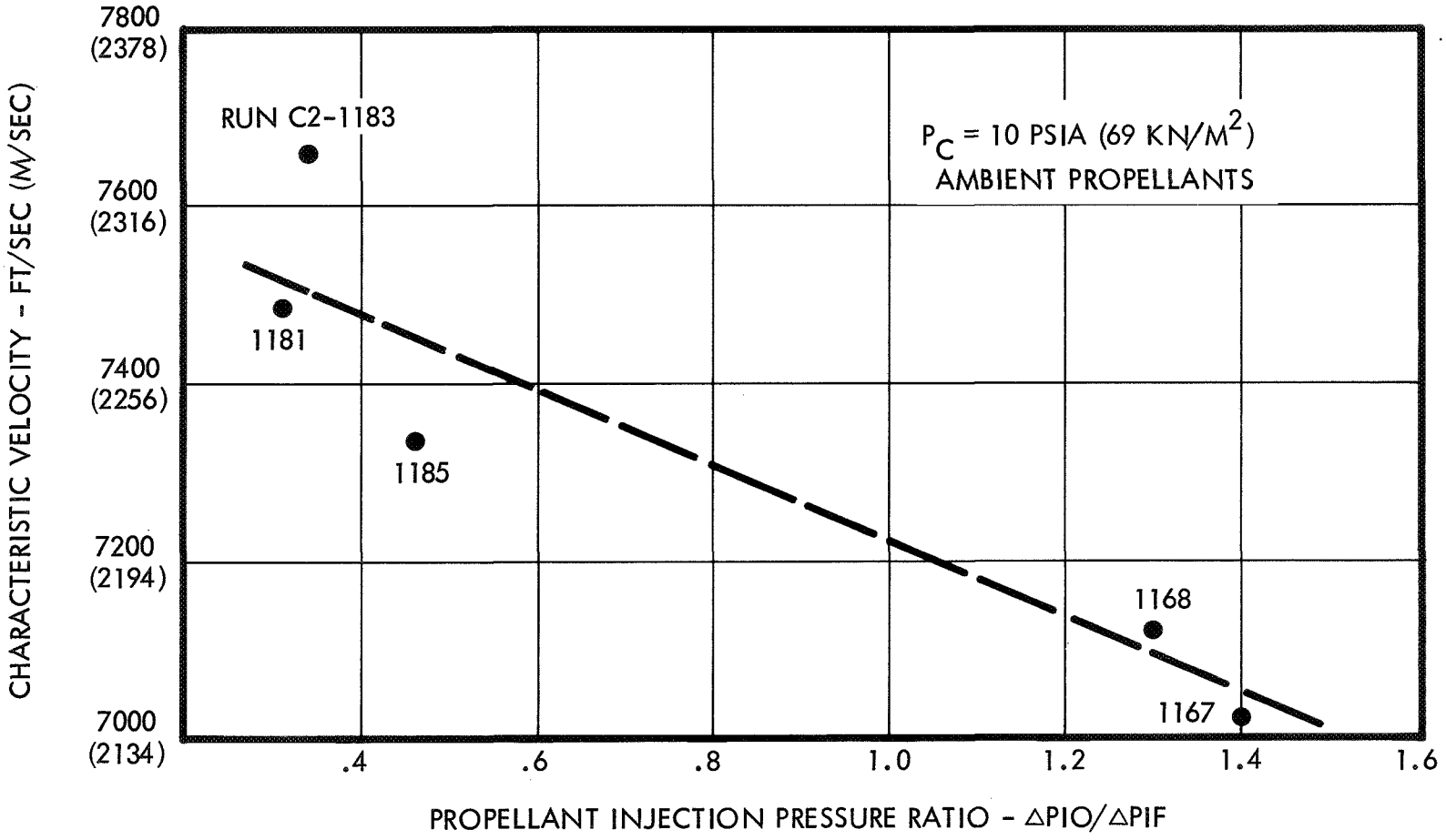

Figure 101. Effect of Injection Pressure on C* Performance— Low P_c Baseline Tests

Table 25. Baseline Performance Summary

	Low Pressure Thruster	High Pressure Thruster
Maximum measured vacuum performance with ambient propellant temperatures	7120[1] ft/sec C*(85% C*theor.) (2170 m/sec) 369 sec ISP (3618 N sec/kg) 7659[2] ft/sec C*(91% C* theor.) (2334 m/sec) 397 sec ISP (3897 N sec/kg)	8032 ft/sec C* (96% C*theor.) (2448 m/sec) 421 sec ISP (4129 N sec/kg)
Maximum measured vacuum performance with -250°F (117°K) propellant temperatures	7262[1] ft/sec C* (89% C*theor.) (2213 m/sec) 376 sec ISP (3688 N sec/kg)	7488 ft/sec C* (92% C*theor.) (2282 m/sec) 398 sec ISP (3899 N sec/kg)

(1) .053 in. (.135 cm) fuel injection gap
(2) .028 in. (.071 cm) fuel gap - increased injection velocity

Table 26. Thruster Pulse Mode Tests Minimum Test Matrix

Propellant inlet temperature: -250°F (117°K)

Catalyst bed/thruster temperature: initially at ambient

Matrix Element No.*	Pulse Duty Cycle**	Igniter Operational Mode***	Propellant Lead/ Lag***
1	1	1	1
2	1	2	1
3	1	3	1
4	1	1	2
5	2	1	2
6	3	1	2
7-12	Repeat 1-6 for 2nd P_c level thruster		

*One or more tests were conducted for each matrix element.

**Pulse duty cycle No. 1 was 10 pulses of 200 ms duration each with 100 ms off time as specified. Two additional duty cycles ("on" time versus "off" time) were selected for evaluation after analysis of initial pulse mode data.

***Three igniter operational modes were evaluated: pulsing of both igniter flows, continuous operation of the igniter between main thruster pulses, and igniter fuel flow only between pulses.

on/100 msec off and 500 msec on/500 msec off for the low pressure thruster; 150 msec on/150 msec off and 500 msec on/500 msec off for the high pressure thruster.

Electronic sequencing control equipment was designed and assembled for the pulse mode test series. Variable delay circuits were incorporated into the pulse control console to allow for precise setting of igniter and thruster propellant valve lead/lags over the maximum ranges anticipated. Variable lead/lags between the igniter and main thruster valves were also pre-set by simple panel adjustments.

Three separate pulse operational sequences were evaluated, as shown in Figure 102. Main thruster pulse mode tests with continuous igniter propellant flow, pulsed igniter oxidizer flow, and pulsing of both igniter flows were conducted. Main oxidizer to fuel valve leads from 10 to 35 milliseconds were evaluated. Simultaneous shutdown of both main propellant valves was performed to minimize the thrust decay time after each pulse. A minimal igniter hydrogen lag was utilized, as shown in Figure 102, to maintain optimum catalyst bed activity by precluding oxygen from the catalyst surface while the bed was at temperature above 1500°F (1089°K).

5.5.2 Discussion of Results

Results of the pulse mode tests at each thruster chamber pressure level, 10 and 100 psia (69 and 690 kN/m^2), are presented in Table 27. All tests were performed with propellants conditioned to -250°F (117°K) and the thruster/igniter hardware initially at ambient temperature, as required.

Tests 1202-1204: Initial low P_c pulse tests were conducted with each of the three igniter pulse sequences, as indicated. The required pulse duty cycle of 200 msec on/100 msec off was performed for these tests, and a main oxidizer to fuel valve lead of nominally 30 msec was evaluated. Satisfactory ignitions were attained on each pulse.

Test 1205: This test was a repeat of 1202, except that the main oxidizer valve lead was decreased to a nominal value of 10 msec, with no detremental effects noted. Thrust data for this test were invalid because the calibration weights were accidently left on during the run.

Tests 1206-1207: A second pulse duty cycle of 500 msec on/500 msec off was evaluated with the low P_c thruster. Ignition did not occur on the first attempt (run 1206), but was achieved by raising the igniter effluent temperature above 1900°F (1309°K) (by increasing igniter mixture ratio).

Tests 1208-1209: The final pulse duty cycle, 100 msec on/100 msec off, was performed with the low chamber pressure hardware. Again, increasing the effluent temperature over 1900°F (1309°K) was required for ignition with propellants at -250°F (117°K).

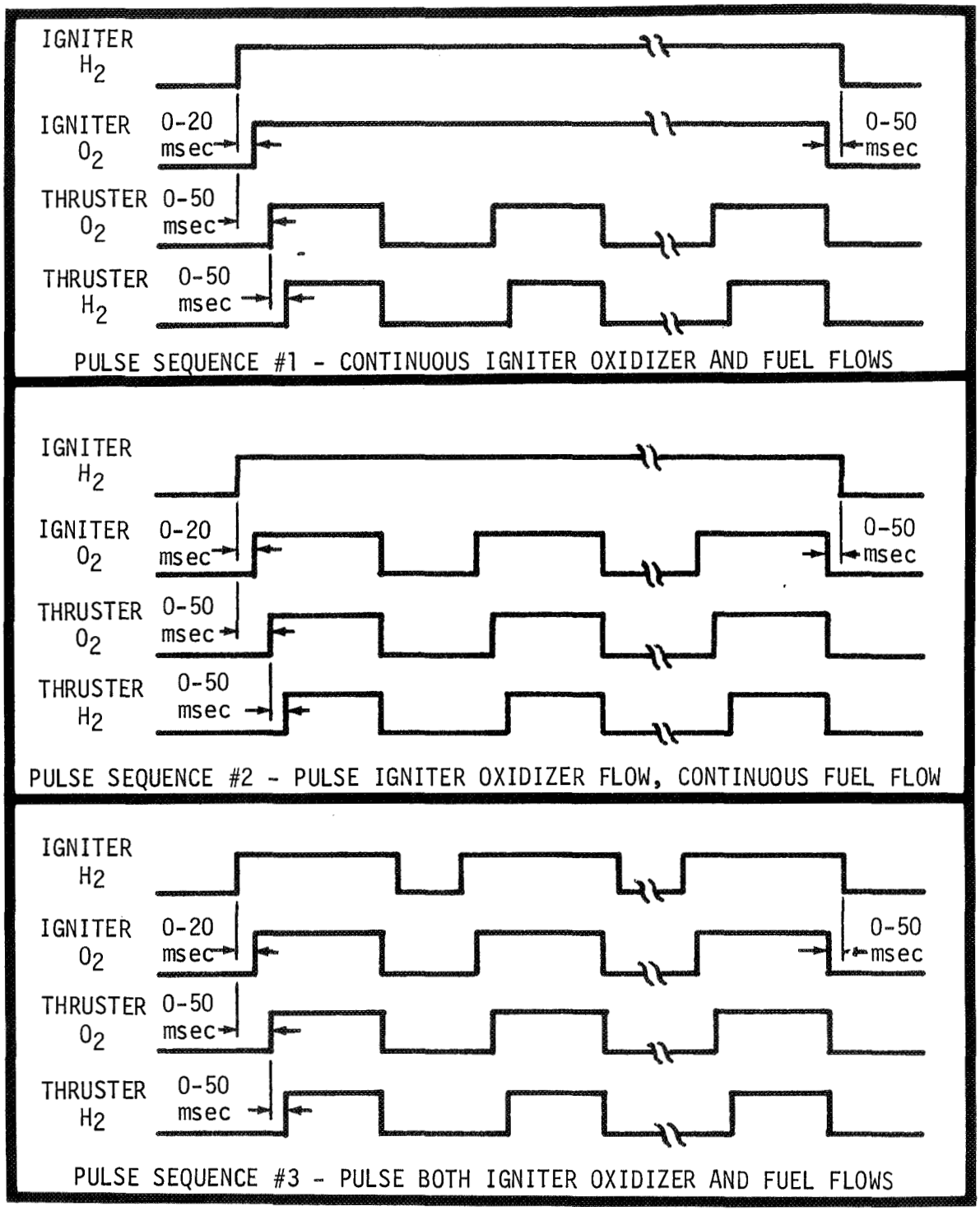

Figure 102. Pulse Mode Valve Sequencing

Table 27. Thruster Pulse Mode Test Data

Run No.	P_c psia	P_c kN/m^2	M.R. O/F	C^* Corr. ft/sec	C^* Corr. m/sec	I_{sp} Corr. lbf sec/lbm	I_{sp} Corr. N sec/kg	Duty Cycle msec on/msec off	Igniter Pulse Sequence	O_2 Lead msec	T Effluent °F	T Effluent °K	Comments
C2-1202	11.2	77.2	2.21	6814	2077	362	3550	200/100	(1) continuous O_2, H_2	32	1933	1329	
1203	9.7	66.9	2.38	6869	2094	350	3432	200/100	(3) pulse O_2, H_2	31	2009	1371	Low P_c thruster pulses—required duty cycle with each igniter sequence, varied main O_2 lead time
1204	8.8	60.7	2.30	6248	1904	311	3050	200/100	(2) pulse O_2, cont. H_2	30	2112	1429	
1205	9.9	68.3	2.64	6843	2086	invalid		200/100	(1)	8	2028	1302	
1206	No ignition—reduced igniter effluent temperature							500/500	(1)	7	1832	1273	Second duty cycle, low P_c thruster, minimum O_2 lead, no ignition at TE = 1832°F (1273°K)
1207	9.9	68.3	2.57	6938	2115	368	3609	500/500	(1)	8	1981	1356	
1208	No ignition—reduced igniter effluent temperature							100/100	(1)	9	1882	1301	Third duty cycle, low P_c, no ignition at TE = 1882°F (1301°K)
1209	8.9	61.4	Digital data not available					100/100	(1)	8	1957	1343	
1210	9.2	63.4	Digital data not available					200/100	(1)	9	2076	1409	Repeat first and second low P_c pulse duty cycles
1211	9.9	68.3	Digital data not available					500/500	(1)	10	2062	4001	
1224	92.7	639.1	2.22	7347	2239	381	3736	200/100	(1)	8	2030	1383	High P_c thruster pulses—required duty cycle, varied igniter pulse sequence
1225	104.3	719.1	2.53	7504	2287	398	3903	200/100	(2)	9	1868	1293	
1226	96.7	666.7	2.35	7406	2257	398	3903	150/150	(1)	8	1882	1301	Second duty cycle, high P_c thruster, varied O_2 lead
1227	99.0	682.6	2.47	7238	2206	386	3785	150/150	(1)	30	1825	1269	
1228	108.7	749.5	2.58	7492	2284	399	3913	500/500	(1)	10	1795	1253	
1229	No ignition—reduced igniter effluent temperature							500/500	(2)	10	1308	982	Third duty cycle, high P_c—catalyst bed cooldown during longer igniter O_2 off times (igniter sequences No. 2 and No. 3) resulted in effluent temperatures below ignition limit.
1230	No ignition—reduced igniter effluent temperature							500/500	(3)	9	1372	1018	
1231	No ignition—reduced igniter effluent temperature							500/500	(3)	10	1222	934	
1232	101.4	699.1	2.60	7248	2209	385	3776	500/500	(1)	9	1958	1343	

Tests 1210-1211: These tests were conducted to repeat the first two duty cycles; however, valid performance data were not acquired on these tests because of a malfunction of the digital tape start circuit.

Tests 1224-1225: The high P_c thruster tests were begun with the required pulse duty cycle, 200 msec on/100 msec off. Igniter pulse sequences (1) and (2) were evaluated at a nominal main oxidizer valve lead of 10 msec with satisfactory operation in each case.

Tests 1226-1227: A pulse program of 150 msec on/150 msec off was evaluated as the second high chamber pressure duty cycle. Main oxidizer leads of nominally 10 and 30 msec were evaluated with satisfactory pulse ignitions for each condition.

Tests 1228-1232: The final high P_c pulse duty cycle was 500 msec on/500 msec off. Each of the three igniter pulse sequences were evaluated, and cooldown of the catalyst bed between pulses was found to preclude ignition, except for igniter sequence (1), where both igniter oxidizer and fuel are flowing continuously through the catalyst bed between main thruster pulses and no catalyst bed cooldown occurs.

All valid pulse performance data, both C* and I_{sp}, from Table 27 are displayed in Figures 103 through 106. Also included in these figures are the corresponding theoretical C* and I_{sp} performance values for each chamber pressure level.

Computer plotted chamber pressure and thrust traces are shown in Figure 107 for the required duty cycle of 200 msec on/100 msec off performed with the high chamber pressure thruster. The same thrust trace is shown in Figure 108, but the thrust cell output has been electronically filtered to remove the thrust stand ringing frequency.

Figure 109 is a thrust output trace recorded during pulse operation of the low pressure thruster. This trace also has been filtered, as described above. The thrust level of about 16 lbf (71N) indicated for each pulse is the measured value, uncorrected for vacuum cell pressure. With the large exit area of the low pressure thruster, this correction was considerable in magnitude, approximately 3 lbf (13N).

Figures 110 and 111 present simulated thruster pulse data from the TRW computer transient start program. Inputs to this program for these plots included the actual valve response times and thruster manifold volumes from the experimental hardware used for the pulse performance tests. The calculated thrust rise times agree quite well with the actual test data of Figures 107 through 109, which are also superimposed on Figures 110 and 111 for comparison. These thrust response times can be significantly improved at each pressure level by minimizing injector manifold volumes and incorporating a close-coupled bipropellant fire valve, as described in the discussion of flightweight thrusters in Section 6.2 (and illustrated in Figures 118 and 119).

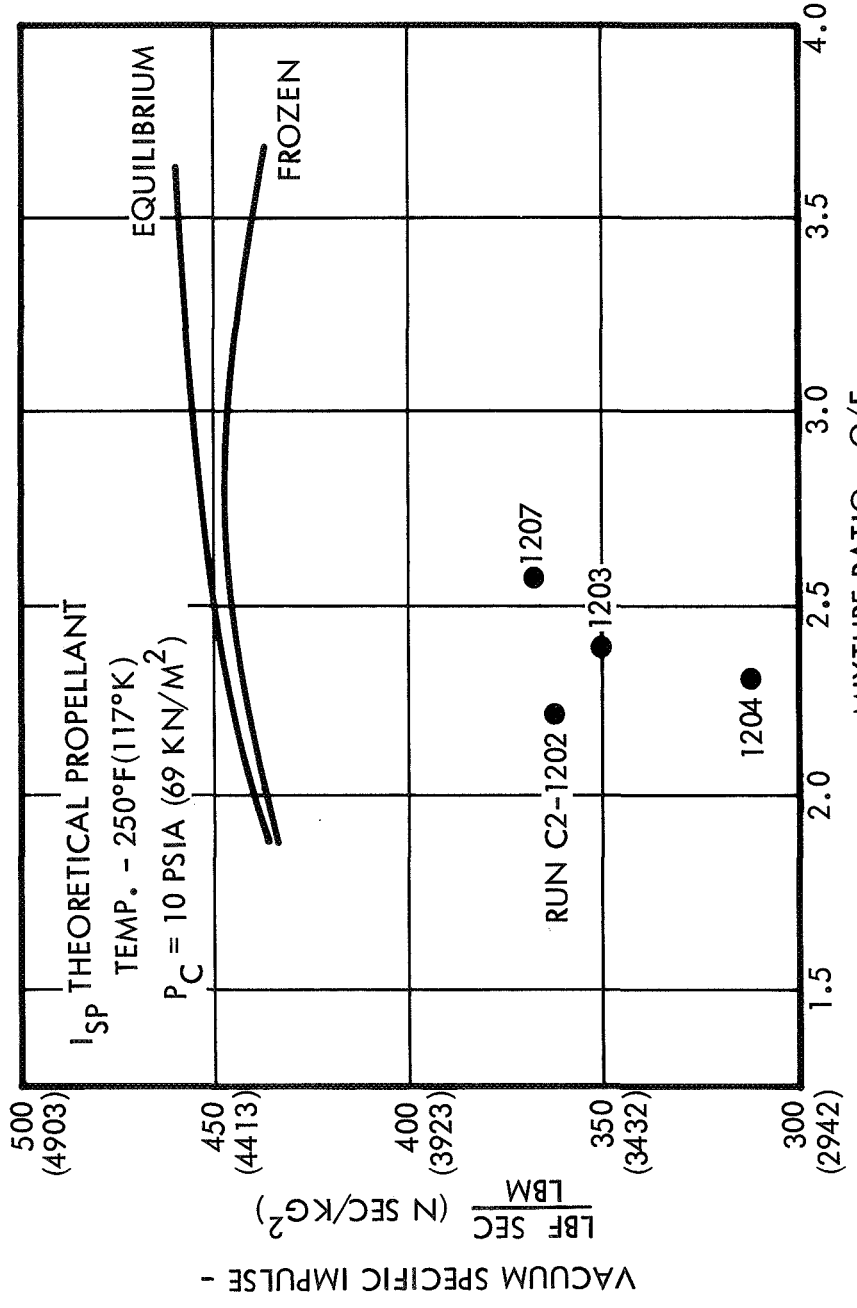

Figure 103. Pulse Mode Impulse Performance—Low P_c Thruster

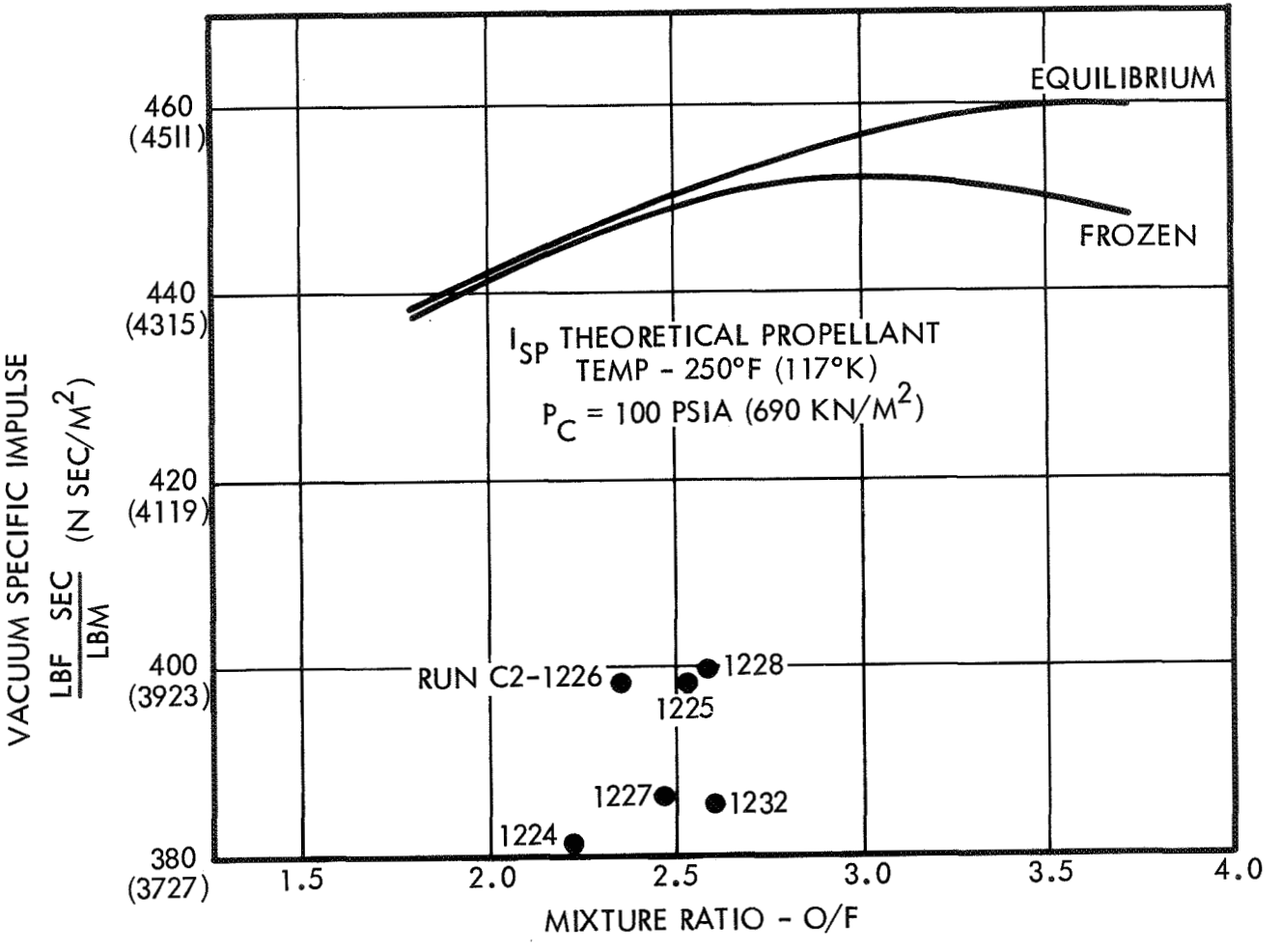

Figure 104. Pulse Mode Impulse Performance—High P_c Thruster

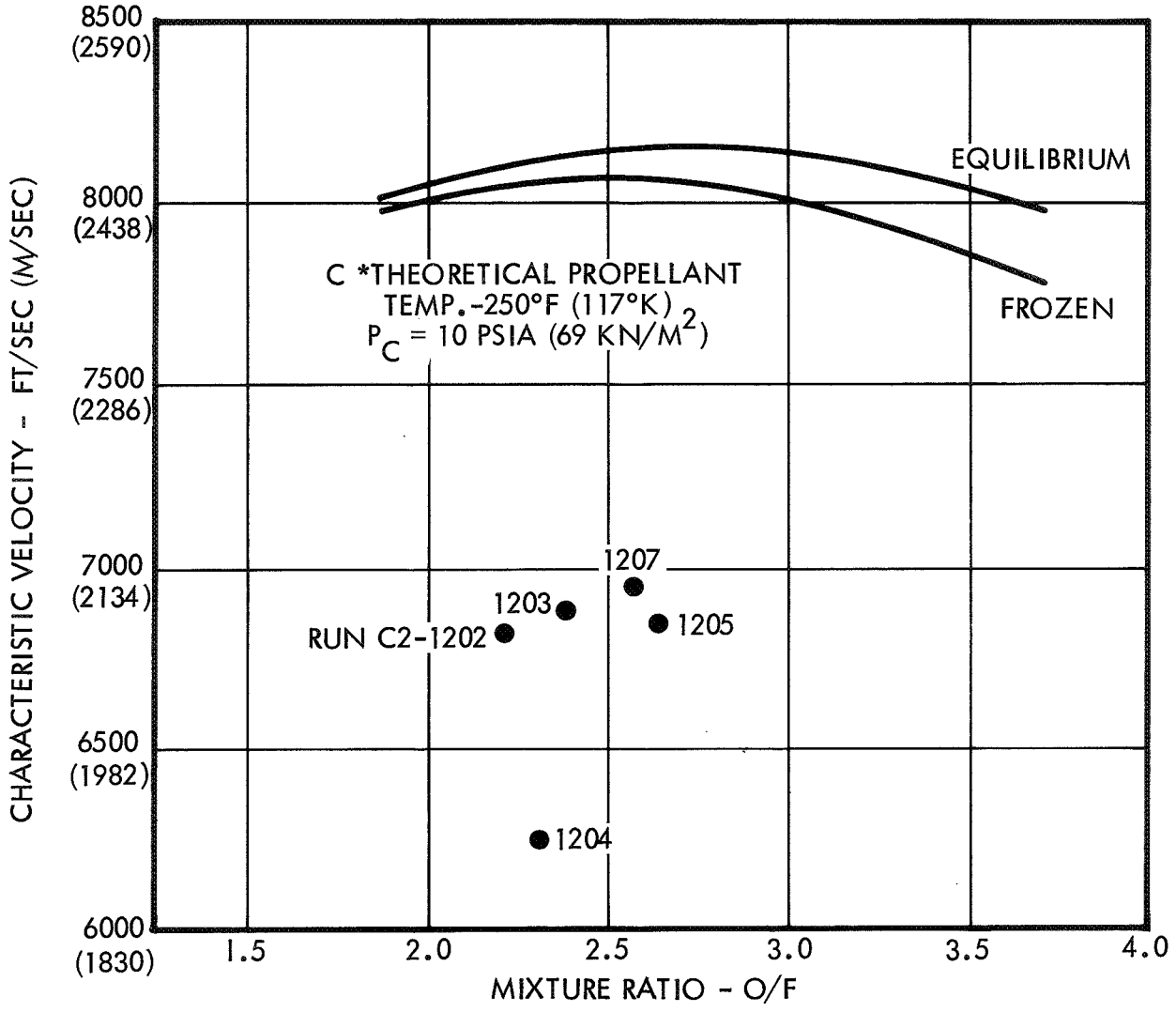

Figure 105. Pulse Mode C* Performance—Low P_c Thruster

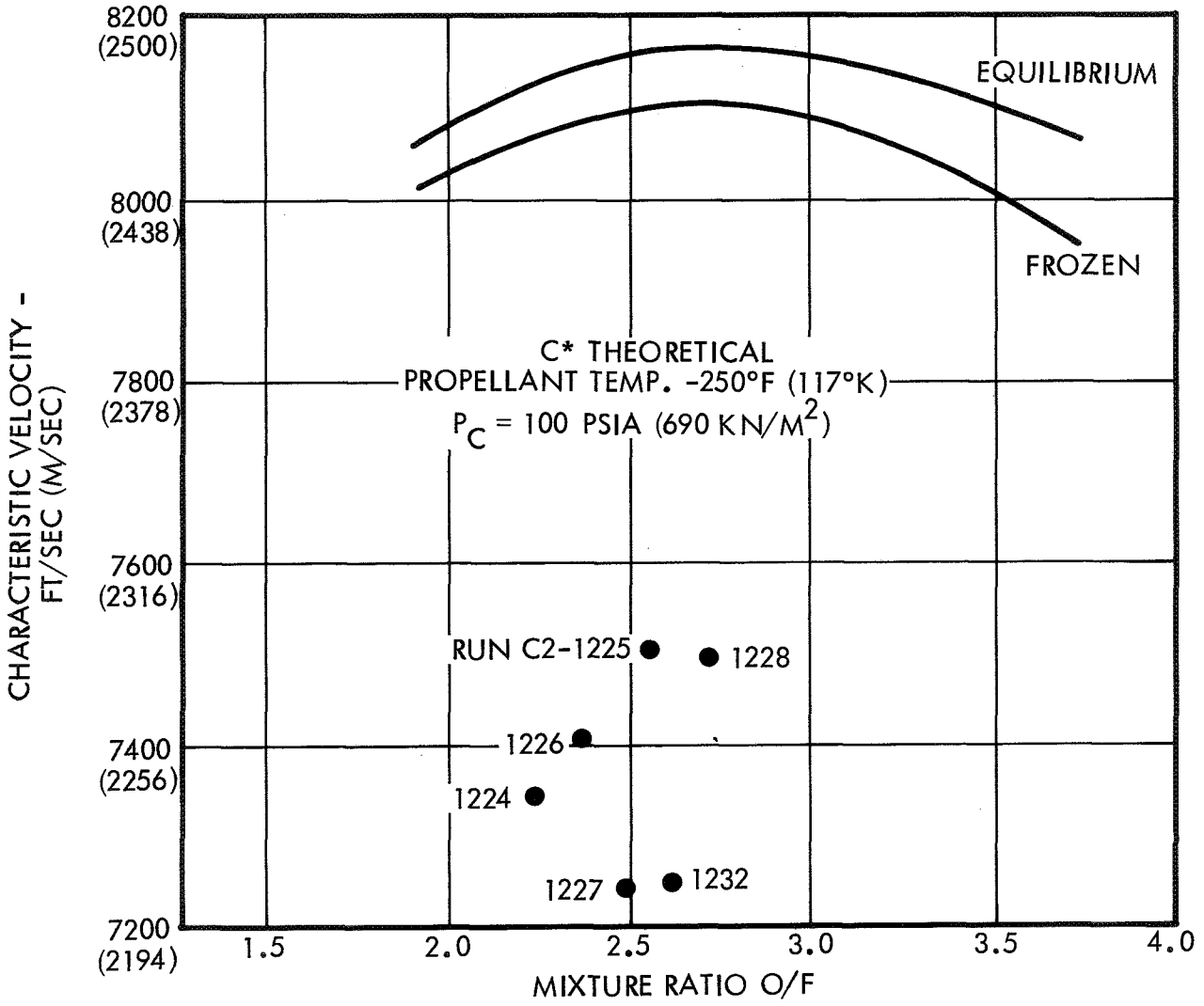

Figure 106. Pulse Mode C* Performance—High P_c Thruster

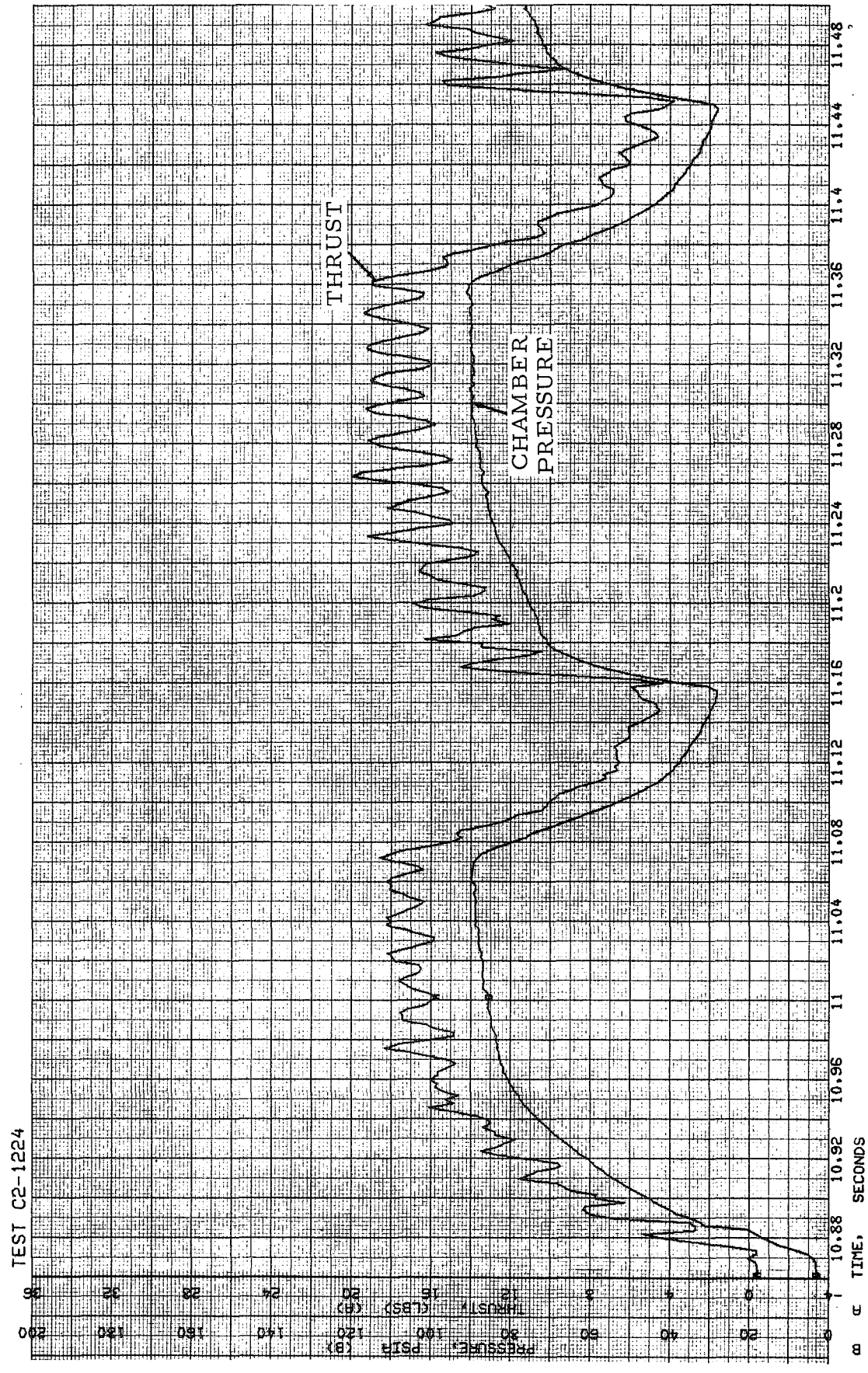

Figure 107. Pulse Mode Thrust and Chamber Pressure—High Pressure Thruster

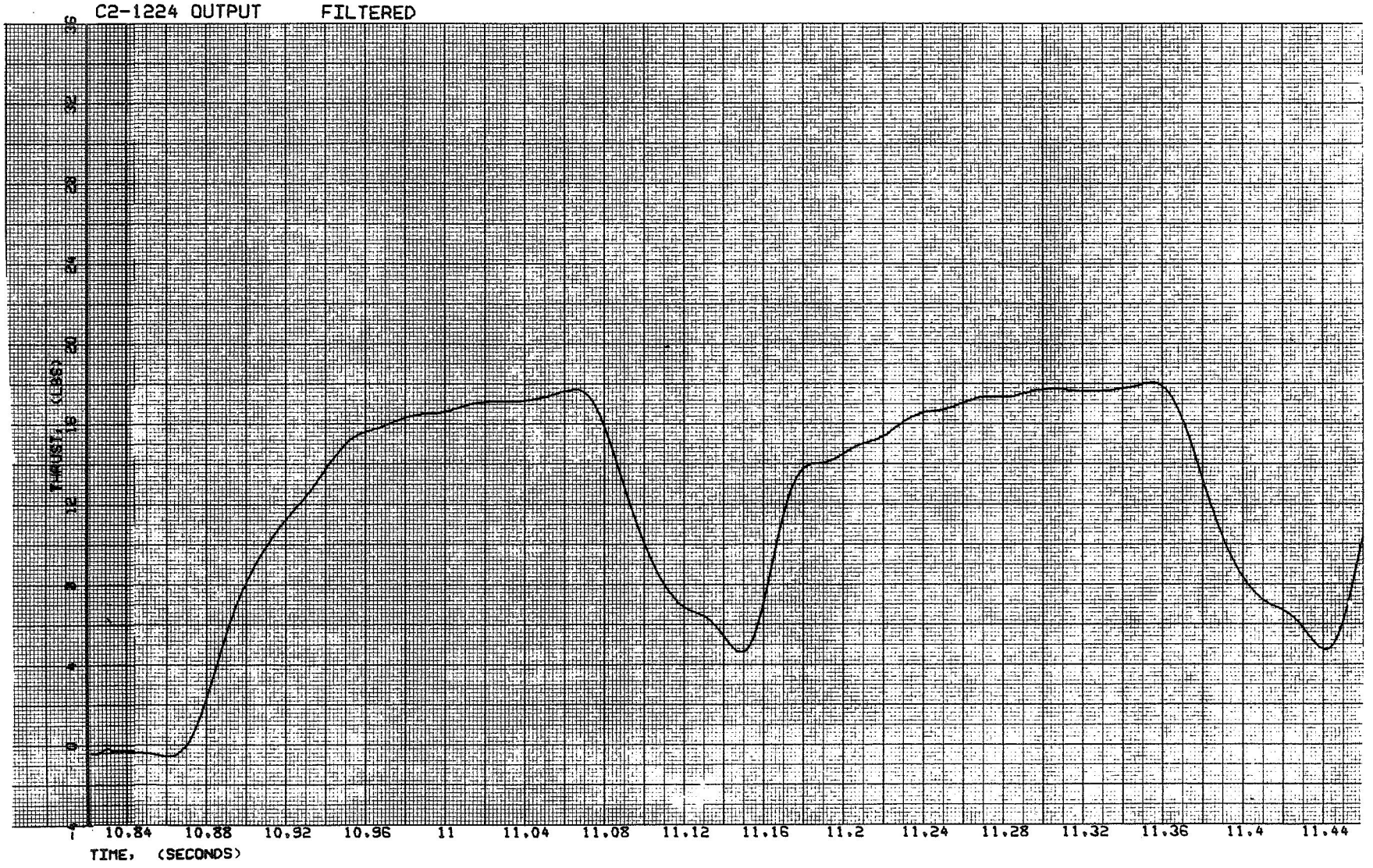

Figure 108. Thrust Trace Filtered to Remove Stand Ringing Frequency— High Pressure Thruster

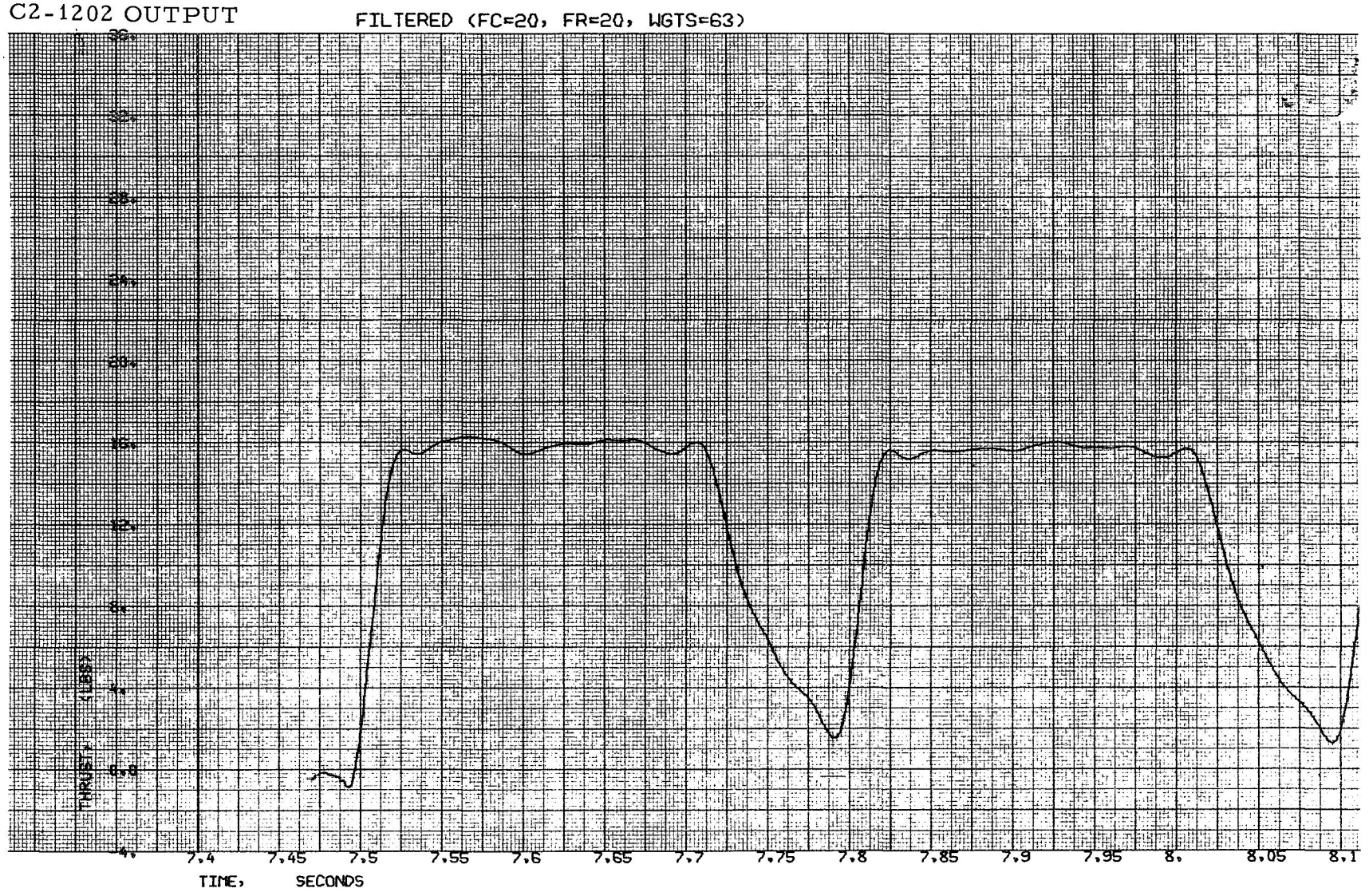

Figure 109. Filtered Thrust Trace— Low Pressure Thruster Pulse Duty Cycle

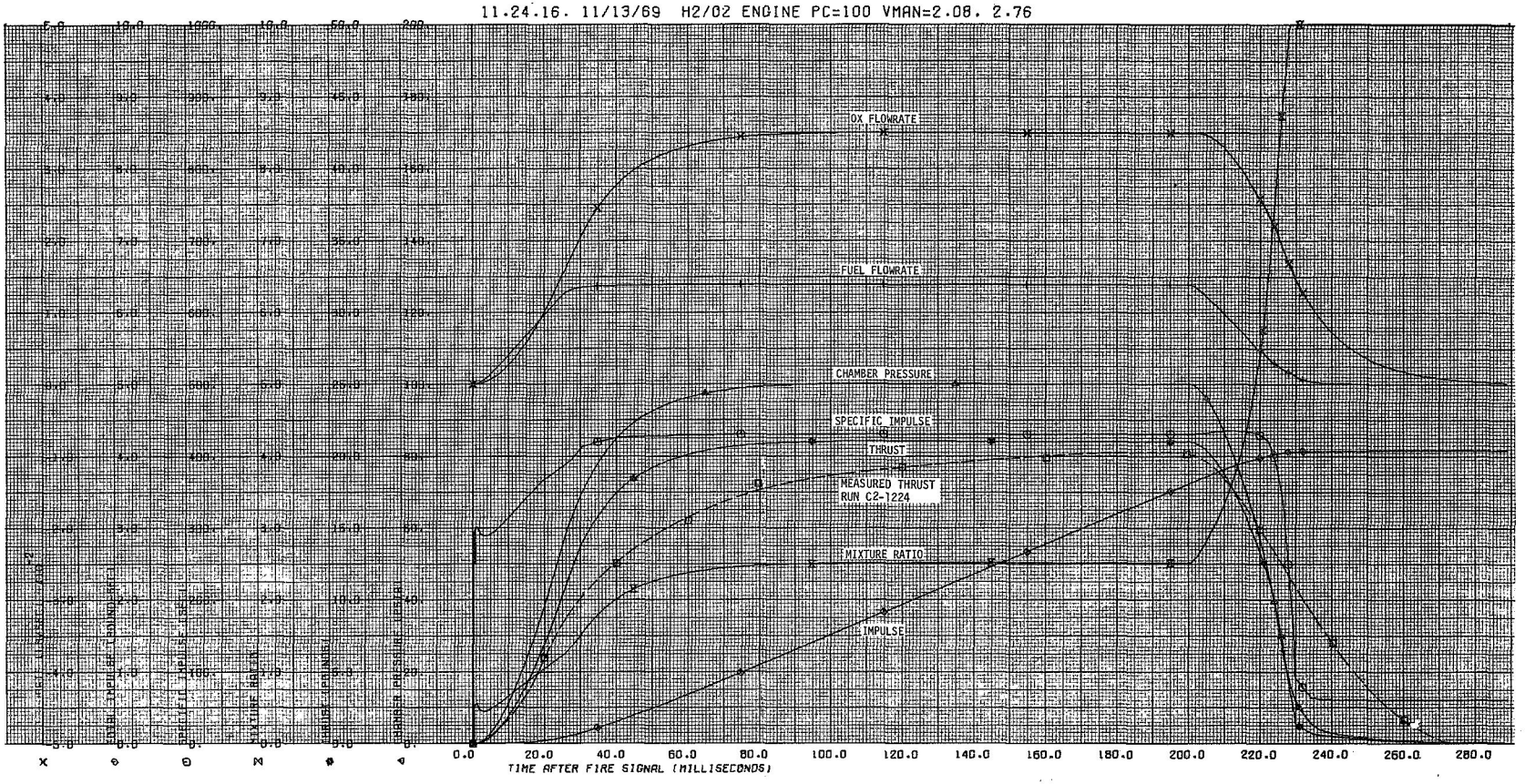

Figure 110. Computer Model for Low P_c Thruster — Actual Propellant Manifold Volumes

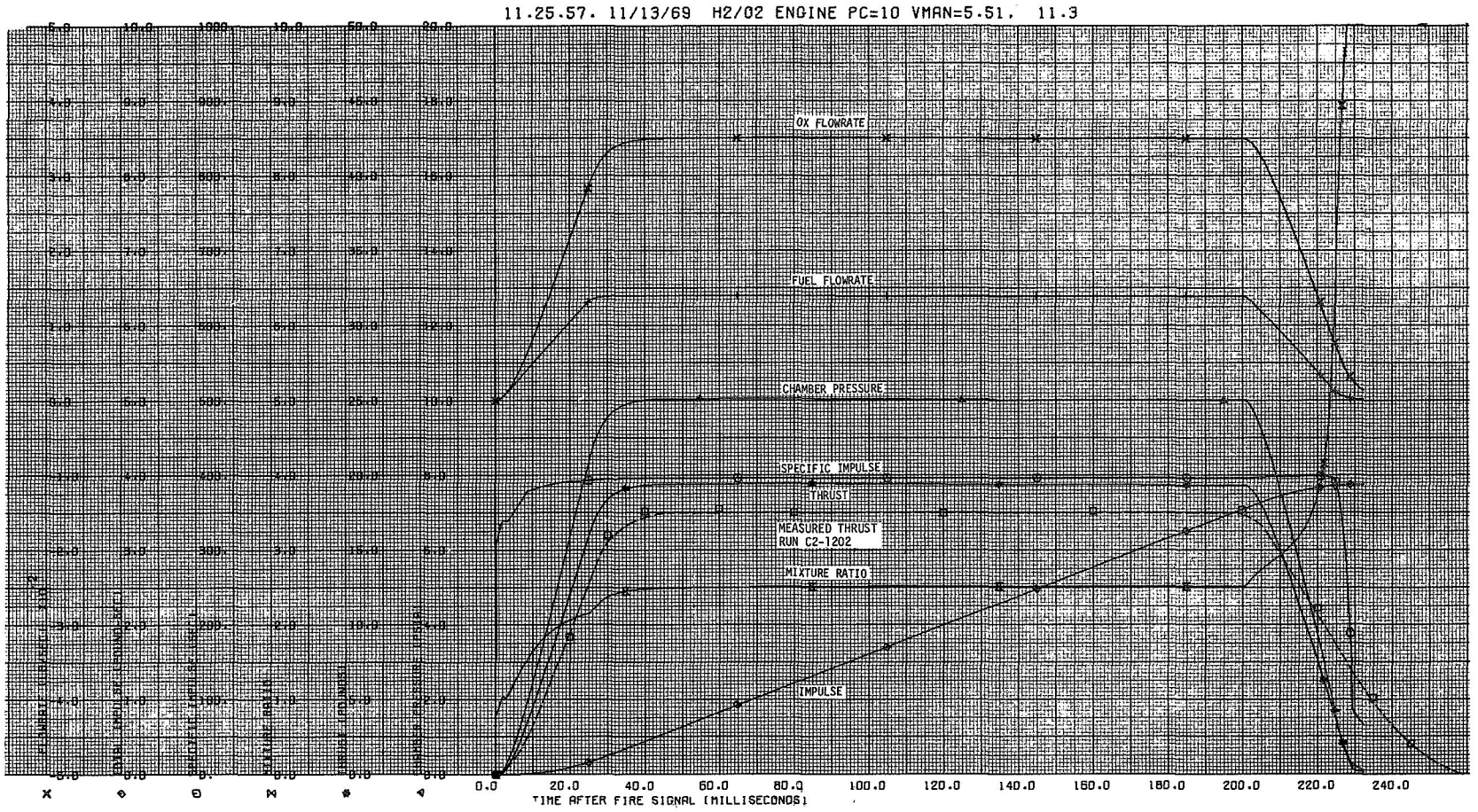

Figure 111. Computer Model for Low P_c Thruster – Actual Propellant Manifold Volumes

Table 28 summarizes the results of the pulse mode duty cycle evaluations. Required test conditions were -250°F (117°K) propellants and (initially) ambient temperature thruster and catalyst bed. Of the different pulse operational sequences evaluated (Figure 102), continuous operation of the igniter (both propellants) resulted in the most consistent pulse repeatability. Termination of igniter oxygen flow between thruster pulses, particularly when low temperature hydrogen flow was continued through the catalyst bed (pulse sequence 2), resulted in bed chilling and led to delayed ignitions as longer off times between pulses were investigated.

5.5.3 Thruster Heat Transfer Evaluations

Chamber temperature measurements obtained with the heat sink hardware were evaluated for both pressure levels at the nominal mixture ratio of 2.5. The total heat loss rate for a 34-second high pressure thruster firing was 23 Btu/sec (5.80 kcal/sec) with 11 Btu/sec (2.77 kcal/sec) chamber loss. The film coefficient at the throat was estimated at 1.98×10^{-3} Btu/in^2-sec-°F (5.79 cal/cm^2 sec-°K).

The total heat loss rate for a 32-second low pressure thruster firing was 14 Btu/sec (3.53 kcal/sec) with 8 Btu/sec (2.02 kcal/sec) chamber loss. The estimated throat film coefficient was 3.1×10^{-4} Btu/in^2-sec-°F (0.907 cal/cm^2-sec-°K). Estimated recovery temperatures of 4340°R (2411°K) for the high pressure thruster and 3700°R (2055°K) for the low pressure thruster are in close agreement with the theoretical values (for 2.5 mixture ratio) presented in Figure 112.

Post-test condition of the thruster/igniter hardware is illustrated by Figures 113 and 114. Except for required catalyst bed configuration changes and modifications to the reactor mixing chamber, the same hardware for each chamber pressure was utilized for all program testing. Steady-state runs of over 30 seconds duration were made with both thrusters.

Table 28. Pulse Mode Test Summary

	Low Pressure Thruster	High Pressure Thruster
Propellant inlet temperatures	-250°F (117°K)	-250°F (117°K)
Initial catalyst bed temperature	ambient	ambient
Pulse duty cycles evaluated	200 msec on/100 msec off[1] 100 msec on/100 msec off 500 msec on/500 msec off	200 msec on/100 msec off[1] 150 msec on/150 msec off 500 msec on/500 msec off
Propellant valve lead/lags	7-32 msec O_2 lead	8-30 msec O_2 lead
Igniter operational modes	1 - constant flow 2 - pulsed O_2 3 - pulsed O_2 and H_2	1,2,3 (same as low pressure)
Pulse mode measured vacuum performance	84% C* theor.[2]	92% C* theor.

(1) Required duty cycle - other duty cycles selected
(2) All low pressure pulse tests performed with .053 in. (.135 cm) fuel gap

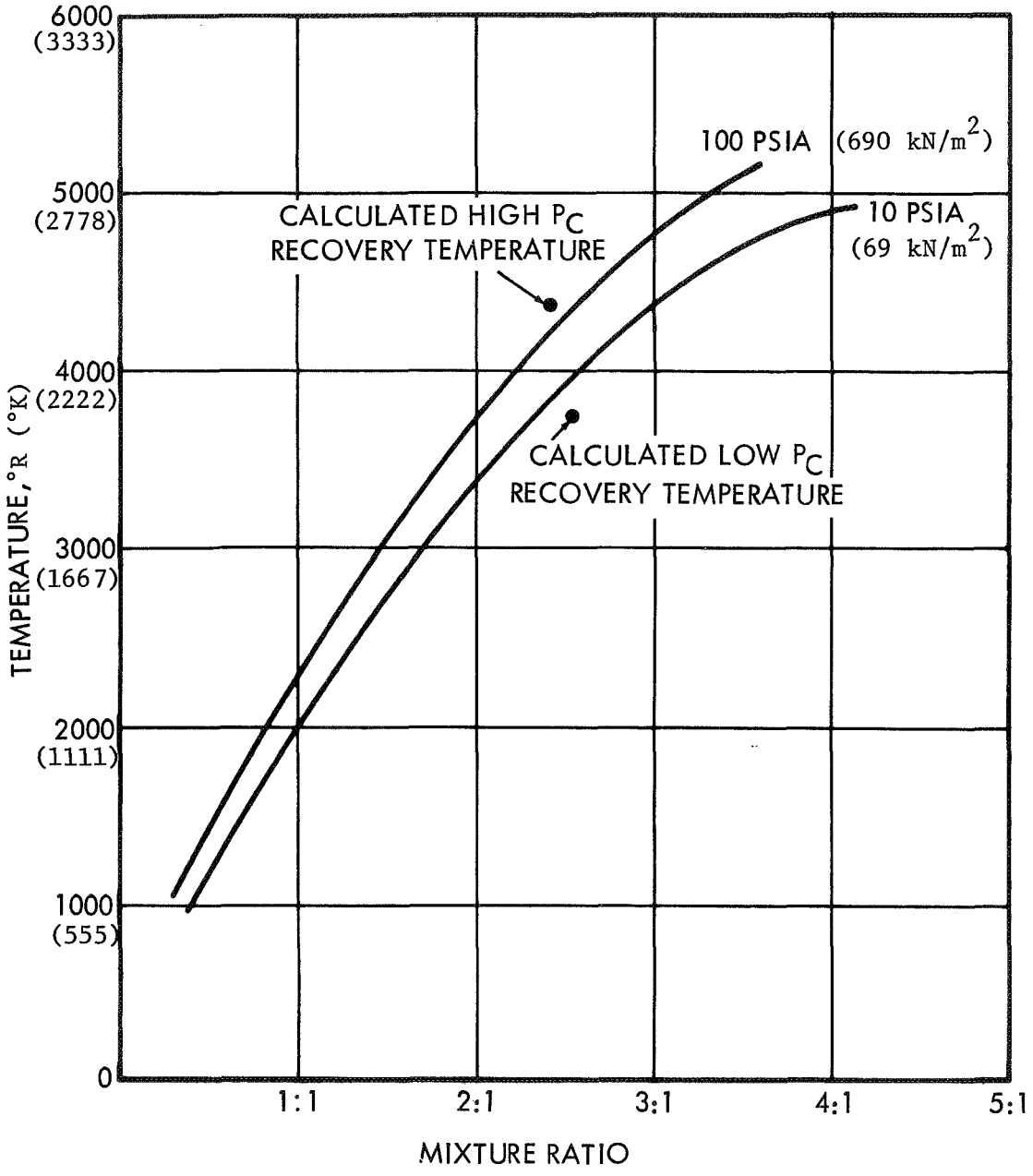

Figure 112. T Versus MR for H_2/O_2 Propellants

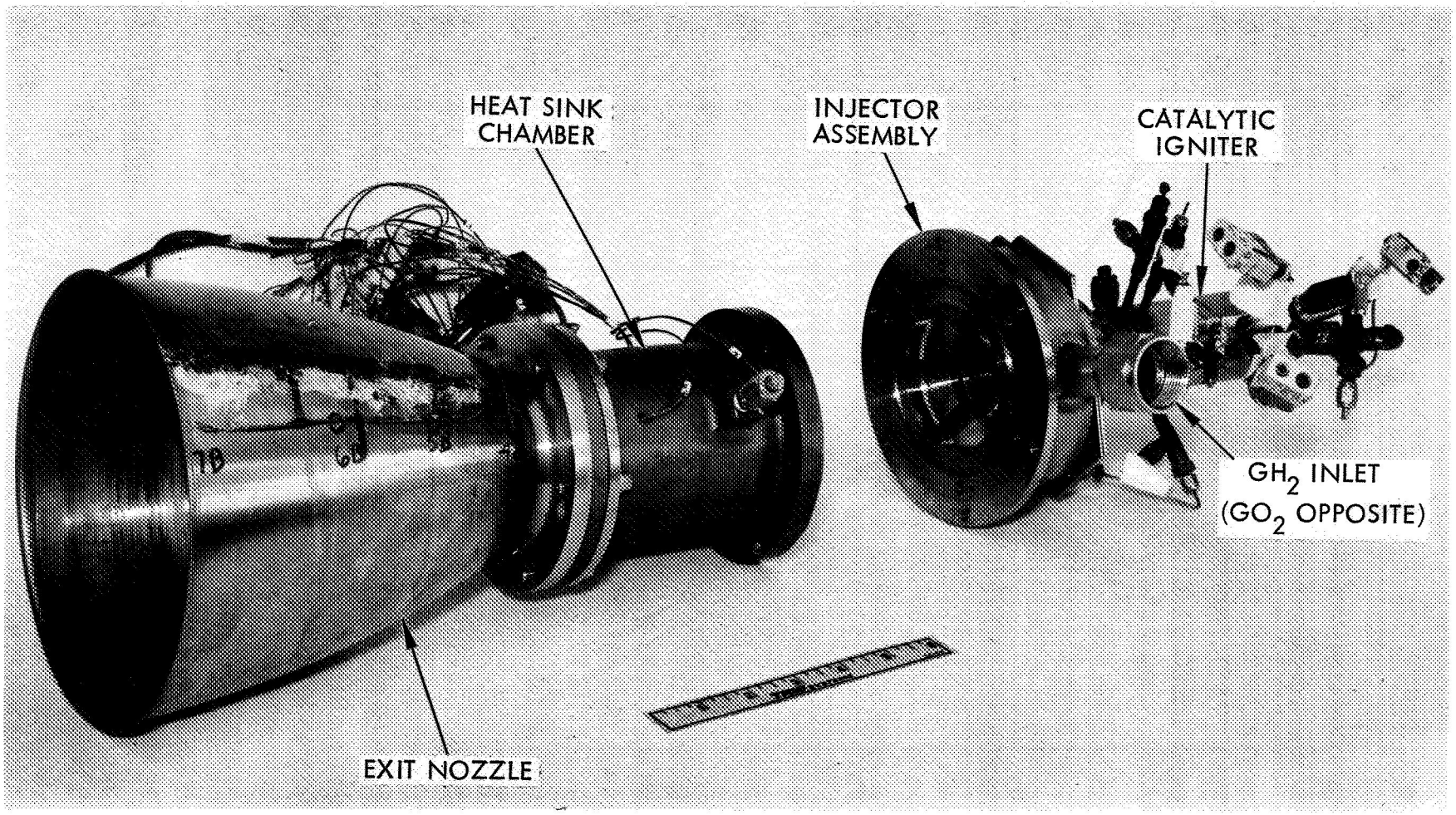

Figure 113. Post-Firing Condition of Low Pressure Thruster/Igniter Hardware

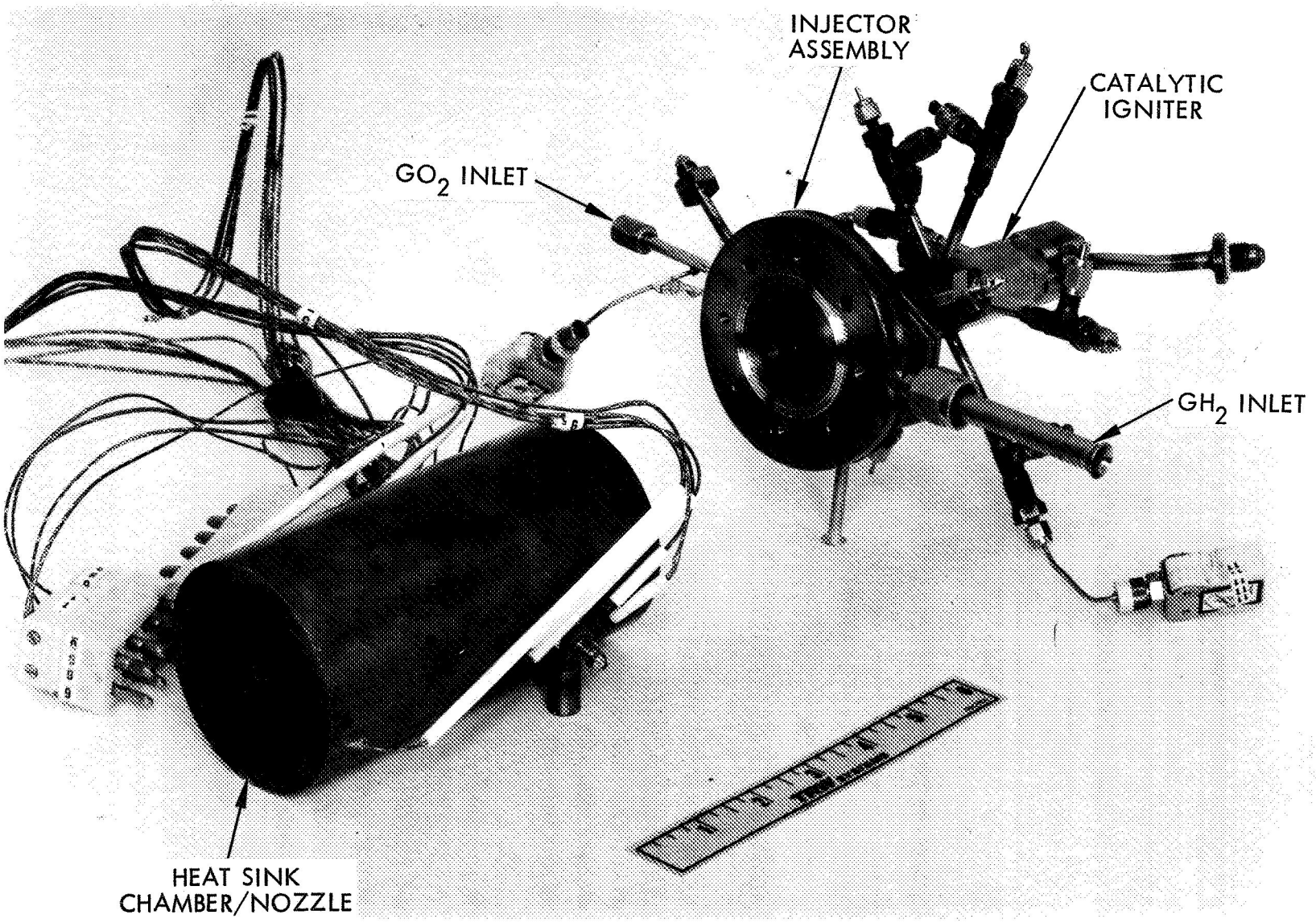

Figure 114. Post-Firing Condition of High Pressure Thruster/Igniter Hardware

6. FLIGHTWEIGHT THRUSTER DESIGN

Data evaluation, analysis and design activities were conducted to define a preliminary 20 lb_f (89N) flightweight thruster design for both the high and low chamber pressure levels. The results of these flightweight design evaluations are presented in the following paragraphs, including overall thruster theoretical performance characteristics, selected thrust chamber thermal operating trends, preliminary valve envelope sizing, and preliminary flightweight thruster design layouts.

6.1 OVERALL THRUSTER PERFORMANCE

The theoretical performance characteristics for these propellants about the nominal 2.5 mixture ratio of interest were presented in Figures 94, 95, 98, and 99 (Section 5.4.2 of this report) for both the 10 (69 kN/m^2) and 100 (69 kN/m^2) psia chamber pressure levels. These figures show the important theoretical equilibrium, frozen, and one-dimensional kinetic performance values for each subject thruster over the mixture range of interest (O/F = 1.5 to 3.5 with ambient temperature gaseous propellants). The calculated kinetic performance can be seen to follow closely the frozen performance trends, with predicted maximum I_{sp} values occurring at approximately the nominal mixture ratio of 2.5 for both chamber pressure levels. These data also show the expected shift in the kinetic performance (to higher mixture ratios) with increased chamber pressure. Each of these figures compares the theoretical equilibrium, frozen, and kinetic calculated performance values. The calculated kinetic performance (both C* and I_{sp}) is near maximum at the nominal mixture ratio of 2.5 for both chamber pressure levels.

Delivered thruster performance estimates were made for both the 10 and 100 psia 200 lb_f thrust H_2/O_2 design at the nominal mixture ratio of 2.5 using the following relationship which utilizes one-dimensional kinetic performance data and accounts for the associated nozzle divergence, viscous, and combustion losses by reduced efficiency terms (η_{div}, η_{vis}, η_{comb}, respectively).

$$I_{sp_{delivered}} = I_{sp_{kinetic}} \times \eta_{div} \times \eta_{vis} \times \eta_{comb}$$

Shown in the table below are the preliminary delivered performance estimates for the subject thrusters assuming both 100 percent combustion efficiency and the actual measured combustion efficiencies. The theoretical predicted thruster vacuum specific impulse values shown agree quite well with the experimental data presented earlier in Figures 94 and 98.

Chamber Pressure psia	Chamber Pressure kN/m^2	Mixture Ratio (O/F)	$I_{sp_{kinetic}}$*	η_{div}	η_{vis}	Estimated Delivered I_{sp} (sec)			
						η_{comb}	I_{sp}	η_{comb}	I_{sp}
10	69	2. 5	460. 8	0. 985	0. 955	1. 00	433. 5	0. 90	390. 1
100	690	2. 5	465. 8	0. 985	0. 965	1. 00	442. 7	0. 95	420. 6

*One-dimensional, 20° Nozzle, ϵ = 40:1

6. 1. 1 Nonuniform/Zonal Mixture Ratio Effects

With the gaseous propellant thruster designs, it is anticipated that reduced combustion efficiencies are caused primarily by nonuniform (zonal) mixture ratio effects. Intentional radial mixture ratio biases are, in many cases, required from the standpoint of resultant thrust chamber durability considerations. Analyses of these factors, as they affect delivered thruster performance, can be accomplished by available multizone computer programs based on the simplified stream-tube approach.

A stream tube approach can be undertaken wherein the overall I_{sp} is a summation of the weighted stream tube I_{sp}, i. e. , :

$$I_{sp} = \sum_i \frac{\dot{m}_i}{\dot{m}_T} \cdot I_{sp,\, i} \qquad (6)$$

where:

$\dot{M}_i/\dot{m}_T$ = Fraction of total flow rate in ith stream tube

I_{sp}, i = Specific impulse of ith stream tube

Zonal performance calculations were conducted to assess, on a theoretical basis, the magnitude of these nonuniform mixture ratio effects. The 100 psia (690 kN/m^2) chamber pressure one-dimensional kinetic performance data were used for these calculations (assuming a simplified two-zone expansion model), since the requirement for chamber wall environment control increases directly with operating chamber pressure. The results of these calculations are shown below for the case where the overall thruster mixture ratio is maintained constant at 2. 5 (O/F) and for a wall zone (zone 1) mixture ratio of 1. 5, which represents a theoretical reduction of the effective wall zone gas temperature of approximately 1200°R (667°K).

$\frac{\dot{\omega}_{zone\ 1}}{\dot{\omega}_{total}}$	$O/F_{overall}$	$O/F_{zone\ 1}$	$O/F_{zone\ 2}$	Estimated* Delivered I_{sp} (sec)	$\frac{I_{sp}}{I_{sp_{O/F\ =\ 2.5}}}$
0	2.5	2.5	2.5	465.8	1.00
20	2.5	1.5	2.9	462.4	0.993
30	2.5	1.5	3.2	459.2	0.987

*Assuming only zonal combustion/expansion losses

The resultant performance losses caused by zonal effects are seen to be quite small for the above selected operating conditions at the nominal thruster mixture ratio of 2.5.

6.2 PRELIMINARY FLIGHTWEIGHT DESIGNS

Preliminary designs for the flightweight thrusters, based on the results of these investigations, are shown in Figures 115 and 116. Both thruster designs are shown employing columbium alloy radiation cooled thrust chambers. An overall envelope of the associated thruster bipropellant valving is shown on these preliminary designs to permit assessment of overall thruster envelope and resultant thruster interfaces.

6.2.1 Flightweight Thruster Thermal Analyses

Thermal analyses were conducted to define the thermal operating characteristics of the selected radiation cooled chamber designs for both the 10 psia (69 kN/m^2) and 100 psia (690 kN/m^2) chamber pressure levels. Primary emphasis of the analyses was to define the operating temperatures of the critical throat region since peak operating temperatures, which occur at this location, determine resultant overall thrust chamber durability. The primary variables evaluated during this analysis were throat station wall thickness and wall zone combustion gas temperature. Heat transfer coefficients for both the high and low chamber pressure designs were calculated using the Bartz simplified techniques with no correction for either recombination or relaminarization.

The primary results of these thermal analyses are shown in Figure 117 for both chamber pressures and a constant wall thickness of 0.3 inch (0.76 cm). The indicated wall thickness is very near optimum for both thruster designs. One can see from Figure 117, that at the nominal engine mixture ratio of 2.5, the low and high chamber pressure thruster designs have computed throat wall operating temperatures of approximately 2550°R (1417°K) and 3720°R (2067°K), respectively.

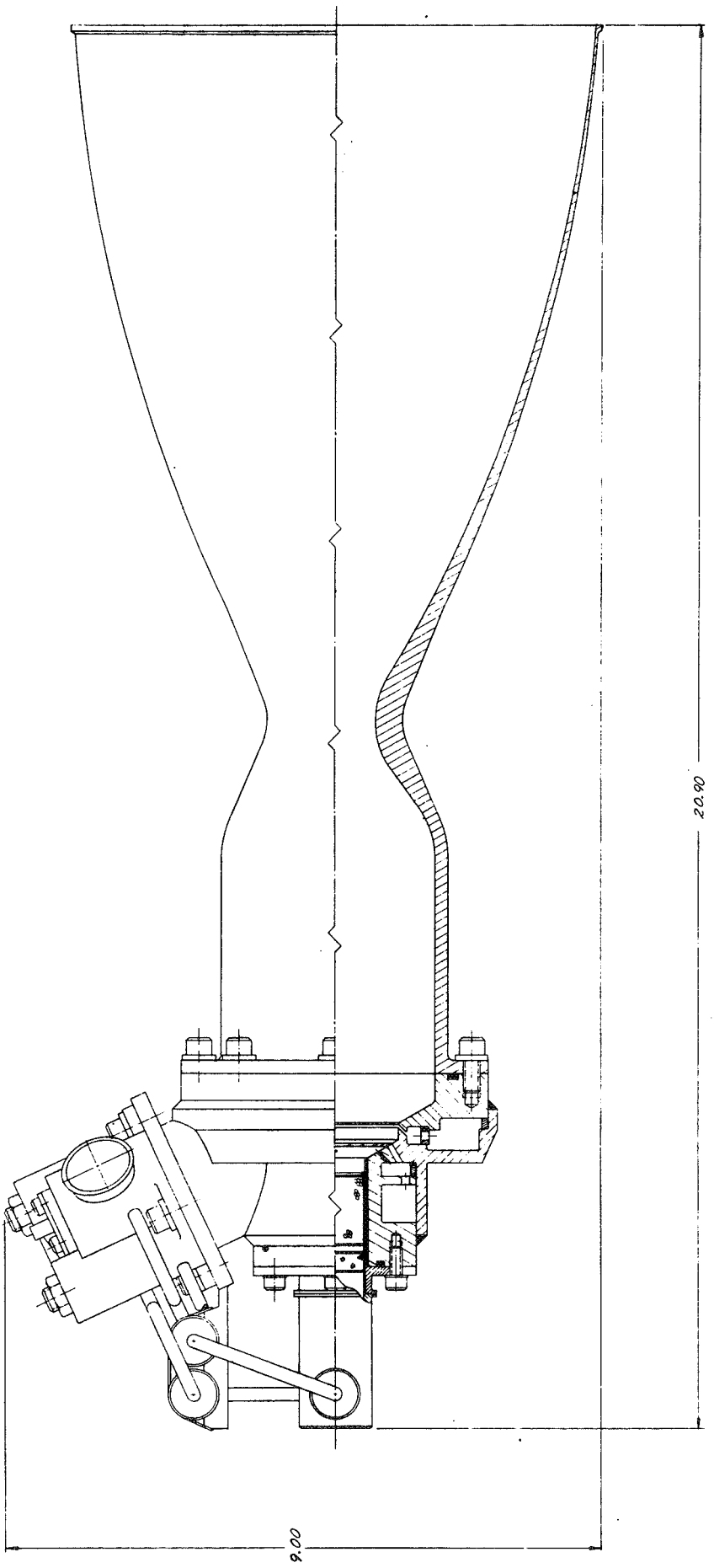

Figure 115. Preliminary Flightweight Thruster Design—Low Chamber Pressure

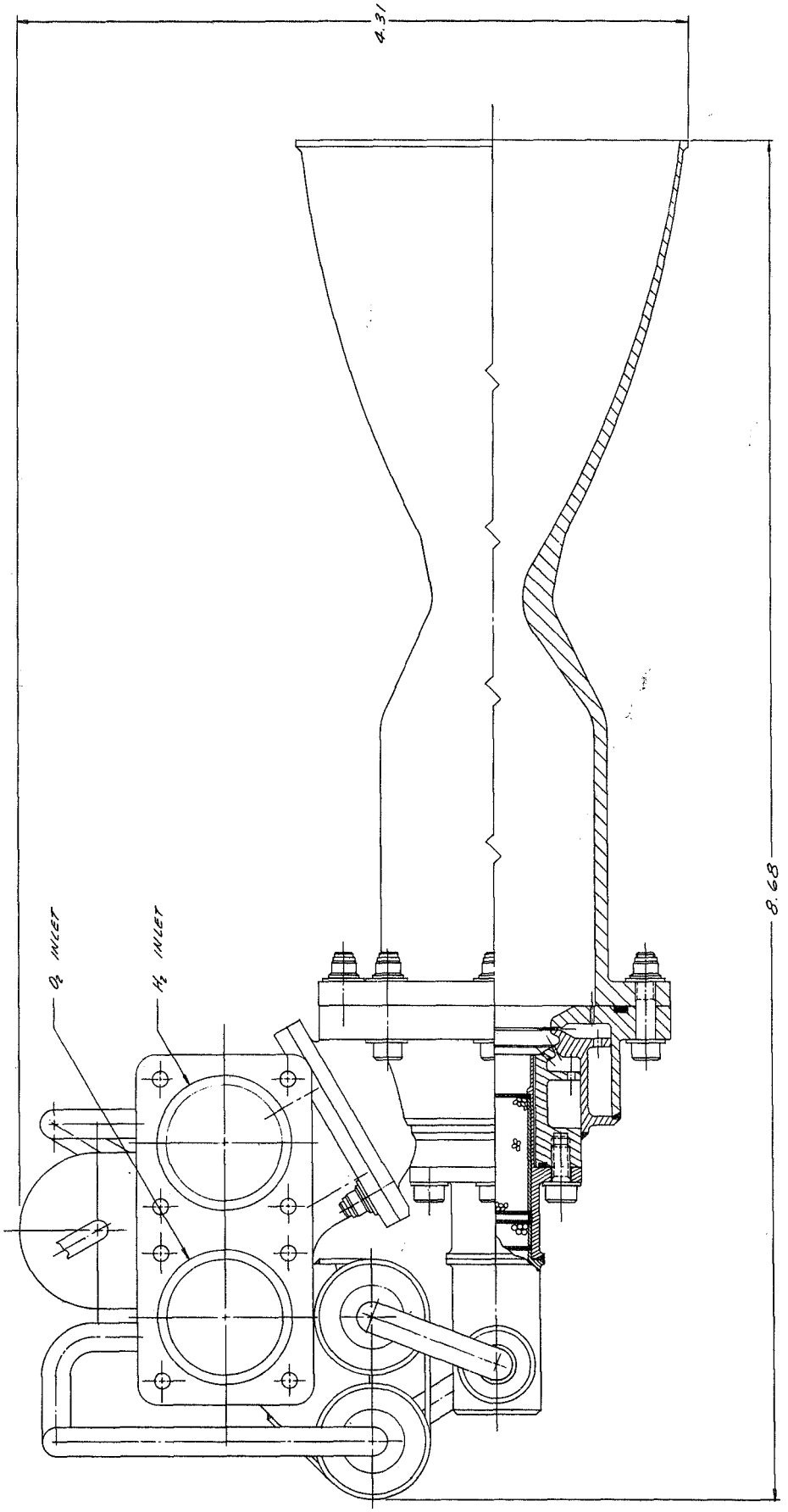

Figure 116. Preliminary Flightweight Thruster Design—High Chamber Pressure

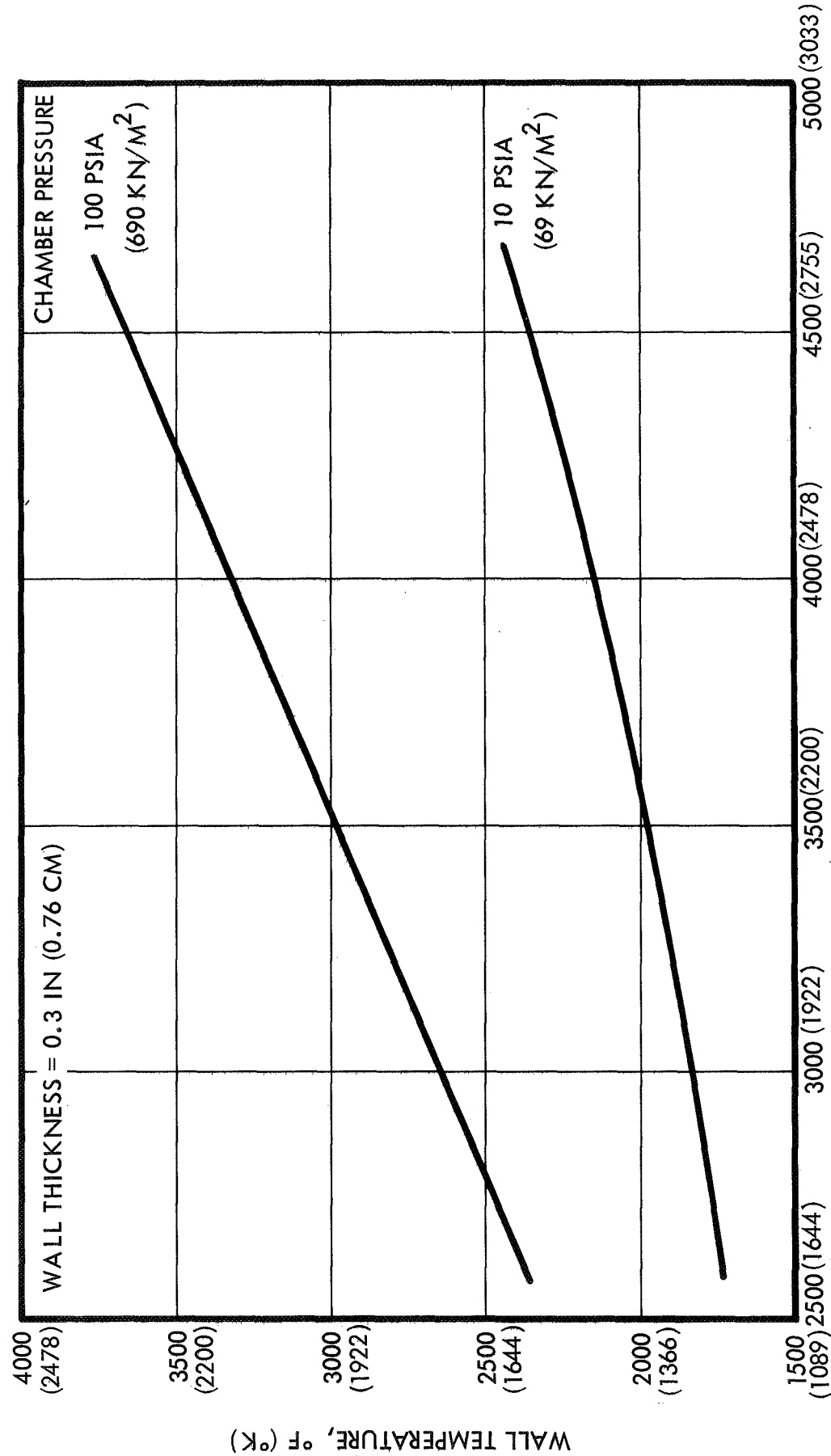

Figure 117. Combustion Chamber Wall Temperature—Flightweight Thruster Design

The allowable wall operating temperatures for the selected refractory metal (columbium) radiation cooled thrust chamber design is determined by the durability characteristics (temperature/life trends) of the oxidation protection coating employed. State-of-the-art silicide coatings, employed on similar thruster designs with the earth storable propellants, have experimentally demonstrated 9-10,000 second durability at steady-state wall temperatures of 3130°R (1739°K). With this data, and the results shown in Figure 117, one can predict the required wall environmental control for both chamber pressure levels. No wall environment control is required for the 10 psia (69 kN/m^2) thruster design at the nominal 2.5 mixture ratio. The 100 psia (690 kN/m^2) thruster requires, to meet the above wall operating temperature constant, reduction in the wall zone mixture ratio from the nominal of 2.5 to approximately 1.85, equivalent to an effective wall zone gas temperature of 3500°R (1944°K). The zonal performance loss associated with this reduced (O/F = 1.85) wall zone mixture ratio are estimated to be approximately 0.5 percent. Higher temperature oxidation protection coating systems for the refractory metals have been evaluated by TRW Systems and other investigators and would permit higher wall operating temperatures, thus removing the necessity of wall environment control for the 100 psia (690 kN/m^2) chamber pressure design at the nominal 2.5 thruster mixture ratio.

6.2.2 Flightweight Thruster Pulse Mode Operational Characteristics

In the preliminary design of the flightweight thrusters shown in Figures 115 and 116, analyses were made of the various injector design factors which have a critical influence on pulse mode performance as well as overall thruster response. Of primary importance are the respective injector manifold volumes and the ratio of the oxidizer/fuel manifold volumes. The basic injector manifold volumes determine, from fill time requirements, the overall thruster response characteristics. The ratio of the oxidizer and fuel manifold volumes are important for the maintenance of nominal thruster mixture ratio during start and shutdown transients, and thus critically affect the resultant pulse mode performance.

A thruster pulse simulation digital computer program was employed to establish the optimal oxidizer/fuel manifold volumes for maximum pulse mode performance. Figures 118 and 119 present the first computer printout data for each chamber pressure thruster. Both of these computer simulations indicate constant propellant mixture ratio during the entire pulse, including start and shutdown transients, resulting in maximum overall impulse performance. Using this same pulse simulation computer program, similar analyses may be readily conducted to include actual propellant valve response characteristics as well as the primary thruster/igniter interactions.

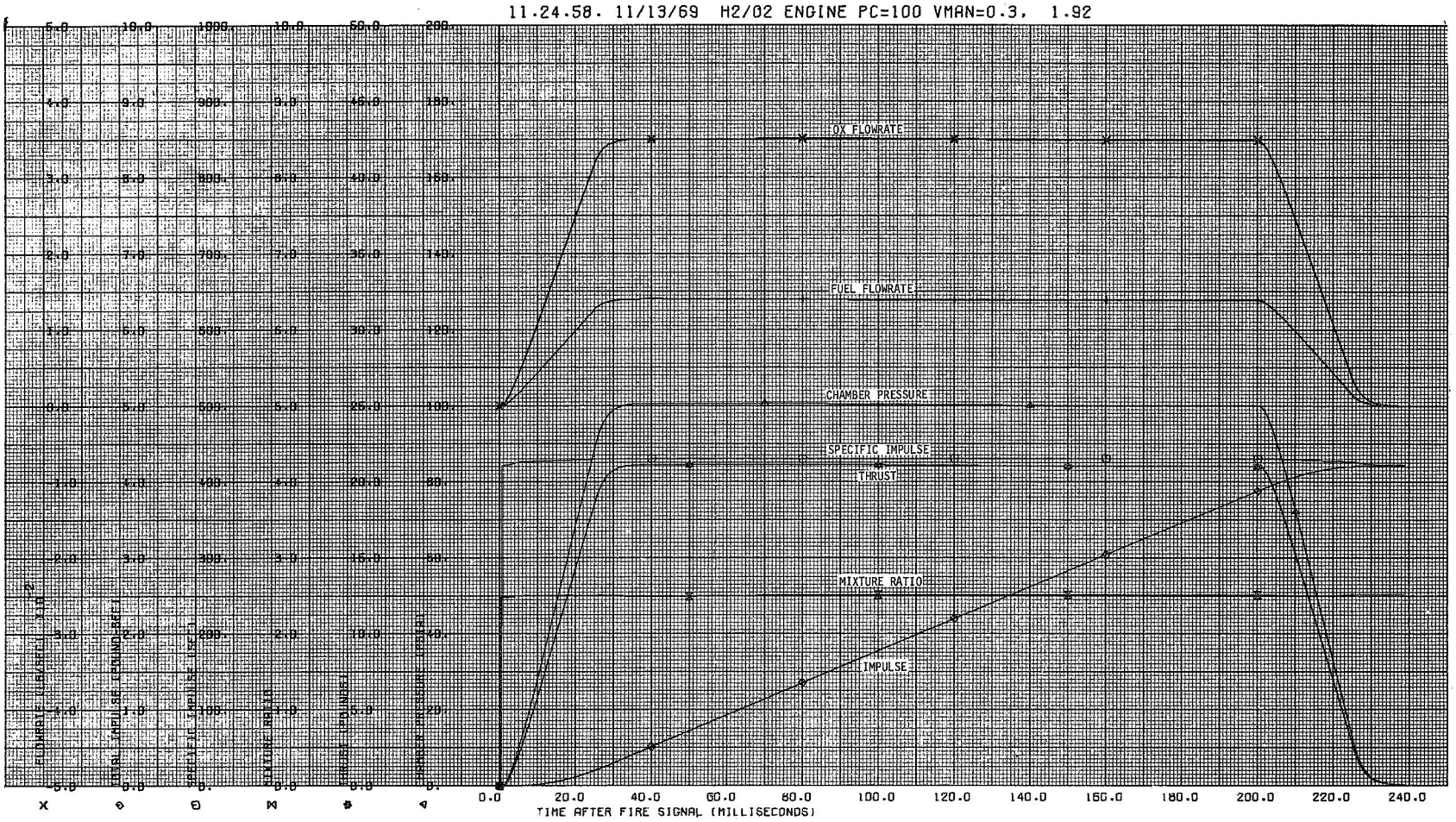

Figure 118. Transient Analysis for High P_c Flightweight Thruster — Optimum Propellant

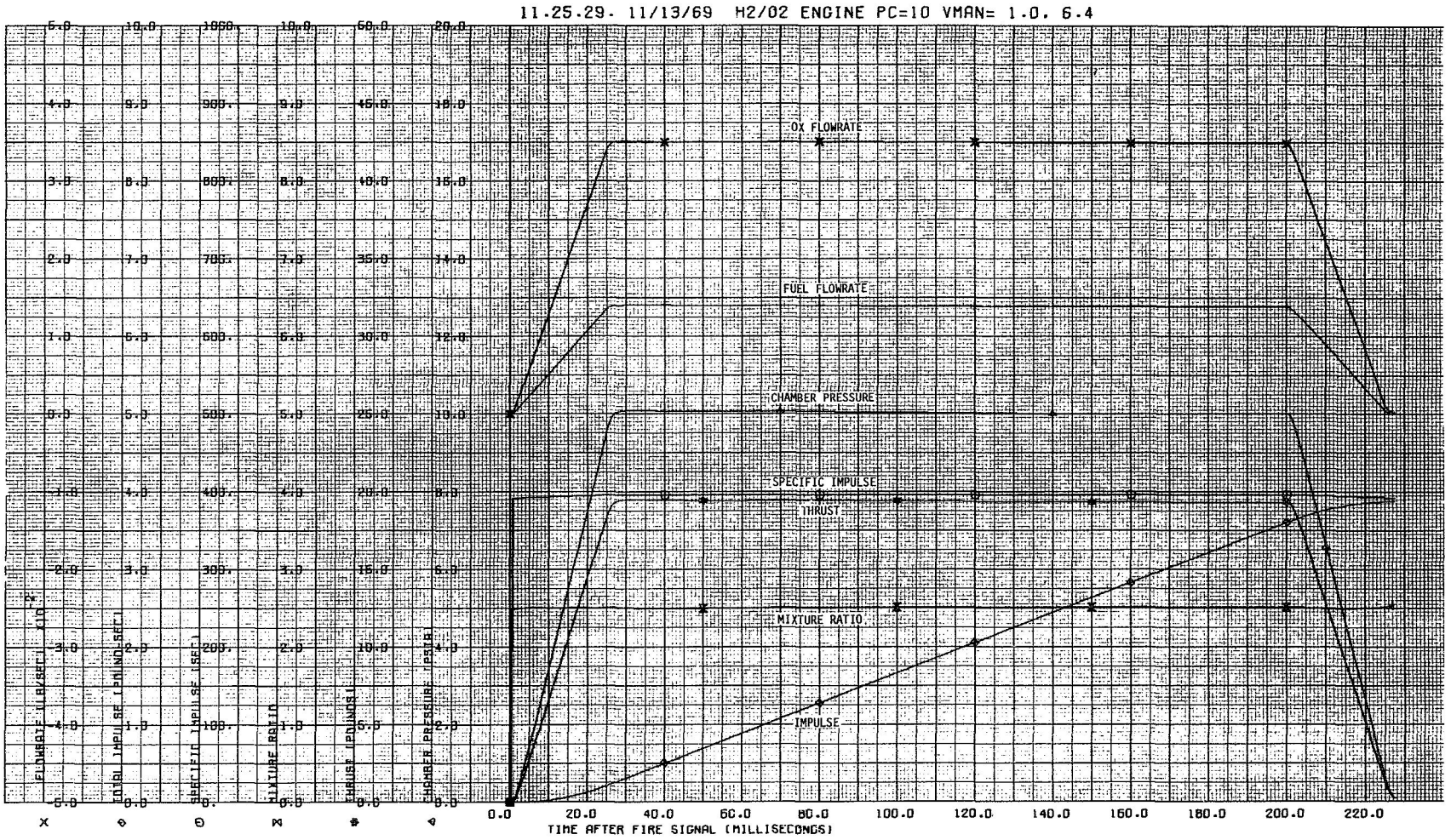

Figure 119. Transient Analysis for Low P_c Flightweight Thruster—Optimum Propellant Manifold Volumes

7. CONCLUDING REMARKS

The experimental evaluations conducted during this program included laboratory investigations of catalyst activity, reactor optimization tests, and combined thruster/igniter firings over a wide range of operating conditions. Evaluation and analysis of the data obtained have provided basic design criteria for catalytic pilot bed reactors as described below, and have defined limits of operation for gaseous hydrogen-oxygen thrusters under specific environmental conditions. The following paragraphs summarize the overall results of this program and present recommendations for continued investigation of this thruster concept.

7.1 SUMMARY OF RESULTS

The laboratory investigations of the candidate Shell 405-ABSG and Engelhard MFSA catalyst formulations have indicated the Shell catalyst tested was superior in activity at temperatures below -125°C (148°K), although the Engelhard catalyst was equally as active in promoting H_2-O_2 reaction at -100°C (173°K) or above. Catalyst pretreatment procedures were developed to remove oxygen and to preadsorb hydrogen on the catalyst surface, which were found to be essential in achieving appreciable catalyst activity at temperatures below -25°C (248°K). These pretreatment techniques were also employed during all subsequent test procedures to insure maximum catalyst activity and thus achieve consistent experimental results.

Final selection of a single catalyst type for thruster testing was intentionally deferred until an extensive evaluation of each catalyst had been conducted with reactor hardware capable of igniting a 20 lbf (89N) gaseous hydrogen-oxygen thruster. These tests confirmed the laboratory results—ignition was achieved with the Shell catalyst at temperatures as low as -250°F (117°K), but not with the Engelhard MFSA catalyst below -100°F (200°K). No evaluations were made at intermediate temperatures during this investigation. Exposure to vacuum environments of 10^{-5} mm Hg prior to ignition did not affect the catalyst activity, as indicated by successive reactor response measurements at different vacuum ignition conditions with no changes observed. Helium dilution of up to 10 percent weight in the hydrogen supply was not detrimental to reactor operation with either catalyst. Ignition with ambient temperature propellants was not attained with He-O_2 dilutions exceeding 25 percent by weight with the low pressure reactor, although reaction occurred with 50 percent He-O_2 dilutions at the higher pressure level. Low temperature dilution tests were not successful at He-O_2 dilutions above 5 percent (no intermediate dilutions between 5 and 25 percent He-O_2 were evaluated). Reaction at both pressure levels was attained with catalyst bed lengths from 0.50 to 1.0 inch (1.27 to 2.54 cm) and with igniter flow rates from 2 to 10 percent of nominal thruster flow.

Both steady-state and pulse mode thruster firings were conducted at each chamber pressure with as little as 2 percent of the total propellant flow directed through the igniter. Thruster ignition was attained by injection of pure oxygen directly into the fuel-rich igniter effluent. Minimum

igniter effluent temperature was found to be the primary requirement for thruster ignition, rather than an energy limit. Combustion efficiencies of 95 percent of theoretical equilibrium C* were attained with the high pressure thruster. Efficiencies from 85 to 90 percent of C* theoretical were measured with the low pressure thruster, depending on the fuel injection velocity. These results indicate that further optimization of thruster performance would be beneficial.

7.2 RECOMMENDATIONS FOR FURTHER INVESTIGATIONS

The experimental and analytic results of this program have demonstrated the feasibility of catalytic pilot bed ignition of gaseous hydrogen-oxygen reaction control thrusters.

The following activities are suggested for further investigation of hydrogen-oxygen reaction control thrusters:

- Analysis and design of flightweight thrusters for each pressure level, including evaluation of a number of chamber cooling concepts
- Performance optimization tests of flight prototype thrusters at each pressure level, and over a range of operating conditions
- Durability demonstrations of each thruster — both steady-state and pulse mode extended duration firings.

DISTRIBUTION

Report Copies R	D	Recipient	Designee
		National Aeronautics & Space Administration Lewis Research Center 21000 Brookpark Road Cleveland, Ohio 44135	
1		Attn: Contracting Officer, MS 500-313	
5		Liquid Rocket Technology Branch, MS 500-209	
1		Technical Report Control Office, MS 5-5	
1		Technology Utilization Office, MS 3-16	
2		AFSC Liaison Office, MS 4-1	
2		Library	
1		Office of Reliability & Quality Assurance, MS 500-111	
1		D. L. Nored, Chief, LRTB, MS 500-209	
3		P. N. Herr, Project Manager, MS 500-209	
1		E. W. Conrad, MS 500-204	
2		Chief, Liquid Experimental Engineering, RPX Office of Advanced Research & Technology NASA Headquarters Washington, D. C. 20546	
2		Chief, Liquid Propulsion Technology, RPL Office of Advanced Research & Technology NASA Headquarters Washington, D. C. 20546	
1		Director, Launch Vehicles & Propulsion, SV Office of Space Science & Applications NASA Headquarters Washington, D. C. 20546	
1		Chief, Environmental Factors & Herodynamics Code RV-1 Office of Advanced Research & Technology NASA Headquarters Washington, D. C. 20546	

Report Copies R	Report Copies D	Recipient	Designee
1		Chief, Space Vehicles Structures Office of Advanced Research & Technology NASA Headquarters Washington, D. C. 20546	
1		Director, Advanced Manned Missions, MT Office of Manned Space Flight NASA Headquarters Washington, D. C. 20546	
6		NASA Scientific & Technical Information Facility P. O. Box 33 College Park, Maryland 20740	
1		Director, Technology Utilization Division Office of Technology Utilization NASA Headquarters Washington, D. C. 20546	
1		National Aeronautics & Space Administration Ames Research Center Moffett Field, California 94035 Attn: Library	
1		National Aeronautics & Space Administration Flight Research Center P. O. Box 273 Edwards, California 93523 Attn: Library	
1		National Aeronautics & Space Administration Goddard Space Flight Center Greenbelt, Maryland 20771 Attn: Library	Dan Grant
1		National Aeronautics & Space Administration John F. Kennedy Space Center Cocoa Beach, Florida 32931 Attn: Library	Dr. Kurt H. Debus
1		National Aeronautics & Space Administration Langley Research Center Langley Station Hampton, Virginia 23365 Attn: Library	Ed Cartwright, Director
1		National Aeronautics & Space Administration Manned Spacecraft Center Houston, Texas 77001 Attn: Library	J. G. Thiobodaux, Jr Chief, Propulsion & Power Division Norm Chaffee Chester Vaughan

Report Copies R	D	Recipient	Designee
1		National Aeronautics & Space Administration George C. Marshall Space Flight Center Huntsville, Alabama 33812 Attn: Library	Keith Chandler James Thomas Ed Jacobs
1		Jet Propulsion Laboratory 4800 Oak Grove Drive Pasadena, California 91103 Attn: Library	Duane Dipprey
1		Defense Documentation Center Cameron Station Building 5 5010 Duke Street Alexandria, Virginia 22314 Attn: TISIA	
1		Office of the Director of Defense Research &Engineering Washington, D. C. 20301 Attn: Office of Asst. Dir. (Chem. Technology)	
1		RTD (RTNP) Bolling Air Force Base Washington, D. C. 20332	
1		Advanced Research Projects Agency Washington, D. C. 20525 Attn: Library	D. E. Mock
1		Aeronautical Systems Division Air Force Systems Command Wright-Patterson Air Force Base, Dayton, Ohio Attn: Library	D. L. Schmidt Code ARSCNC-2
1		Air Force Systems Command Andrews Air Force Base Washington, D. C. 20332 Attn: Library	Capt. S. W. Bowen SCLT
1		Air Force Rocket Propulsion Laboratory (RPR) Edwards, California 93523 Attn: Library	
1		Air Force Rocket Propulsion Laboratory (RPM) Edwards, California 93523 Attn: Library	

Report Copies R	D	Recipient	Designee
1		Air Force FTC (FTAT-2) Edwards Air Force Base, California 93523 Attn: Library	Donald Ross
1		Air Force Office of Scientific Research Washington, D. C. 20333 Attn: Library	SREP, Dr. J. F. Masi
1		Space & Missile System Organization Air Force Unit Post Office Los Angeles, California 90045 Attn: Technical Data Center	
1		Office of Research Analyses (OAR) Holloman Air Force Base, New Mexico 88330 Attn: Library	Major R. E. Bracken, Code MDGRT
1		U. S. Air Force Washington, D. C. Attn: Library	Col. C. K. Stambaugh, Code AFRST
1		U. S. Army Missile Command Redstone Scientific Information Center Redstone Arsenal, Alabama 35808 Attn: Document Section	Dr. W. Wharton
1		Bureau of Naval Weapons Department of the Navy Washington, D. C. Attn: Library	J. Kay, Code RTMS-41
1		Commander U. S. Naval Weapons Center China Lake, California 93557 Attn: Library	W. F. Thorm Code 4562
1		Picatinny Arsenal Dover, New Jersey 07801 Attn: Library	L. Forsten
1		Propulsion Division Aerojet-General Corporation P. O. Box 15847 Scramento, California 95803 Attn: Technical Library 2484-2015A	R. Stiff
1		Aeronutronic Division of Philco Ford Corp. Ford Road Newport Beach, California 92663 Attn: Technical Information Department	D. A. Carrison Dr. L. H. Linder

Report Copies R	D	Recipient	Designee
1		Aerospace Corporation 2400 E. El Segundo Blvd. Los Angeles, California 90045	J. G. Wilder
1		Astropower Laboratory McDonnell-Douglas Aircraft Company 2121 Paularino Newport Beach, California 92163 Attn: Library	Dr. George Moc Director Research
1		Astrosystems, International 1275 Bloomfield Avenue Fairfield, New Jersey 07007	A. Mendenhall
1		Susquehanna Corporation Altantic Research Division Shirley Highway & Edsall Road Alexandria, Virginia 22314 Attn: Library	Dr. Ray Friedman
1		Beech Aircraft Corporation Boulder Facility Box 631 Boulder, Colorado Attn: Library	Douglas Pope
1		Bell Aerosystems, Inc. Box 1 Buffalo, New York 14205 Attn: Library	T. Reinhardt W. M. Smith F. Herud
1		Bendix Systems Division Bendix Corporation 3300 Plymouth Street Ann Arbor, Michigan Attn: Library	John M. Brueger
1		Bellcomm 955 L'Eufant Plaza, S. W. Washington, D. C. Attn: Library	H. S. London
1		Boeing Company Space Division P. O. Box 868 Seattle, Washington 98124 Attn: Library	J. D. Alexander

Report Copies R	D	Recipient	Designee
1		Chemical Propulsion Information Agency Applied Physics Laboratory 8621 Georgia Avenue Silver Spring, Maryland 20910	Tom Reedy
1		Chrysler Corporation Space Division New Orleans, Louisiana Attn: Librarian	
1		Curtiss-Wright Corporation Wright Aeronautical Division Attn: Library	G. Kelley
1		Fairchild Stratos Corporation Aircraft Missiles Division Hagerstown, Maryland Attn: Library	J. S. Kerr
1		Research Center Fairchild Hiller Corporation Germantown, Maryland Attn: Library	Ralph Hall
1		Republic Aviation Fairchild Hiller Corporation Farmington, Long Island New York	
1		General Dynamics/Convair P. O. Box 1128 San Diego, California 92112 Attn: Library	Frank Dore R. Roberts P. Stephens
1		Missiles and Space Systems Center General Electric Company Valley Forge Space Technology Center P. O. Box 855 Philadelphia, Pa. 190101 Attn: Library	A. Cohen F. Schultz
1		General Electric Company Flight Propulsion Lab. Department Cincinnati, Ohio Attn: Library	D. Sulchu Leroy Smith
1		Grumman Aircraft Engineering Corporation Bethpage, Long Island, New York Attn: Library	Joseph Gavin

Report Copies R	D	Recipient	Designee
1		Honeywell Inc. Aerospace Division 2600 Ridgeway Road Minneapolis, Minnesota Attn: Library	Gordon Harris
1		Kidde Aerospace Division Walter Kidde & Company, Inc. 567 Main Street Belleville, N. J. 07107	R. J. Hanville
1		Ling-Temco-Vought Corporation P. O. Box 5907 Dallas, Texas 75222 Attn: Library	Warren G. Trent
1		Lockheed Missiles and Space Company P. O. Box 504 Sunnyvale, California 94087 Attn: Library	V. C. Lee J. Guill
1		Marquardt Corporation 16555 Saticoy Street Box 2013 - South Annex Van Nuys, California 91409	L. R. Bell Jr. C. Coulbert T. Hudson
1		Martin-Marietta Corporation (Baltimore Division) Baltimore, Maryland 21203 Attn: Library	John Calathes
1		Denver Division Martin-Marietta Corporation P. O. Box 179 Denver, Colorado 80201 Attn: Library	Dr. Morganthaler
1		Western Division McDonnell Douglas Aircraft Company, Inc. 3000 Ocean Park Blvd. Santa Monica, California 90406 Attn: Library	R. W. Hallet
1		McDonnell Douglas Aircraft Corporation P. O. Box 516 Lambert Field, Missouri 63166 Attn: Library	R. A. Herzmark

Report Copies R	D	Recipient	Designee
1		Rocketdyne Division North American Rockwall Inc. 6633 Canoga Avenue Canoga Park, California 9134 Attn: Library, Department 596-306	Dr. R. J. Thompso S. F. Iacobellis
1		Space & Information Systems Division North American Rockwell 12214 Lakewood Blvd. Downey, California Attn: Library	
1		Northrop Space Laboratories 3401 West Broadway Hawthorne, California Attn: Library	Dr. William Howard
1		Radio Corporation of America Astro-Electronics Products Princeton, New Jersey Attn: Library	S. Fairweather
1		Rocket Research Corporation Willow Road at 116th Street Redmond, Washington 98052 Attn: Library	F. McCullough, Jr.
1		Thiokol Chemical Corporation Redstone Division Huntsville, Alabama Attn: Library	John Goodloe
1		United Aircraft Corporation Corporation Library 400 Main Street East Hartford, Connecticut 06108 Attn: Library	Dr. David Rix Frank Owen
1		United Aircraft Corporation Pratt & Whitney Division Florida Research & Development Center P. O. Box 2691 West Palm Beach, Florida 33402 Attn: Library	R. J. Coar Dr. Schmitke

Report Copies R	D	Recipient	Designee
1		United Aircraft Corporation United Technology Center P. O. Box 358 Sunnyvale, California 94038 Attn: Library	Dr. David Altman
1		Vickers Incorporated Box 302 Troy, Michigan	
1		Vought Astronautics Box 5907 Dallas, Texas Attn: Library	W. C. Trent